SYNTHESIS OF NITROGEN CONTAINING HETEROCYCLES AND ACID CATALYZED REACTIONS OF AROMATIC AMINES OVER MEDIUM AND LARGE PORE ZEOLITES

THESIS

Submitted to the

UNIVERSITY OF PUNE

for the degree of

DOCTOR OF PHILOSOPHY

in

CHEMISTRY

By

R. ANAND

CATALYSIS DIVISION

NATIONAL CHEMICAL LABORATORY

PUNE 411 008, INDIA

APRIL 2002

Dedicated to

My parents

And

Sisters

CERTIFICATE

This is to certify that the work incorporated in the thesis, "**Synthesis of Nitrogen Containing Heterocycles and Acid Catalyzed Reactions of Aromatic Amines Over Medium and Large Pore Zeolites**" submitted by **Mr. R. Anand**, for the degree of *Doctor of Philosophy*, was carried out by the candidate under my supervision in the Catalysis Division, National Chemical Laboratory, Pune, India. Such material as has been obtained from other sources has been duly acknowledged in the thesis.

Dr. B. S. Rao
Research Guide

ACKNOWLEDGEMENTS

R. Anand

CONTENTS

CHAPTER 1

List of Figures

List of Tables

Chapter –1

Introduction

1.1. INTRODUCTION: FINE CHEMICALS

Fine chemicals are synthesis products aimed at chemical uses as intermediates (or with the function of bulk chemicals), in the manufacturing of various chemical substances such as: pharmaceuticals, flavors, essences, agro-chemicals and detergents, etc., Around 95% of all industrial heterogeneous catalysts are used in the production of bulk chemicals and only 3–5% in the synthesis of fine chemicals. In that industrial segment, on the other hand, this low percentage accounts for approximately 20% of the profit. With respect to fine and intermediate chemicals manufacture, the multiplication factor seems to be much higher than in petrochemical or refinery processes. That underlines the economic importance and the need of catalysis not only in petrochemical industry but also in speciality chemical production [1,2].

Processes employed for the synthesis of organic chemicals generate copious amounts of waste, mainly in the form of inorganic salts, which end up in aqueous effluent. The magnitude of the waste problem is readily apparent from a consideration of the *E factors*, defined as the amount of waste (in kg) generated per kg of desired product, in various segments of the chemical industry [3,4].

With respect to the homogeneous catalysis no catalyst regeneration is possible, and their application causes unavoidable problems with corrosion of the reactors, tubes, machinery etc. with separation and recycling of the catalysts, with the salt formation due to the neutralization in the working up procedure and with the high costs for waste disposal and polluted water treatment. Solid acid–base catalysts play an extremely important economical and ecological role in chemical and petrochemical industry as well as refinery technology. Among the solid acid-base catalyst that are employed in various industrial process for the production of fine chemicals zeolite catalysts represent 45% in different processes such as for alkylation, isomerization, amination, cracking, etherification,

esterification, condensation reactions, etc. Even though great progress of petroleum and petrochemical industry for the last 40 years contribute to a high demand of acid heterogeneous zeolite catalyst, it is noteworthy to mention that about 40 processes in the field of fine and intermediate chemicals are catalyzed by such materials.

The use of zeolites as catalysts for organic reactions began in the early 1960s. Initially, zeolite-based catalysts were investigated for applications in the petrochemical industries. In 1968, Venuto and Landis provided the first comprehensive overview of zeolite catalysts for organic reactions within and outside the area of fuels synthesis [5]. Over the past few decades, zeolites have had a significant impact on the petrochemical industries and Venuto has provided another extensive review of the literature in 1994 [6]. In addition to increased use in petrochemical manufacture, zeolite catalysis is expanding into the areas of speciality and fine chemicals synthesis.

As the number of zeolite structures increased and as the basic knowledge of zeolite acidity and shape selectivity grew, it became evident that molecular sieves would play a greater role in organic synthesis. The pores of zeolites are similar in size to small organic molecules and have shown the ability to recognize, discriminate and organize molecules with precisions that can be less than 1Å [7,8]. The first report of shape-selective, acid catalysis using a zeolite catalyst was by Weisz et al. [9] who selectively dehydrated n-butanol in the presence of iso-butanol (difference in kinetic diameter less than 1Å). Another reason for the success of zeolites as commercial catalysts is the ability to control the catalytic properties by a variety of synthetic and post-synthetic methods. By choosing the appropriate organic template and synthesis conditions, the pore size and pore shape (dimensionality, intersections, cages) may be directly influenced. The acidity of the zeolite may also be controlled through various methods such as silicon/aluminum ratio, ion exchange, and calcination conditions. Their high thermal stability permits them to be used

at high temperatures that often result in higher yields and easier heat recovery. All of these characteristics, and especially the control of structure and acidity, make zeolites well suited as catalysts for organic reactions. A number of excellent review papers have dealt with the use of zeolites as acid catalysts for a wide variety of organic syntheses [6,10-19].

1.2. ZEOLITES: HISTORICAL DEVELOPMENT OF ZEOLITE CHEMISTRY

Zeolites are natural volcanic minerals with a number of unique characteristics. Zeolites were formed when volcanic ash was deposited in ancient alkaline lakes. The interaction of the volcanic ash with the salts in the lake water altered the ash into various zeolite materials. The Swedish mineralogist Cronstedt introduced the name "zeolite" in 1756 [20] for certain silicate minerals in allusion to their behavior on heating in a borax bead (Greek *zeo* = boil; *lithos* = stone). Three such minerals were listed by Haüy (1801) namely stilbite, analcime, and harmotome, together with "mesotype", which has not survived. Chabazite and leucite had been named even earlier. Forty-six zeolites were listed by Gottardi and Galli (1985), and new species continue to be described. The first crystal-structure determination of a zeolite was done on analcime (Taylor, 1930); following this, Hey (1930) concluded that zeolites in general have aluminosilicate frameworks with loosely bonded alkali or alkali-earth cations, or both. There was little interest in zeolites until the late 1930's when the modern founder of zeolite chemistry, Barrer began the characterization of zeolite structure and chemistry. His many papers gave details of the first method of laboratory synthesis of zeolites from silicate alumina gels, the changes that occur upon ion exchange and their use as strong environmental friendly, shape selective catalysts. These discoveries sparked huge interest in the synthesis of shape selective zeolite catalysts in companies such as Union Carbide and Mobil. In the 1950s and early 1960s Union Carbide made several discoveries, which proved to be of great economic significance, and propelled them to the forefront of zeolite science. Milton and Breck of the

Linde division of Union Carbide, over a period of 5 years, developed and characterized three novel zeolites Linde A, X and Y, which have become 3 of the most profitable synthetic zeolites.

1.3. ZEOLITES: GENERAL INTRODUCTION

Zeolites are highly crystalline alumino-silicate frameworks comprising $[SiO_4]^{-4}$ and $[AlO_4]^{-5}$ tetrahedral units. T atoms (Si,Al) are joined by an oxygen bridges. Introduction of an overall negative surface charge requires counter ions e.g. Na^+, K^+ and Ca^{2+}. The first zeolite, stilbite, was discovered by Cronstedt in 1756 [20] who found that the mineral loses water rapidly on heating and thus seems to boil. A representative empirical formula of a zeolite is

$$M_{x/n}[(AlO_2)_x(SiO_2)_y]zH_2O$$
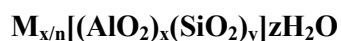
where M represents the exchangeable cation of valence n. M is generally a Group I or II ion, although other metal, non-metal and organic cations may also balance the negative charge created by the presence of Al in the structure. The ratio x/y can have the value 1 to ∝. The framework may contain cages and channels of discrete size, which are normally occupied by water [21]. Z represents the number of water molecules, which can be reversibly adsorbed or desorbed in the pores.

In addition to Si^{4+} and Al^{3+}, other elements can also be present in the zeolitic framework. They need not be isoelectronic with Si^{4+} or Al^{3+}, but must be able to occupy framework sites. Aluminosilicate zeolites display a net negative framework charge, but other molecular sieve frameworks may be electrically neutral.

Most of the natural zeolites are aluminum isomorphs. Therefore zeolite is one of the most interesting classes of tectosilicate having open framework in which $[AlO_4]^{-5}$ is partially substituted for $[SiO_4]^{-4}$ in silicate polymorph.

1.4. STRUCTURAL FEATURES OF ZEOLITES

The framework of a molecular sieve is based on an extensive three-dimensional network in which the polyhedral sites, usually tetrahedral, are linked by oxygen atoms. The crystalline framework contains cages and channels of discrete size and 3-30 Å in diameter. The primary building unit of a molecular sieve is the individual tetrahedral unit. The topology of all known molecular sieve framework types can be described in terms of a finite number of specific combinations of tetrahedra called "secondary building units" (SBU's)[22]. In figure 1.1 [23] the T atom belonging to a TO_4 tetrahedron is located at each corner, but the oxygens located near the midpoints of the lines joining each pair of T atoms are not shown. A molecular sieve framework is made up of one type of SBU only.

It is the way that these SBUs join together that gives rise to the huge number of different zeolites with and their intriguing properties. The SBUs join to form structurally and chemically important zeolite channels known as oxygen windows that pass through the zeolite. It is the pore system in the zeolites that gives rise to interesting properties. The pores can pass through the zeolite in 1,2 or 3 directions, vary in size and in the case of ZSM-5, can also be sinusoidal.

Description of the framework topology of a molecular sieve involves "tertiary" building units corresponding to different arrangements of the SBU's in space. Various alternative ways have been proposed. The framework may be considered in terms of large polyhedral building blocks forming characteristic cages. For example, sodalite, zeolite A and zeolite Y can all be generated by the truncated octahedron known as the [beta]- cage [24].

Figure 1.1: Secondary building units (SBU's) found in zeolite-like molecular sieve structures.
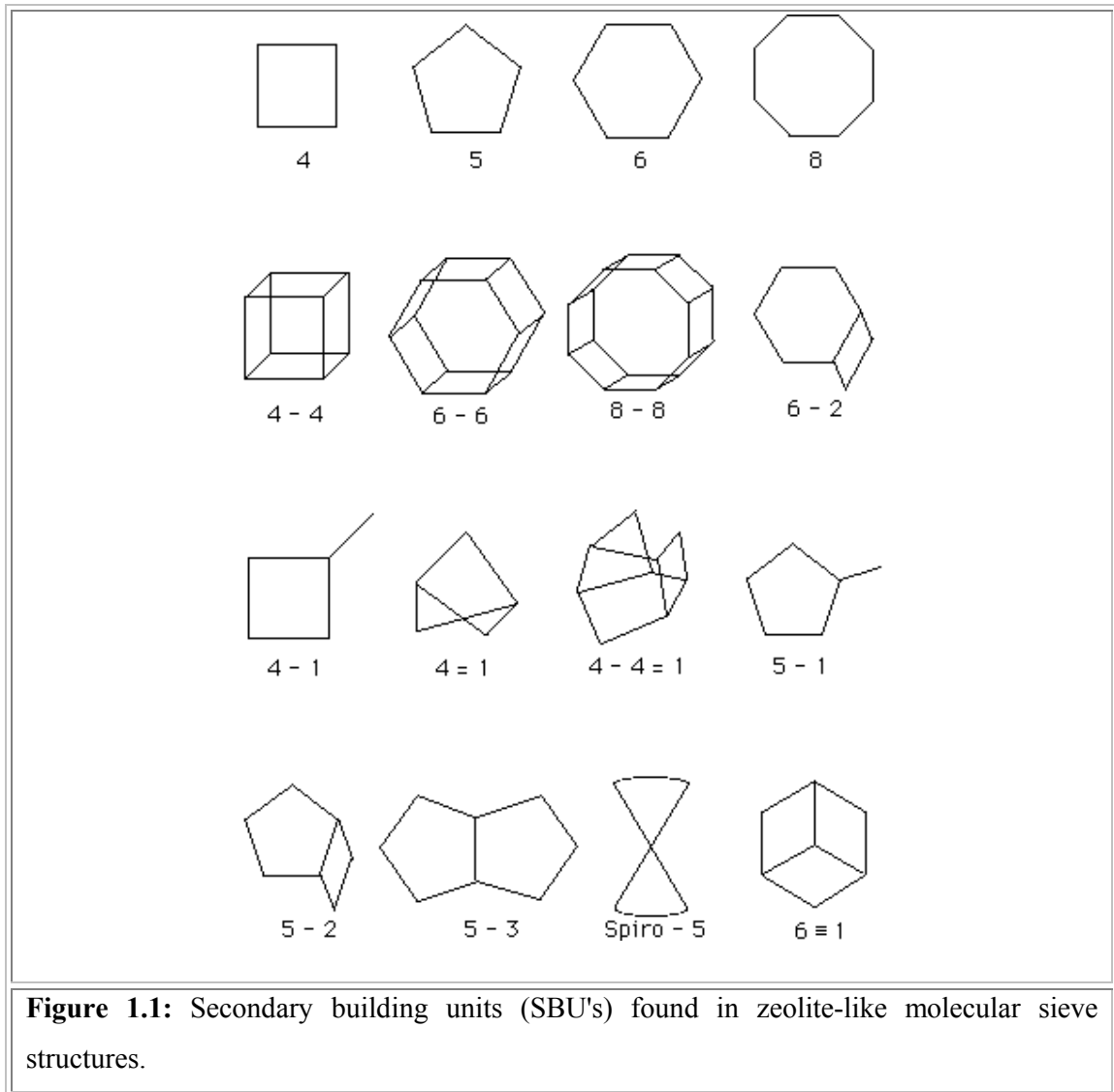
According to the so-called Loewenstein rule [25], Al-O-Al linkages in zeolitic frameworks are forbidden. As a result, all aluminate tetrahedra must be linked to four silicate tetrahedra, but a silicate tetrahedron may have five different possible environments: Si(0Al,4Si), Si(1Al,3Si), Si(2Al,2Si), Si(3Al,1Si) and Si(4Al,0Si).

1.5. CLASSIFICATION OF ZEOLITES

Zeolites have been classified on the basis of their morphological characteristics [24], crystal structure [23], chemical composition [24], effective pore diameter [26] and

natural occurrence [24]. The classification of zeolites on the basis of morphology was made initially by Bragg [27]. On the basis of effective pore diameters they can be classified as

(a) *Small pore zeolites* (diameter, d < 5 Å)

(b) *Medium pore zeolites* (d = 5.0-6.5 Å)

(c) *Large pore zeolites* (d = 6.5 – 13.0 Å)

(d) *Extra large pore zeolites* (d =13.0-20 Å)

(e) *Mesoporous zeolites* (d = 20.0-100 Å)

These pore openings are made up of 8-, 10-, 12-, 14-, 18-, and 24-membered oxygen rings. Table 1.1 represents some of the examples.

Table 1.1: Classification based on effective pore opening size of oxygen ring

Small Pore, 8-ring	Intermediate Pore, 10- ring	Large Pore, 12-ring	Extra large pore, 14-, 18-, and 24-ring	Mesoporous Zeolites
Li-A	Dachiardite	Cancrinite	Cloverite,	MCM-41
Chabazite	Epistilbite	LindeX,Y,L		
Erionite	Ferrierite	Gmelinite		
ZK-5	Heulandite	Mazzite		
Linde-Y	Laumontite	Mordenite		
Natrolite	ZSM-5	Offretite		
Phillipsite	ZSM-11			
Rho	Stilbite			
Thomsonite				

Aluminium is the element, which replaces silicon most easily. The limits of the Si/Al ratio are 0.5 (e.g., bicchulite) and infinity (e.g., silicalite-1). Zeolites are also classified on the basis of silica: alumina ratio [26] as follows.

(a) *Low Si:Al ratio*, between 1 and 1.5 like Zeolite A, X and Sodalite.

(b) *Intermediate Si:Al ratio*, between 2 to 5 like Zeolite Y, L, Mordenite and Omega.

(c) *High Si:Al ratio* from 10 to several thousands like highly siliceous variants of Y, Erionite, Mordenite prepared by thermo chemical framework modifications, like EU-1, EU-2, ZSM-11, ZSM-5, ZSM-23, ZSM-48 prepared by direct synthesis and pure silica polymorphs, Silicalite-1 and Silicalite-2.

The Classification of zeolites according to structure types was also reported [22]. Wilson et al. [28] have reported a new class of molecular sieves called aluminophospate (AlPO$_4$) containing equal moles of Al^{3+} and P^{5+} ions in the lattice. Davis et al. [29] have synthesized a new AlPO$_4$ type, 18 membered ring, large pore molecular sieve designated as VPI-5 having a pore diameter of 12 Å. Esterman et al. [30] reported gallophosphate molecular sieve with a pore diameter of 29-30Å. The metal substitution in the aluminophosphate (MeAlPO) such as Si, Ti, V, Fe, Mg, Ga, Co, Zn, Mo and Cr have also been reported by different authors [31-33].

1.6. NOMENCLATURE

The Structure Commission of the International Zeolite Association and IUPAC has assigned the structural codes to the synthetic and natural zeolites [23,24]. The topology of the framework defines a structure type symbolized by a group of three letters, e.g., MFI for the structure type of zeolite ZSM-5. These codes are decided on the basis of the types of species and not on the number or composition, distribution of tetrahedral atoms (e.g., Ti, Be, Ge, Ga, P etc), cell dimensions or crystal symmetry.

A list of the 98 currently accepted structure types, with their type materials, can be found in the ATLAS OF ZEOLITE STRUCUTRE TYPES [34] which contains an additional list of zeolite material designations related to known structure types. Updated data can be found on the World Wide Web (**http://www.iza-structure.org).** Few of them are given in the table 1.2.

Table 1.2: Structural codes to the synthetic and natural zeolites

Code	Type Material	Date	Code	Type Material	Date
AEI	AlPO-18	1992	LTA	Linde Type A	1978
AEL	AlPO-11	1987	LTL	Linde Type L	1978
AET	AlPO-8	1992	LTN	Linde Type N	1987
AFI	AlPO-5	1987	MEL	ZSM-11	1978
ANA	Analcime	1978	MFI	ZSM-5	1978
BEA	Beta	1992	MOR	Mordenite	1978
CHA	Chabazite	1978	MTW	ZSM-12	1987
CLO	Cloverite	1992	MWW	MCM-22	1997
EPI	Epistilbite	1978	OFF	Offretite	1978
ERI	Erionite	1978	STI	Stilbite	1978
FAU	Faujasite	1978	STT	SSZ-23	1998
FER	Ferrierite	1978	VFI	VPI-5	1992

http://www.iza-structure.org

1.7. BRÖNSTED ACIDITY IN ZEOLITES

In addition to shape and size selective catalysis, the generation of acidic sites within the zeolite pores gives rise to a highly efficient solid acid catalysis. The isomorphous replacement of silicon with aluminium in a T site gives rise to a charge imbalance because aluminium has lower co-ordination ability than silicon and must be neutralized. This is achieved in two ways in natural zeolites: The Al-O bond length becomes slightly longer. A coordination site is made available for a cation to counter the excess negative charge.
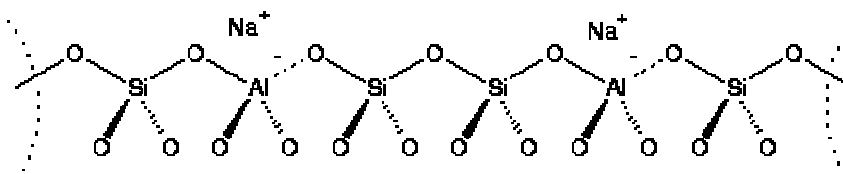
Figure 1.2: Neutral sodium balanced zeolite framework
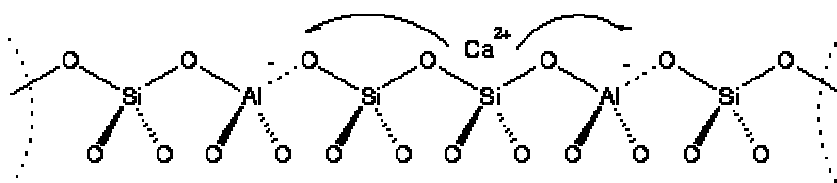
Figure 1.3: Neutral calcium balanced zeolite framework

In natural zeolites, the excess negative charge is balanced by whatever ions are present in the surrounding environment e.g. K^+, Na^+, Ca^{2+} and Mg^{2+}. The type of counter ion used to balance the charge plays an important part in the use of the zeolite.
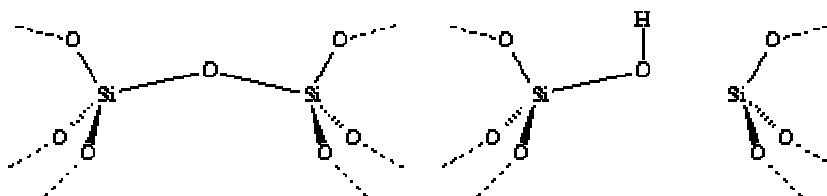
Figure 1.4: i) Siliceous zeolite ii) Zeolite Brönsted acid site

The acid site formed behaves as a classic Brönsted, proton donating acid site. The highly acidic sites, combined with the high selectivity arising from shape selectivity and large internal surface area makes the zeolite an ideal industrial catalyst. The significance of this acidic proton can be shown quite easily by comparisons of experiments in H exchanged zeolites and their equivalent cation form zeolites. We can modify zeolite structure and activity so as to increase the catalytic effect of the zeolites, a very economically important step for industry.

1.8. SYNTHESIS OF ZEOLITES

Zeolites are synthesized hydrothermally from basic reaction gels at temperatures between 60°C and 200°C under an autogeneous pressure and in the presence of a large excess of water. Most of the highly siliceous zeolites are formed in the presence of organic bases known as templates, introduced in the early 1960's [35]. The template must be

present, lest a dense phase be crystallized. The structure and properties of the zeolite product are highly dependent on the physical and chemical nature of the reactants used in preparing the reaction mixture, its overall chemical composition, and on the type of cations or organic templates and the conditions (temperature, pressure and duration) of the hydrothermal treatment.

Most of the synthetic molecular sieves are produced under non-equilibrium conditions and are considered, in a thermodynamic sense, as metastable phases. Upon mixing of the reagents used in the synthesis, the system is in a disordered state with a higher entropy than the ordered crystalline molecular sieve. For crystalline systems, which can exist in several different polymorphic forms, the one with the highest entropy will develop from the highly disordered synthesis mixture. According to the Ostwald rule of successive transformations, at long reaction times metastable molecular sieves recrystallize to other more stable structures under certain conditions.

In contrast to the wide diversity of structures prepared from aqueous systems, only a handful of molecular sieves are known to crystallize from solvents such as hexanol, propanol, glycol, glycerol, sulfolane and pyridine [39]; ferrierite was synthesized from pyridine [36]; silicalite, ZSM-39, ZSM-48, AlPO$_4$-5, AlPO$_4$-11 and AlPO$_4$-21 from ethylene glycol [37, 38], hydroxysodalite, kaliophilite and zeolite BaT from glycol [39].

The tetrahedral sites are occupied only by silicon, the organic species may be acting both as a template and a solvent, and it creates a new road to synthesize zeolites and other molecular sieves. Crystals prepared under normal synthesis conditions are generally rather small. Large crystal can be grown in the "fluoride system" [36,40] and the multihydroxyl alcohol system [41].

1.8.1. Incorporation of Heteroatoms by Hydrothermal Methods

Elements isoelectronic with Al^{3+} or Si^{4+} can enter the zeolite framework during synthesis. These include B^{3+}, Ga^{3+}, Fe^{3+} and Cr^{3+}, all of which substitute for Al^{3+}; and Ge^{4+} and Ti^{4+} which substitute for Si^{4+}.

Goldsmith [42] was the very first to report isomorphous substitution of Si^{4+} by Ge^{4+} in the lattice. The substitution of Si by Ge when a trivalent element is present has been reviewed by Barrer [24, 43] Ti incorporation into the structure types BEA [44,45] and MFI [46-48.] has been reported. The isomorphous substitution of Si^{4+} and Al^{3+} by elements such as B [49-53], Fe [50,51], Ga [50,52], Ti [54-56], V [57,58], Zr [59] are reported. The number of acid sites and strength depend on the amount and nature of the incorporated metal. Such materials find application in acidic reactions, oxidations and various other organic transformations.

1.9. POST-SYNTHESIS MODIFICATION OF ZEOLITES

Several post-synthesis methods have been used to modify the properties of zeolites.

1.9.1. Ion Exchange of zeolites

The ion-exchange capacity of a zeolite depends on the chemical composition, i.e., a higher ion-exchange capacity is observed in zeolites of low Si/Al ratio [ref.21, p.537]. The specific ion exchange capacity varies with the structure of the zeolite and the exchange cation. Ion exchange is generally carried out in aqueous system. Solid-state ion exchange using fused salts has been the subject of some recent work.

Cations in the zeolites, which compensate the negative charge on the framework and are exchangeable by other cations from solution, play an important part in determining their adsorption and catalytic properties. Ion exchange is an effect and sufficiently simple means for the chemical modification of zeolite crystals. A significant number of

publications are available containing data on exchange by transition metal cations in type X and Y zeolites. [60].

Zeolites with low Si/Al ratios have strongly polar anionic frameworks. The exchangeable cations create strong local electrostatic fields and interact with highly polar molecules such as water. Cation exchange in a zeolite is accompanied by an alteration of stability, adsorption behaviour and selectivity, catalytic activity and other properties.

The cation-exchange behaviour of zeolites depends on

(a)   the nature of the cation species, the cation size (both anhydrous and hydrated) and cation charge,

(b)   the temperature,

(c)   the concentration of the cationic species in the solution, the anion associated with the cation in solution,

(d)   the solvent (most exchange has been carried out in aqueous solutions, although some work has been done in organics),

(e)   and the structural characteristics of the particular zeolite.

1.9.2. Metals supported on zeolites

A metal function, e.g., for reduction, hydrogenation, or oxidation, can be combined with the acid function of a zeolite. There are basically two procedures by which precursors of metals can be introduced into a zeolite (a) by ion exchange, if the metal forms cations and [61,62] (b) by sorbing neutral metal compounds, e.g., carbonyl complexes [63].

A third method frequently applies to bound catalysts is impregnation, which introduces anions as well as cations. In order to impregnate a zeolite of low Si/Al ratio, a high concentration of the solution is required to over come the anion-repelling effect of the negative charges around the pore mouth. A convenient method involves evaporation of the impregnating solution in contact with the zeolite.

Impregnation of a zeolite is employed when the quantity of metal ion to be introduced is greater than would be obtained by ion exchange of, e.g., high-silica zeolites, but the distribution is more uniform in the ion-exchanged sample [64].

1.9.3. Dealumination / Steaming

For use as acid catalysts, zeolites are frequently applied in the acid form, which can most conveniently be prepared by calcination of the ammonium form. The acid forms of low-silica zeolites are inherently unstable. Even mild hydrothermal treatment causes loss of crystal structure [65-67]. Most zeolites with SiO_2/Al_2O_3 molar rations above 20 are crystallized in the presence of an organic cation, usually a quaternary ammonium ion. The ratio can be increased significantly by chemical treatment leading to removal of some of the Al from the framework (so-called Dealumination). Dealumination by steaming, $SiCl_4$ treatment, reaction with chelating agents like EDTA, acetylacetone, ammonium hexafluorosilicate, oxalic acid etc. acid leaching with HCl are some of the post synthesis methods used to control the acidity of the zeolites [68].

In some cases, for e.g., under the action of acids, when Al migrates from the zeolite framework, it then passes into solution, and chemical analysis indicates an increase in the Si/Al ratio in the zeolite crystals. In other cases, for e.g., heating H-zeolites in the presence of water vapor, the Si/Al ratio in the catalyst remains unchanged, while the content of tetrahedral Al in the framework decreased. In both the cases, dealumination can lead to significant changes in the properties of the zeolites. In general, thermal stability and catalytic activity of zeolites are increased substantially as a result of dealumination.

1.10. CHARACTERIZATION OF ZEOLITES

Characterization of zeolite samples can be split into various simple and complex techniques. In the case of naturally occurring zeolite samples, simple analysis of the mineralogy of the sample, e.g. colour, shape of crystallite, hardness can be used to identify

the zeolite type. Unfortunately many man-made zeolite samples do not allow this type of analysis, as many of these samples are simple white powders with small crystal sizes (<300 angstroms). Characterizations that have been utilized in this work only are described here.

1.10.1. X-Ray Diffraction

X-Ray Diffraction can be used in the determination of zeolite structure as a basic fingerprinting technique [69]. In most cases XRD is used to identify the basic zeolite structure type, phase purity, degree of crystallinity, unit cell parameters, crystallite size and in understanding the kinetics of crystallization. As the powder pattern is the "fingerprint" of the molecular sieve structure, phase purity and percent crystallinity of the synthesized molecular sieve can be ascertained by comparing with the standard pattern for the molecular sieve under investigation. Thus, zeolite structures can be easily identified by comparison of the d-spacings or 2θ positions of the typical Bragg reflections with those given for known zeolites in straightforward compilations. Even in mixtures with other zeolites or crystalline materials the identification of a zeolitic phase generally does not encounter difficulties.

1.10.2. IR spectroscopy

For a long time, IR spectroscopy had been the mainly used spectroscopic technique to characterize zeolites and zeolite/adsorbate systems. IR studies on zeolites and zeolite/adsorbate systems reported in the literature before 1975 have been extensively reviewed by Ward [70] and in 1992, a very concise overview has been published by Foerster [71].

The main areas of application of IR spectroscopy are

(a) Investigation of framework properties

(b) Study of sites of the zeolite lattice for adsorption or catalysis

(c) Characterization of zeolite/adsorbate systems

(d) Measurements related to the motion of guest molecules in the pores and cavities of the zeolites.

1.10.2.1. Study of Framework vibrations of zeolites

Flanigen et al. [72] studied the relationship between IR spectral features of zeolites and structural properties. The bands observed in mid infrared were classified into two main categories, viz. bands due to internal vibrations of the TO_2 tetrahedra (T= Si or Al) and external vibrations of tetrahedral linkages e.g., in double rings (as in A-, X-, Y- type) or pore openings (e.g., as in mordenite). Assignments of zeolite lattice vibrations are listed in table 1.3.

Table 1.3: Assignments of Zeolite lattice vibrations

Internal Tetrahedra	Vibrations, cm^{-1}	External Linkages	Vibrations, cm^{-1}
Asym. stretch	1250-950	Double ring	650-500
Sym. stretch	720-650	Pore opening	420-300
T-O bend	500-420	Sym. Stretch	820-750
		Asym. Stretch	1150-1050 sh

sh: shoulder

1.10.2.2. IR investigation of Acidic and Basic sites in zeolites

Acidic sites, such as acidic OH groups (Brönsted acid centers), true Lewis sites (aluminium-containing extra-framework species) and cations as well as basic sites (such as basic oxygen atoms or alkaline metal clusters) are encountered in zeolites and are of paramount importance in acid-base catalysis on zeolites. By IR spectroscopy, only the Brönsted acid sites may be investigated with and without probe molecules, whereas acidic Lewis sites, cations and basic sites can be identified and quantitatively determined only with the help of probes. Probe molecules frequently employed for acidic sites are pyridine, substituted pyridine, ammonia, amines, carbon monoxide, methane, hydrogen and fluoro-

/chloroethane and ethane for acidic centers and carbon dioxide or pyrrole for basic sites. A detailed description about determination of zeolite acidity is discussed in section 1.11.

1.10.3. Atomic Adsorption Spectroscopy (A.A.S/A.A.E)

Atomic Absorption Spectroscopy (A.A.S) is used to determine the chemical composition of zeolite samples. Although it is a destructive technique, the sample size needed is very small (typically about 10 milligrams - i.e. one hundredth of a gram) and its removal causes little damage. Samples are typically made up by first dissolving approximately 0.1g of zeolite sample in a solution of 1ml HF / 5ml. Dissolution times are generally in the region of 1 hour, although it can take up to 5 days for natural zeolite samples to completely dissolve. After complete dissolution of the zeolite the solutions are then diluted to decrease their element concentrations to within the linear range for the particular element under study. The resulting solution is sprayed into the flame of the instrument and atomized. Light of a suitable wavelength for a particular element is shone through the flame, and some of this light is absorbed by the atoms of the sample. The amount of light absorbed is proportional to the concentration of the element in the solution, and hence in the original object. Measurements are made separately for each element of interest in turn to achieve a complete analysis of an object, and thus the technique is relatively slow to use. However, it is very sensitive and it can measure trace elements down to the part per million level, as well as being able to measure elements present in minor and major amounts. These elements are Na, K, Fe, Al, Mg, Zn, Cd, Cu, Co, Ni, Mn, Ca, Sr, Ag, Pt, Au, etc. where as some of the elements which are not detectable by atomic absorption are Ti, Si, Ta, W, Mo, V, Ir and few others. This may be due to the fact that these elements form oxide in the flame. This method is also independent of flame temperature since atoms usually used in this method are in ground state.

1.10.4. Adsorption measurements

Molecular sieves have the ability to adsorb probe molecules of different sizes. The Braunauer-Emmett-Teller (BET) volumetric gas adsorption technique using nitrogen, argon, etc., is a standard method for the determination of the surface areas and pore size distribution of finely divided porous samples [73]. The relation between the amount adsorbed and the equilibrium pressure of the gas at constant temperature is defined by the adsorption isotherm. Sorption studies on zeolites can provide information about their void volumes, pore size, percentage crystallinity, surface area, acidity, diffusion properties and pore blockage if any. Low temperature (77 K) nitrogen sorption isotherms help in determining pore volume, pore size distribution as well as the surface area of zeolite under study [74,75]. Adsorption and diffusion properties of zeolite play an important role on the rate of chemical reaction at the active sites. Barrer et al. [76] studied in detail the diffusion process in zeolites. Diffusion in zeolites has been categorized as Configurational, Knudsen and Bulk diffusion.

1.10.5. X-ray Fluorescence Spectroscopy

In this method a suitable sample is radiated by high energy X-rays by which electrons can be expelled from the different atoms, leaving empty space (holes) in low-lying orbitals. The main mechanism for relaxation then is, that an upper electron falls into this vacancy. The energy released may result either in the generation of radiation, which is called X-ray fluorescence, or in the ejection of another electron, the secondary electron of the so-called Auger effect. Both X-ray fluorescence radiation and the Auger electrons are characteristic for the emitting atoms and can be used for quantitative elemental analysis.

The sample preparation consists of making a solid solution of the zeolite in a $LiBO_2$ melt followed by rapid cooling to a glassy material For callibration standard zeolite samples with known composition are used.

1.10.6. X-ray Photoelectron spectroscopy (XPS)

Instead of measuring the emitted X-rays or secondary electrons it is also possible to measure the energy spectrum of the primary electrons. This is done in X-ray photoelectron spectroscopy and the resulting spectrum can be used for qualitative analysis and after calibration also for quantitative analysis of the sample.

Because the escape depth of the electrons is limited to a few atom-layers only the surface composition of the samples is obtained. In combination with suputtering of the sample by bombarding the sample with noble gas ions it is possible to obtain a depth profile of the chemical composition of the sample.

X-ray photoelectron spectroscopy (XPS) is a surface-sensitive technique, which uses a monochromatic X-ray source to excite photoelectrons from the sample. The energy of these electrons is characteristic of elements in the sample for "core-level" electrons but may also represent hybridized molecular orbitals for "valence-level" electrons. This technique shows changes in the binding energy (BE) of electrons on Si, Al and O with changes in the zeolite framework Si/Al ratio. In addition, there is a large shift in BE of Al on changing from tetrahedrally coordinated to octahedrally coordinated [77]. This provides a method of detecting nonframework Al in steamed zeolites, as does solid-state NMR [78].

1.11. DETERMINATION OF ZEOLITE ACIDITY

The acidity of zeolites is mainly caused by the presence of Brönsted acid sites but also some Lewis acid sites may be present especially after high temperature treatments. The measurement of the number, type and strength of acid sites provides the key experimental data regarding zeolite acidity.

For a complete characterization of zeolite acidity it is, therefore, necessary to determine number and strength of both types of acid sites. Several methods have been developed for this purpose from which the most important are

(i)   Titration methods

(ii)   Adsorption and desorption of bases

(iii) IR spectroscopy of –OH groups

(iv)   IR spectroscopy of adsorbed species

(v)   NMR spectroscopy of –OH groups

(vi)   NMR spectroscopy of adsorbed groups

1.11.1. Desorption of bases: Temperature programmed Desorption

When an acid is neutralized by a reaction with a base the heat of neutralization is evolved. This heat of neutralization is larger the stronger the acid and so it can be used to characterize acid-strength. This principle can be used to characterize the acid sites present on a zeolite sample. Temperature programmed desorption (TPD) of probe molecules like ammonia and pyridine is a popular method for the determination of acidity of solid catalysts as well as acid strength because it is an easy and reproducible method. Ammonia is used frequently as a probe molecule because of its small molecular size, stability and strong basic strength [79]. The acidity measurements have been carried out by ammonia TPD method. First the zeolite is contacted with a base (NH_3 or pyridine) to neutralize the acidic sites present. Then the temperature is raised at a constant rate and the amount of desorbed base is recorded. As a result, a desorption spectrum is obtained. In short, TPD consists of heating a sample at a constant rate and measuring the quantity of material desorbed at each temperature. TPD data provide a partially averaged value for acid strength. It is a simple and rapid method to characterize zeolite acidity.

Numerous theoretical and experimental studies have been devoted to the adsorption of NH_3 [80-93]. NH_3-TPD is one of the most often used methods [84-92]. In principle, both the concentration of sites having similar acid strength and the average adsorption heat or activation energy of NH_3 desorption can be determined using the TPD method. Often the

temperature of maximum desorption rate, i.e., the temperature of a TPD peak, is used as a rough measure of the acid strength of the sorption sites. Among the limitations of the method is that it can distinguish sites by sorption strength only, but not L- and B-type sites. Moreover, desorption may proceed simultaneously from sites of different types resulting in more or less overlapping TPD.

In a TPD spectrum, two peaks were observed one at low temperature (LT) corresponding with NH_3 desorbing from the weaker acidic sites (also observed for non-acidic silicates) and another one at higher temperature (HT) corresponding with the stronger acidic sites. The area under these peaks gives information about the amount of these strong acidic sites whereas the peak-maximum-temperature (T_m) gives information about its acid-strength.

1.11.2. IR spectra of OH groups

Hardly any property of a solid acid catalyst has been studied so frequently as the nature and concentration of the functional (hydroxyl) groups [94-97]. The origin of these hydroxyl groups may be (i) the relaxation of the terminating lattice by dissociative sorption of water or (ii) the balancing of charges arising from substitution of lattice cations with cations of different valency.

A more direct study of the Brönsted acidic –OH groups in zeolites is possible by IR-spectroscopy. The weaker the O-H bond, the lower the stretching frequency and the higher the acid-strength. A general IR spectrum of zeolite shows three peaks in the O-H stretching region. The peak at 3740cm^{-1} is assigned to the non-acidic silanol groups that are present at the outer surface of the zeolite crystals and at structural defects.

The peak at 3640 and 3540cm^{-1} correspond with -OH groups having lower O-H bond strength and so more acidic character. From these bands the one at 3640 cm^{-1}

disappears after adsorption of pyridine and so this band is assigned to the accessible acidic –OH groups. This method only gives qualitative information on the number of acid sites.

1.11.3. IR spectroscopy of adsorbed bases

Instead of looking to the acidic –OH groups it is also possible to study the IR absorption of bases that have reacted with the acid sites of the zeolite. Frequently, the reaction with pyridine is used for this purpose. Pyridine can react with Brönsted acid sites as well as with the Lewis acid sites of the zeolites. The reaction of the Brönsted acid sites results in the formation of pyridinium ion while the pyridine molecule is coordinatively bound on the Lewis acid sites. Both the pyridinium ion and the coordinatively bound pyridine have characteristic IR absorption bands. The intensity of these bands corresponds to the number of these sites; however, it is impossible to obtain information on the acid-strength. The presence of the absorption bands only shows that acid-sites are present with an acid-strength large enough to react with the basic probe molecule pyridine.

FTIR analysis of adsorbed pyridine allows a clear distinction between Brönsted and Lewis acid sites, the absorption bands appearing at 1545 and 1455 cm^{-1} in the IR difference spectra being acceptably assigned to adsorbed pyridinium ions and pyridine coordinated to Lewis acid sites, respectively [98-100].

1.12. ZEOLITE CATALYSTS IN THE SYNTHESIS OF NITROGEN-CONTAINING ORGANIC COMPOUNDS

1.12.1. Introduction

Nitrogen-containing intermediates and fine chemicals play an important role in the chemical industry, e.g., in the synthesis of active substances and the production of dyestuffs as well as solvents. Attempts are being made to devise improved routes for synthesis of nitrogen-containing compounds. Zeolite catalysts find a broad spectrum of applications, including acid, non-acid and base-catalyzed organic reactions leading to

intermediates [5,10-11,19, 101-106]. Zeolites with their numerous adjustable catalytic properties can be useful in synthesizing these materials.

1.12.2. Rearrangement Reactions: Beckmann Rearrangement

The Beckmann rearrangement features migration of an R (alkyl or aryl) group from carbon to nitrogen, and is known to be catalyzed by a wide variety of acidic reagents [107,109]. The cyclohexanone oxime to ε-caprolactam transformation is the most important industrial example of the Beckmann rearrangement. ε-caprolactam is an important fiber precursor, in particular for synthetic fibers like Nylon, and its production via. Beckmann Rearrangement of cyclohexanone oxime results in the formation of a large amount of by-product, ammonium sulfate. The classical synthetic route involves the oximation of cyclohexanone with hydroxylamine-sulphate and the subsequent rearrangement of the oxime in concentrated sulfuric acid. Aprrox. 4-5 t $(NH_4)_2SO_4$ per t caprolactam is inevitably obtained as co-product [108]. Further problems encountered include handling a large amount of oleum and corrosion of the apparatus caused by that acid. There are a number of references concerning the use of heterogeneous catalysts like alumina, heteropolyacids, boronphosphate, phosphoric acid or Lewis acids on inert carriers, silica-alumina and boric-acid on alumina for the rearrangement of a variety of ketoximes to amides [108,109].

There are several studies to rearrange the cyclohexanone oxime to ε-caprolactam over zeolitic catalysts. Compared with the conventional method, this is an energetically and economically favorable as well as environmentally friendly alternative route, e.g. there is no formation of a waste product like ammonium sulphate. Zeolites as catalysts for this reaction were attempted in 1960s by P.S. Landis and P.B. Venuto [5,110]. Table 1.4 shows Beckmann rearrangement of cyclohexanone oxime to ε-caprolactam catalyzed by both large and medium pore molecular sieves.

Table 1.4: Beckmann Rearrangement

Cyclohexanone oxime ———————➤ Caprolactam + 5-cyano-1-pentene
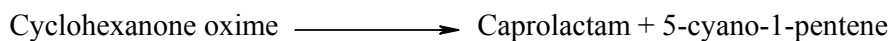
Catalyst reported: Temperature	Reference
HY, RE-, Co-, Zn-, Ni-X, H-Mor: 250-400°C	[109]
TS-1, ZSM-5: 340°C	[112]
B-ZSM-5	[113]
ZSM-5 : 350°C	[114]
H-ZSM-5, MgZSM-5, LiZSM-5: 350°C	[115]
SAPO-11, -41 : 350°C	[116]
NaHY : 335°C	[117]
H-, Ni-ZSM-5, H-ZSM-11, -23; REY : 350°C	[118]
ZSM-5, SiO_2-ZSM-5 : 350°C	[119]

The principal by-product is 5-cyano-1-pentene together with traces of cyclohexanone and cyclohexanol. According to Hoelderich [111] and from the literature data, the optimum reaction temperature for high caprolactam selectivity is between 250-380°C with the selectivity increasing with increasing temperature. Above 400°C caprolactam decomposition is observed. Atmospheric pressure is favored. Since at elevated pressure 5-cyano-1-pentene is formed as principal product. Non-polar solvents such as cyclohexane, benzene or toluene are much more favourable than the more polar solvents. Nitrogen and particularly CO_2 as non-basic carrier gas are very useful for the Beckmann rearrangement.

As to mechanistic considerations, a Brönsted acid catalyzed reaction was assumed: protonation of the OH group followed by concerted dehydration/migration and subsequently water addition. As shown by the selective phenyl migration in (E)-acetophenone oxime [109] the group trans with respect to the OH group migrates. This is

24

also observed in the homogeneous Beckmann rearrangement. The key role of the zeolitic acid sites is probably to convert the OH of the oxime into a better leaving group by protonation, although there are different opinions on this issue [115,119]. Sato and co-workers [115,119] also conclude that the Beckmann rearrangement occurs on the external surface of ZSM-5 type zeolites.

Recently, Hoelderich et al. [120–122] reported that only extremely weak acidic sites on zeolitic catalysts are needed for the Beckmann-rearrangement. In particular, vicinal silanol groups and silanol nests at the outer surface of zeolites with MFI structure are thought to be the most suitable species for the rearrangement as their appearance is connected to a remarkable increase of conversion, selectivity and lifetime. Dai et al. [123] studied the catalysis of H-USY zeolite with different SiO_2/Al_2O_3 ratios in the presence of 1-hexanol. They showed that an appropriate amount of relatively weak acid sites of H-USY were effective for a high selectivity.

Polar solvents with high dielectric constant usually enhance this rearrangement in homogeneous systems. The opposite effect was observed over rare earth modified-X at 250°C [109], suggesting that the polar solvents (e.g. acetic acid, methanol) blocked contact of reactant with zeolite acid sites by competitive adsorption.

1.12.3. Cyclocondensation with ammonia: Synthesis of pyridine and methyl pyridines

Introduction of heteroatoms, such as N, S or O, into hydrocarbon molecules adds substantial value, and new routes for such reactions are of continuous interest to the chemical industry. There are two main classes of aromatic N-containing hydrocarbons, the arylamines and the aromatic N-heterocycles. The arylamines which are required industrially are exclusively obtained by synthesis, namely by nitration of aromatics, to nitro aromatics, followed by hydrogenation to aryl amines [124,125]. Pyridine and the like are

important intermediates for the production of pharmaceuticals, herbicides and agrochemicals [126]. Because of the lower demand of aromatic heterocycles than for arylamines, coal tar is still an important source for pyridine and methylpyridines. Increasing demands for aromatic heterocycles have increased, the interest in synthetic routes, and processes in which aldehydes and ketones are condensed with NH$_3$ to pyridine and alkylated pyridines have been realized.

Although there are numerous possible methods for preparing pyridine bases from acyclic molecules (such as carbonyls and dicarbonlys [127,128], dicyano- alkanes [129], alkenes [130] and alkynes [128,131]), only a limited number of these processes (notably the condensations of aldehydes with ammonia [130,132,133]) have achieved industrial application. For e.g., when acetaldehyde, formaldehyde and ammonia are reacted in fluid bed reactor over H-ZSM-5, the principal product is pyridine (40-50%) and β-picoline is obtained as a by-product in 20-30% yield [111,134].

The synthesis of pyridines and substituted pyridines can be carried out by the vapour phase reaction of aldehydes, ketones and alcohols with ammonia over acidic zeolites, especially H-ZSM-5, promoted occasionally with heavy metal ions such as lead or zinc [134-138]. The synthesis of pyridine bases from various aldehydes or ketones with ammonia is tabulated in table 1.5 [139].

1.12.4. Pyrazine and alkylpyrazines

Pyrazine and alkylpyrazines are used in flavors, fragrances and pharmaceutical intermediates. Among them, 2-methylpyrazine is used as a raw material of anti-tuberculosis drug, i.e. pyrazinamide. Okada found, for the first time, that pyrazine compounds can be produced by the catalytic reaction of diamines with diols in a vapor-phase reaction in the presence of granular alumina [140]. Catalytic systems such as copper-chromium [141], copper-zinc-chromium [142], zinc-phosphoric acid-manganese [143] and

silver [144] are also patented as catalysts for preparation of 2-methylpyrazine (2-MP) from ethylene diamine (ED) and propylene glycol (PG).
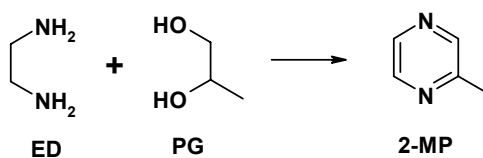
The table 1.6 shows some of the commercialized product for the production of pyrazine and alkylpyrazines.

Apart from patented literature, the optimum conditions for vapor-phase condensation of ED and PG over $MnSO_4$-H_3PO_4-ZnO to give 2-MP was reported [149]. The catalytic behavior of the Pd-promoted ZnO-$ZnCr_2O_4$ mixture for the above said reaction was studied by Forni et al. [150]. However, there are very few reports on the synthesis of 2-MP over zeolite catalysts. Kulkarni et al.[151] reported its synthesis over ZSM-5.
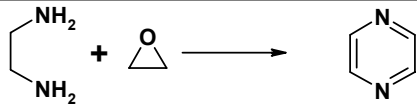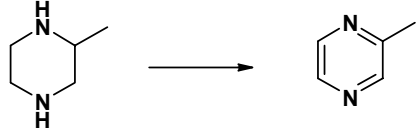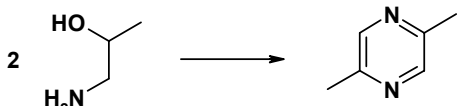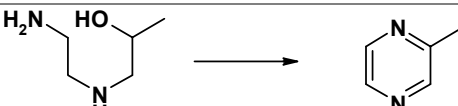
1.12.4.1 Formation of bicyclic compounds

Analogous to cyclic ethers, cyclic or bicyclic amines can be prepared from corresponding educts by elimination of H_2O or NH_3. Thus 1,4-diazabicyclo[2.2.2]octane (DABCO) has been prepared from precursors such as N-hydroxylethyl- and N-aminoethylpiperazine by interamolecular nucleophilic substitution. The industrially used catalysts are silica, alumina or tungsten catalyst. Due to severe reaction conditions (T ≥ 400°C), cracking and condensation reaction of the reactants take place resulting in lower yields of DABCO. Also wide variety of undesired products like piperazines, N-alkylpiperazines and pyrazine derivatives lead to expensive purification of DABCO via distillation or fractional crystallization.

Table 1.5: Synthesis of pyridine bases from aldehydes or ketones with ammonia [139]

Material	Product
Acetaldehyde	2-Metylpyridine, 4-methylpyridin
Acetoaldehyde, formaldehyde	Pyridine, 3-methylpyridine
Acrolein	3-Methylpyridine
Acrolein, acetaldehyde	Pyridine
Acetone, formaldehyde	2,6-Dimethylpyridine
Acrolein, propionaldehyde	3-Methylpyridine
Acrolein, acetone	2-Methylpyridine
Propionaldehyde, formaldehyde	3,5-Dimethylpyridine

Table 1.6: Commercialized product for the production of pyrazine and alkylpyrazines

Reactions	Company	Catalysts	Ref.
	Koei Chemical Co.	$Cu-Cr_2O_3$	[145]
	BASF A.-G.	$Pd-MgCl_2-Al_2O_3$	[146]
	Wyandotte Chemical Co.	$Cu-Cr_2O_3$	[147]
	Hasegawa T. Co.	$Cu-Cr_2O_3$	[148]

Zeolites give higher selectivities than existing industrial catalysts in the synthesis of DABCO. It is reported that high-silica zeolite [152] with Si/Al = 33-55, such as ZSM-5, ZSM-11, ZSM-12 or USY zeolite provide increased selectivities when the reaction is carried out between 250-550°C and at pressure between 0.5-2 atm in the vapor phase and contact time between ca. 0.2 and 3sec. At 400°C 10% conversion and 87% selectivity are

obtained [152] over H-ZSM-5 (Si/Al 35-55). Conventional catalysts, e.g. alumina, are more active but less selective leading to difficulty separable byproducts. When using a high silica zeolite, the only byproduct is piperazine. It is also possible [153] to use ethanolamine as the starting material for DABCO. At 400°C and WHSV 10h^{-1} a 64% yield of DABCO is claimed using ZSM-5 catalyst.

1.12.5. Alkylation of aromatic amines

Alkylation is an electrophilic substitution reaction. The electrophile i.e., the carbonium ion is formed from the alkylating agent viz., olefins, alcohol or alkyl halide with the help of the acid sites on the catalyst surface. The solid acids, because of the presence of both Lewis and Brönsted acid sites, function successfully as alkylation catalysts. The alkylation of aromatic amines includes the reaction of aniline with methanol [154,155], olefins [156-158] and dimethyl carbonate [159-161] in the presence of zeolitic and nonzeolitic molecular sieves. In principle, the reaction can take place at the N-containing groups forming N-alkylated compounds or at the nucleus forming C-alkylated compounds. The alkylation of aniline by acid catalysts is difficult, due to high basicity of aniline. Zeolites as Brönsted acids are effective catalysts for aniline alkylation with methanol [6]. At 275°C, 100% N-alkylation occurs, yielding N-methylaniline and N,N-dimethylaniline. At 450°C, C-alkylated toluidine is produced with only 0.3% N-methylaniline. The toluidines contain mostly the para isomer at short contact time, but reach thermodynamic equilibrium at longer time, with the meta isomer as the major component. All these products are useful intermediates for dyestuffs, agrochemicals and drugs as well as for the organic synthesis. Methylation of aniline over zeolites HY and H-ZSM-5 generally gives mixture of N- and C-methylated products [154]. Ione et al. [162] demonstrated that product composition obtained over ZSM-5 is strongly affected by the reaction temperature. Within the C-alkylate the regioselectivity depends on temperature, WHSV and on zeolite chemical

composition. Narayanan et al. [163] recently reviewed aniline alkylation over various solid acid catalysts. However, there are very few reports on the alkylation of o-toluidine. V_2O_5 [164], $V_2O_5 - Cr_2O_3 - Al_2O_3$ [165] and γ-alumina supported V_2O_5 [166] were reported as catalysts for this reaction recently.

1.12.6. Isomerization of aromatics containing functional groups

The isomerization of substituted aromatics over zeolites is the best example of the shape selectivity of zeolites and is of industrial interest [167]. The isomerization of xylenes is one of the most important examples of this and was carried out on a large industrial scale using zeolite as catalysts. The principle of the xylenes isomerization is applicable to a number of toluene derivatives carrying functional groups such as hydroxyl, amino, nitrilo and halogen. The excellent isomerization capacity of pentasil zeolites is also applicable to aromatic compounds bearing N-containing substituents such as toluidines [168-172]. As shown, e.g. by Weigert [171,172], zeolites of the ZSM-5 type are particularly suited for such equilibrations. The highly acidic H-ZSM-5 is able to protonate the aromatic nucleus, to form the intermediate carbenium ion, also when strongly deactivating groups as cyano are present. Thus a contact time of 3s at 500°C suffices [172] to establish the three-component equilibrium of 46% ortho-, 34% meta- and 20% para-toluinitrile over H-ZSM-5. A zirconium-MFI-containing zeolites is able to isomerize o- and/or p-toluidine into mixtures of the o-, m- and p- isomers and is superior to the H-ZSM-5 catalyst in terms of both product yield and catalyst lifetime [168]. At 430°C o-toluidine is converted on the zirconium zeolite to an o-, m- and p- mixture in a weight ratio of 37:45:15. Aniline can be used as a diluent [173]. In contrast to the isomerization of xylenes, this toluidine isomerization does not yield preferentially the para- but the meta- isomer [5,101].

1.13. OBJECTIVES OF THE PRESENT INVESTIGATION

The objectives of the present work are:

- To synthesize medium pore zeolites (ZSM-5 and FER) and wide or large pore zeolite (Beta).

- To modify ZSM-5 with zinc by various techniques like wet impregnation and ion exchange.

- To modify FER, Beta, MOR with zinc by wet impregnation method.

- To characterize these modified samples in detail using various techniques and tools such as X-ray diffraction, X-ray Fluorescence, EDX, elemental analysis, XPS, NH_3-TPD, FT-IR, and N_2 adsorption measurements.

- To evaluate catalytic activity of FER samples in the synthesis of pyridine bases and Beckmann rearrangement of cyclohexanone oxime to ε-caprolactum.

- To evaluate zinc modified ZSM-5 samples in the synthesis of alkyl pyrazine and to compare them with the catalytic activity of zinc modified FER, MOR and Beta samples.

- To study the catalytic activity of H-form of medium (FER and ZSM-5) and wide/large pore zeolites (HY, H-Beta and H-MOR) in the synthesis of a bicyclic amine (DABCO), alkylation of aromatic amine (*o*-toluidine) and isomerization of *o*-toluidine.

The thesis has been divided into five chapters.

Chapter I presents the general introduction on fine chemicals and zeolites. It also summarizes the available literature on the zeolites involved in synthesis of some important nitrogen containing heterocycles and acid catalyzed reactions of aromatic amines. It also briefs the characterization techniques used in the characterization of zeolites and the objectives of the present work.

Chapter II describes the synthesis of medium pore (FER and ZSM-5) and wide pore (Beta) zeolites and their post-synthesis modification with zinc. It also gives an account of the physico-chemical characterization of the above-mentioned zeolites by various methods especially employing both NH_3-TPD and pyridine FT-IR techniques for determining acidity of these zeolites.

Chapter III deals with the synthesis of nitrogen containing heterocycles and is divided in to two sections.

Section one deals with the catalysis over FER zeolite in which vapor-phase Beckmann rearrange of cyclohexanone oxime to ε-Caprolactam and liquid phase synthesis of pyridine bases were evaluated.

Section two deals with the catalysis over zinc-modified zeolites in which catalytic activity of the zinc modified ZSM-5 samples in the synthesis of methyl- and ethyl-pyrazine were evaluated. Also the results were compared with those of zinc modified FER, Beta and MOR samples.

Chapter IV deals with the synthesis of amines over H-zeolites. In particular, synthesis of a bicyclic amine, DABCO, Isomerization of *ortho*-toluidine and methylation of *ortho*-toluidine were evaluated over these zeolites.

Finally, in **Chapter** V, a summary of the results obtained and the conclusions drawn are presented.

1.14. REFERENCES

1.   W.F. Hoelderich, *Stud. Surf. Sci. Catal.,* **75** (1993) 127.
2.   W.F. Hoelderich *Catalysis Today,* **62** (2000) 115.
3.   R.A. Sheldon, *Chem. Rev.,* **9**(5), (2000) 10.
4.   R.A. Sheldon, *Pure Appl. Chem.,* **72**(7), (2000) 1233.
5.   P.B. Venuto, P.S. Landis, *Adv. Catal.,* **18** (1968) 259.
6.   P.B. Venuto *Micropor. Mater.,* **2** (1994) 297.

7. M.E. Davis, *Ind. Eng. Chem. Res.,* **30** (1991) 1675.

8. M.E. Davis, R.F. Lobo, *Chem. Mater.,* **4** (1992) 756.

9. P.B. Weisz, V.J. Frilette, R.W. Mastman, E.B. Mower, *J. Catal.,* **1** (1962) 307.

10. W.F. Hoelderich in: M. Guisnet, J. Barrault, C. Bouchoule, D. Duprez, C. Montassier, G. Perot (Eds.), *Stud. Surf. Sci. Catal.*, **41** (1988) 83.

11. W.F. Hoelderich, M. Hesse, F. Naumann, *Angew. Chem. Int. Ed. Engl.,* **27** (1988) 226.

12. W.F. Holderich in: K. Tanabe, H. Hattori, T. Yamaguchi, T. Tanaka (Eds.), *Acid-Base Catalysis*, Kodansha, Tokyo, 1988, pp. l-20.

13. G. Perot, M. Guisnet, *J. Mol. Catal.,* **61** (1990) 173.

14. IC. Smith, *Bull. Sot. Chim. Fr.,* **2** (1989) 272.

15. R.F. Parton, J.M. Jacobs, D.R. Huybrechts, P.A. Jacobs, *Stud. Surf. Sci. Catal.,***46** (1988) 163.

16. W.F. Hoelderich, H. van Bekkum, *Stud. Surf. Sci. Catal.,* **58** (1991) 631.

17. W.F. Hoelderich, *Proc. 1st Tokyo Conf Adv. Catal. Sci.Technol.*, 1990, pp. 31-46.

18. Y. Ono, *Stud. Surf. Sci. Catal.*, **5** (1980) 19.

19. H. van Bekkum, H.W. Kouwenhoven, *Stud Surf Sci. Catal.*, **41** (1988) 45.

20. A.F. Cronstedt, *Kongl Vetenskaps Acad. Handl. Stockholm,* **17** (1756) 120.

21. D.W. Breck, *Zeolite Molecular Sieves: Structure, Chemistry and Use*, John Wiley, London, (1974).

22. W.M. Meier, *Molecular Sieves*, Society for Chemical Industry, London, 10 (1968).

23. W. M. Meier, D. H. Olson, *Atlas of Zeolite Structure Types*, 3rd edn., Butterworths, (1992).

24. R.M. Barrer, *Hydrothermal Chemistry of Zeolites*, Academic Press, New York (1982).

25. W. Loewenstein, *Am. Mineral.*, **39** (1954) 92.

26. E. M. Flanigen, *Proc.of 5th Int. Zeol. Conf.*, Ed. L.V. C. Rees, Heydon London, June 2-6, (1980) P 760.

27. W. L. Bragg, *The Atomic Structure of Minerals*, Cornell University Press, Ithaka, New York (1937).

28. S.T. Wilson, B.M. Lok, C.A. Messina, T.R. Cannan, E. M Flanigen, *J. Am. Chem. Soc.,* **104**(4) (1982)1146.

29. M.E. Davis C. Saldarriaga, C. Montes, J. Garces, C. Crowder, *Nature,* **331** (1988) 698.

30. M. Estermann, L.B. McCusker, C. Baerlocher, A. Merrouche, H. Kessler, *Nature*, **352** (1991) 320.

31. B.M. Lok, C.A. Messina, R.L. Patton, R.T. Gajek, T.R. Cannan, E.M. Flanigen, *J. Am. Chem. Soc.,* **106**(20) (1984) 6092.

32. E.M. Flanigen, B.M.T. Lok, R.L. Patton, S.T. Wilson, US 4738837 (1988).

33. E.M. Flanigen, B.M.T. Lok, B.K. Marcus, C.A. Messina, CA 1242180 (1988).

34. W.M. Meier, D.H. Olson, C.H. Baerlocher, *Atlas of zeolite structure types* (1996) 4th revised edition, Elsevier, London.

35. R. M. Barrer, P. J. Denny, *J. Chem. Soc.,* 971 (1961).

36. A. Kuperman, S. Nadimi, S. Oliver, G. A. Ozin, J. M. Garcés, M.M. Olken, *Nature,* **365** (1993) 239.

37. Q. Huo, S. Feng, R. Xu, *J. Chem. Soc. Chem. Commun.,*(10) (1988) 1486.

38. Q. Huo, R. Xu, *J. Chem. Soc., Chem.Commun.,* (22) (1990) 783

39. W. A Van Erp, H. W. Kouwenhoven, J. M. Nanne, *Zeolites*, **7** (1987) 286.

40. J. L. Guth, H. Kessler, R. Wey, *Proc. 7th Int. Zeolite Conf.* Tokyo, 121 (1986).

41. Y. Long, H. He, P. Zheng, G. Wu, B. Wang, *J. Inclusion Phenomena,* **5**, (1987) 355.

42. T.R. Goldsmith, *Min. Mag.,* **29** (1952) 952.

43. R. M Barrer, in *Proceedings of the 6th International Zeoilte Conference.* Butterworth, Guildford, Olson D, Bisio A (eds) (1984) pp 870-886.

44. N.Y. Chen, S.M. McCullen, EP 3,25,053 (1989).

45. M.A. Camblor, A. Corma, J. Perez-Pariente, *Zeolites,* **13** (1993) 82.

46. M. Taramasso, G. Perego, B. Notari. US Pat 4410401 (1983).

47. J.M. Popa, J.L. Guth, H. Kessler, EP 292363 (1988).

48. B. Kraushaar, J.H.C. Van Hooff, *Catal. Lett.,* **1**(4), (1988) 81.

49. K. Becker, H. John, K. Steinburg, M. Weber, K. Nestler, "*Catalysis on Zeolites*'' (D. Kallo., Kh. M. Minachev, Eds.), Akademia Kiado, Budapest (1988) 515.

50. C. Naccache, Y. Ben Tarrit, "*Zeolite Science and Technology*", (F. R. Riberio, A.E. Rodrigues, L.D. Rollmann, E. Naccache, Eds.) Martinus Nijhoff, The Haque (1984) 373.

51. A.N. Kotasthane, V.P.Shiralkar, S.G. Hegde, S.B. Kulkarni, *Zeolites,* **6** (1986) 233.

52. G.N. Rao, V.P. Shiralkar, A.N. Kotasthane, P. Ratnasamy, *Molecular Sieves; Synthesis of Microporous Materials,* Vol 1, Ed. M.L. Occelli and H.E. Robson, Van Nostrand Reinhold-New York.

53. Kh. M Minachev, V.V. Khariamov, V.I. Garanin, "*Catalysis on Zeolites*" (D. Kallo., Kh. M. Minachev, Eds.), Akademia Kiado, Budapest (1988) 489.

54. G. Pergo, G. Bellusi, C. Corono, M. Taramasso, F. Buonomo, *Stud. Surf. Sci. Catal.,* **28** (1986)129.

55. T. Sen, M. Chatterjee, S. Sivasanker, *JCS Chem. Commun.,* (1995) 207.

56.   A. Tuel *Zeolites,* **15** (1995) 236.

57.   J. Kornatowki, M. Sychev, V. Goncharuk, W.-H. Bauer, *Stud. Surf. Sci. Catal.,* **65** (1991) 581.

58.   K.R. Reddy, A.V. Ramaswamy, P. Ratnasamy *JCS Chem. Commun.,* (1995) 1613.

59.   M. K.Dongare, P. Singh, P. P. Moghe, P. Ratnasamy, *Zeolites*, **11**(7) (1991) 690.

60.   A. Cremers, *Molecular sieves II*, ACS symp. Series. No. 40, Washington, 179 (1977).

61.   R. T. Obermyer, L. N. Mulay, C. Lo, M. Oskooie-Tabrizi, V.U.S. Rao, *J. Appl. Phys.,* **53**(3, Pt. 2), (1982) 2683.

62.   T.A. Lin, L.H. Schwartz, J.B. Butt, *J. Catal.,* **97**(1), 177-87 (1986).

63.   P. Gallezot, G. Coudurier, M. Primet, B. Imelik, *ACS Symp. Ser.,* **40**(Mol. Sieves-2, Int. Conf., 4th), (1977) 144.

64.   T.I. Koranyi, L. J. M. Van de Ven, W. J. J. Welters, J. W. De Haan, V.H.J. De Beer, R.A Van Santen, *Catal. Lett.,* **17**(1-2), (1993) 105.

65.   D. P. Roelofsen, E. R. J. Wils, H. van Bekkum., *J. Inorg. Nucl. chem.,* **34** (1972) 1437.

66.   G. H. Kuhl., *J. Catal.,* **29** (1973) 270.

67.   G. H. Kuhl, A. E. Schweizer., *J. Catal.,* **38** (1975) 469.

68.   P.A. Jacobs, M. Tielen, J.B. Nagy, G. Debras, E.G. Derouane, Z. Gabelica, in: D.H. Olson, A. Bisio (Eds.), *Proc.6th Int. Zeolite Conf.* Butterworth, Guildford, 1984, p-783.

69.   R. Von Ballmoos, "*Collection of Simulated XRD Powder Patterns for Zeolites*", Butterworths, London (1984).

70.   J. W. Ward in *Zeolite Chemsitry and Catalysis*. J. A Rabob. (ed) Am. Chem. Soc, Mon 171, Washington, DC, (1976) p 118.

71.   H. Foerster in *Spectroscopic And Computational Studes of Supramolecular Systems*, J.E. Davies (ed) Kluver Academic Publishers, dordrecht, The Netherlands, (1992) p 29.

72.   E.M. Flanigen, H.A. Szymanski, H. Khatami. *Adv. Chem Ser.,* **101** (1971) 201.

73.   S. Brunauer, P.H. Emmett, E. Teller *J. Am. Chem. Soc.,* **60** (1938) 309.

74.   -Xin. Li. Hong, J.A. Martens, P.A. Jacobs, "*Innovation in Zeolite Material Sci.*", P. J. Gribit, (Eds.) (1985) 75.

75.   N.J. Tapp, N.B. Milestone, D.M. Bibby, "*Innovation in Zeolite Material Sci.*", P. J. Gribit, (Eds.) (1985) 393.

76.   R.M. Barrer, *Adv. Chem. Ser.,* **102** (1971) 41.

77. R.L. Patton, E.M. Flanigen, L.G. Dowell, D.E. Passoja, *ACS Symp. Ser.,* **40** (1977) 64.

78. E. Brunner, H. Ernst, D. Freude, M. hunger, C.B. Krause., D. Preger, W. Reschetilowski, W. Schwieger, K.H. Bergk., *Zeolites,* **9** (1989) 282.

79. A. Satsuma, Y. Kamiya, Y. Westi, T. Hattori, *Appl. Catal. A,* **194** (2000) 253.

80. B. M. Lok, B. K. Marcus, C. L. Angell, *Zeolites,* **6**(3), (1986) 185.

81. M. Sawa, M. Niwa, Y. Murakami, Y. *Zeolites,* **10**(4), (1990) 307.

82. J. Valyon, Gy. Onyestyak, L.V.C. Rees, *Langmuir,* **16** (2000) 1331.

83. A Martin, U. Wolf, H. Berndt, B. Lucke, *Zeolites,* **13** (1993) 309.

84. H. Sato, *Catal. Rev. –Sci. Eng.,* **39** (1997) 395.

85. C.V. Hidalgo, H. Itoh, T. Hattori, M. Niwa, Y. Murakami, *J. Catal.,* **85** (1984) 362.

86. N.-Y. Topsoe, K. Pedersen, E.G. Derouane, *J. Catal.,* **70** (1981) 41.

87. N.R. Meshram, S.G. Hegde, S.B. Kulkarni, *Zeolites,* **6** (1986) 434.

88. G.L. Woolery, G.H. Kuehl, H.C. Timken, A.W. Chester, J.C. Vartuli, *Zeolites,* **19** (1997) 288.

89. H.G. Karge, *Stud. Surf. Sci. Catal.,* **65** (1991) 133.

90. H.G. Karge, V. Dondur, *J. Phys. Chem.,* **94** (1990) 765.

91. L. Froni, F.P. Vatti, E. Ortoleva, *Micropor. Mater.,* **3** (1995) 367.

92. G. Bagnasco, *J. Catal.,* **159** (1996) 249.

93. A. Alberti *Zeolites,* **19** (1997) 411.

94. J.W. Ward., *J. Catal.,* **18** (1970) 348.

95. P.A. Jacobs, *Catal. Rev. –Sci. Eng.,* **24** (1982) 415.

96. P.O. Fritz, J.H. Lunsford, *J. Catal.,* **118** (1989) 85.

97. J. Datka, M. Boczar and B. Gil, *Langmuir,* **9** (1993) 2496.

98. T. Barzetti, E. Selli, D. Moscotti, L. Forni, *J. Chem. Soc., Faraday Trans.,* **92** (1996) 1401.

99. T.R. Hughes, H.M. White, *J. Phys. Chem.,* **71** (1967) 2192.

100. C.A. Emeis, *J. Catal.,* **141** (1993) 347.

101. Y.I. Isakov, K.M. Minachev, *Russ. Chem. Rev.,* **51** (1982) 1188.

102. W.F. Hoelderich, *Pure Appl. Chem.,* **58** (1986) 1383.

103. Y. Ono in B. Imelik et al. (Editors), *Catalysis by Zeolites*, Elsevier, Amsterdam, 1980, pp. 19-27.

104. D. Barthomeuf, G. Coudurier, J.C. Vedrine, *Mat. Chem. Phys.,* **18** (1988) 553.

105. L.R. Martens, P.J. Grobet, W. J. Vermeiren, P.A. Jacobs, *Stud. Surf. Sci. Catal.,* **28** (1986) 935.

106. L. R. Martens, W. J. Vermeiren, D.R. Huybrechts, P.J. Grobet, P.A. Jacobs in M.J. Phillips, M. Ternan (Editors), *Proc. 9th Int. Congr. Catal. Calgary*, Canada, 1988, Chem. inst. Canada, Ottawa, 1988, Vol 1 pp. 420.

107. P.Sykes, *A Guide book to Mechanism in Organic Chemistry*, John Wiley & Sons, New York, NY, 1986.

108. O. Immel, H.H. Schwarz, G. Starke, W. Swodenk, *Chem.-Ing.-Techn.,* **56** (1984) 612.

109. P.B. Venuto, P.S. Landis, *J. Catal.,* **6** (1966) 245.

110. W.F. Hoelderich, E. Gallei, *Ger. Chem. Eng.,* **8** (1985) 337.

111. W.F. Hoelderich, *Stud. Surf. Sci. Catal.,* **46** (1989) 193.

112. A. Thangaraj, S. Sivasanker P. Ratnasanly, *J. Catal.,* **137** (1992) 252.

113. T. Takahashi, T. Kai and M. Nishi, in J.B. Higgins, R. von Ballmoos, M.M.J. Treacy (Eds.), *9th International Zeolite Conference*, Butterworth- Heinemann, Boston, MA, 1992, FP6 (Abstracts).

114. W.K. Bell and C.D. Chang, EP 056698 (1985).

115. H. Sato, N. Ishii, K. Hirose and S. Nakanlura, *Stud. Surf. Sci. Catal.,* **28** (1986) 755.

116. K.D. Olson, Eur. Pat., 251 168 (1988).

117. A. Aucejo, M.C. Burguet, A. Corma, V. Fornes, *Appl. Catal.,* **22** (1986) 187.

118. W.K. Bell, C.D. Chang, U.S. Pat. 4359 421 (1982).

119. H. Sato, K. Hirose, M. Kitamura and Y. Nakanlura, *Stud. Surf. Sci. Catal.,* **49** (1989) 1213.

120. J. Röseler, G. Heitmann, W.F. Hölderich, *Appl. Catal. A,* **144** (1996) 319.

121. G.P. Heitmann, G. Dahlhoff, W.F. Hölderich, *J. Catal.* **186** (1999) 12.

122. G. Dahlhoff, G.P. Heitmann, J.P.M. Niederer, W.F. Hölderich, *J. Catal.,* **194** (2000) 122.

123. L. Dai, K. Koyama, M. Miyamoto, T. Tatsumi, *Appl. Catal. A,* **189** (1999) 237.

124. H.G. Franck, J.W. Stadelhofer, *Industrial Aromatic Chemistry*, Springer, Berlin, 1988.

125. K. Weissermel, H.-J. Arpe, *Industrial Organic Chemistry*, VCH, Weinheim, 1992.

126. S. Shimizu, N. Watanabe, T. Kataoka, T. Shoji, N. Abe, S. Morishita, H. Ichimura, in: B. Elvers, S. Hawkins, S. Russey, G. Schulz (Eds.), *Ullmann's Encyclopedia of Industrial Chemistry*, vol. A22, VCH, Weinheim, 1993, p. 399.

127. *Kirk-Othmer Encycl. Chem. Technol.,* 3rd edit vo1.19, 1983, p.454; D.M. Smith. *Rodd's Chemistry of Carbon Compounds*, Elsevier (New York) (1976) p.30.

128. T.D. Bailey, G.L. Goe, E.F.V. Striven, *Chem. Heterocycl. Compd.,* vol.14 suppl. (5), (1984) p.1.

129. D.M. Smith. *Rodd's Chemistry of Carbon Compounds*, Elsevier (New York) (1976) p.30.

130. Y. Kusunoki, H. Okazaki, (a) *Hydrocarbon Process,* **53**(11) (b) Shokubai, **18** (1976) 26.

131. N.S. Boodman, *Chem. Heterocycl. Compd.* (New York), **14**(l), (1974) 183.

132. A. Nenz, M. Pieroni, *Hydrocarbon Process*, (a) **47**(11),(1968)139, (b) **47**(12) (1968) 103.

133. D.J. Berry, *Spec. Chem.,* **3** (1983) 13

134. S.E. Golunski, D. Jackson, *Appl. Catal.,* **23**, (1986) 1.

135. A.V. Rama Rao, S.J. Kulkarni, R. Ramachandra Rao, M. Subrahmanyam, *Appl. Catal. A* **111** (1994) L101.

136. S.J. Kulkarni, R. Ramachandra Rao, M. Subrahmanyam, A.V. Rama Rao, *Appl. Catal. A* **113** (1994) 1.

137. H. Sato, S. Shimizu, N. Abe, K.-i. Hirose, *Stud. Surf. Sci. Catal.,* **84** (1994) 1951.

138. S.J. Kulkarni, R. Ramachandra Rao, Y.V. Subba Rao, M. Subrahmanyam, A.V. Rama Rao, *Appl. Catal. A,* **136** (1996) L1.

139. Y. S. Higasio, T. Shoji *Appl. Catal. A,* **221** (2001) 197–207.

140. J. Okada, Japan 49,25,947 (1974).

141. Koei Chemical Co., Japan 53,43512 (1978).

142. Korea Research Institute of Chemical Technology, Japan 05,52829 (1993).

143. Tokai Electro-Chemical Co., Japan 55,50024 (1980).

144. Koei Chemical Co., Japan 09,48763 (1997).

145. Koei Chemical Co., Japan 49,101391 (1974).

146. BASF A.-G., Japan 05,35140 (1993).

147. Wyandotte Chemical Co., US 2,813,869 (1957).

148. T. Hasegawa Co., Japan 55,45610 (1980).

149. G. T.Fedolyak, L. A. Krichevskii, A. D. Kagarlitskii, *Izv. Akad. Nauk Kaz. SSR, Ser. Khim.,* **5** (1989) 50.

150. L. Forni, S. Nestori, *Stud. Surf. Sci. Catal.,* **41** (1988) 291.

151. S. J. Kulkarni, M. Subrahmanyam, A. V. Rama Rao*, Indian J. Chem., Sect. A:* **32A**(1) (1993) 28.

152. R.A. Budnik, M.R. Sandner, EP 158139 (1989).

153. H. Sato, M. Tsuzuki, Int. Appl. WO 8703592 (1987).

154. P.Y. Chen, M.C. Chen, H.Y. Chu, N.S. Chang, T.K. Chuang, *Stud. Surf. Sci. Catal.,* **28** (1986) 739.

155. H. Sato, M. Tsuzuki, IP 62,195,350 (1986).

156. D.D. Dixon, EP 226,781 (1986).

157. R. Agarwal, S. Auvil, M. Deeba, EP 240,018 (1987).

158. R. Pierantozzi, EP 245,797 (1987).

159. Z. Fu, Y. Ono, *Catal. Lett.,* **22** (1993) 277.

160 P.R.H.P. Rao, P. Massiani, *Catal. Lett.,* **31** (1995) 115.

161. S. Yuvaraj, V.V. Balasubramanian, M. Palanichamy, *Appl. Catal. A:* **176** (1999) 111.

162. K.G. Ione and O.V. Kikhtyanin, *Stud. Surf. Sci. Catal.,* **49** (1989) 1073.

163. S. Narayanan, K. Deshpande *Appl. Catal. A,* **199** (2000) 1.

164. X. Zhang, L. Chen, W. Dong, *Shiyou Huagong,* **29**(2), (2000) 93.

165. L. Chen, X. Zhang, W. Dong, H. Chen, *Jingxi Huagong,* **17**(1), (2000) 19.

166. L. Chen, X. Zhang, L. Yu, *Ranliao Gongye,* **36**(1), (1999) 35-37,40.

167. J.A. Martens, M. Tielen, P.A. Jacobs, J. Weitkamp, *Zeolites*, **4** (1984) 98.

168. K. Eichler, E. Leupold, H.J. Arpe, H. Balter, DE 3420707 (1985).

169. H.J. Arpe, H. Litterer EP 092,103 (1983).

170. F. J. Weigert, U.S. 4,593,124 (1986).

171. F. J. Weigert, *J. Org. Chem.,* **52** (1987) 3296.

172. F. J. Weigert, *J. Org. Chem.,* **51** (1986) 2653.

173. R.H. Hardy, H. Burton. *J. Catal.,* **111** (1988) 146.

Chapter –2

Experimental
&
Characterization

2.1.INTRODUCTION

The range of catalytic transformations has grown steadily in the past two decades as experimental modifications of zeolites were explored. It has been found that adjusting the strength of the acid sites, doping the structure with other metals, and changing the "pore" sizes lead to a wide variety of possible reactions that are performed everyday in organic synthesis. The use of zeolites, due to their small pore size are not ideal for use on most natural synthetic targets, but led to important advances in areas of industry for intermediate chemicals [1]. The scope of reactions that zeolites can catalyze is very broad. Zeolites are now widely used in the petrochemical industry, selective synthesis of chemical intermediates, and numerous other industrial processes such as the MTG (methanol to gasoline) process etc., [2].

Zeolites occur in nature and have been known for almost 250 years as alumino-silicate minerals. Examples are clinoptilolite, mordenite, offretite, ferrierite, erionite and chabazite. Today, most of these and many other zeolites are of great interest in heterogeneous catalysis, yet their naturally occurring forms are of limited value as catalysts because nature has not optimized their properties for catalytic applications and the naturally occurring zeolites almost always contain undesired impurity phases.

Zeolites and other porous materials need to be characterized to elucidate their structural features, pore architecture and catalytic behaviour. A complete characterization of molecular sieves requires information from a number of physical, chemical and spectroscopic techniques. The insight into catalytic processes can be achieved through spectroscopic analysis of the interactions of probe molecules with active sites.

In this chapter, the procedures adopted for the preparation of the various zeolites such as ZSM-5, FER and Beta are described. These zeolites were modified with zinc by impregnation. Zeolite ZSM-5 has also been modified with zinc cation by ion exchange.

Commercially obtained MOR and Y zeolites have been converted to their protonic forms and MOR zeolite has also been impregnated with zinc. FER zeolite was modified by steaming/dealumination. The various methods used in the characterization of these samples and their physicochemical characteristics are presented. Detailed characterization of the acidity of the zeolite samples has been carried out by TPD of ammonia and FTIR of adsorbed pyridine.

2.2. PREPARATION OF CATALYSTS

2.2.1. Medium pore Zeolites

2.2.1.1. ZSM-5 Zeolite

ZSM-5 is a synthetic high-silica zeolite first reported by Argauer and Landolt [3]. The MFI- type topology shows a three-dimensional 10-membered channel system. A large number of patents and publications are available on its synthesis [4]. The first syntheses were performed in the presence of Na^+ and organic additives. About 25 organic species were claimed to be useful [5], among which the tetrapropylammonium cations are the most structure directing. Indeed, ZSM-5 is easily synthesized with this template in a very broad range of experimental conditions. The organic-free synthesis in the presence of Na^+ cations has also been reported [6-8].

2.2.1.2. Synthesis of zeolite H-ZSM-5

Synthesis of ZSM-5 was carried out according to the published procedure [3] using a molar gel composition of

$$2(TPA)_2O.\ 11.8\ Na_2O.\ Al_2O_3.\ 250\ SiO_2.\ 3200\ H_2O$$

The gel was stirred vigorously for 2h and autoclaved in a 300 ml stainless steel Parr autoclave (4842, 300 ml) and heated at $180\pm5°C$ for 96h. The autoclave was quenched, filtered, washed and product was dried at $100°C$ for 6-8 h. The resulting material was calcined in air at $550°C$ for 18-20 h.

framework viewed along [010]

10-ring viewed along [100]

10-ring viewed along [010]

Channels: {[100] **10** 5.1 x 5.5 ↔[010] **10** 5.3 x 5.6}
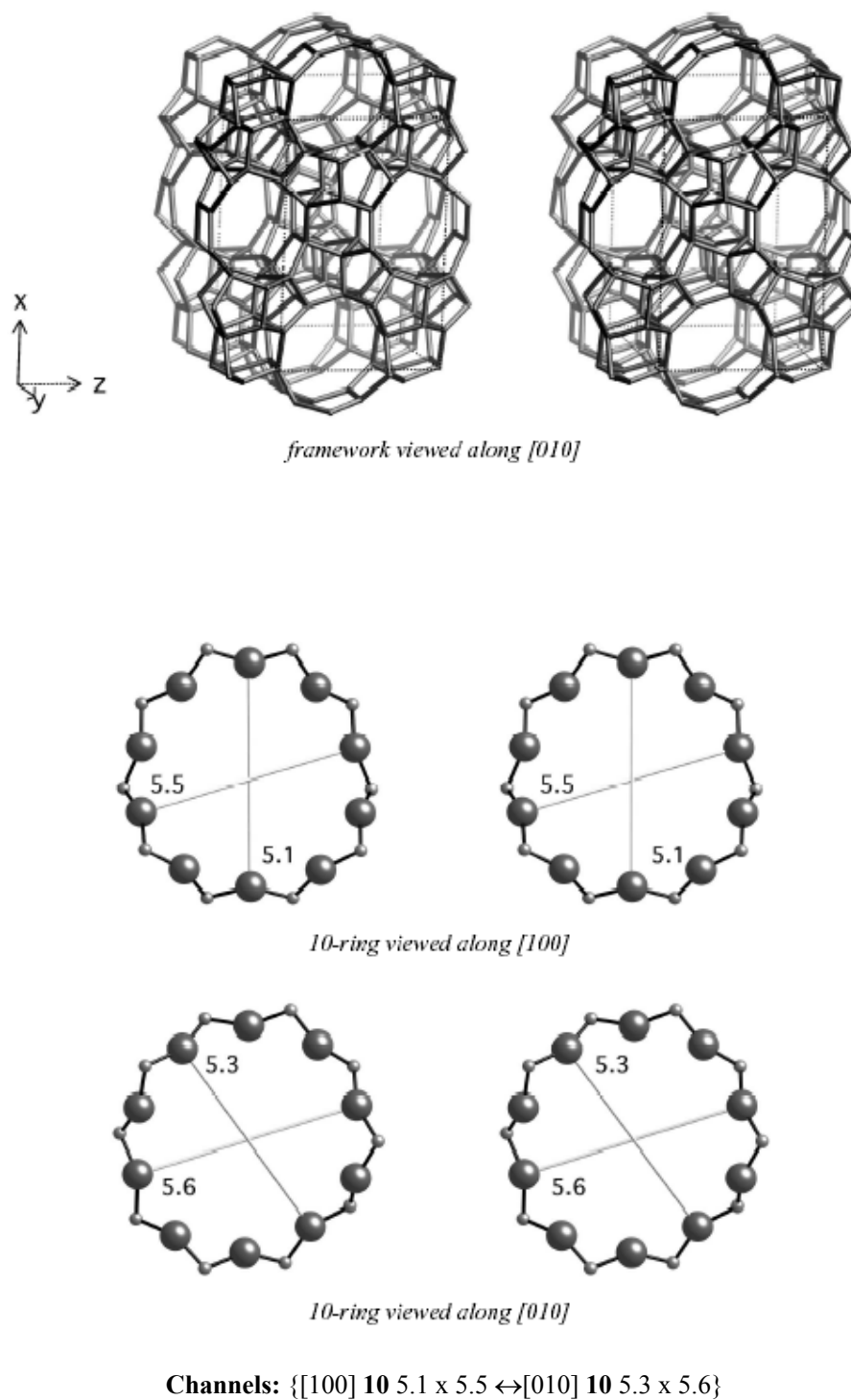
Figure 2.1:. Framework structure of zeolite ZSM-5 [9]

42

2.2.1.3. Ferrierite Zeolite

Ferrierite (FER) is a natural zeolite mineral, which occurs near Kamloops Lakes, British Columbia. Staples [10] in 1955 reported the unit cell composition as

$$(Na,K)_4 \, Mg_2 \, (Si_{30}Al_6)O_{72} \, (OH)_2. \, 18H_2O$$
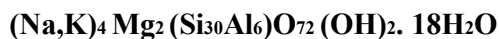
Vaughan [11] and Kerr [12] solved its crystal structure. Breck [13] classified ferrierite zeolite along with mordenite, dachiardite, epistilbite and bikatite. More than a decade ago Kibby et al. [14] reported synthesis of ferrierite using quaternary ammonium cations namely tetramethyl ammonium hydroxide. Since then a number of N- containing molecules and also oxygenated hydrocarbons have been used in FER synthesis. Gies and Gunawardane [15] first synthesized the siliceous form of ferrierite from aqueous medium. On the contrary a non aqueous route in presence of fluoride ions has been reported by Kuperman et al.[16].

2.2.1.4. Synthesis of zeolite H-FER

In a typical synthesis [17], 52.5g of sodium silicate (in 25ml of distilled water) was stirred with 10ml pyrrolidine. To this solution, 2.4g of aluminum sulphate hexadecahydrate (in 25ml distilled water) and 1.8g of sulphuric acid (in 10 ml distilled water) was added. Finally, 30ml of distilled water was added and the gel (pH 11.5 ± 0.2) was stirred vigorously for 2h and autoclaved in a 300 ml stainless steel Parr autoclave (4842, 300 ml) and heated at 160°C for 60 h. The initial gel composition was:
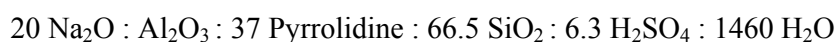
$$20 \, Na_2O : Al_2O_3 : 37 \, Pyrrolidine : 66.5 \, SiO_2 : 6.3 \, H_2SO_4 : 1460 \, H_2O$$

The autoclave was quenched, filtered, washed and product was dried at 100°C for 6-8 h. The resulting material was calcined in air at 550°C for 18-20 h.

Similarly FER with different silica to alumina ratios were synthesized by varying the input ratio of the reactants.

framework viewed along [001]

10-ring viewed along [001]

8-ring viewed along [010]
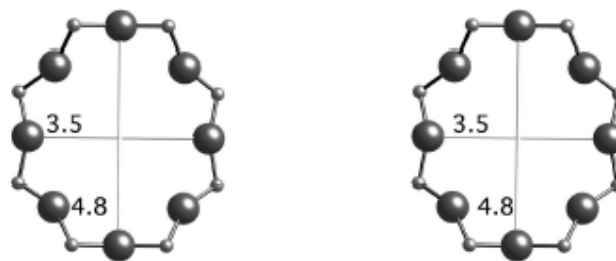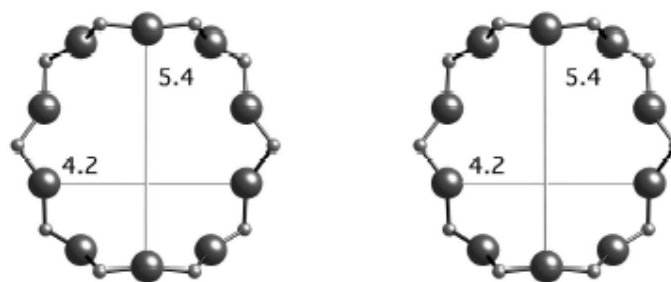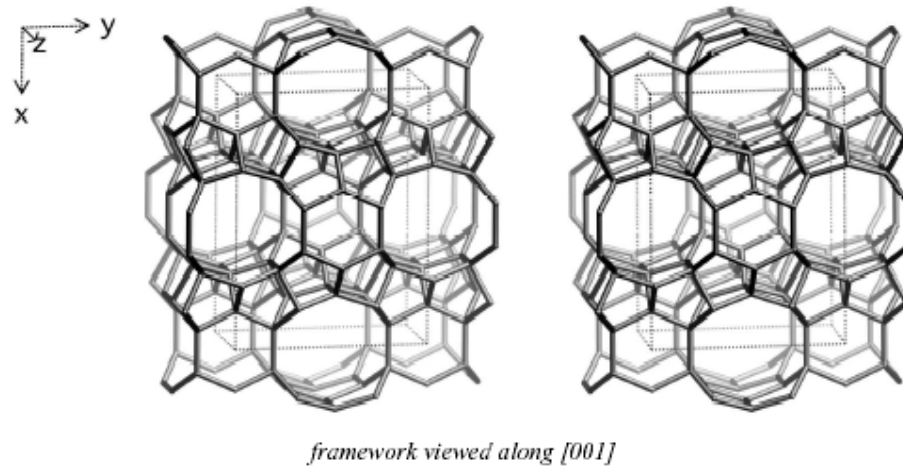
Channels: [001] **10** 4.2 x 5.4 ↔[010] **8** 3.5 x 4.8*

Figure 2.2: Framework structure of zeolite Ferrierite [9]

2.2.1.5. Steaming of H-FER

Dealuminated H-FER was prepared by subjecting it to heating in steam at $550° \pm 10°C$ for 2-3 h. This steamed sample was then acid treated by making slurry of the powder in 10% oxalic acid solution at 80-90°C for 2 h. The sample was filtered, repeatedly washed with demineralized water, dried and finally calcined in a flow of air at a temperature of 550°C for 6-8 h.

2.2.2. Large Pore Zeolites

2.2.2.1. Beta Zeolite

Zeolite Beta is a large pore (12-membered ring apertures), high silica zeolite (Si/Al from ca. 10 to 100) which was first synthesized in 1967 [18] from alkaline aluminosilicate gels in the presence of sodium and tetraethylammonium cations. It was also prepared from near neutral aqueous aluminosilicate gels in the presence of fluoride as the mineralizing agent and 1,4-diazabicyclo[2,2,2]octane (DABCO) and methylamine as the organic species [19]. With this route the zeolite obtained is less siliceous (Si/Al = 9-22) than when prepared in alkaline medium with Na^+ and Et_4N^+ cations.

2.2.2.2.Synthesis of BETA

In a typical synthesis [20], 1.42g sodium aluminate, 1.28g sodium hydroxide, 30g TEAOH and 18.18g distilled water were mixed together and stirred vigorously to obtain a homogeneous mixture. The mixture was then added slowly to 31.21g silica sol in a polyethylene beaker and the mixture was stirred vigorously for 1h. The pH of the final gel was 13.8 and the calculated molar composition of the gel was

$$4.5 Na_2O: 7.5\ (TEA)_2O: 30\ SiO_2: Al_2O_3: 593 H_2O$$
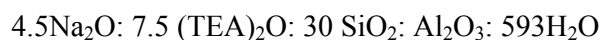
The final gel was transferred to a Teflon lined stainless steel autoclave (capacity 200ml) and hydrothermally treated at 150°C and autogeneous pressure for 7days. After that the autoclave was quenched to room temperature in cold water. The solid material obtained

was filtered, washed with distilled water and dried at 120°C. The occluded organics were burnt off at 500°C for 24h. The protonic form of the zeolite was obtained by repeated exchange with 1M ammonium acetate solution thrice followed by calcination at 500°C for 24h in a flow of dry air.

framework viewed along [010]

12-ring viewed along <100>

12-ring viewed along [001]
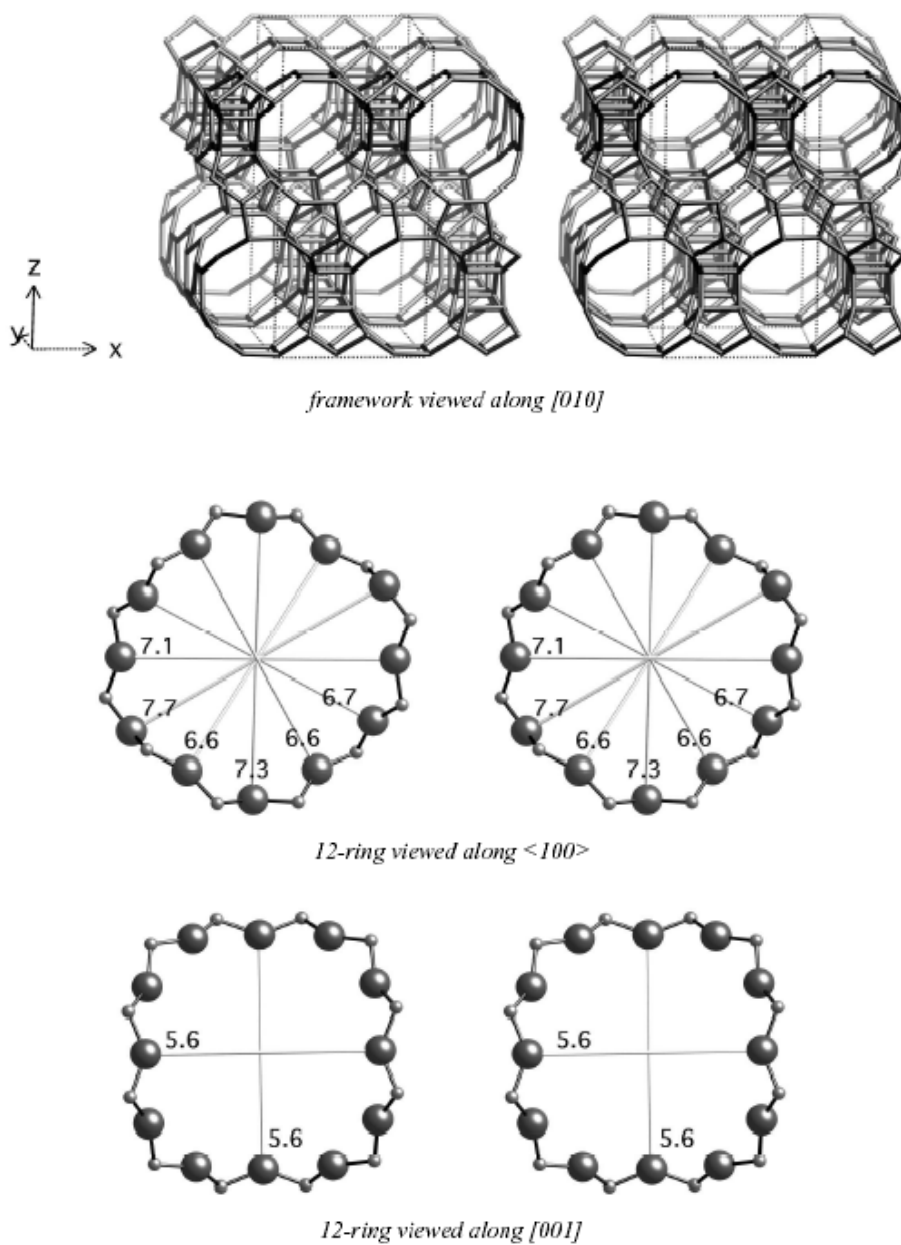
Channels: <100> **12** 6.6 x 6.7 ↔ [001] **12** 5.6 x 5.6

Figure 2.3: Framework structure of zeolite Beta [9]

2.2.2.3. Mordenite (MOR) zeolite

Mordenite is a natural high-silica zeolite whose typical unit cell formula is $Na_8Al_8Si_{40}O_{26} \cdot 24H_2O$. The crystal structure [9] shows a 12-membered ring channel system parallel to c axis (opening 6.5 X 7.0 Å). These channels are interconnected through small side channels parallel to b direction and circumscribed by 8-membered rings (2.6 X 5.7Å). Thus, mordenite can be considered as having an essentially one-dimensional channels system.

The sample of MOR used in this study was obtained from PQ Corporation, The Netherlands. The H-form of the sample was prepared by 3 exchanges of the Na-form with aqueous ammonium acetate solution followed by calcination of the NH_4^+-form at 550°C for 16h in presence of air.

2.2.2.4. Zeolites with FAU-type structures: Zeolite Y

Several material comprising a cubic and hexagonal packing of faujasitic sheets are known. The FAU-type zeolites X [21,22] Y [23] can be obtained from starting mixtures differing essentially in the Si/Al ratio (larger for Y than for X) in the temperature range 20-120°C and 20-175°C [13]. A crystallization temperature around 100°C is preferred.

Zeolite Y consists of linked truncated octahedra called sodalite units, which have a cage of diameter 6.5Å (β cage) and accessible through six membered rings of oxygen atoms [23]. These units are connected along two six membered rings giving rise to hexagonal prism. The polyhedra formed in this way enclosed a super cage (α cage) with an internal diameter of 12.5Å and accessible through four 12-membered rings of oxygen atoms with a free aperture of 7.4Å.

framework viewed along [001]

12-ring viewed along [001]

limiting 8 ring along [001]
between 12-ring channels
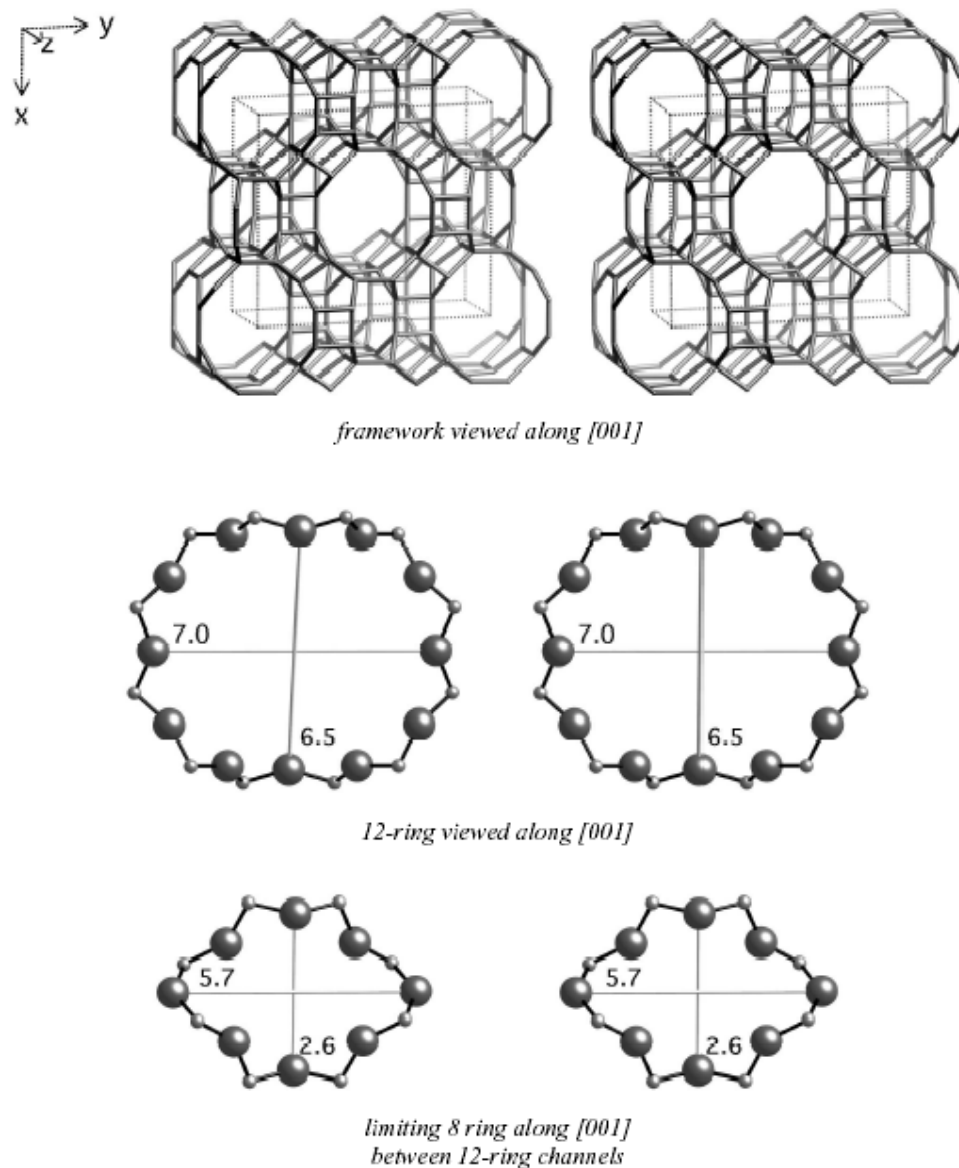
Channels: [001] **12** 6.5 x 7.0 ↔ {[010] **8** 3.4 x 4.8 ↔ [001] **8** 2.6 x 5.7}

Figure 2.4: Framework structure of zeolite Mordenite [9]

The zeolite Y (Na-Y, SK-40) used in this study was obtained commercially from Union Carbide, USA. The H-form of the sample was prepared by 3 exchanges of the Na-form with aqueous ammonium nitrate solution followed by calcination of the NH_4^+-form at 500°C for 24h in presence of air.

framework viewed along [111] (top left: projection down [110])

12-ring viewed along <111>
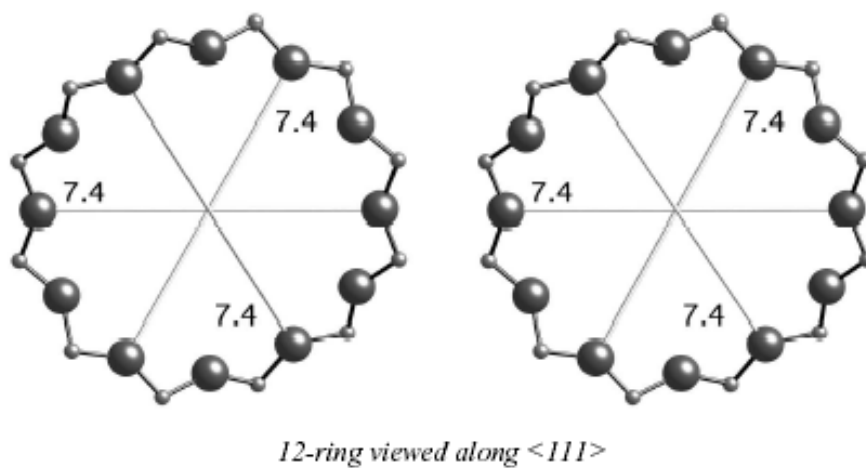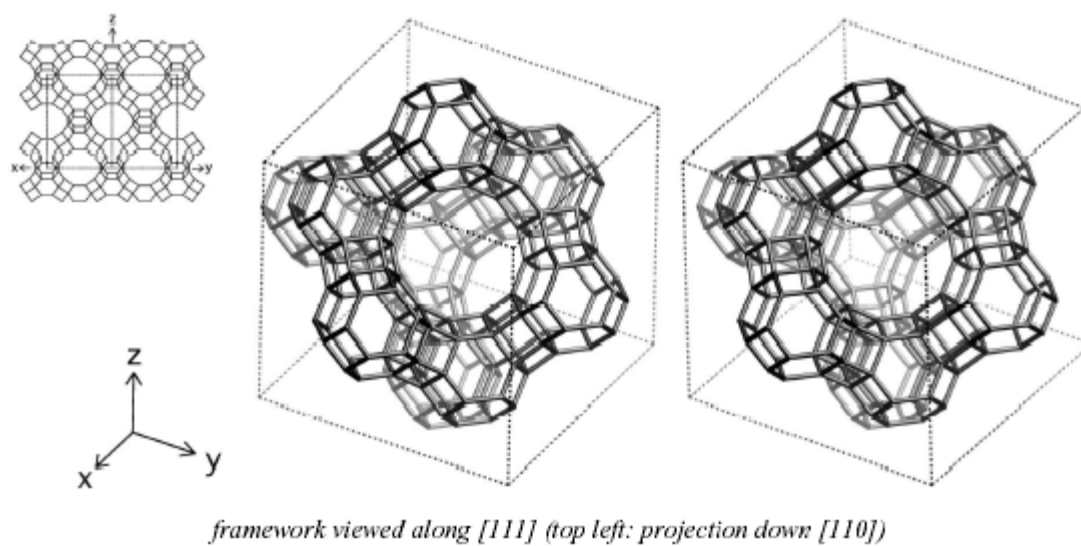
Channels: <111> **12** 7.4 x 7.4

Figure 2.5: Framework structure of zeolite Faujasite [9]

2.2.3. Modification

2.2.3.1. Impregnation

The ZnO-modified catalysts were prepared by mixing hydrogen forms of respective zeolites with zinc acetate (1.35g) in distilled water (100 ml). The mixture was digested at 80°C for 5hrs, dried at 110°C for 3h and calcined at 550°C in the presence of air for 12h. The zeolite ZSM-5 with different amounts of ZnO loading was prepared by mixing appropriate amount of zinc acetate in 100ml of distilled water and digested at 80°C for 5hrs, dried at 110°C for 3h and calcined at 550°C in the presence of air for 12h.

2.2.3.2. Ion exchange

Ion exchange of zeolite ZSM-5 was carried out at 90°C using 0.5M zinc acetate solution for 16h. The ion exchanged zeolite was washed with deionised water and dried over night at 110°C and calcined at 550°C in the presence of air for 12h. The preparation of various zinc modified catalysts and the preparation conditions are detailed in table 2.1.

Table 2.1: Conditions of catalyst preparation

Materials	Preparation Conditions
ZnO	Heating of Zinc acetate at 550°C in air for 12h
Zn-ZSM-5	Ion exchange of H-ZSM-5 with 200ml of 0.5M zinc acetate solution for 16h at 90°C, through washing with water to free acetate ions, dried over night at 110°C and calcined in air at 550°C for 12h.
ZnO-ZSM-5	A mixture of H-ZSM-5 and zinc acetate (1.35g) in distilled water (100 ml) was digested at 80°C for 5hrs, dried at 110°C for 3h and calcined at 550°C in the presence of air for 12h.
ZnO-FER	A mixture of H-FER and zinc acetate (1.35g) in distilled water (100 ml) was digested at 80°C for 5hrs, dried at 110°C for 3h and calcined at 550°C in the presence of air for 12h.
ZnO-Beta	A mixture of H-Beta and zinc acetate (1.35g) in distilled water (100 ml) was digested at 80°C for 5hrs, dried at 110°C for 3h and calcined at 550°C in the presence of air for 12h.
ZnO-MOR	A mixture of H-MOR and zinc acetate (1.35g) in distilled water (100 ml) was digested at 80°C for 5hrs, dried at 110°C for 3h and calcined at 550°C in the presence of air for 12h.

2.3. CHARACTERIZATION

2.3.1. Powder X-ray diffraction (XRD)

The samples prepared and used during the course of the present work were analyzed by X-ray powder diffraction for quantitative and qualitative phase identification. The XRD patterns of the samples were recorded using a computer-automated diffractometer (Model D-MAX III VC, Rigaku, Japan) using a Ni-filter Cu K_α radiation (λ=1.5404Å). Data were collected in the 2θ range of 4-50° at a scan rate of 2°/min with silicon as an internal standard.

2.3.2. Determination of Chemical Composition

The chemical composition of the samples was analyzed by using combination of techniques like, atomic absorption spectroscopy (AAS, the procedure detailed in chapter 1), X-ray fluorescence spectroscopy (XRF) and energy-dispersive x-ray analyzer (EDX) depending up on the nature of the sample.

2.3.2.1. X-ray Fluorescence Spectroscopy

Wavelength dispersive X-ray fluorescence spectrometer (Rigaku 3070) with rhodium target energized at 45KV and 40MA was used for the experiment. For XRF measurements, borate fusion technique was applied to prepare glassy beads of reference standards and of samples. A calibration curve was made using standards for the analysis of Si and Al. For all analysis, K_α lines were selected and pulses were collected for 40s. Then background correction was applied before getting the results. The sample beads were prepared by fusing the sample in a platinum crucible with appropriate amount of sample, potassium bromide and lithium tetra borate flux by heating to 1200°C. For accurate quantitative analysis, glass beads of standard compositions were made and calibration curve was obtained before analysis of the sample. The composition of the sample with respect to SiO_2/Al_2O_3 and SiO_2/ZnO ratio was calculated.

2.3.2.2. Energy Dispersive X-ray Analysis (EDX)

An energy-dispersive x-ray analyzer (EDX) is a common accessory, which gives the scanning electron microscope (SEM) a very valuable capability for elemental analysis. The electron beam in an SEM has energy typically between 5,000 and 20,000 electron volts (eV). The energy holding electrons in atoms (the binding energy) ranges from a few eV up to many kilovolts. Many of these atomic electrons are dislodged as the incident electrons pass through the specimen, thus ionizing atoms of the specimen. Ejection of an atomic electron by an electron in the beam ionizes the atom, which is then quickly neutralized by other electrons. In the neutralization process an x-ray with an energy characteristic of the parent atom is emitted. By collecting and analyzing the energy of these x-rays, the constituent elements of the specimen can be determined.

2.3.3. Surface Area Measurement

A commercial adsorption apparatus (Ominisorb 100 CX; Coulter Corporation, USA) was employed for the measurement of surface area of the samples. The samples were activated at 400°C for 2h under high vacuum (10^{-6}mm). The anhydrous weight of the sample was measured and the sample was then cooled to 94K using liquid nitrogen and allowed to adsorb nitrogen gas. Finally surface area of the sample was calculated by the BET method [24].

2.3.4. Fourier Transform Infrared Spectroscopy

The potassium bromide (KBr) pellete technique was used to record the FTIR spectra in the region 1300 - 400cm^{-1}. For the preparation of KBr pellets, 300mg of previously dried KBr was mixed thoroughly with 0.5mg of the sample and pressed in to pelletes of 13mm diameter with a pressure of 7tons/inch^{2}. The spectrum was recorded using NICOLET 60 SXB spectrometer with resolution of 2cm^{-1} and averaging over 250 scans [25].

For the nature of the surface hydroxyl groups and the nature of acidity, thin wafers of the samples weighing nearly 5-6mg/cm^2 were made by pressing a thin layer of the sample at a pressure of 7ton/inch^2. The wafer was placed on the sample holder. It was then placed inside the heating compartment of the transmittance cell, which was connected to a high vacuum system. The sample was evacuated to 10^{-6} Torr at 400°C for 3h and then cooled to 100°C before recording the spectrum of the pure sample. Then the sample was allowed to adsorb pyridine at an equilibrium pressure of 20mm of Hg for 30min. The loosely adsorbed and free vapor of pyridine was removed by evacuating the cell for 1h. Then the spectrum was recorded. Thereafter, the sample was further heated to 200, 300 and 400°C successively for 1h at each temperature before recording the spectrum again. The spectrum was recorded with 2cm^{-1} resolution after averaging over 500 scans.

2.3.5. Temperature Programmed Desorption of ammonia

Temperature programmed desorption (TPD) studies were carried out using an Autochem 2910 instrument (Micromeritics, USA). The unit has a programmable furnace with a maximum operating temperature of 1100°C. The instrument was interfaced to a computer which performs tasks such as programmed heating and cooling cycles, continuous data recording, gas valve switching, data storage and analysis. In a typical experiment for TPD studies, about 200 mg of oven-dried sample (dried at 110°C for 16 h) was taken in a U-shaped quartz cell. The catalyst sample was packed in one arm of the sample tube on a quartz wool bed. The temperature was monitored with the aid of thermocouples located near the sample from outside and one on the top of the sample. The gas flows were monitored by highly sensitive mass-flow controllers. Prior to TPD studies, the catalyst was pretreated at 300°C for 1h by passing very pure helium (50ml/min). After pretreatment of the sample, it was saturated by passing (75ml/min) high pure anhydrous ammonia at 80°C and subsequently flushed at 105°C for 2h to remove the physisorbed

ammonia. The sample was then cooled to 50°C and TPD analysis was carried out up to 700°C at a heating rate of 10°C/min. The ammonia concentration in the effluent stream was monitored with the thermal conductivity detector and the area under the peaks were integrated using GRAMS/32 software to determine the amount of ammonia desorbed during TPD.

2.3.6. XPS

X-ray photoelectron spectra (XPS) were recorded in the Vacuum Generator's Microtech ESCALab 3000 spectrometer with Mg Kα x-ray source in a vacuum of $1-3 \times 10^{-9}$ Torr range during the analysis. Energy resolution of the instrument is set to 0.8eV at a pass energy of 20eV. Energy resolution was measured from the full-width at half-maximum (FWHM) of clean gold surface from its $4f_{7/2}$ core level. Accuracy of the binding energy (BE) reported is within ±0.1 eV. Adventitious carbon, appears at a BE of 284.9 eV on clean metal surfaces, was utilized as an internal standard for charge correction for all samples. Photoionization cross section (σ) [26] was used to obtain compositions of the surface and atom ratios from peak areas.

2.4. RESULTS AND DISCUSSIONS

2.4.1. X-ray diffraction (XRD)

The XRD patterns of the zeolite samples ZSM-5, Ferrierite, Beta, Mordenite and Y were all highly crystalline and matched with the reported literature [11,27-30]. There was no change in the peak intensities of the zeolite samples modified with zinc by impregnation. However, at higher loadings of zinc (>5wt%), there was slight decrease in the peak intensity. The XRD figures of the samples are given in figure 2.6(a,b).

2.4.2. Elemental analysis and Surface area

Chemical compositions of the various zeolites used in the work are calculated from combined analytical techniques like XRF, AAS and EDX. The surface area of the samples

was calculated from N_2 sorption isotherms using the BET procedure. The surface area of the various samples along with their chemical composition is presented in table 2.2. The surface area of zinc modified zeolites decreased as compared with their parent sample. Also in the case of ZSM-5 zeolite, the surface area decreased with increase in the amount of zinc in the zeolite sample.
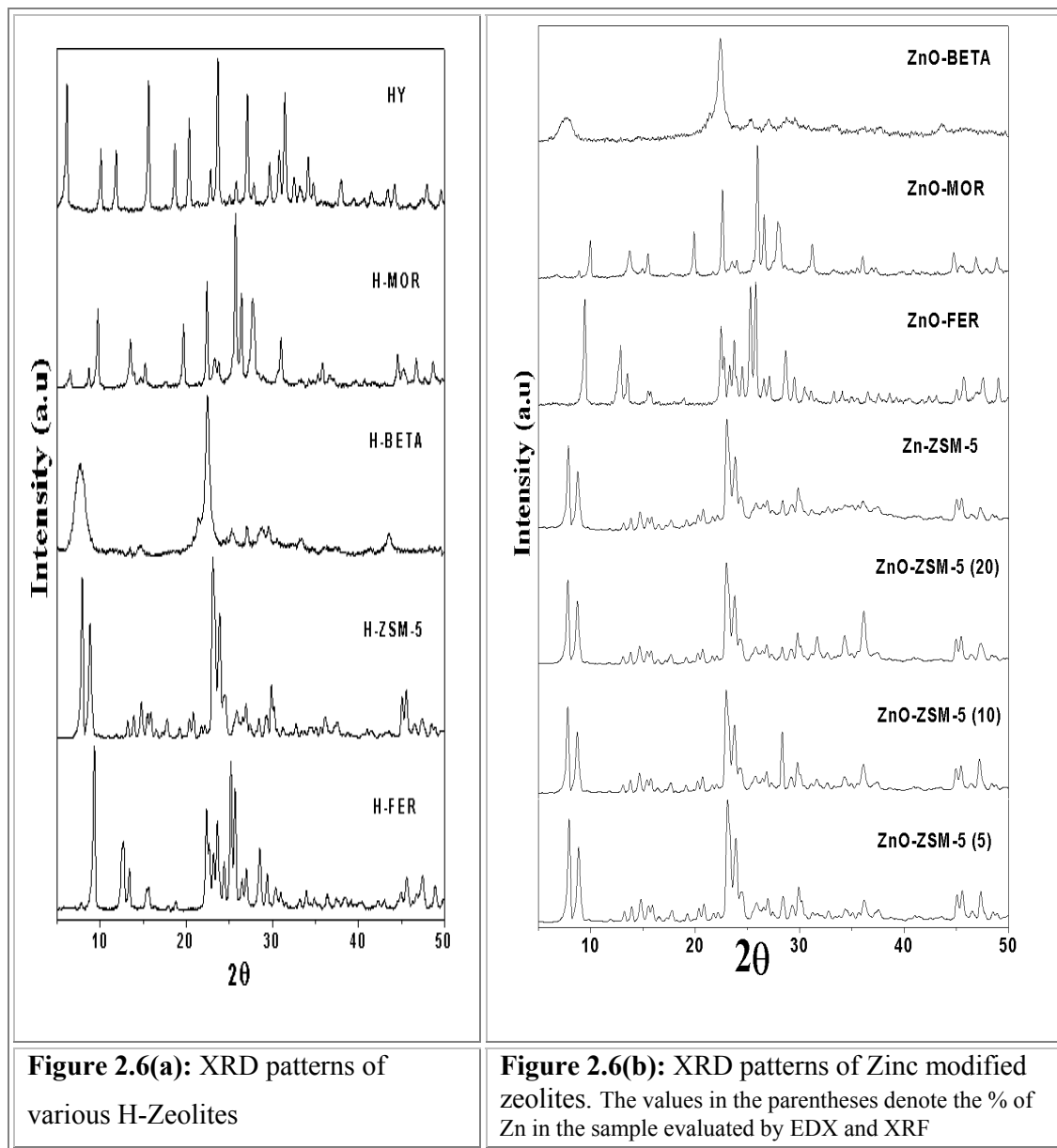
| Figure 2.6(a): XRD patterns of various H-Zeolites | Figure 2.6(b): XRD patterns of Zinc modified zeolites. The values in the parentheses denote the % of Zn in the sample evaluated by EDX and XRF |

Table 2.2: Composition and surface area of zeolites under study

Sample	SiO$_2$/Al$_2$O$_3$ ratio[*]	Zn (wt%)[#]	Surface Area (m^2/g)
H-ZSM-5	200	-	372.6
H-FER	34	-	335.5
H-BETA	30	-	706.1
H-MOR	25	-	421.5
HY	4.76	-	836.9
St-H-FER	72	-	262.5
H-FER (10)	20		272.7
H-FER (25)	50		315.9
Si-FER[b]	-	-	119.2
ZnO-ZSM-5	200	4.52	314.7
Zn-ZSM-5	200	2.11	322.6
ZnO-FER	34	4.6	214.4
ZnO-Beta	30	4.5	367.4
ZnO-MOR	25	4.76	288.9
ZnO-ZSM-5 (10)[a]	200	10.2	283.9
ZnO-ZSM-5 (20)[a]	200	19.8	249.6

* Obtained by combination of AAS, XRF and EDX. [#]Zinc weight percentage calculated from XRF and EDX.
[a]The value in the parentheses represents the amount of zinc impregnated by post synthesis modification.
[b]Siliceous FER was prepared according to [16].

2.4.3. Temperature Programmed Desorption of Ammonia

2.4.3.1. H-Zeolites

Acid sites of zeolites are often characterized by temperature programmed desorption using ammonia as basic probe molecule (NH$_3$-TPD) [31-34]. In the NH$_3$-TPD curves of H-zeolites, peaks are generally observed in two temperature regions. The regions below and above 673K (400°C) are referred to as low-temperature region (LT) and high temperature region (HT), respectively [35,36]. The peaks in the HT region can be attributed

to desorption of NH_3 from strong acid Brönsted sites (B sites) and Lewis sites (L sites), which are of catalytic importance [33].

For zeolites like Beta and HY, the LT and HT peaks may extensively overlap. In general, the HT peak is attributed to decomposition of NH_4^+ ions formed over strong acid B sites. Some L sites, related to the presence of specific kinds of extra-framework Al-species [37] were found to have acid strength close to that of the protonic B sites. If both strong acid B and L sites are present, they release ammonia in the HT region [31-33].

TPD spectra of NH_3 on various H-Zeolites (H-ZSM-5, H-FER, H-MOR, H-BETA and HY) are shown in figure 2.7. Spectra exhibited a fairly good resolution of two peaks (LT and HT peaks). The peaks are further resolved by Gaussian function and the resolved peaks are shown as dotted lines in the figure 2.7. The acid site densities (total acidity) of the different zeolites under study are shown in table 2.3. The TPD profile of large pore zeolites (HY, H-Mordenite and H-Beta) exhibited peaks having two maxima corresponding to low and high acid strength whereas H-ZSM-5 and H-FER showed four and three peaks respectively corresponding to weak, medium and strong acid sites. It has already been reported that three peaks are observed in the TPD of NH_3 from ZSM-5 zeolite [31]. Due to more resolution, four peaks are observed for H-ZSM-5 zeolite (2 each for LT and HT peaks). The second peak in the LT region may be due to possible formation of $NH_4^+.nNH_3$ associations [34,38]. The most weakly adsorbed ammonia is however out of the scope of the present study, since the weakest acid site is believed to play little role in the usual catalytic reaction. In the HT region of H-ZSM-5 and H-FER, the peak seems to consist of atleast two components: a dominating large peak and a smaller peak with maximum at somewhat higher temperature. Out of these resolved peaks, the peak having larger area can be assigned to desorption from strong B sites, while the smaller peak at higher temperature is assigned to desorption from strong L sites. These B and L sites were related to

framework Al atoms charge compensated by acidic protons and to extra-framework Al atoms, respectively [33]. The HT B acid peak of H-ZSM-5 and H-FER appeared at 417, and 401°C respectively whereas HT L acid peak appeared at 593 and 566°C respectively. The total amount of ammonia desorbed from these zeolites was respectively 0.27 and 0.92mmol/g.

Figure 2.7: TPD spectra of NH_3 on various H-Zeolites
 (a) H-ZSM-5
 (b) H-FER
 (c) H-BETA
 (d) H-MOR
 (e) HY
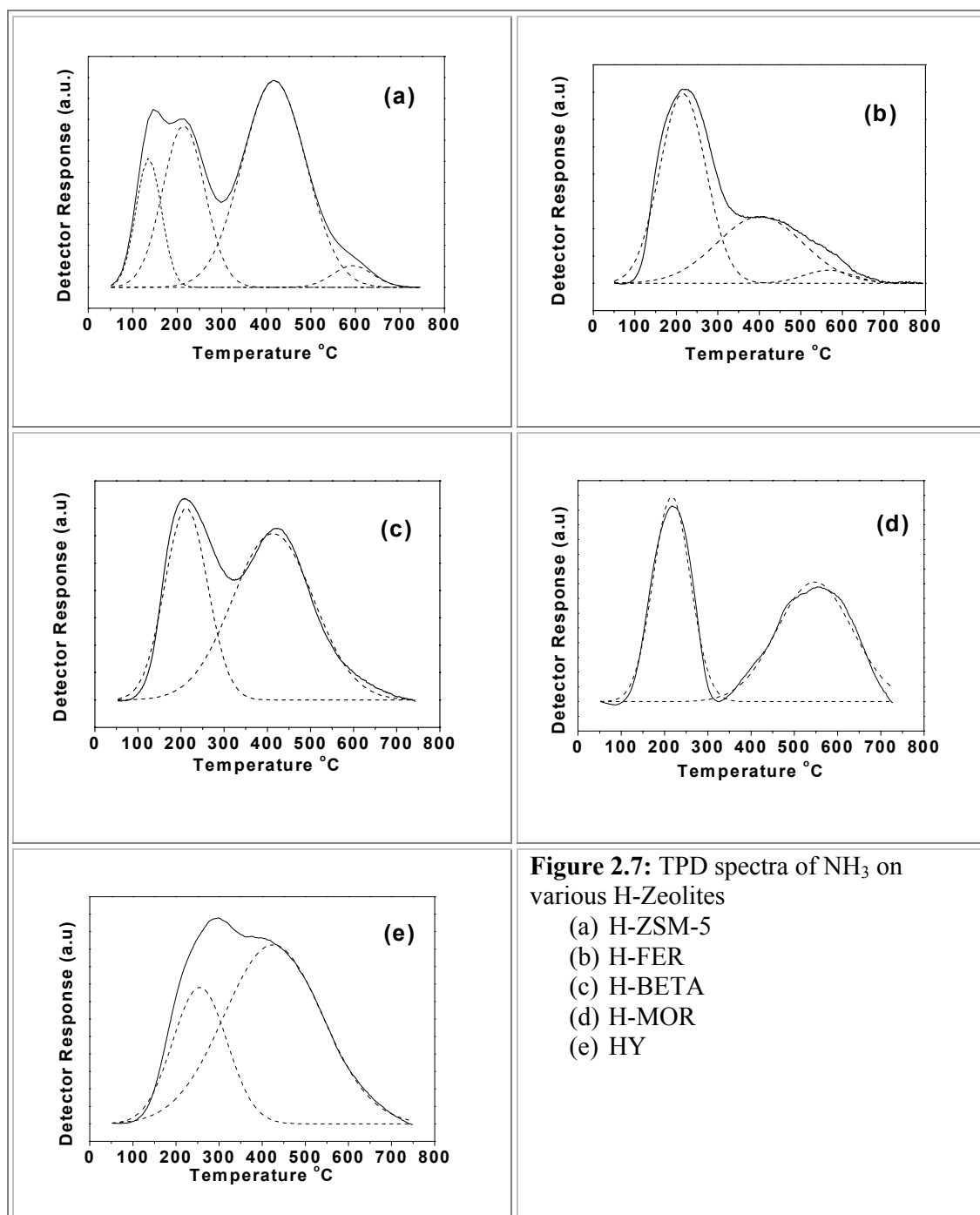
In the case of large pore zeolites (H-MOR, H-BETA and HY) first peak corresponds to weak + medium acid sites and second one is for stronger B and L acid sites as only two peaks were resolved for these zeolites. HY had a long tailing and showed broad unresolved spectra. Improper resolution indicates the overlap of various components desorbing in relatively broad temperature range. Such a complexity in the TPD spectra of NH_3 taken from faujasite-type zeolites has already been reported by Cattanach et al. [39]. The HT component of TPD spectra of HY is most likely to be associated with the water desorption as a result of dehydroxylation of surface hydroxyl groups. The HT B peak of H-Beta and HY appeared at temperatures 413 and 425°C respectively, whereas that of H-mordenite appeared at a temperature (547°C) about 100°C higher than the corresponding peak of other zeolites under study. The H-Zeolites used in the work have the following order according to their total acidity, i.e., HY > H-BETA > H-MOR > H-ZSM-5 > H-FER.

Table 2.3: Amount of desorbed ammonia and temperature of peak maximum of various H-zeolites

Zeolite	Peak	T°C	Acidity mmol/g	Total acidity mmol/g
H-ZSM-5 (200)	1	135.9	0.04	0.27
	2	214.5	0.08	
	3	417.5	0.15	
	4	593.7	0.01	
H-FER (34)	1	215.9	0.53	0.92
	2	401.6	0.35	
	3	566.6	0.04	
HY (4.76)	1	255.4	1.34	4.54
	2	425.5	3.20	
H-Beta (30)	1	211.9	0.69	1.83
	2	413.2	1.14	
H-MOR (28)	1	216.6	0.80	1.76
	2	547.1	0.96	

The value in the parentheses represents the SiO_2/Al_2O_3 ratio

2.4.3.2. Zinc modified ZSM-5

The NH$_3$-TPD profiles of pure H-ZSM-5 and zinc modified ZSM-5 samples (impregnated and ion-exchanged) are shown in figure 2.8. The resolved peaks are shown in dotted lines. The Si/Al ratio of ZSM-5 used for modification with zinc was 100. The unmodified sample showed four peaks as discussed earlier (figure 2.7). Table 2.4 shows ammonia TPD results for zinc modified ZSM-5 zeolite. Figure 2.8 also reveals overall widening and shift of the HT peak of the ammonia desorption to higher temperatures as compared to unmodified sample. Moreover, generation of new adsorption sites is visible by further changes of the profile shape. The HT shows a shoulder towards higher temperatures and the LT peak is widened and shifted towards higher temperature. These changes could be attributed to generation of strongly acidic Lewis sites. Both the zinc modified ZSM-5 zeolite showed distinct increase of ammonia desorption by 0.30mmol/g and 0.17mmol/g for impregnated and ion-exchanged samples respectively compared to H-ZSM-5.

Figure 2.8: TPD spectra of NH$_3$ on Zinc modified ZSM-5 zeolite (a) ZnO-ZSM-5 (b) Zn-ZSM-5
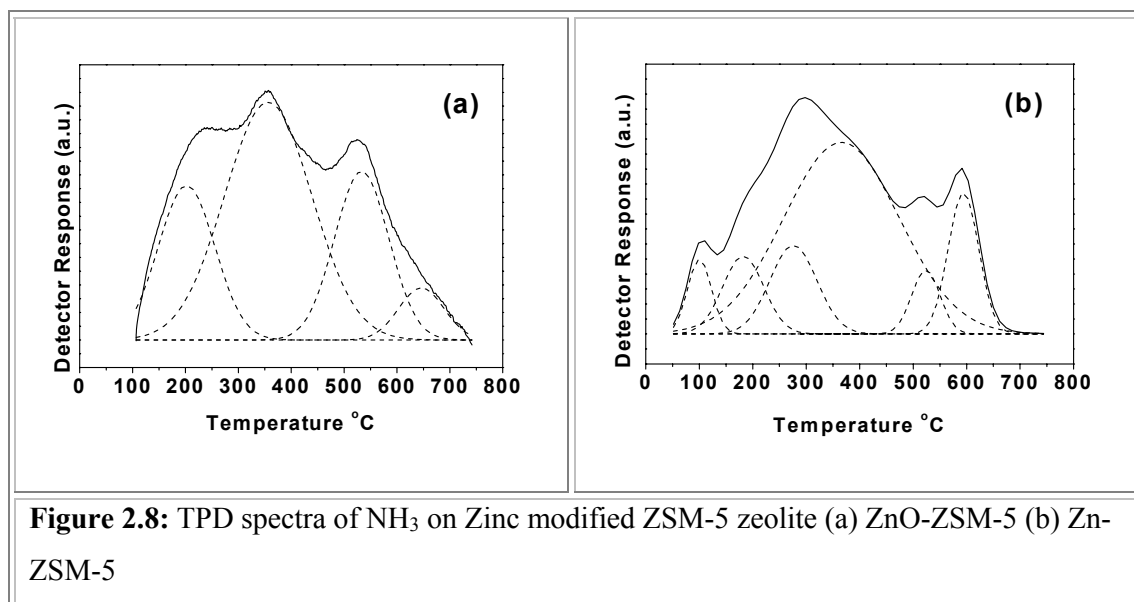
Table 2.4: Amount of desorbed ammonia and temperature of peak maximum of H-ZSM-5 and zinc modified H-ZSM-5 samples.

Zeolite	Peak	T°C	Acidity Mmol/g	Total acidity mmol/g
H-ZSM-5 (200)	1	135.9	0.04	0.27
	2	214.5	0.08	
	3	417.5	0.15	
	4	593.7	0.01	
ZnO-ZSM-5	1	202.2	0.12	0.57
	2	356.5	0.29	
	3	533.3	0.13	
	4	646.2	0.03	
Zn-ZSM-5	1	100.4	0.02	0.44
	2	182.2	0.04	
	3	276.1	0.05	
	4	366.0	0.26	
	5	523.8	0.02	
	6	594.1	0.05	

The value in the parentheses represents the SiO_2/Al_2O_3 ratio

Osaka et al. [40] have reported a shift of the LT peak indicating interaction of zinc species with ammonia. This would mean that the zinc species behave similar to exchanged Zn^{2+} ions, causing an increase of the LT peak only [41]. Roessner et al. [42] also relate the increase of LT peak to the formation of Lewis sites generated by zinc ions but they pointed out that an additional tailing of the HT peak is due to strongly acidic Lewis sites. According to the total acidity of the samples, following order can be observed for zinc modified samples: ZnO-ZSM-5 > Zn-ZSM-5 > H-ZSM-5.

2.4.3.3. Ferrierite Series

The results of the normalized NH_3-TPD measurements of various FER zeolites are depicted in figure 2.9. The FER zeolite releases ammonia over a wide temperature range. It is a reported fact that the difference in the catalytic performance of zeolites is due to the difference in their acidity. Desorption of ammonia with increasing the temperature showed

three peaks for H-FER (34) at 215, 401 and 566°C corresponding to weak, medium and strong acid sites. All the spectra are deconvoluted (resolved) and the acidity corresponding to each peak is reported in table 2.5. For increasing SiO_2/Al_2O_3 ratio from 34 to 50, the area of LT peak remains almost the same (even though a increase in height of the LT peak), however in HT region peak is observed at a higher temperature of 465°C with small decrease in the area of the same.

Table 2.5: Amount of desorbed ammonia and temperature of peak maximum of FER zeolites

Zeolite	Peak	T°C	Acidity mmol/g	Total acidity mmol/g
H-FER (50)	1	208.8	0.51	0.88
	2	465.8	0.37	
H-FER (20)	1	230.7	0.81	1.23
	2	468.8	0.42	
Na-FER (34)	1	221.6	0.82	1.27
	2	435.8	0.45	
H-FER (34)	1	215.9	0.53	0.92
	2	401.6	0.35	
	3	566.6	0.04	
St-H-FER (72)	1	206.6	0.35	0.79
	2	395.3	0.43	
	3	578.7	0.01	

The value in the parentheses represents the SiO_2/Al_2O_3 ratio

A decrease in Si/Al ratio from 17 to 10 resulted in a decrease of LT peak and an increase in HT peak and its concentration. According to Topsoe et al. [31], the TPD peak around 500°C (550°C in case of FER) is due to Brönsted acid sites. An additional observation is the shift in the TPD peak to the lower temperature as silica to alumina ratio increases. In the case of St-H-FER, the three peaks are well resolved and appeared at 206, 395 and 578°C. Upon steaming of H-FER (17), apart from decrease in the area and shifting of LT peak to a lower temperature, the HT peak in the resulting sample is shifted to a higher temperature showing strong HT L peaks (578°C).

Siliceous ferrierite (Si-FER) did not adsorb (or desorb) any ammonia. The spectrum of Na-FER exhibits maximum at 221°C, thereafter ammonia desorption decreases softly and showed a decrease in HT peak area as compared to its counterpart H-FER. The area of LT peak of Na-FER is more than the other FER zeolites under study. Based on the total acidity, the FER zeolites can be arranged in the following order: Na-FER > H-FER (20) > H-FER (34) > H-FER (50) > St-H-FER (37) > Si-FER.
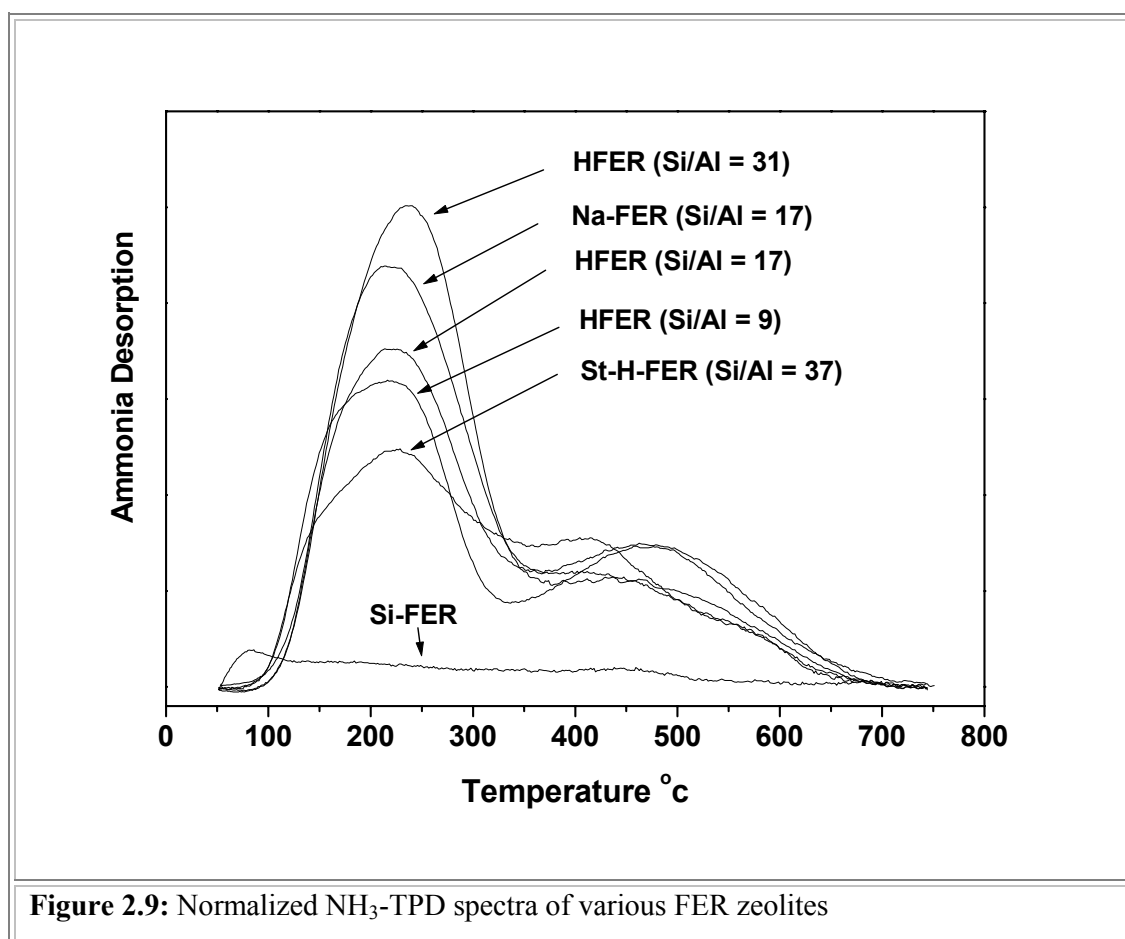
Figure 2.9: Normalized NH$_3$-TPD spectra of various FER zeolites

2.4.3.4. Zinc modified Zeolites

The normalized NH$_3$-TPD spectra of zinc impregnated MOR, BETA, ZSM-5 and FER along with their parent sample is shown in figure 2.10 and the temperature maxima and total acidity are shown in table 2.6. It can be seen in the case of BETA upon impregnation with zinc, two peaks appeared in the HT region: one shifting to lower

temperature (318°C) and another one at higher temperature (530°C), where as the parent

sample showed only one HT peak at 413°C. Also it is worth noting an increase in the total

acidity of ZnO-Beta compared to parent sample.

Figure 2.10: TPD spectra of NH$_3$ on Zinc modified zeolites: (a) ZnO-ZSM-5 (b) ZnO-FER (c) ZnO-BETA (d) ZnO-MOR
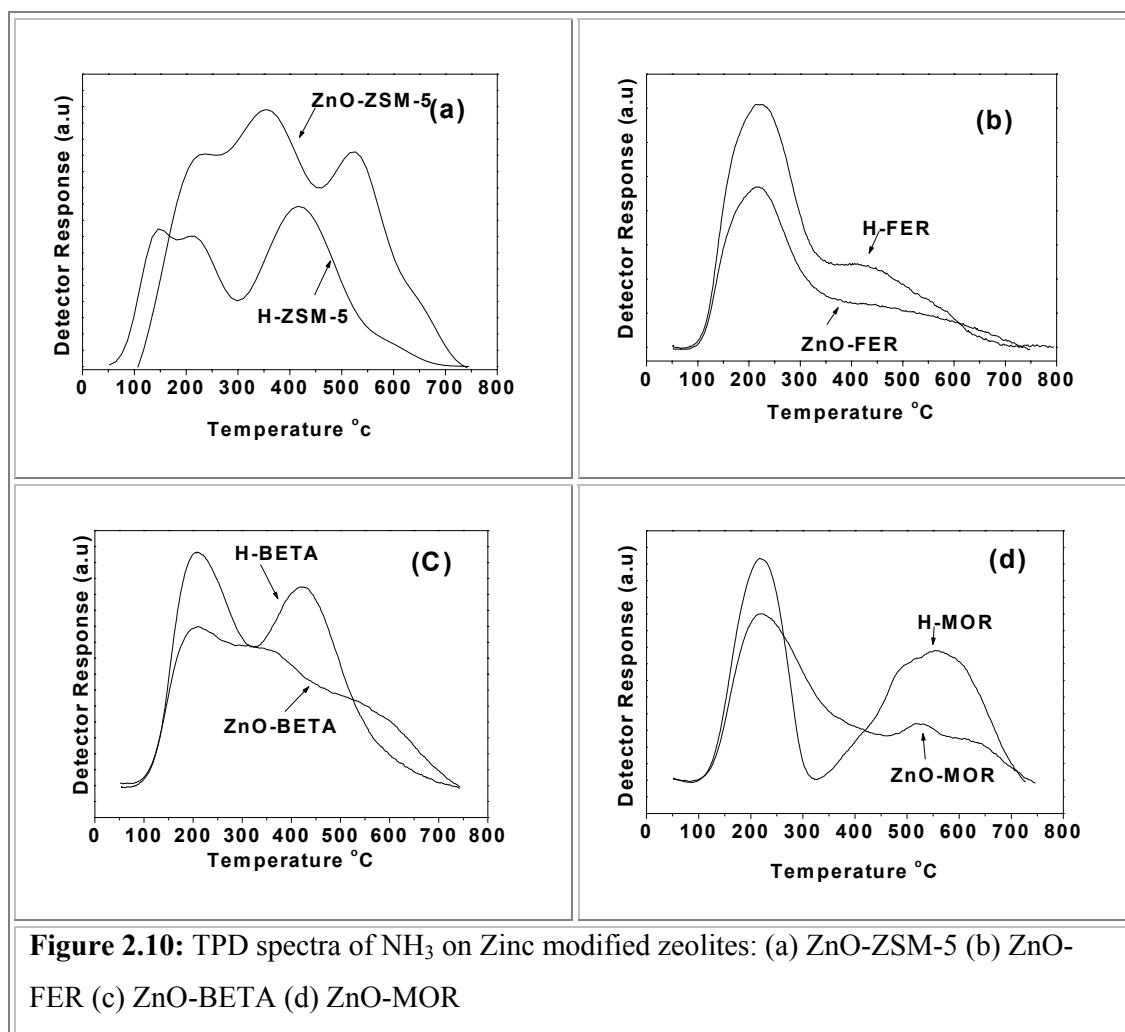
The HT peak is completely suppressed in the case of H-FER and had a long tailing up to

750°C and also a decrease in the LT peak is observed. H-MOR showed well-resolved

peaks in both the regions, where as the ZnO-MOR showed two peaks in the HT region at

high temperatures (523 and 646°C) with a decrease in the HT area. Both ZnO modified

FER and MOR showed a decrease in total acidity as compared with their parent sample.

Table 2.6: Amount of desorbed ammonia and temperature of peak maximum of zinc-modified zeolites

Zeolite	Peak	T°C	Acidity mmol/g	Total acidity mmol/g
ZnO-ZSM-5 (200)	1	202.2	0.12	0.57
	2	356.5	0.29	
	3	533.3	0.13	
	4	646.2	0.03	
ZnO-FER (34)	1	214.0	0.35	0.41
	2	*	0.06	
ZnO-BETA (30)	1	193.4	0.38	2.0
	2	318.4	0.98	
	3	530.6	0.64	
ZnO-MOR (28)	1	214.4	0.73	0.84
	2	523.0	0.06	
	3	646.3	0.05	

The value in the parentheses represents the SiO_2/Al_2O_3 ratio

For ZnO-BETA and ZnO-MOR zeolites, there are two new adsorption sites: one below and one above the adsorption temperature of corresponding parent zeolite. The decrease of HT peaks in the above samples indicate an exchange of protons of Brönsted sites by zinc ions which acts as Lewis sites adsorbing ammonia. A similar trend is also observed for ZnO-ZSM-5 zeolite, however showing more acidity than the parent sample. This may be due the fact that the parent sample used for modification has Si/Al ratio of 100 and hence the Lewis sites generated by zinc ions are much more stronger than the parent zeolite. The zinc modified zeolites are placed in the following order based on their total acidity: ZnO-BETA > ZnO-MOR > ZnO-ZSM-5 > ZnO-FER.

2.4.4. FTIR

2.4.4.1. Framework vibrations

Mid-infrared spectroscopy has been applied to identify zeolite structures. The infrared spectrum in the region of 400-1300cm^{-1} is a sensitive tool indicating structural features of zeolite frameworks. FTIR spectra in the region of framework vibrations of H-Zeolite samples are presented in the figure 2.11 and the frequencies of vibrations are given in the table 2.7.

The characteristic absorption bands found for H-ZSM-5 (figure 2.11a) are at 1228, 1101, 796, 624, 586, 545 and 449cm^{-1}. The bands around 1093 (in this case 1101), 796 and 449 cm^{-1} correspond to asymmetric stretching, symmetric stretching and T-O bending vibrations of internal tetrahedra respectively [43] and band around 550cm^{-1} (545, in this case) indicates the presence of double five membered ring in the framework [44].

Ferrierite (figure, 2.11b) showed strong absorption band in 1000-1200cm^{-1} region which is assigned to internal vibration of SiO$_4$, AlO$_4$ tetrahedra, which are also reported for silica and quartz [45]. The broad shoulder at 1226cm^{-1} was assigned to external asymmetric vibration [46]. The absorbance at 580cm^{-1} was assigned by Jacobs et al. [47] to a highly distorted double five membered rings present in the zeolite framework structure. The strongest band around 1090cm^{-1} is assigned to the asymmetric stretching vibrations of T-O-T linkage.

The major absorption bands found for H-Beta (figure 2.11c) are 1226, 1093, 792, 721, 619, 570, 520, 459 and 426cm^{-1}. Among these, the bands around 575 and 525cm^{-1} (570 and 520cm^{-1} in the present study) are characteristic structural bands of zeolite Beta [48]. The bands around 1093, 792 and 459cm^{-1} correspond to asymmetric stretching, symmetric stretching and T-O bending vibrations of internal tetrahedra respectively [43]. The band at 1226cm^{-1} indicates the presence of 5-membered ring in the zeolite framework

[44]. The absorption bands of HY and H-MOR are in accordance with the published literature [43].

Table 2.7: Characteristic absorption bands of framework vibrations for different Zeolites

Zeolite	Frequency of vibration, cm^{-1}								
H-ZSM-5	1228	1101	796	-	-	625	586	546	449
H-FER	1226	1097	800	721	675	-	586	538	463
H-Beta	1226	1093	793	721	-	619	571	521	459
H-MOR	1222	1086	808	-	696	632	584	563	459
HY	1146	1018	787	721	-	-	575	503	455

2.4.4.2. Hydroxyl group stretching region

FTIR spectra of surface hydroxyl groups of HY, H-Beta, H-Mordenite, H-ZSM-5 and H-FER samples are presented in figure 2.12. The HY zeolite (figure 2.12a) shows characteristic bridging hydroxyl groups (Si-OH-Al) at 3640 (high frequency, HF) and 3550cm^{-1} (low frequency, LF) and surface silanol (Si-OH) groups at 3744cm^{-1} respectively. The HF band arises due to -OH groups situated in the super cages and the LF band arises due to -OH groups in the sodalite cages.

The bands at 3737, 3659 and 3598cm^{-1} for H-Beta (figure 2.12b) and at 3737, 3678 and 3614cm^{-1} for H-mordenite (figure 2.12c) are observed. The assignments of these bands are very well documented in the literature [49-51]. The bands near 3775 and 3670cm^{-1} are due to extralattice aluminum species, around 3745cm^{-1} to silanol groups. The bridging hydroxyl groups (Brönsted acid OH groups) at 3614 and 3588 cm^{-1} of H-MOR are assigned the positions at 12-membered straight channels and 6 or 8-membered channels respectively. There is only one kind of bridging hydroxyl groups in H-Beta giving band at 3614cm^{-1}.

The spectrum of H-ZSM-5 (figure 2.12d) contains two main bands, at 3611 and 3744cm^{-1}. The band at 3611cm^{-1} is associated with the acidic OH groups (–Si–OH–Al–) and the 3744cm^{-1} band with external silanol groups [52,53]. A weak band at 3663cm^{-1}, are also detected; they are assigned to hydroxyls linked to aluminum atoms dislodged from the framework [54,55].

Ferrierite (figure 2.12e) exhibits two principal bands at 3735 and 3587cm^{-1} and another one at 3647cm^{-1}. The 3587cm^{-1} band is assigned to bridging hydroxyl groups (Si-OH-Al) while 3735cm^{-1} band corresponds to terminal silanol groups. A weak band was observed in the region of Al-OH groups at 3647cm^{-1}.

Figure 2.11: FTIR spectra in the region of framework vibrations (a) H-ZSM-5, (b) H-FER, (c) H-BETA, (d) H-MOR and (e) HY	**Figure 2.12:** FTIR spectra in structural hydroxyl group vibrations (a) HY (b) H-BETA (c) H-MOR (d) H-ZSM-5 and (e) H-FER
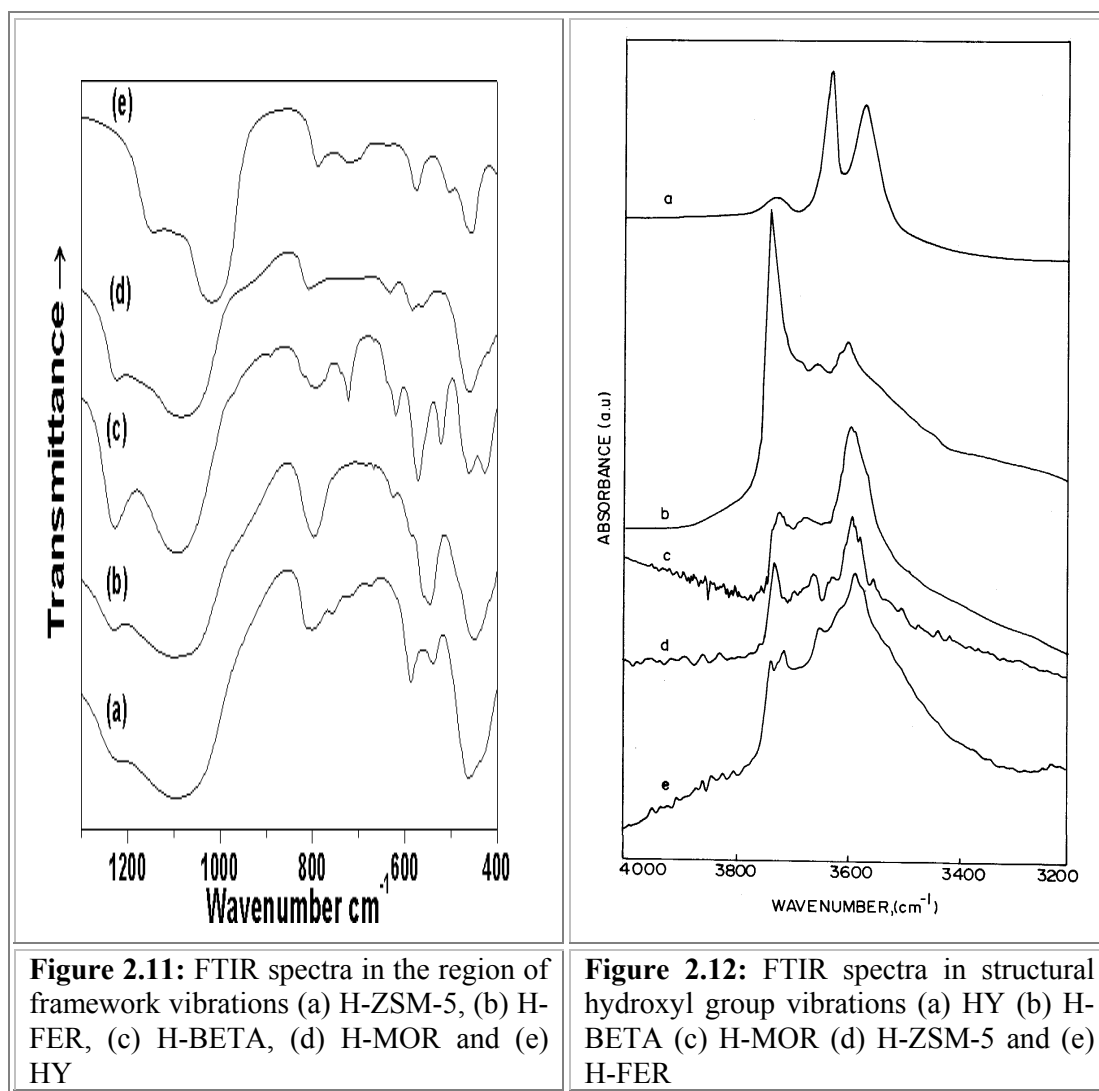
2.4.4.3. Pyridine Adsorption

One of the most reliable tools to investigate the acidity of zeolites is the Fourier transform infrared spectroscopy (FTIR) of adsorbed pyridine, which gives a clear distinction between Brönsted and Lewis acidic sites at around 1540 and 1450cm^{-1} respectively. Brönsted acid sites are generated by protons associated with negatively charged oxygen adjacent to Al tetrahedra in the framework as well as electrostatic dissociation of adsorbed water over cations in to OH$^-$ and H$^+$ ions. Lewis acid sites may occur because of several reasons: (i) Heating may lead to partial disintegration of the zeolite lattice and the formation of sub-nanoscale metal oxide particles within the channels of the microporous materials [56]. (ii) The exchangeable metal cations affiliated with the tetrahedrally coordinated aluminum acts as Lewis acid sites [57]. (iii) Larger and, hence, accessible di- or trivalent metal cations, e.g. Co, Mg, Cr, are incorporated in the lattice [58]. (iv) Reversible hydrolysis of metal-oxygen bonds allows access of polar molecules to the metal cations [59].

Ever since the pioneering work of Parry [60], the IR spectroscopy of adsorbed pyridine has been used as characteristic tool to detect and measure the presence of Brönsted and Lewis acid centers on the solid surfaces. The IR bands of pyridine of interest to this study are the C-H and N-H stretching as well as the C-C and the C-N stretching in pyridine ring [61]. In the figure 2.13-2.17, FTIR spectra of adsorbed pyridine at 100, 200, 300 and 400°C on the H-zeolite samples listed in the table 2.8 are depicted. The spectra were normalized with respect to 5mg/cm^2 weight of the wafer and the relative concentration of Brönsted and Lewis acid sites are presented in the table 2.8.

Pyridine adsorption on H-ZSM-5 (figure 2.13a-d) exhibits IR bands characteristic of pyridinium ion (PyH$^+$) vibrating at 1545cm^{-1} reflecting its interaction with Brönsted sites. In addition, IR bands around 1445 to 1460cm^{-1} result from coordinatively bonded

pyridine on electron acceptor sites (Lewis centers). The FTIR spectrum of H-ferrierite (figure 2.14a-d) after adsorption of pyridine showed characteristic bands of its interaction with protons of the bridging groups at 1545cm^{-1} and with Lewis sites at 1455, 1445 and 1440cm^{-1}, of much lower intensity. The IR spectra of pyridine adsorbed on H-Beta zeolite (figure 2.15a-d) exhibited several peaks due to Lewis bound pyridine (1618 and 1456cm^{-1}) and pyridinium ion on Brönsted acid sites (1546 and 1641cm^{-1}). Both HMOR (figure 2.16a-d) and HY (figure 2.17a-d) zeolites exhibited characteristic peaks of pyridine adsorption on Brönsted and Lewis acid sites.

Table 2.8: Acid strength distribution of zeolite samples.

Sample	HY	H-Beta	H-MOR	H-ZSM-5	H-FER	ZnO-ZSM-5	Zn-ZSM-5	T °C
Relative concentration of Brönsted acid sites	45	4	30	18	4	8	8	100
	44	3	28	16	3	6	6.5	200
	39	2.5	22	12	1.8	4	4	300
	33	1	15	9	1.2	2	2	400
Relative concentration of Lewis acid sites	46	6	3	3	2	25	31	100
	28	3	1.5	1.5	0.45	15	13	200
	21	0.9	1	-	0.3	13	8	300
	21	-	1	-	-	10	6	400
Brönsted / Lewis (B/L) acid sites	0.98	0.7	10	6	2	0.32	0.26	100
	1.56	1	18.7	10.7	6.66	0.4	0.5	200
	1.85	2.7	22	-	6	0.31	0.5	300
	1.56	-	15	-		0.2	0.33	400
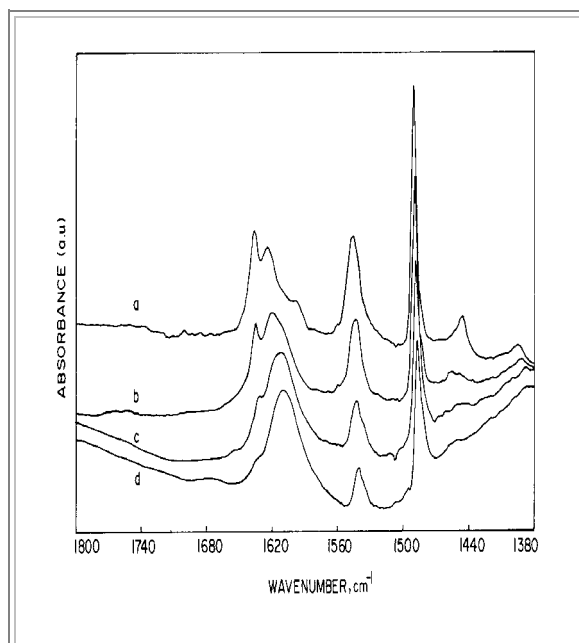
Figure 2.13: FTIR difference spectra of adsorbed pyridine on H-ZSM-5 at (a) 100°C (b) 200°C (c) 300°C and (d) 400°C
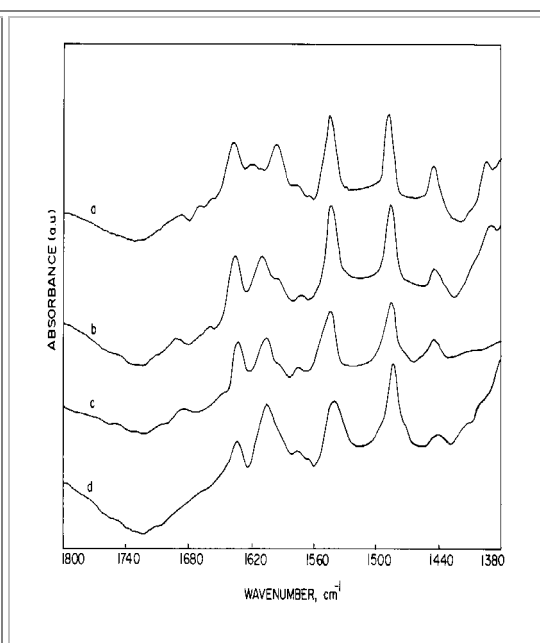
Figure 2.14: FTIR difference spectra of adsorbed pyridine on H-FER at (a) 100°C (b) 200°C (c) 300°C and (d) 400°C
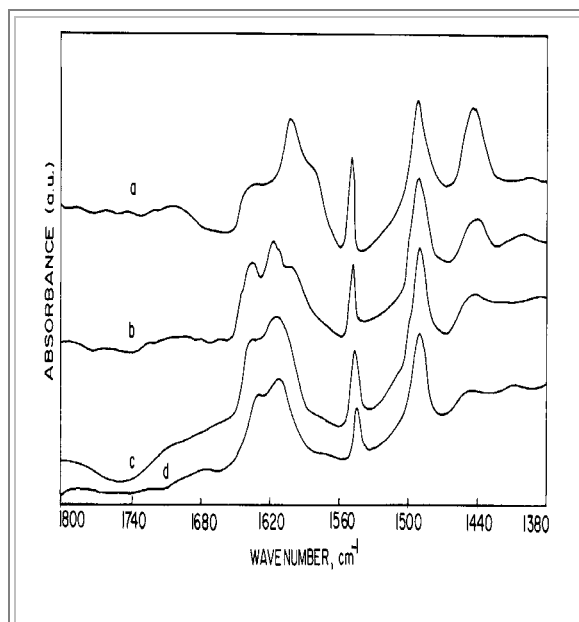
Figure 2.15: FTIR difference spectra of adsorbed pyridine on H-BETA at (a) 100°C (b) 200°C (c) 300°C and (d) 400°C
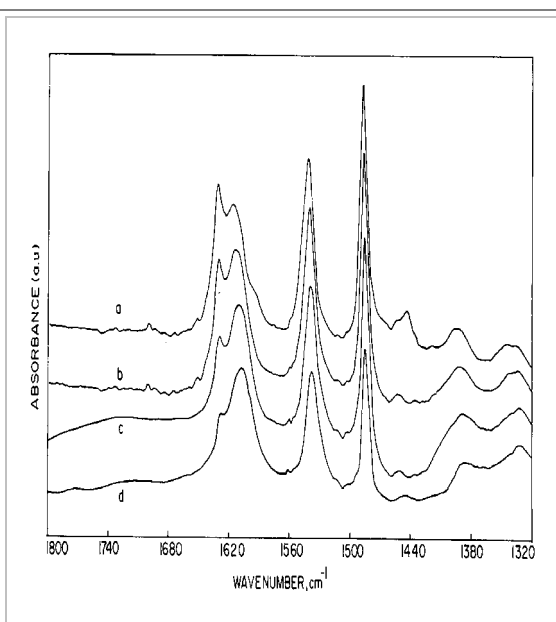
Figure 2.16: FTIR difference spectra of adsorbed pyridine on H-MOR at (a) 100°C (b) 200°C (c) 300°C and (d) 400°C

2.4.4.4 FTIR spectra of Zinc modified ZSM-5

Usually, Zinc or gallium cations are incorporated into a zeolite via ion exchange or impregnation of the zeolite with aqueous solution of the respective metal salt. Biscardi and Iglesia [64] showed that ion exchange leads directly to intrazeolitic zinc centers, while impregnation leads to exchanged centers and extracrystalline ZnO. In the figure 2.18, FTIR spectra of structural hydroxyl groups of zinc modified H-ZSM-5 samples are given in comparison with that of pure H-ZSM-5. A remarkable difference in the relative concentration of different kind of –OH groups should be noted. In the spectrum for zinc containing H-ZSM-5 samples, despite having higher amount of Zn^{2+} compared to ion exchanged sample (4.5% Vs 2.1%) the decrease in concentration of bridging hydroxyl groups due to Zn^{2+} exchange of a H^+ cation is considerably less in zinc impregnated sample.

Figure 2.17: FTIR difference spectra of adsorbed pyridine on HY at (a) 100°C (b) 200°C (c) 300°C and (d) 400°C	**Figure 2.18:** FTIR spectra in structural hydroxyl group vibrations (a) H-ZSM-5 (b) ZnO-ZSM-5 and (c) Zn-ZSM-5
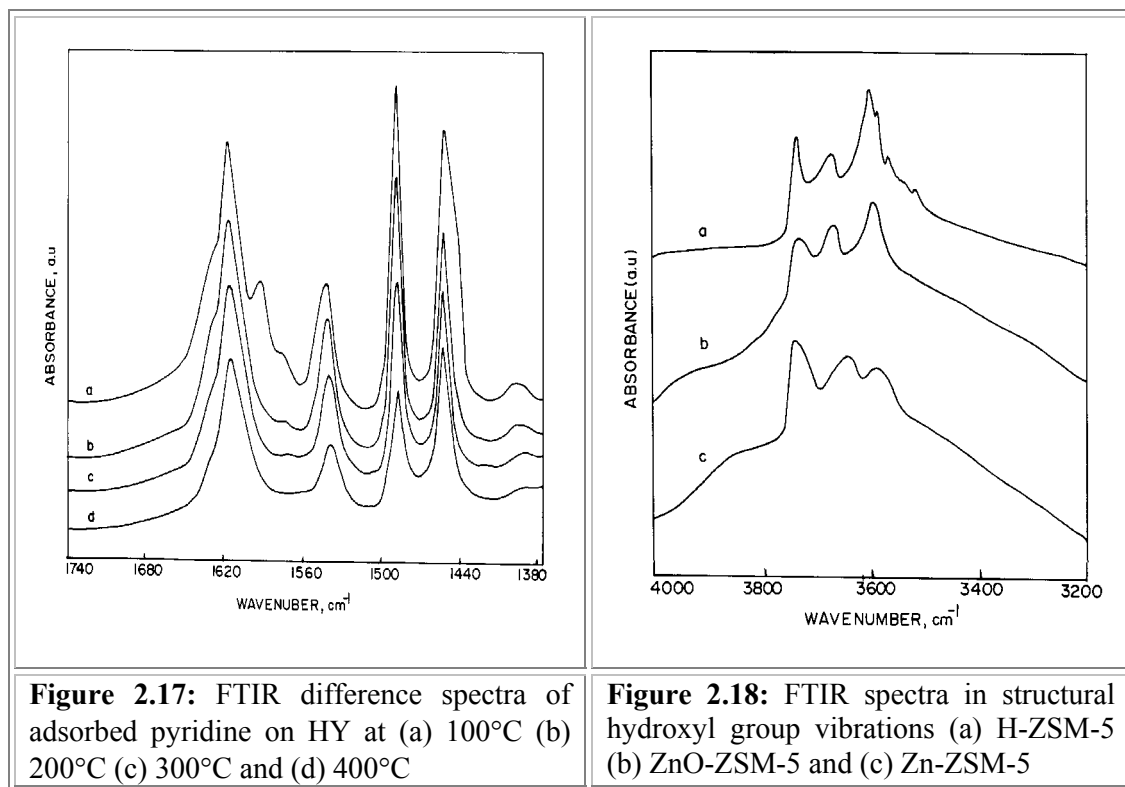
It is evident from FTIR spectra of surface hydroxyl groups (figure 2.18) as well as FTIR spectra of adsorbed pyridine (figure 2.19-2.21). Where in the concentration of the internal surface silanol groups at 3740cm^{-1} in impregnated sample has decreased more than that in ion-exchanged sample. It indicates that in impregnated sample, in addition to ion exchangeable positions, zinc may be present as bulk ZnO on the surface of the sample in not much dispersed state. The concentration of Lewis acid sites is also less in impregnated sample compared to ion-exchanged sample due to the same reason. Overall, zinc incorporation in H-ZSM-5 decreased the concentration of Brönsted acid sites and increased Lewis acid sites. The change in nature of acid site distribution is manifested in their reactions as described in the latter part.
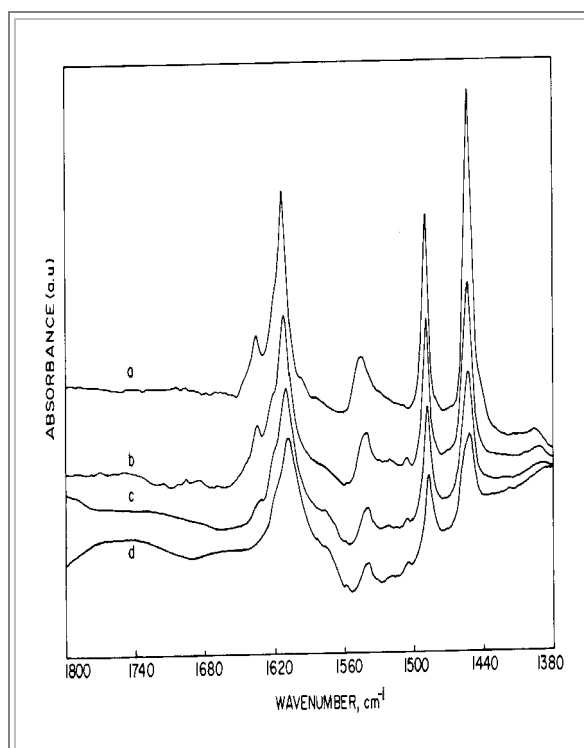
Figure 2.19: FTIR difference spectra of adsorbed pyridine on ZnO-ZSM-5 at (a) 100°C (b) 200°C (c) 300°C and (d) 400°C
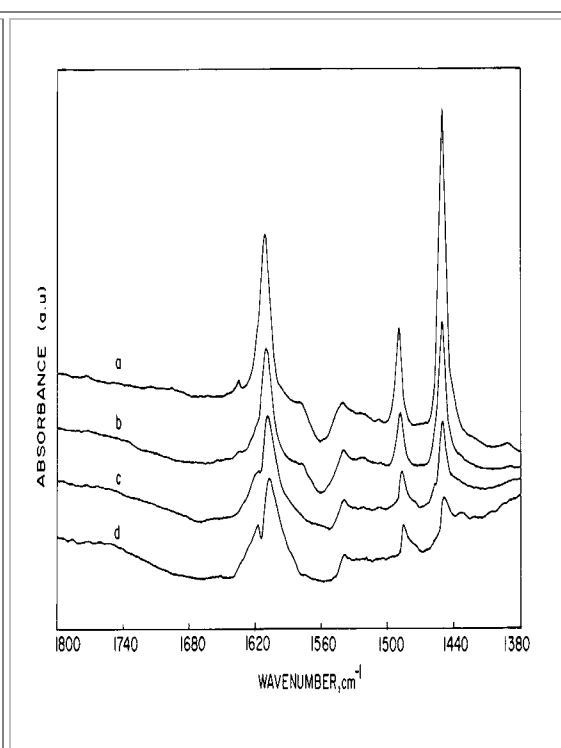
Figure 2.20: FTIR difference spectra of adsorbed pyridine on Zn-ZSM-5 at (a) 100°C (b) 200°C (c) 300°C and (d) 400°C

73
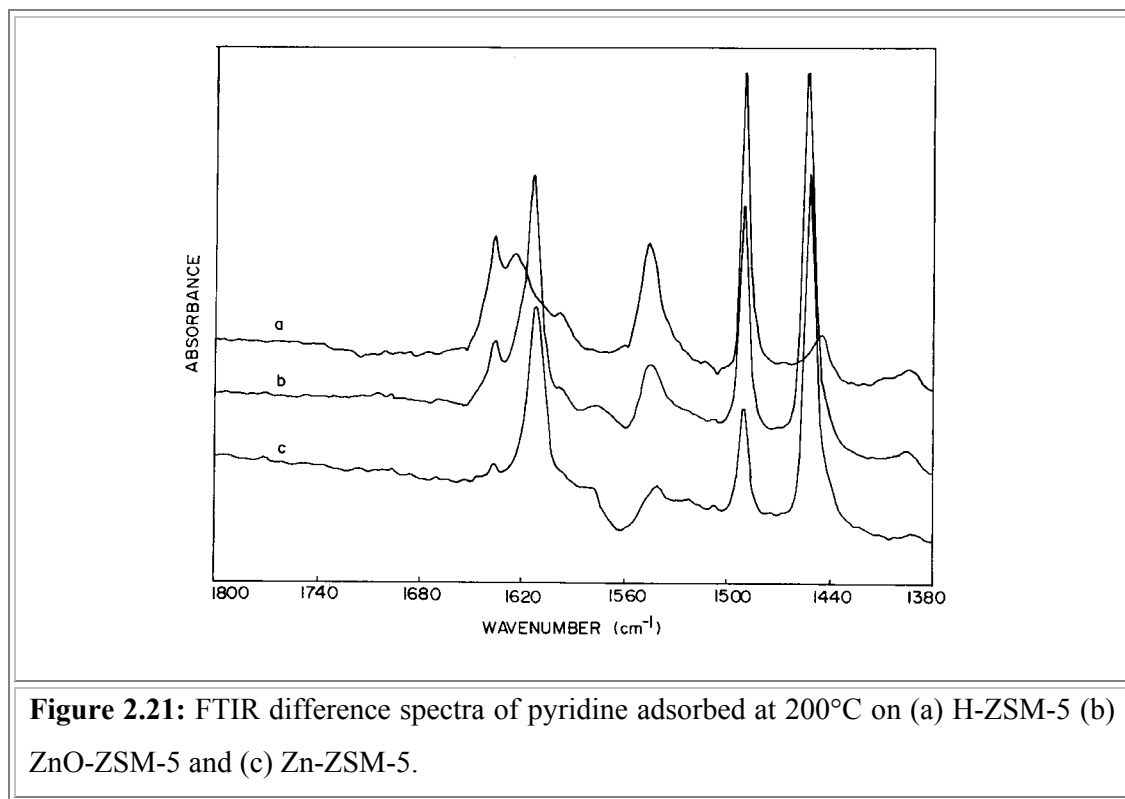
Figure 2.21: FTIR difference spectra of pyridine adsorbed at 200°C on (a) H-ZSM-5 (b) ZnO-ZSM-5 and (c) Zn-ZSM-5.

2.4.5. XPS

XPS studies were carried out on ZnO-ZSM-5 catalysts to understand the nature and distribution of zinc species. Figure. 2.22(a) shows the Zn $2p_{3/2}$ core level spectrum from Zn impregnated ZSM-5, ion exchanged Zn-ZSM-5, a physical mixture of ZnO (5%) and ZSM-5 and pure ZnO. Further the Zn 2p spectrum from the impregnated and ion exchanged zeolites are deconvoluted (figure 2.22(b) and 2.22(c)). XPS parameters derived from all the above catalysts are given along with Si 2p BE in table 2.9. It is clear from figure 2.22(a) that the BE of Zn 2p core level from all the above catalysts are comparable to ZnO and in good agreement with the results reported earlier [66]. This clearly indicates the nature of zinc species is close to that of ZnO. However there is a broadening associated with all catalysts indicates that there might be more than one species and the deconvolution clearly shows that there are two different zinc species at different BE. Species 2 appears at

1023.3eV in both impregnated as well as in ion-exchanged cases is similar to that of ZnO. Additionally, species 2 is the majority of Zn species in both the above catalysts. However, species 1 appears at lower BE than that of ZnO and low in intensity. It is speculated here that the species 1 could be from the Zn species that are incorporated into the zeolite lattice.
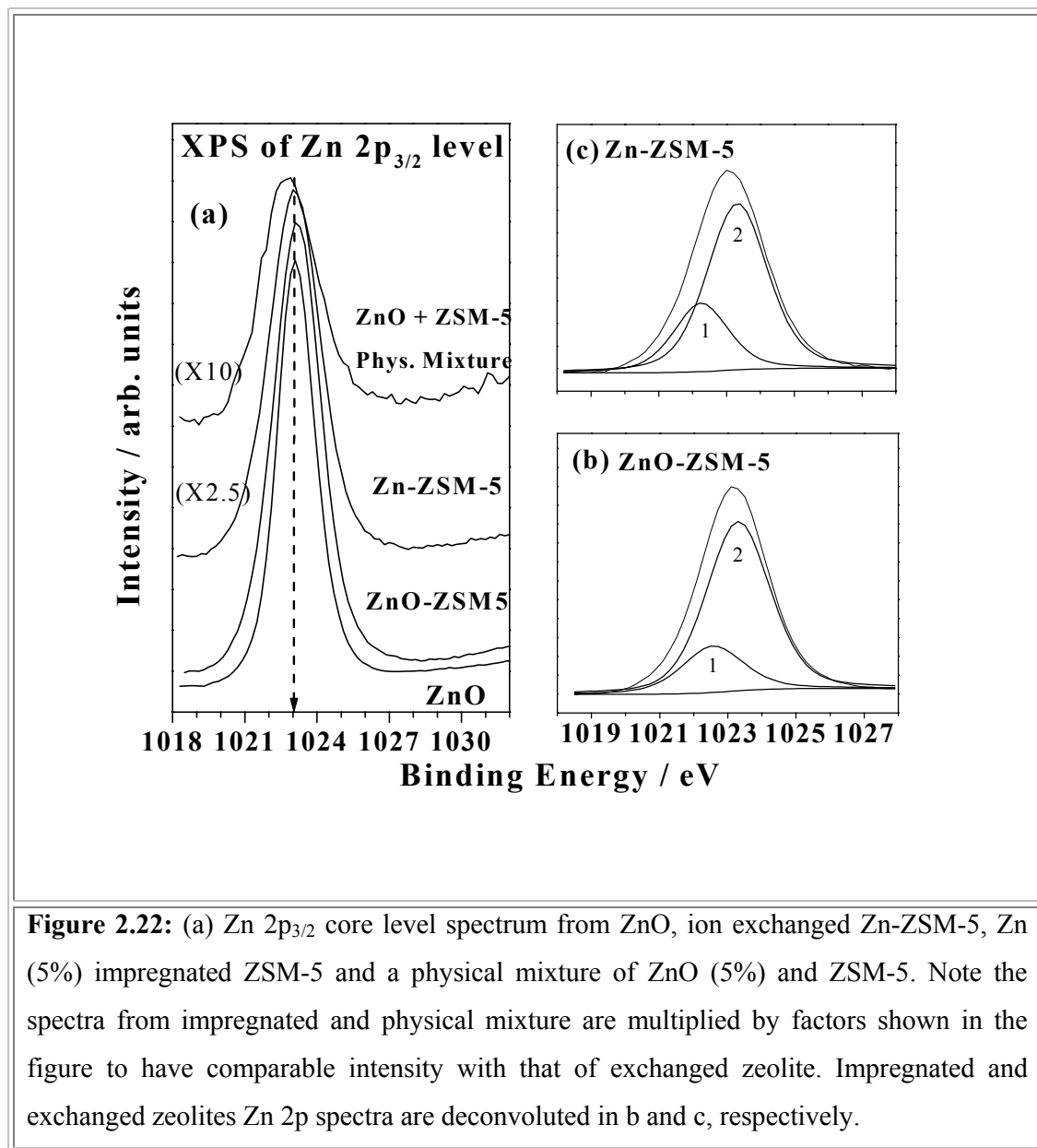
Figure 2.22: (a) Zn $2p_{3/2}$ core level spectrum from ZnO, ion exchanged Zn-ZSM-5, Zn (5%) impregnated ZSM-5 and a physical mixture of ZnO (5%) and ZSM-5. Note the spectra from impregnated and physical mixture are multiplied by factors shown in the figure to have comparable intensity with that of exchanged zeolite. Impregnated and exchanged zeolites Zn 2p spectra are deconvoluted in b and c, respectively.

Table 2.9 demonstrates the surface Zn/Si ratio is low for ion exchanged ZSM-5 compared to impregnated ZSM-5. In the case of physical mixture it is too low. The intermediate value obtained for surface Zn/Si ratio suggests that the distribution of Zn

species is more uniform and well separated in Zn-ZSM-5 and this is not the case with physical mixture and ZnO-ZSM-5 zeolite. The results are in accordance with FTIR –OH spectra of these species as discussed early (figure 2.18)

Table 2.9: XPS parameters of different Zn-ZSM-5 Catalysts and ZnO.

Material	Zn 2p$_{3/2}$ (FWHM) (eV)		Si 2p (eV)	(Zn/Si)$_{XPS}$	
	Species 1	Species 2		Species 1	Species 2
ZnO	--	1023.1 (1.9)	---	--	--
ZnO-ZSM5	1022.6 (2.1)	1023.3 (2.2)	103.3	0.0724	0.263
Zn-ZSM-5	1022.3 (1.9)	1023.3 (2.1)	103.4	0.05	0.131
ZnO (5%) and ZSM-5 Physical Mixture	1022.8 (2.6)		103.8	0.027	

2.5. CATALYTIC REACTOR SYSTEMS

In the present study of catalytic evaluations, two types of reactors were used depending on the reactions, (i) Continuous flow fixed bed atmospheric reactor: Catalytic studies were carried out at atmospheric pressure, in a fixed bed, down flow, integral silica reactor (figure 2.23a). All heating and temperature measurements were carried out using Aplab temperature controller and indicator. About 3.0g of catalyst (10-20 mesh) was placed at the center of the silica reactor supported by porcelain beads, which was placed vertical in the heating shell (Geomechanique, France). Liquid reactants were fed with a syringe pump (Sage instruments, USA), and carrier gas was used at a desired rate using a mass flow controller (Matheson, USA). Reaction products were condensed by passing through cold water condenser and samples were collected at various intervals. Samples were analyzed on gas chromatograph (Shimadzu, model GC 15A). (ii) Liquid phase high-pressure reactor: Liquid phase high-pressure reactions were carried out in pressurized and stirred autoclaves (figure 2.23b).

Figure 2.23: Catalytic reactors used in this work. (a) Schematic representation of continuous down-flow fixed bed vertical reactor and (b) High pressure stirred autoclaves (Photo of PAAR reactor, Model 4842, USA)
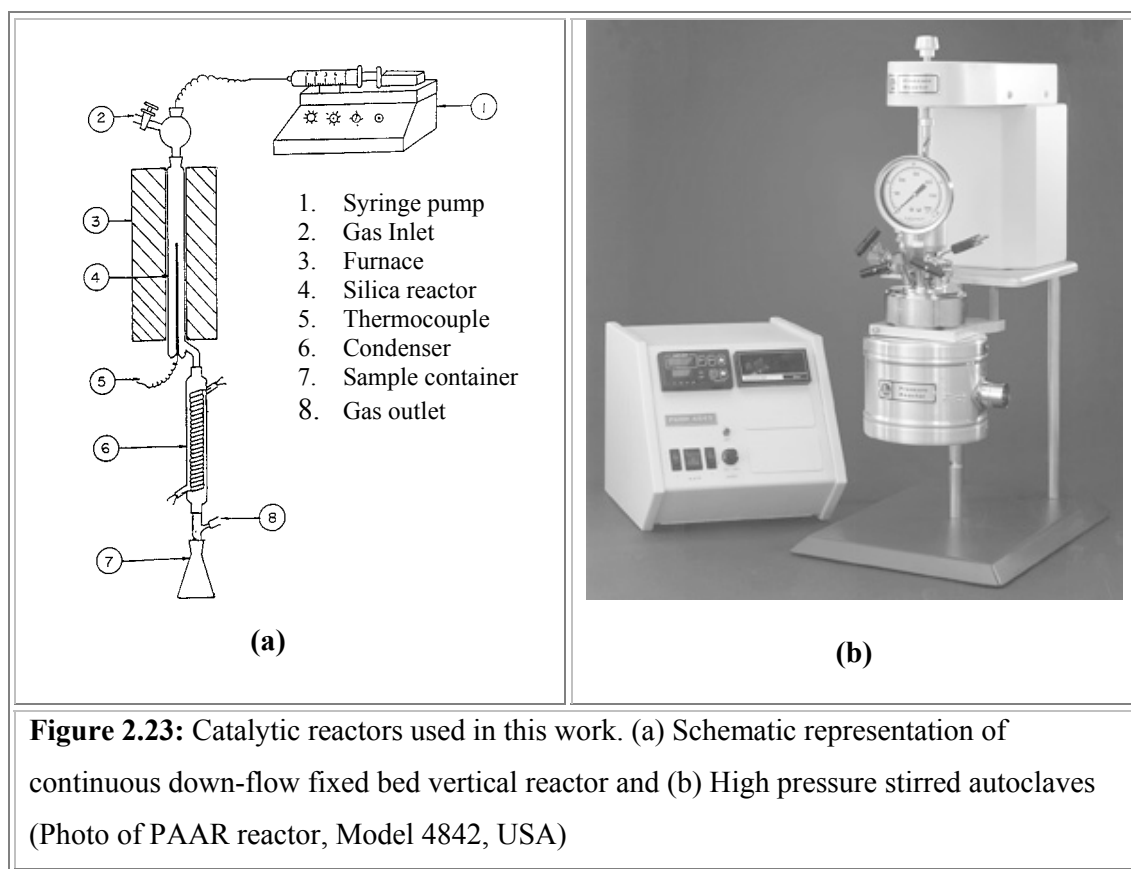
2.6. CONCLUSIONS

The zeolites ZSM-5, FER and BETA were synthesized with good crystallinity and surface area. These zeolite samples and commercially obtained MOR and Y zeolite were also modified with zinc by impregnation. The zeolite ZSM-5 was also modified with zinc by various methods (ion exchange, impregnation and physical mixing). At higher loading of zinc, a slight decrease in intensity of XRD peaks was observed. Also surface area decreased on zinc loading. From the TPD of ammonia studies, the samples are graded according to the total acidity. They are: HY > H-Beta > H-MOR > H-ZSM-5 > H-FER. FTIR of pyridine adsorption also confirmed similar results. In the zinc-modified sample, the generation of strongly acidic Lewis sites is observed. From FTIR studies, we conclude that for ZnO-ZSM-5 sample, zinc may be present as bulk ZnO on the surface of the sample

in not much dispersed state as compared to Zn-ZSM-5. Similar results are also obtained by XPS from Zn/Si ratio.

2.7. REFERENCES

1. X. Teng, E.J. Munson, J.F. Haw, *J. Am. Chem. Soc.,* **116** (1994) 1962.
2. S. L. Meisel, J.P. McCollough, C.H. Lechthaler, *CHEM-TECH.*, **6 (**1976) 86.
3. R.J. Argauer, G.R. Landolt US Pat 3702886 (1972).
4. P.A. Jacobs, J.A. Martens in Synthesis of high-silica aluminosilicate zeolites. Elsevier Amsterdam, *Stud. Surf. Sci. Catal.,***33** (1987).
5. B.M. Lok, T.R. Cannan, C.A. Messina, *Zeolites,* 3 (1983) 282.
6. C.J. Plank, E.J. Rosinski, M.K. Rubin, US Pat 4175114 (1979).
7. R.W. Grose, E.M. Flanigen, US Pat 4257885 (1981).
8. W.J. Bale, D.G. Stewart Eur Pat Appl. 30811 (1981).
9. Ch. Baerlocher, W.M. Meier and D.H. Olson, *"Atlas of Zeolite Framework Types"*, 5th ed., Elsevier: Amsterdam, 2001.
10. L.W. Stapes, *Amer. Min.,* **40** (1955) 1095.
11. P.A. Vaughan, *Acta. Cryst*., **21** (1966) 983.
12. I.S. Kerr, *Nature,* **210** (1966) 294.
13. D.W. Breck, *Zeolite molecular sieves. Structure chemistry and use*. John Wiley, New York (1974).
14. C.L. Kibby, A.J. Perotta, J. Massoth, *J. Catal.,* **35** (1974) 256.
15. H. Gies, R. Gunawardane, *Zeolites,* **7** (1987) 442.
16. A. Kuperman, S. Nadami, S. Oliver, G.A. Ozin, J.M. Graces, M.M. Olken, *Nature,* **365** (1993) 239.
17. R.K. Ahedi, A. N. Kotasthane. *J.Por.Mat.,* **4** (1997) 171.
18. R.L. Wadlinger, G. T. Kerr, E.J. Rosinski US Pat 3308069 (1967).
19. P. Caullet, J. Hazm, J. L. Guth, J.F. Joly, J. Lynch, F. Raats *Zeolites,* **12** (1992) 240.
20. Rajib Bandhyopadhyay, Ph.D Thesis, University of Pune (1996)
21. R.M. Milton US Pat 2882244 (1959).
22. Union Carbide French Patent 1286136 (1962).
23. D.W. Breck US Pat 3130007 (1964).
24. S.J. Gregg, K.S.W. Sing in "*Adsorption, Surface Area and Porosity*", Academic Press, New York, 2nd Edn. (1982).

25. S. G. Hegde, R.A. Abdullah, R.N. Bhat, P. Ratnasamy, *Zeolites*, **12** (8), (1992) 951.

26. J.J. Yeh, I. Lindau, *At. Data Nucl. Data Tables,* **32** (1985) 1.

27. H. van Koningsveld, J. C. Jansen, H. van Bekkum, *Zeolites,* **10** (1990) 235.

28. M.A. Camblor, J. Perez-Pariente, *Zeolites,* **11** (1991) 202.

29. G.J. Kim, W.S. Ahn *Zeolites,* **11** (1991) 745.

30. D.M. Ginter, A.T. Bell, C.J. Radke, in M.L. Occelli, H.E. Robson (eds), *Synthesis of Mircroporous Materials*. Vol. 1, Molecular Sieves, Van Nostrand Reinhold, New York, 1992, p6.

31. N.-Y. Topsoe, K. Pedersen, E.G. Derouane, *J. Catal.,* **70**(1), 41-52 (1981).

32. C. V. Hidalgo, H. Itoh, T. Hattori, M. Niwa, Y. Murakami, *J. Catal.,* **85**(2), (1984) 362.

33. H.G. Karge, *Stud. Surf. Sci. Catal.,* **65** (1991) 133.

34. R. Barthos, F. Lonyi, Gy. Onyestyak, J. Valyon, *J. Phys. Chem. B*, **104**(31), (2000) 7311.

35. M. Sawa, M. Niwa, Y. Murakami, *Zeolites,* **10**(4), (1990) 307.

36. H. Sato, *Catal. Rev. – Sci. Eng.,* **39**(4), (1997) 395.

37. F. Lonyi, J.H. Lunsford, *J. Catal.,* **136**(2), (1992) 566.

38. W.L. Earl, P.O. Fritz, A.A.V. Gibson, J.H. Lunsford, *J. Phys. Chem.,* **91**(8), (1987) 2091.

39. J. Cattanach, E.L. Wu, P.B. Venuto, *J. Catal.,* **11** (1968) 342.

40. K. Osako, K.N. Nakashiro, Y. Ono, *Bull. Chem. Soc. Jpn.,* **66**(3), (1993) 755.

41. U. Kuerschner, B. Parlitz, E. Schreier, G. Oehlmann, J. Voelter, *Appl. Catal.,* **30**(1), (1987) 159.

42. F. Roessner, A. Hagen, U. Mroczek, H.G. Karge, K.H. Steinberg, *Stud. Surf. Sci. Catal.,* **75**B, (1993) 1707.

43. E.M. Flanigen, H. Khatami, H.A. Szymanski, *Adv. Chem. Ser.,* **101** (1971) 201.

44. R. Szostak, in *Molecular sieves, Principles of Synthesis and Modification,* Van Nostrand Reinhold, New York (1989).

45. M. Ghamami, L.B. Sand., *Zeolites,* **2** (1982) 143.

46. Yong Shu Jin, Aline Auroux, Jacques C. Vedrine *Appl. Catal.,* **37** (1988) 1.

47. P.A. Jacobs, H.K. Bayer, J. Valyon, *Zeolites,* **1** (1981) 161.

48. J. Perez-Pariente, J.A. Martens, P.A. Jacobs *Appl. Catal.,* 31 (1987) 35.

49. J.W. Ward, in *Zeolite Chemistry and Catalysis*, J. Rabo (Ed) ACD Monograph, 1976.

50. E. Bourgeat-Lami, P. Massiani, F. Di Renzo, P. Espiau, F. F. Des Courieres *Appl. Catal.*, **72** (1991) 139.

51. M. Maache, A. Janin, J. C. Lavalley, E. Benazzi *Zeolites,* **15** (1995) 507.

52. P.A. Jacobs, R. von Ballmoos, *J. Phys. Chem.,* **86** (1982) 3050.

53. C.T.W. Chu, C.D. Chang, *J. Phys. Chem.,* **89** (1985) 1569.

54. V.L. Zholobenko, L.M. Kustov, V.Y. Borovkov, V.B. Kazasky, *Zeolites,* **8** (1988) 150.

55. I. Kiricsi, C. Flego, G. Pazzuconi, W.O. Parker, R. Millini, C. Perego Jr., G. Bellussi, *J. Phys. Chem.,* **98** (1994) 4627.

56. R. Szostak, *Stud. Surf. Sci. Catal.,* **58** (1991) 153.

57. J.W. Ward, *J. Catal.,* **10** (1968) 34.

58. H.G. Karge, in E.G. Derouane et. al. (Editors), *Zeolite Microporous solids: Synthesis, Strucutre and reactivity*, Kluwer, Dordrecht, 1992, p. 273

59. G. Muller, G. Eder-Mirth, J.A. Lercher, *J. Phys. Chem.,* **99**(32) (1995) 12327.

60. E.P. Parry, *J. Catal.,* **2** (1963) 371

61. S.G. Hedge, P. Ratnasamy, L.M. Kustov, V.B. Kazansky, *Zeolites*, **8**(2), (1988) 137

62. J. A. Biscardi, E. Iglesia, *Catal. Today*, **31** (1996) 207.

63. C.D. Wagner, W.M. Riggs, L.E. Davis, J.F. Moulder, G.F. Muilenberg, *Handbook of x-ray photoelectron spectroscopy*, Perkin-elmer Corporation, Physical Electronics Division, Eden Prairie, MN, 1979, and references therein

Chapter –3

Synthesis of Nitrogen containing

Heterocycles

Section –1

Catalysis over Medium pore zeolite

(Ferrierite)

3.1.VAPOR PHASE BECKMANN REARRANGEMENT OF CYCLOHEXANONE OXIME OVER DIFFERENT FERRIERITE ZEOLITE CATALYSTS

3.1.1. INTRODUCTION

When ketoximes are treated with a strong Brönsted or Lewis acid, they are converted to amides in a reaction known as the Beckmann rearrangement [1]. The most commercially important reaction of Beckmann rearrangement is that of cyclohexanone oxime to ε-caprolactam. Almost all of the world's annual production of ca. 3×10^6 tons of ε-caprolactam is consumed as the monomer for nylon-6 fibers and plastic. There are five major commercial routes to ε-caprolactam, which are practiced today [2]. Conventional methods of preparation of ε-caprolactam involve treating cyclohexanone oxime with concentrated sulfuric acid or phosphoric acid as the catalyst, followed by neutralization with liquid ammonia. The process suffers from number of disadvantages, such as, requirement of large quantity of ammonia for the neutralization of sulfuric acid, separation of ε-caprolactam from the product mixture, undesirable large quantities of ammonium sulfate or ammonium phosphate than the desired ε-caprolactam and equipment corrosion due to concentrated acids.

To overcome these problems, a vapor phase Beckmann rearrangement of cyclohexanone oxime using various solid catalysts has been extensively investigated. Catalysts studied include silica and borophosphoric acid [3], phosphoric acid supported on Kieselguhr [4], Keargy-type aluminum orthophosphates and γ-alumina mixtures [5], apatites, ortho-, pyro-, meta-, and triphosphates [6], boron oxide supported on alumina [7-10.] or silica [11], silica-supported tantalum oxide catalysts [12] and silica monolayers on γ-Al_2O_3, ZrO_2, and TiO_2 [13].

More recently, a good deal of attention has been focused on zeolites as solid acids for the Beckmann rearrangement. Deactivation is a commonly reported phenomenon.

Zeolites like Y [14,15], ZSM-5 [16] Beta [18] and mordenite [19] have been proposed for the Beckmann rearrangement of cyclohexanone oxime to ε-caprolactam. However, the efficiency of these solid acid catalysts is low since they are deactivated rapidly during the reaction. Figure 3.1.1 shows the schematic representation of both the conventional and new processes for the preparation of ε-caprolactam.

The principal byproduct was 5-cyanopent-1-ene with traces of cyclohexanone and cyclohexanol [14]. Aucejo et a1.[15] reported that byproduct 5-cyanopent-1-ene was formed mainly on the Na^+ ions of the zeolite.

Sato et al. [20,21] studied the vapor phase Beckmann rearrangement with some MFI zeolites (equivalent to ZSM-5) as a catalyst and summarized their interesting results (i) the catalytic activity and selectivity to ε-caprolactam increased, to some extent (Si/Al ≤ 1000) proportionally to the Si/Al ratio, (ii) The activity and selectivity were almost inversely proportional to the acid amount on the external surface of MFI crystals, (iii) The external surface area of the zeolite crystals affected the catalytic activity. The zeolites of large external surface area gave high conversion of cyclohexanone oxime. They strongly suggested that the vapor phase Beckmann reaction took place on the outer surface of the catalyst, and the active sites might be different from the acid sites caused by Al. Hoelderich et al. [22] found by SIMS-XPS studies that the deactivation of the B-MFI catalyst takes place at the outer surface and concluded that the reaction occurs at the outer surface of the zeolitic catalyst. They also pointed out a pore blocking effect caused by an enrichment of nitrogen containing species inside the pore system, which were formed by oligomerization or polymerization of hexane nitriles. Also Hoelderich and co-workers concluded that the silanol nests were most suitable for the reaction and that the vicinal silanol groups were more favorable than the terminal silanols. This research group also demonstrated that such

weakly acidic zeolitic catalysts can be generated by using B-MFI catalyst as the starting

material [23-25].
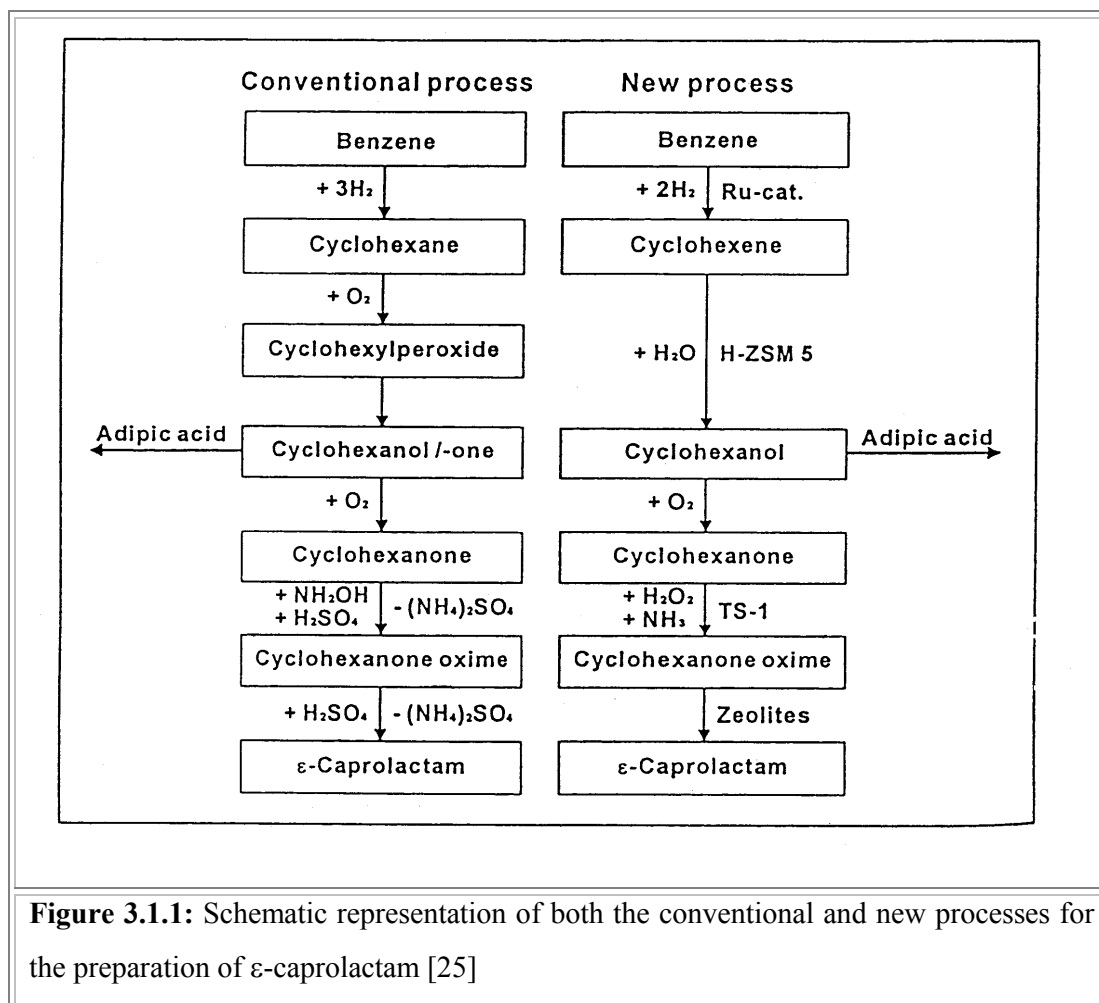
Figure 3.1.1: Schematic representation of both the conventional and new processes for the preparation of ε-caprolactam [25]

Yashima et al. [26] studied the vapor phase Beckmann rearrangement of

cyclohexanone oxime on some zeolite catalysts that had different pore windows, and

reported that the catalyst which had a smaller pore window than the molecular size of

cyclohexanone oxime showed a high selectivity for caprolactam formation, and therefore,

the selective rearrangement reaction was performed on the external surface of zeolite

crystals. However, percent conversion of the oxime and percent selectivity to the lactam

still decreased with time in all cases. Thangaraj et al. [27] examined ZSM-5, silicalite, and

titanium silicalite (TS-1) and found that incorporation of Ti increased the percent selectivity and lowered the deactivation rate.

A detailed study of Beckmann rearrangement of cyclohexanone oxime was not reported so far in the literature over H-ferrierite. In this study, we synthesized ferrierite zeolite in presence of pyrrolidine template (Chapter 2). The purpose of this study is to clarify the influence of various ferrierite zeolite catalysts on the oxime conversion and selectivity for ε-caprolactam formation. The application of ferrierite zeolite is expected to give better results due to its acidic nature and stable performance as in other hydrocarbon conversion reactions.

3.1.2. EXPERIMENTAL

3.1.2.1. Materials and Catalysts

Cyclohexanone oxime (> 99% purity, Aldrich), acetonitrile, benzene, and ethanol were obtained from s.d. fine chemicals, India (>99% purity). The vapor phase Beckmann rearrangement of cyclohexanone oxime to ε-caprolactam was investigated over four different FER zeolite catalysts, Viz., (i) H-FER, (ii) St-H-FER, (iii) Si-FER, and (iv) Na-H-FER with different exchange levels of Na. Their preparation and detailed characterization of some of the catalyst was described in the chapter 2.

3.1.2.2. Reactor and experimental setup

The powdered catalysts are pressed, pelleted, crushed and sieved to obtain 10-20 mesh particles. All the reactions are carried out at atmospheric pressure in a fixed bed down flow reactor (figure 2.23(a), chapter 2). About 3g of catalyst was placed in a cylindrical glass reactor (1.5cm i.d; 30cm length), having thermowell of 4mm at the centre. The catalyst was packed in-between inert ceramic beads in such a way that the thermowell top was at the centre of the catalyst bed. Also the portion above the catalyst bed served as preheater. The reactor was placed in a constant temperature zone of an electrically heated

furnace. The catalyst was activated at 500° C for 5 h in a flow of dry air. The catalyst was then flushed with dry nitrogen and cooled to the desired temperature. The cyclohexanone oxime was dissolved in acetonitrile (10 wt%) and injected using a high precision feed pump (ISCO, Model 500D,USA) at the required rate. Nitrogen was used as a carrier gas. The reactions were carried out at different temperatures between 300 and 450°C. The liquid products were analyzed by gas chromatography (HP 6890 series, fitted with HP-1 capillary column and FID as detector, the carrier gas being nitrogen) and confirmed by GCMS (QP 2000A, Shimadzu SE-52 column, non-polar silicon fluid).

3.1.3. RESULTS AND DISCUSSIONS

The vapor phase Beckmann rearrangement of cyclohexanone oxime mainly yielded ε-caprolactam and the by-products being cyclohexanone, cyclohexenone, 1-cyanopentane and 1-cyanopentene and polymer of ε-caprolactam which was shown as in the tables under 'others'.

3.1.3.1. Effect of reaction time

The oxime conversion and selectivity of ε-caprolactam with time is shown in figure 3.1.2. The catalyst activity and product selectivity reached an equilibrium level after 3 to 4h and hence all the experimental data were obtained after the stabilization of the activity. Influence of different reaction parameters on the conversion of oxime and selectivities of different products are discussed below.

3.1.3.2. Influence of temperature

The conversions of cyclohexanone oxime and caprolactam yield at different temperatures over H-FER, Si-FER and St-H-FER are shown in table 3.1.1. It can be observed from table 3.1.1 that with increase in temperature from 300 to 450°C, oxime conversion increases. However, the selectivity towards ε-caprolactam increased with temperature up to 400°C and then decreased.

85
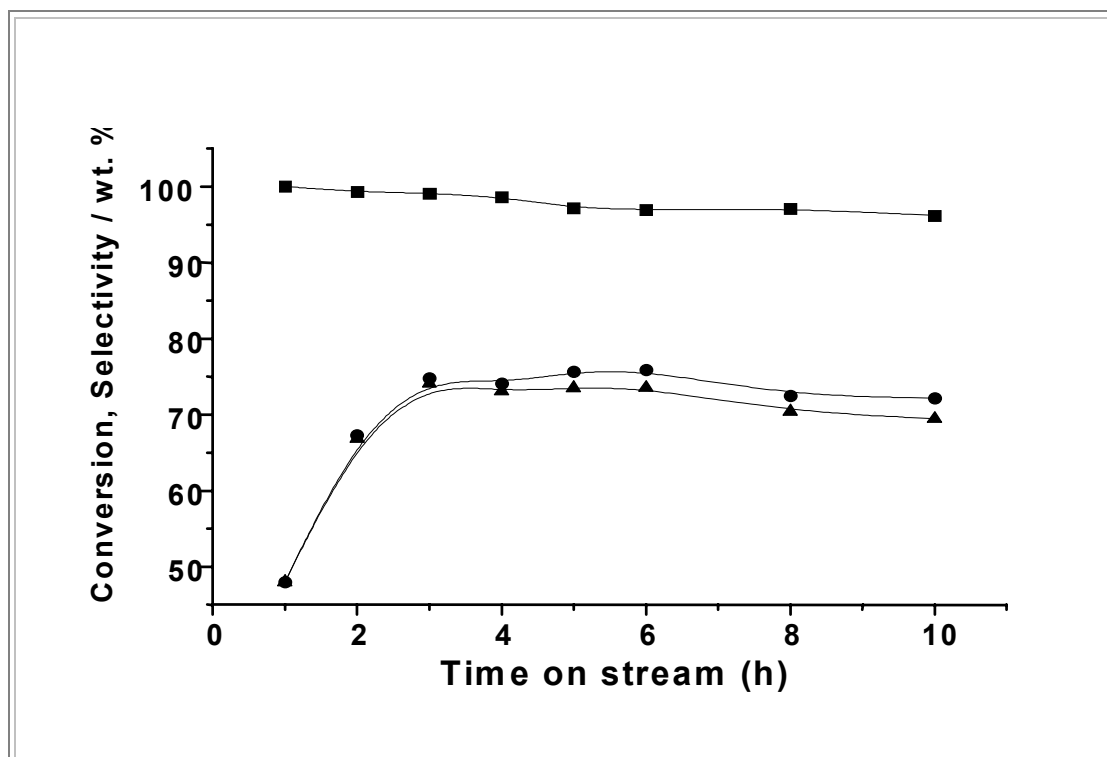
Figure 3.1.2: Influence of time on the conversion and selectivity for Beckmann rearrangement of cyclohexanone oxime over H-ferrierite (■) conversion, wt. % of oxime; (●) selectivity, wt. % of caprolactam; (▲) yield, wt. % caprolactam.

Reaction conditions: Temp. = 400°C ; Pressure = 1 atm.; WHSV = $1h^{-1}$; Oxime concentration in feed = 10wt.% in acetonitrile; Nitrogen flow rate = 20 ml min^{-1}; Catalyst wt. = 3g.

At higher temperature (450°C) the conversion for oxime was 99.9 and 95.4% while the selectivity towards ε-caprolactam was 73.5% and 79.9% for the sample H-FER and St-H-FER. This low selectivity as compared with the data of reaction temperature 400°C is due to decomposition of ε-caprolactam at high temperature on the catalyst surface. Table 3.1.1 also shows that H-FER at 350°C gives better performance towards conversion and yield as compared with the steamed sample. This is due to the acidic differences as detailed in the TPD studies in chapter 2.

Table 3.1.1: Influence of different temperature on the conversion of oxime and selectivity of ε-caprolactam using ferrierite catalyst.

Catalyst	Temp (°C)	Oxime Conv. (Wt%)	Selectivities (Wt%)[a]				Yield[b]
			A	B	C	D	
H-FER	300	80.6	77	8.2	13.8	0.9	62.06
	350	91.3	84.3	6.8	12.7	2.2	76.96
	400	99.3	74.8	9	13.4	2.8	74.28
	450	99.9	73.5	9.2	14.1	3.2	73.43
Si-FER	350	43.3	20.7	29.9	38.4	11	8.96
	400	64.2	42.1	19.9	29.5	8.5	27.03
	450	93.1	24	13.7	25.7	36.5	22.34
St-H-FER	300	71.7	79.3	8.1	9.4	3.2	56.85
	350	82.1	79	7.7	8.6	4.6	64.85
	400	84.2	85.3	6.1	6.5	2.1	71.82
	450	95.4	79.9	4.9	6.5	8.6	76.22

[a]Selectivity (wt.%) = (Wt.% of product formed / Conversion of cyclohexanone oxime) X 100

[b]Yield (wt.%) of caprolactam = (Selectivity wt.% X Conversion wt.%) / 100

A= ε-caprolactam; B= Cyclohexanone; C= Cyanopentane + Cyanopentene; D= Others

Reaction conditions: Pressure = 1 atm.; WHSV = 1h^{-1}; Oxime concentration in feed = 10 wt.% in acetonitrile; Nitrogen flow rate = 20 ml min^{-1}; Time on stream of the reaction = 3h; Catalyst wt. = 3g.

3.1.3.3. Influence of different FER catalysts

The results of the catalytic reactions of the cyclohexanone oxime over different ferrierite catalysts at 400°C are presented in table 3.1.2. The St-H-FER catalyst shows good selectivity towards caprolactam. This is due to the high ratio of SiO_2/Al_2O_3 (73). Increase in SiO_2/Al_2O_3 ratio decreases the total acidity of H-ferrierite zeolites, oxime conversion decreased. It is known that the catalytic activity for Beckmann rearrangement depends upon the acidity and the nature of hydroxyl group of catalysts. Corma et al. [28] reported that the strong Brönsted acidity of Y zeolite is responsible for the formation of lactam.

However, the majority of previous reports have suggested that the very weak [22,24,25] or medium-strength acidity [29] or almost neutral hydroxyl groups [16] of zeolites are favorable for Beckmann rearrangement reaction, while the strong acid sites accelerate the formation of by-products [12]. This is in good agreement with the results of our study, since St-H-FER is weakly acidic as compared to other samples under study. Si-FER showed poor conversion and yield of ε-caprolactam towards this reaction and this may be due to large zeolite crystals and the reaction on the surface. Also, this is in contrast with other studies [30], silanol groups (Si-OH) are not active in the case of FER.

The H-FER shows good conversion of cyclohexanone oxime. Also the Si/Al ratio of H-FER samples was varied and tested at 400°C for this reaction. As the Si/Al ratio increases, the conversion decreases but there is not much difference in the selectivity towards ε-caprolactum. In order to find out effect of sodium on activity, Na-FER was exchanged to different levels with NH_4NO_3 and performed the title reaction with these catalysts. The results are tabulated in table 3.1.2. As the Na % decreases, increase in conversion and selectivity is noticed. The following studies were carried out with H-FER as catalyst.

3.1.3.4. Influence of space velocity (WHSV)

The increase in WHSV of the feed on the conversion of oxime and selectivity of the products is shown in figure 3.1.3 over H-FER catalyst. It can be seen from figure 3.1.3 that as the WHSV increases there is decrease in oxime conversion and increase in caprolactam selectivity. Due to lesser contact time of the reactant, the formation of secondary products cyclohexanone, 5-cyanopentane and 5-cyanopent-1-ene was suppressed at higher WHSV. The maximum yield of caprolactam is at WHSV = 1.

Table 3.1.2: Conversion of cyclohexanone oxime and selectivity for ε-caprolactam over various ferrierite type zeolites**.**

Catalyst	Oxime Conv. (Wt%)	Selectivities (Wt%)[a]				Yield[b]
		A	B	C	D	
Na-FER	92.9	41.2	20.6	20.6	14.7	38.3
Na-H-FER-1 (1.3)[#]	94.4	47.2	19.4	22.2	5.6	44.5
Na-H-FER-2 (1.1)[#]	98.3	65	15.1	16.4	1.9	63.9
H-FER (10)[*]	100	76	5.4	10.9	5.4	76
H-FER (17)[*]	99.3	74.8	9	13.4	2.8	74.3
H-FER (25)[*]	98.3	77.5	8.5	9.4	4.6	76.2
St-H-FER	84.2	85.3	6.1	6.5	2.1	71.8
Si-FER	64.2	42.1	19.9	29.5	8.5	27

[a, b] See footnotes in Table 3.1.1

[#] The value in the parentheses represents the Si/Al ratio by EDX.

[*] The value in the parentheses represents the Na weight percent by EDX.

A= ε-caprolactam; B= Cyclohexanone; C= Cyanopentane + Cyanopentene; D= Others

Reaction conditions: Temp. = 400°C ; Pressure = 1 atm.; WHSV = 1h^{-1}; Oxime concentration in feed = 10 wt.% in acetonitrile; Nitrogen flow rate = 20 ml min^{-1}; Time on stream of the reaction = 3h; Catalyst wt. = 3g.

3.1.3.5. Influence of solvent

Table 3.1.3 shows the influences of various solvents for cyclohexanone oxime on the catalytic performance of H-FER. There is not much appreciable change in the conversion but the selectivity of ε-caprolactam was strongly influenced by the type of solvent used. The selectivity increases by increasing the dipole moment of solvent. The selectivity in presence of benzene (0 D) was low (69.4 wt.%), selectivity in presence of ethanol (1.44D) was 70.7 wt.% while selectivity in presence of acetonitrile (3.92 D) was high (74.8 wt.%). Roseler et al. [24] have reported the deactivation of MFI borosilicate in the Beckmann rearrangement of cyclohexanone oxime using different organic solvents and

found that the degree of deactivation depends on the kind of solvent used. Komatsu et al. [31] have reported that the solvent with medium polarity was preferable for the Beckmann rearrangement on silicalite-1. But for ferrierite it is observed that the solvent with high polarity is preferable for this reaction.

Figure 3.1.3: Influence of W.H.S.V. data on the conversion and selectivity for Beckmann rearrangement of cyclohexanone oxime over H-ferrierite
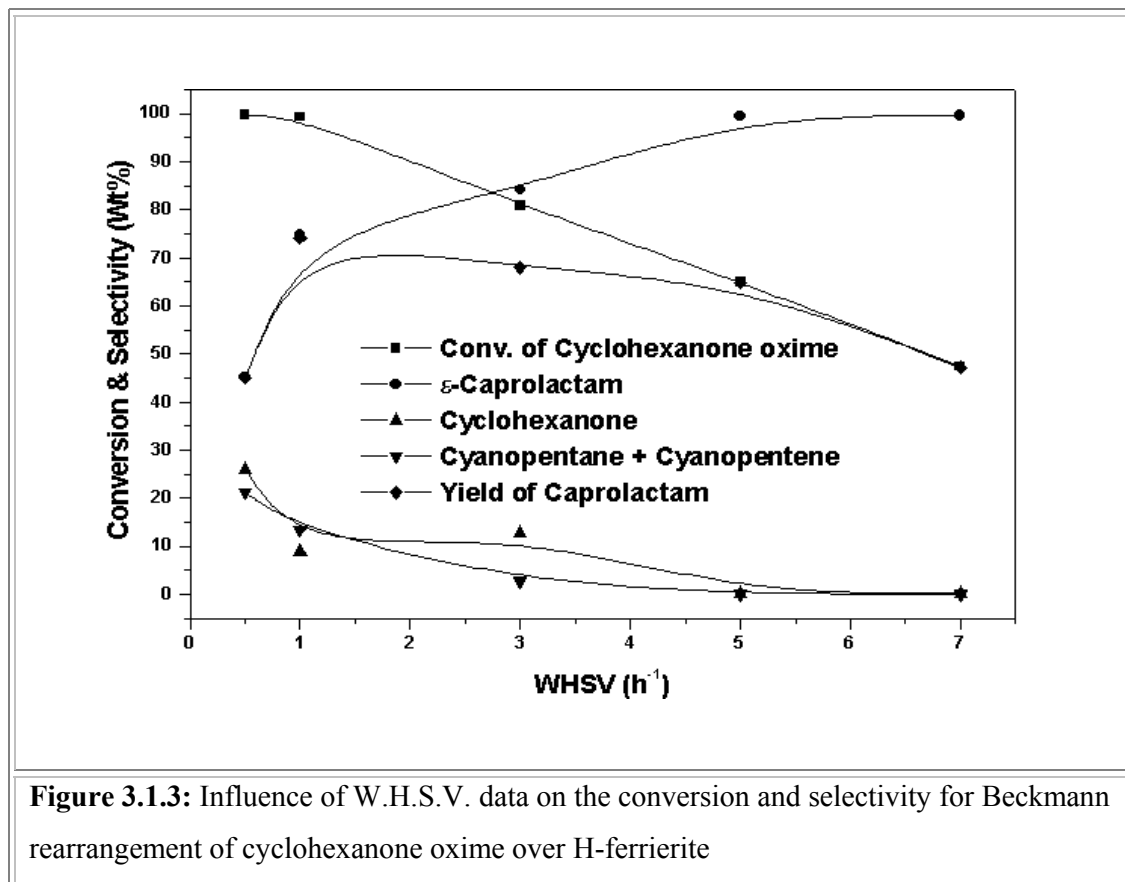
Reaction conditions: Temp. = 400°C ; Pressure = 1 atm.; Oxime concentration in feed = 10 wt.% in solvent; Nitrogen flow rate = 20 ml min^{-1}; Time on stream of the reaction = 3h; Catalyst wt. = 3g.

3.1.3.6. Influence of concentration of cyclohexanone oxime

It can be seen from table 3.1.4 that the dilution of the cyclohexanone oxime in acetonitrile improves the conversion and the selectivity of caprolactam. At low oxime concentration (2.5 wt.%) the yield of caprolactam was high. At high oxime concentration (20 wt.%) in acetonitrile the formation of by-products cyclohexanone, cyanopentane and cyanopentene were high. Also with higher concentration of oxime deactivation of the catalyst is rather faster.

Table 3.1.3: Influence of various solvents for cyclohexanone oxime on the catalytic performance of H-FER

Solvent	Oxime Conv. (Wt%)	Selectivities (Wt%)[a]				Yield[b]
		A	B	C	D	
Ethanol	99.5	70.7	7.8	20.3	1.2	70.35
Acetonitrile	99.3	74.8	9	13.4	2.8	74.28
Benzene	95.7	69.4	9.5	12.2	8.9	66.41

[a, b] See footnotes in Table 3.1.1

A= ε-caprolactam; B= Cyclohexanone; C= Cyanopentane + Cyanopentene; D= Others

Reaction conditions: Temp. = 400°C ; Pressure = 1 atm.; WHSV = 1h^{-1}; Oxime concentration in feed = 10 wt.% in solvent; Nitrogen flow rate = 20 ml min^{-1}; Time on stream of the reaction = 3h; Catalyst wt. = 3g.

Table 3.1.4: Influence of oxime concentration on oxime conversion and caprolactam selectivity using H-FER as a catalyst.

Oxime Concentration (Wt%)	Oxime Conv. (Wt%)	Selectivities (Wt%)[a]				Yield[b]
		A	B	C	D	
2.5	99.8	95.5	3.2	0.9	0.4	95.31
5	99.6	87.7	6.7	4.4	1.2	87.35
10	99.3	74.8	9	13.4	2.8	74.28
20	90.1	49	20.3	18.1	12.6	44.15

[a, b] See footnotes in Table 3.1.1

A= ε-caprolactam; B= cyclohexanone; C= Cyanopentane + Cyanopentene; D= Others

Reaction conditions: Temp. = 400°C ; Pressure = 1 atm.; WHSV = 1h^{-1}; Solvent = acetonitrile; Nitrogen flow rate = 20 ml min^{-1}; Time on stream of the reaction = 3h; Catalyst wt. = 3g.

3.1.3.7. Influence of N$_2$ feed

Table 3.1.5. shows the influence of nitrogen flow on the conversion of oxime and selectivity of ε-caprolactam. Increase in flow rate of N$_2$, reduces the residence time of reactants over the catalyst leading to increase in selectivity and decrease in conversion of oxime. The yield of ε-caprolactam is maximum when the carrier gas flow rate was 20ml/min. At higher nitrogen flow rate the selectivity of cyclohexanone is seen to increase.

Table 3.1.5: Influence of nitrogen feed on the oxime conversion and caprolactam selectivity using H-FER as a catalyst.

N$_2$ Feed	Oxime Conv. (Wt%)	Selectivities (Wt%)[a]				Yield[b]
		A	B	C	D	
140	94.3	70.4	25.9	1.2	2.5	66.39
90	96.6	70.1	22.4	3.4	4.1	67.72
60	98.6	71.4	17	7.7	3.9	70.40
20	99.3	74.8	9	13.4	2.8	74.28

[a, b] See footnotes in Table 3.1.1

A= ε-caprolactam; B= cyclohexanone; C= Cyanopentane + Cyanopentene; D= Others

Reaction conditions: Temp. = 400°C ; Pressure = 1 atm.; WHSV = 1h^{-1}; Oxime concentration in feed = 10 wt.% in acetonitrile; Time on stream of the reaction = 3h; Catalyst wt. = 3g.

3.1.3.8. Mechanism

Based on the above studies, following mechanism similar to that one proposed earlier [31] can hold here also: Protonation of the OH group followed by concerted dehydration/migration and subsequently water addition (figure 3.1.4.).
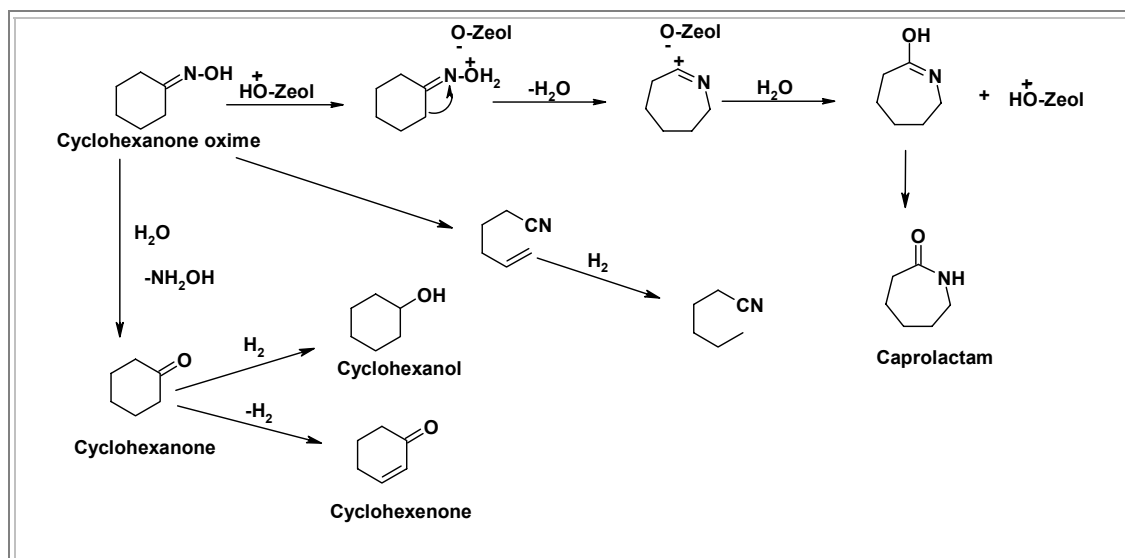
Figure 3.1.4: Mechanism for Beckmann rearrangement of cyclohexanone oxime over zeolite catalysts.

3.1.4. CONCLUSIONS

In conclusion, using appropriate Si/Al ratio or highly dealuminated H-ferrierite and an appropriate diluent can increase catalytic performance of H-ferrierite zeolite catalysts for the vapor phase Beckmann rearrangement of cyclohexanone oxime. H-FER and St-H-FER catalysts show good activity at 350°C. It is also seen that the type of solvent used for this rearrangement strongly affects the conversion of cyclohexanone oxime and selectivity of ε-caprolactam. Acetonitrile has been found to be the best solvent for cyclohexanone oxime to improve the selectivity for ε-caprolactam formation.

3.2. LIQUID PHASE SYNTHESIS OF PYRIDINE BASES OVER FERRIERITE ZEOLITE CATALYST

3.2.1. INTRODUCTION: PYRIDINE BASES

Nitrogen-containing compounds are used as structural components of pharmaceuticals and agrochemicals due to their high biological activities. There are many nitrogen-containing chemicals, from simple structured compounds as pyridine bases to complicated compounds as pharmaceutical ingredients and their number is growing rapidly year-by-year. Among the nitrogen containing compounds, pyridine bases are produced in by far the largest quantity.

Apart from the long established uses of pyridine and alkylpyridines (known collectively as pyridine bases) as solvents [33,34], catalysts [34] and acid scavengers [34], a large and growing demand for them as intermediates in the formation of medicines [33-36], dietary supplements [33-36], herbicides [33,34], disinfectants [34] and pesticides.

These compounds can be prepared by the heterogeneous gas-phase cyclization of simple organic molecules in the presence of ammonia. Most of the pyridine bases have been mass-produced by Chichibabin condensation, which includes gas phase dehydration

and dehydrogenation reactions between acetaldehyde, formaldehyde and ammonia on an amorphous silica-alumina catalyst [37].

In the industrial process, formaldehyde, acetaldehyde and ammonia are condensed over alumino-silicate catalyst (80's and early 90's), at temperatures between 300 and 550°C to give pyridine and β-picoline.
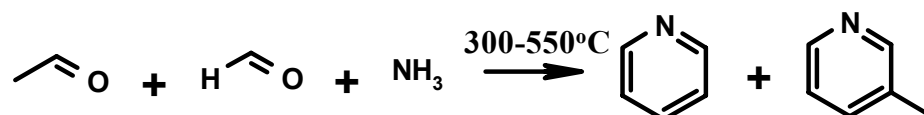
3.2.1.1. Mechanism

Formation of imines by both Homogeneous and heterogeneous reactions

(a) Homogeneous reaction
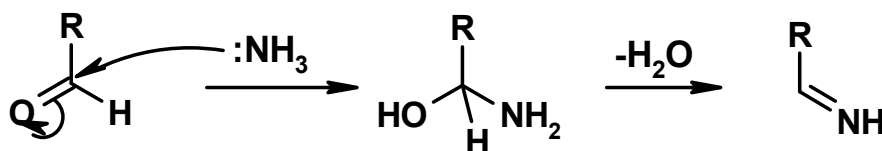
(b) Heterogeneous reaction
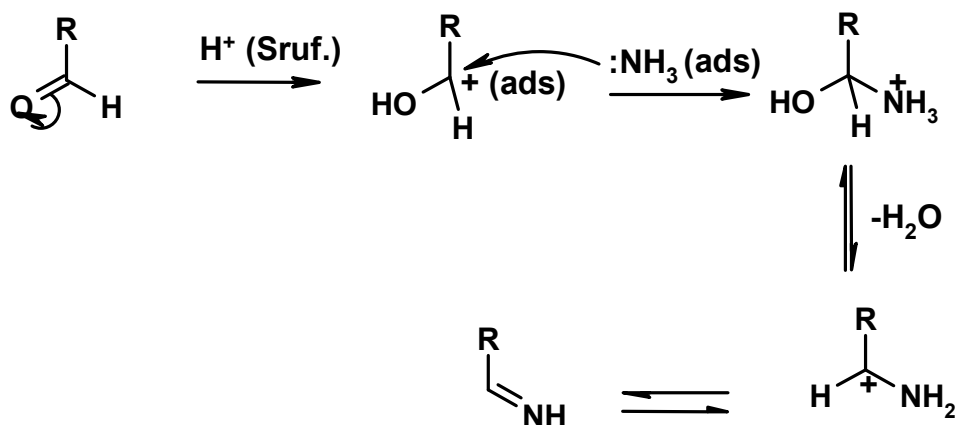
Nucleophilic addition of ammonia to an aldehyde can occur homogeneously, but catalysts (aluminosilicates, zeolites) readily adsorb ammonia and also promote the formation of carbocations.

94

So the first step is the adsorption of reactants to near or acidic sites, forming adsorbed ammonia and carbonium ions. Nucleophilic addition of ammonia occurs at the surface of the catalyst, followed by loss of water to leave adsorbed imines.

Formation of pyridine bases

(i) Homogeneously catalyzed cyclization of allylamines
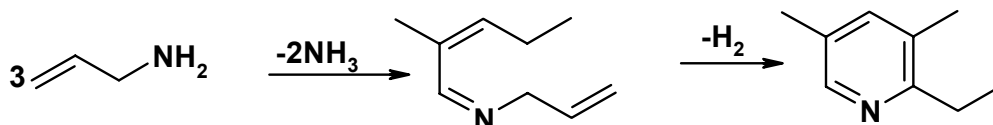
(ii) Heterogeneously catalyzed cyclization of allylamines
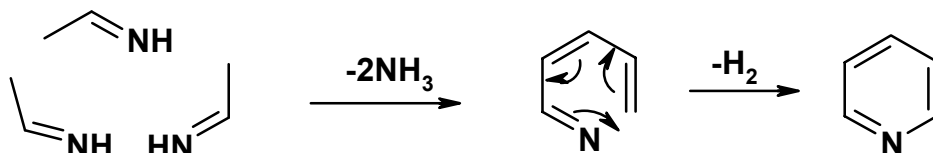
Analysis of intermediates in homogeneously catalyzed reaction of allylamines in liquid phase shown two molecules of ammonia are eliminated and loss of a hydrogen molecule occur before ring closure. Similar mechanisms are proposed for latter stages of both homogeneous and heterogeneous conversion of carbonyl compounds to pyridine bases.

3.2.1.2. Catalysts employed in synthesis of pyridine bases

The alumino-silicate catalyst is best employed in a fluidised-bed reactor [38]. Its performance can be improved by the addition of halides [39-42] and/ or metal oxides [43, 44]. Alternative catalysts include mixed-metal phosphates [45,46] and crystalline zeolites. In particular, highly siliceous ZSM-5 may prove very useful as it allows high conversion (up to 93%) to bases that include dimethylpyridines (lutidines) [47]. Antonova and coworkers [48] have deduced that if the acidity is too high, the reaction is retarded because of unreactive adsorbed ammonium ions. Therefore, the overall acidity of the solid is not as

important as the nature and distribution of acid sites at its surface. Brönsted acid sites would be involved in the creation of carbonium ions, where as Lewis sites would allow the formation of labile adsorbed ammonia.

3.2.1.3. Zeolites

Zeolites have been extensively used for the condensation of carbonyl compounds in presence of ammonia to form heterocyclics, notably alkylpyridines. A wide section of substituted pyridines have been generated using industrial aldehydes and ketones or mixtures thereof as reactants. To obtain adequate conversion in such systems, temperatures must be relatively high, i.e. in the 300-450°C range, in order to counteract the poisoning adsorption of NH_3 and the basic products on the acid sites [49]. Analyzing the product distributions and assessing side reactions in these transformations can be challenging, since the already complex chemical pathways of aldol condensation are superimposed upon ammonia addition, water elimination and other processes. The appreciable resonance energy of pyridine (23 kcal/mol) [50] provides a driving force for the dehydrogenation step. In the reaction of acetone, methanol and NH_3 to from 2,6-lutidine [51] Van der Gaag et al. found, using ^{13}C-labelled methanol that the ^{13}C appeared exclusively at the 4-position. An argument for methanol dehydrogenation to formaldehyde seems reasonable in this case, although numerous mechanistic options exists [51]. Also in the oxidative cyclocondensation of ethanol and NH_3 to pyridines [49,52], dehydrogenation of ethanol to acetaldehyde followed by aldol-type condensation, ammonia addition, cyclization, dehydrogenation, etc. is plausible. The synthesis of pyridine bases from various aldehydes or ketones with ammonia over zeolite catalyst was tabulated in table 3.2.1.

In this study, the application of ferrierite zeolite for the synthesis of pyridine bases from simpler molecules like acetone, acetaldehyde/formaldehyde and ammonia in liquid phase at autogeneous pressure was attempted.

Table 3.2.1: Synthesis of pyridine bases using zeolite catalyst reported in the literature.

Materials	Product	Catalyst: Conditions	Ref.
Acetaldehyde, NH$_3$	α + γ-picolines	NaX, H-MOR : 300-420°C	[53]
		H-ZSM-5, Cd, Cu-, Ni-ZSM-5: 427°C	[54]
Acetaldehyde, formaldehyde, NH$_3$	Pyridine, β-picoline	Zeolites: 450°C	[55]
		H-ZSM-5, H-MOR: 427°C	[54]
Acrolein, butanal, NH$_3$	β-ethylpyridine	B-ZSM-5: 400°C	[56, 57]
Acrolein, hexanal, NH$_3$	β-butylpyridine	B-ZSM-5: 400°C	[56, 57]
Acrolein, octanal, NH$_3$	β-hexylpyridine	B-ZSM-5: 400°C	[56, 57]
Acetone, NH$_3$	2,6-lutidine, 2,4,6-trimethylpyridine	H-ZSM-5: 454°C	[51]
Acetone, methanol, NH$_3$	2,6-lutidine	H-ZSM-5, H-MOR: 450°C	[51]
Acetone, methylamine, SO$_2$	4-methylthiazole	Cs-, Rb-, K-ZSM-5, -β: 450-500°C	[58]
Glutaraldehyde, NH$_3$	Pyridine	H-ZSM-5, B-, Co-, La-ZSM-5, LaY: 400°C	[59]
Acetylene or methylacetylene, NH$_3$	Methylpyridines	Ag-X: 100-300°C	[60]
Phenylacetylene, acetonitrile	Diphenylmethylpyridines	NaCo-Y, -MOR: ~100°C	[61]
Ethanol, NH$_3$, O$_2$	Pyridine, α-picoline	H-ZSM-5: 320-380°C	[49]
		H-, B-, Fe-ZSM-5: 340-400°C	[51]

3.2.2. EXPERIMENTAL

The synthesis of pyridine bases was carried out in a batch reactor (100 ml PARR autoclave Model No.4842 USA, figure 2.34b, chapter 2) in the temperature range 140-250°C under autogeneous pressure. All the chemicals (acetone, acetaldehyde, formaldehyde and ammonia solution) were obtained from E-Merck (AR Grade) and used without further purification. A typical reaction mixture contains acetone, acetaldehyde and ammonia solution (30%) in the molar ratio 2:1:4 respectively. To this mixture 10 wt% of freshly activated catalyst (200°C, 2h) was added. The reaction temperature was then raised slowly to the desired value.

The samples of the reaction mixture were isolated from the catalyst after 6h by quenching the reactor in ice-cold water and the collected samples were analyzed by HP 6890 series GC (HP-1, crosslinked methyl siloxane, 30m X 0.32mm X 0.25μm). The GC-MS measurements were performed on a GCMS-QP2000A mass spectrometer equipped with a Shimadzu 14A gas chromatograph. The products were further identified by GC-FTIR (Perkin Elmer FT-IR spectrometer, Spectrum 2000, equipped with Perkin Elmer GC-IR system 2000 and Perkin Elmer Autosystem Chromatograph). The selectivity to a product is expressed as the amount of the particular product divided by the total amount of products and multiplied by 100.

3.2.3. RESULTS AND DISCUSSIONS

The experimental data regarding the effect of the reaction temperature on the synthesis of pyridine bases are given in table 3.2.2. The reaction of acetone, acetaldehyde with ammonia (molar ratio of 2:1:4 respectively) was carried out at 150-250°C in a batch reactor under autogeneous pressure. The products of this reaction are picolines (mainly 2- and 4-picoline), lutidines (2,6- and 2,4-lutidines), 2,4,6-collidine, ethylmethylpyridine (5-ethyl,2-methylpyridine) and 2-ethyl,2,6-dimethylpyridine along with other high boiling

fractions (grouped under others in tables). The major product is collidine. The conversion of acetone and acetaldehyde increases with temperature, however, there is not much effect of the reaction temperature on the selectivity towards collidine. The formation of 2- + 4-picoline is high at lower temperature and with increase of temperature an increase in other higher alkyl pyridines are observed by successive reactions/alkylations.

Table 3.2.2: Liquid phase synthesis of pyridine bases: Effect of reaction temperature

Temperature °C	150	180	200	225	250
Conv. Acetone	37.4	44.7	45.9	50.8	55.3
Conv. Acetaldehyde	85.3	88.6	94.6	100	100
Product Distribution (wt%)					
Low Boilers	1.6	1.4	2.9	2.1	1.8
2- and 4-Picoline	15.3	7.8	2.5	3.1	4
2,6-Lutidine	11.6	15	10.8	15.9	15.6
2,4-Lutidine	5.2	4.4	8.8	9.2	11
2,4,6-Collidine	51.7	53.7	57.3	51.8	50.6
5-ethyl-2-methyl pyridine	7	6.1	5.4	7	5.1
2-ethyl,2,6-dimethyl pyridine	2.2	5.1	6.5	4.5	4.5
Others[a]	5.4	6.5	5.8	6.4	7.4

Reaction Conditions: Catalyst 0.1g; time 6h; Acetone:Acetaldehyde:NH_3 molar ratio (2:1:4)

[a]Others include higher alkyl pyridines and oligomers of acetaldehyde

The reaction was studied at 180°C with different catalyst amount and the results of influence of the catalyst concentration are shown in table 3.2.3. With an increase in catalyst concentration from 0.1g to 0.5g, the conversion of both acetone and acetaldehyde increases. However, a decrease in the selectivity of collidine with concomitant increase in low boiling fractions was observed. This indicates that the converted acetone and acetaldehyde are not utilized in the cyclization reaction towards pyridines. Further when

the above reaction was carried out in the absence of a catalyst the conversion of acetone and acetaldehyde decreased (~ 27 and 80 % respectively) and low boiling compounds and oligomers of acetaldehyde are the major products. This result indicates that the presence of catalyst leads to the dehydrocyclization reaction and subsequent pyridine formation reaction.

Table 3.2.3: Liquid phase synthesis of pyridine bases: Effect of catalyst concentration

Catalyst amount (g)	0.1	0.25	0.5	Thermal*
Conv. Acetone	44.7	50.8	53.4	27.4
Conv. Acetaldehyde	88.6	95.7	100	80.1
Product Distribution (wt%)				
Low Boilers	1.4	9.7	11.2	81.6
2- and 4-Picoline	7.8	5.6	4.3	1.8
2,6-Lutidine	15	13.2	12.7	1.2
2,4-Lutidine	4.4	3.4	4.4	1.6
2,4,6-Collidine	53.7	49.9	45	3.4
5-ethyl-2-methyl pyridine	6.1	5.4	7.5	0
2-ethyl,2,6-dimethyl pyridine	5.1	6	7.5	0
Others[a]	6.5	6.8	7.4	10.4

* Reaction carried out without catalyst at 180°C

Reaction Conditions: Temperature 180°C; time 6h; Acetone:Acetaldehyde:NH_3 molar ratio (2:1:4)

[a]Others include higher alkyl pyridines and oligomers of acetaldehyde

Table 3.2.4. depicts the influence of reaction time over FER zeolite under the reaction conditions (T=180°C; acetone/acetaldehyde/ammonia molar ratio of 2/1/4 respectively). It is observed that the conversion of acetone and acetaldehyde increases with reaction time along with increase in selectivity of collidine with a decrease in picoline and lutidine selectivities.

Table 3.2.4: Liquid phase synthesis of pyridine bases: Effect of reaction time

Time (h)	2	6	12	24
Conv. Acetone	45.3	44.7	49.1	52.6
Conv. Acetaldehyde	83.8	88.6	100	100
Product Distribution (wt%)				
Low Boilers	1.4	1.4	1.5	0.6
2- and 4-Picoline	7.6	7.8	3.7	2.4
2,6-Lutidine	14.4	15	10.5	8.3
2,4-Lutidine	8.6	4.4	7.1	6.5
2,4,6-Collidine	55.3	53.7	59.6	64.3
5-ethyl-2-methyl pyridine	7.6	6.1	5.5	5.1
2-ethyl,2,6-dimethyl pyridine	2.1	5.1	6.2	6.5
Others[a]	3	6.5	5.9	6.3

Reaction Conditions: Temperature 180°C; time 6h Acetone:Acetaldehyde:NH$_3$ molar ratio (2:1:4) Catalyst 0.1g. [a]Others include higher alkyl pyridines and oligomers of acetaldehyde

The possible mechanism can be explained with respect to the product distribution, as given in figure 3.2.1. The mechanism explains the variation in the selectivity. The first step may be the formation of imine by the reaction of acetaldehyde and ammonia. This imine reacts with two molecules of acetone and by cyclization and dehydration leads this intermediate compound to 2,4,6-collidine. To confirm this mechanism a reaction of acetone and formaldehyde with ammonia (molar ratio of 2:1:4 respectively) was carried out at 180°C in a batch reactor under autogeneous pressure, which yielded 2,4-lutidine as major product.

Mechanism of reaction of acetone and acetaldehyde with ammonia
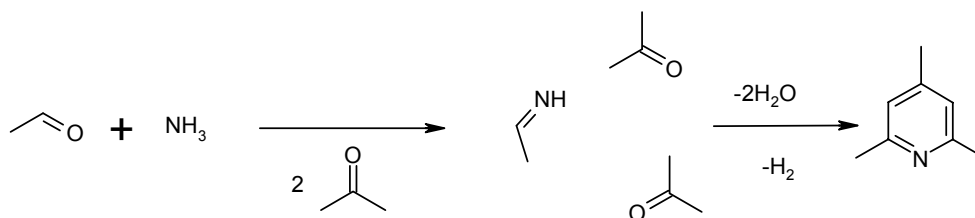
Mechanism of reaction of acetone and formaldehyde with ammonia
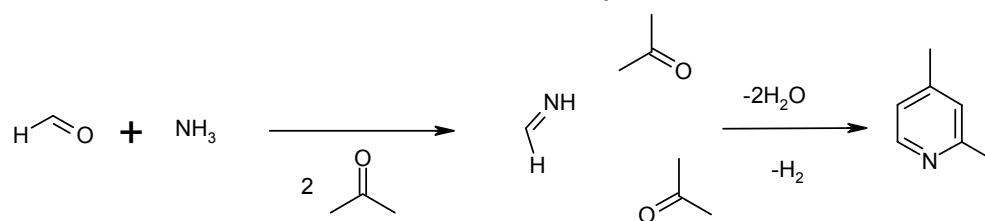
Figure 3.2.1: Plausible route for the synthesis of Pyridine bases (collidine and lutidine)

3.2.4. CONCLUSIONS

The synthesis of pyridine bases from acetone, acetaldehyde and ammonia were carried out under batch conditions in 100 ml PARR autoclave in the temperature range of 140-250°C at autogeneous pressure. FER zeolite affords higher yields of 2,4,6-collidines along with other alkylpyridines. There is no deactivation of the catalyst during the period of study.

Section –2

Catalysis over Zinc-modified

zeolites

3.3. SYNTHESIS OF 2-METHYL PYRAZINE OVER ZINC MODIFIED ZEOLITE CATALYSTS

3.3.1. INTRODUCTION

Pyrazine and alkylpyrazines are used in flavors, fragrances, and pharmaceutical intermediates. Among them, 2-methylpyrazine is used as a raw material of anti-tuberculosis drug, i.e. pyrazinamide. Pyrazines play an important role as intermediates for perfumes, pharmaceuticals and agricultural chemicals. Especially, amides and sulfonamides of pyrazines have been used as anti-tuberculosis, oral anti-diabetics, nutrition supplement, insecticides and fungicides. Okada, for the first time, observed that pyrazine compounds can be produced by the catalytic reaction of diamines with diols in a vapor-phase reaction in the presence of granular alumina [62]. Catalytic systems such as copper-chromium [63], copper-zinc-chromium [64], zinc-phosphoric acid-manganese [65] and silver [66] are patented as catalysts for preparation of 2-methylpyrazine (2-MP) from ethylene diamine (ED) and propylene glycol (PG).

Forni et al. extensively studied this reaction over palladized zinc-chromium oxide

[67] and Pd-promoted ZnO-$ZnCr_2O_4$ mixture [68]. Other studies include those over $MnSO_4$-H_3PO_4-ZnO [69], Ag-La/Al_2O_3 [70], ZnO-WO_3 mixture [71] modified ZSM-5 and chromite catalysts [72]. However, this title reaction was not reported so far over acidic zeolites (both medium and large pore) due to the complexity involved in such cyclization reactions and cracking of the substrates over these acidic zeolites. It is also reported that zinc modified MFI type zeolites are important catalyst for conversions of paraffins [73-76] and also known that ZnO catalyzes effectively in both dehydration and dehydrogenation reactions [77]. Further ZnO prepared from oxalate, or acetate is more active than that prepared from hydroxide [77]. The zeolites H-ZSM-5, H-

FER and H-Beta were selected for studying this reaction and zinc acetate is used for the modification of these zeolites in this investigation.

3.3.2. EXPERIMENTAL

3.3.2.1. Materials and Catalysts

Ethylene diamine and propylene glycol (> 99% purity) were obtained from E-Merck and used as such with out further purification. The title reaction was investigated over three different zinc modified zeolite catalysts, viz., (i) ZnO-FER, (ii) ZnO-ZSM-5, and (iii) ZnO-Beta with almost same amount of zinc impregnated in the zeolite. Their preparation and detailed characterization are discussed in the chapter 2.

3.3.2.2. Catalytic reactions and product analysis

The catalytic activity measurements were carried out at atmospheric pressure in a fixed bed down flow glass reactor (figure 2.23(a), chapter 2) using 3g of the catalyst (10-20 mesh sizes) and the reaction was studied in a temperature range 300 - 450°C. The catalyst was activated in a flow of dry air at 500°C for 5h prior to catalytic runs. The catalyst was then flushed with dry N_2 and cooled to desired temperature. The feed was prepared by mixing an aqueous solution of propylene glycol and ethylene diamine. The liquid reactants were fed into the reactor by a syringe feed pump (SAGE instruments, model 352, USA) at the required rate. The liquid products were collected in an ice-cooled condenser and were analyzed by GC (15-A, Shimadzu) using OV-101 column and confirmed by GC-MS (QP 2000A, Shimadzu) and GC-FTIR (Perkin Elmer, FTIR spectrometer spectrum 2000). The mass balance was > 90%. In the absence of water, high coking is observed.

3.3.3. RESULTS AND DISCUSSIONS

The products formed by intermolecular cyclization reaction of propylene glycol and ethylene diamine are 2-methylpyrazine (2-MP) the desired product and, 2-methyl piperazine (MPIP), the intermediate product. In addition, pyrazine was also formed in large

quantities. Some of the other compounds formed are alkyl pyrazines like dimethyl pyrazines, ethyl pyrazine, methyl-ethyl pyrazines, propyl pyrazine, and low boilers like CO_2, acetaldehyde, ethanol, acetone, propionaldehyde, 2-propen-1-ol, n-propanol and 2-butanone.

Ethylene diamine and propylene glycol combine to form 2-methyl piperazine, which dehydrogenates to form 2-methylpyrazine. The alkylpiperazines dehydrogenate to corresponding alkylpyrazines. Pyrazine is also formed by the dealkylation of alkylpyrazines. It is reported that this reaction involves a rate-determining step of Rideal-Eley type between propylene glycol and ethylene diamine [67]. The reactant feed is prepared by mixing ethylene diamine, propylene glycol and water in the mole ratio (1:1:5). The solvent (water) enables in reducing the viscosity and smooth feeding of the reactants. It also increases the lifetime of the catalyst by desorption of the basic product molecules from the catalyst.

When feeding pure propylene glycol over ZnO-modified FER, a very large number of products were observed. Surprisingly, the above-mentioned low boilers were found in fewer amounts. The major products were acetone, aromatics like benzene, toluene, and xylenes (BTX). When ethylene diamine is fed alone in the absence of propylene glycol, the most abundant products were pyrazine and piperazine, along with considerable amounts of methyl pyrazine, ethyl pyrazine and dimethyl pyrazine. With both ethylene diamine and propylene glycol in the feed, aromatics (BTX) were not found indicating that intermolecular cyclization is the main reaction. A general reaction scheme for the 2-MP synthesis based on the product formation is shown in figure 3.3.1. The decomposition products of ethylene diamine and/or propylene glycol interact with piperazines and pyrazines to form other alkyl pyrazines. The amount of these products is less as compared

to those obtained during the cyclization reaction. The catalysts can be regenerated and used

again by heating the deactivated samples in a flow of air at 500°C for 5h.

Figure 3.3.1: A general reaction scheme for synthesis of 2-MP from ethylene diamine
and propylene glycol over zinc modified zeolites
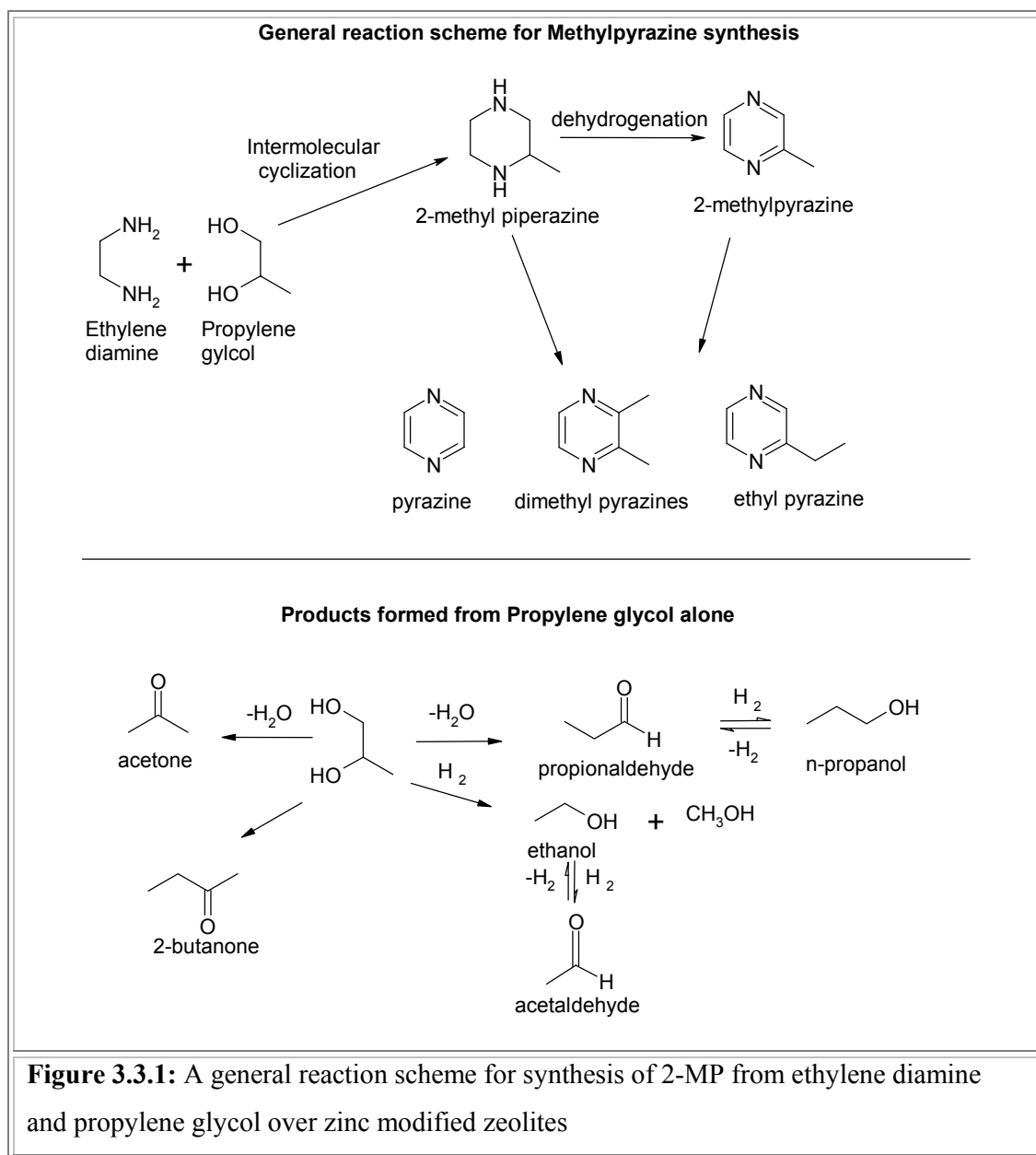
3.3.3.1. Effect of temperature

The effect of temperature on the conversion and product selectivity in the case of

ZnO-ZSM-5 is presented in figure 3.3.2(a). The propylene glycol conversion increased

from 55 % at 300°C to 100 % at 400°C. Considerable amounts of lower boilers (11-34%)

were detected which include methanol, acetaldehyde, ethanol, acetone, propanal, allyl alcohol, n-propanol, butan-2-one. At lower temperatures these were considerable and at higher temperatures even though they are expected to be high, due to the reaction of some of these compounds like methanol, acetaldehyde, with piperazine and pyrazine forming alkyl pyrazines, a reduction in their concentration is observed. It is reported that piperazine or its alkyl derivatives were dehydrogenated easily to corresponding pyrazine derivative over ZnO modified catalyst. At all the temperatures studied, formation of ethyl pyrazine, dimethyl pyrazine, ethyl-methyl pyrazine and propyl pyrazine were observed with all the catalysts studied. The pyrazine and alkyl pyrazines may also be formed by the transalkylation of the adsorbed reaction intermediates.

The product pattern for ZnO-FER (figure 3.3.2(b)) is similar to that obtained for ZnO modified ZSM-5 zeolite. But the selectivity of methyl pyrazine was low at 300°C (7.1%) and increased sharply to 38% at 400°C. In this case, formation of a higher amount of lower boilers was noticed at lower temperatures (63%). Since the conversion of propylene glycol is less at lower temperatures, the formation of alkyl pyrazines, pyrazines and piperazines were very less compared to that of other catalyst system under study.

The activity of the ZnO-Beta (figure 3.3.2(c)) catalyst was high at 300°C, for methyl piperazine (about ~ 30%) however at 400°C it was 1.8 %. In comparison to other two catalysts, ZnO modified Beta afforded a large amount of 2-methylpiperazine and pyrazine showing the high activity towards the cyclization reaction.

107
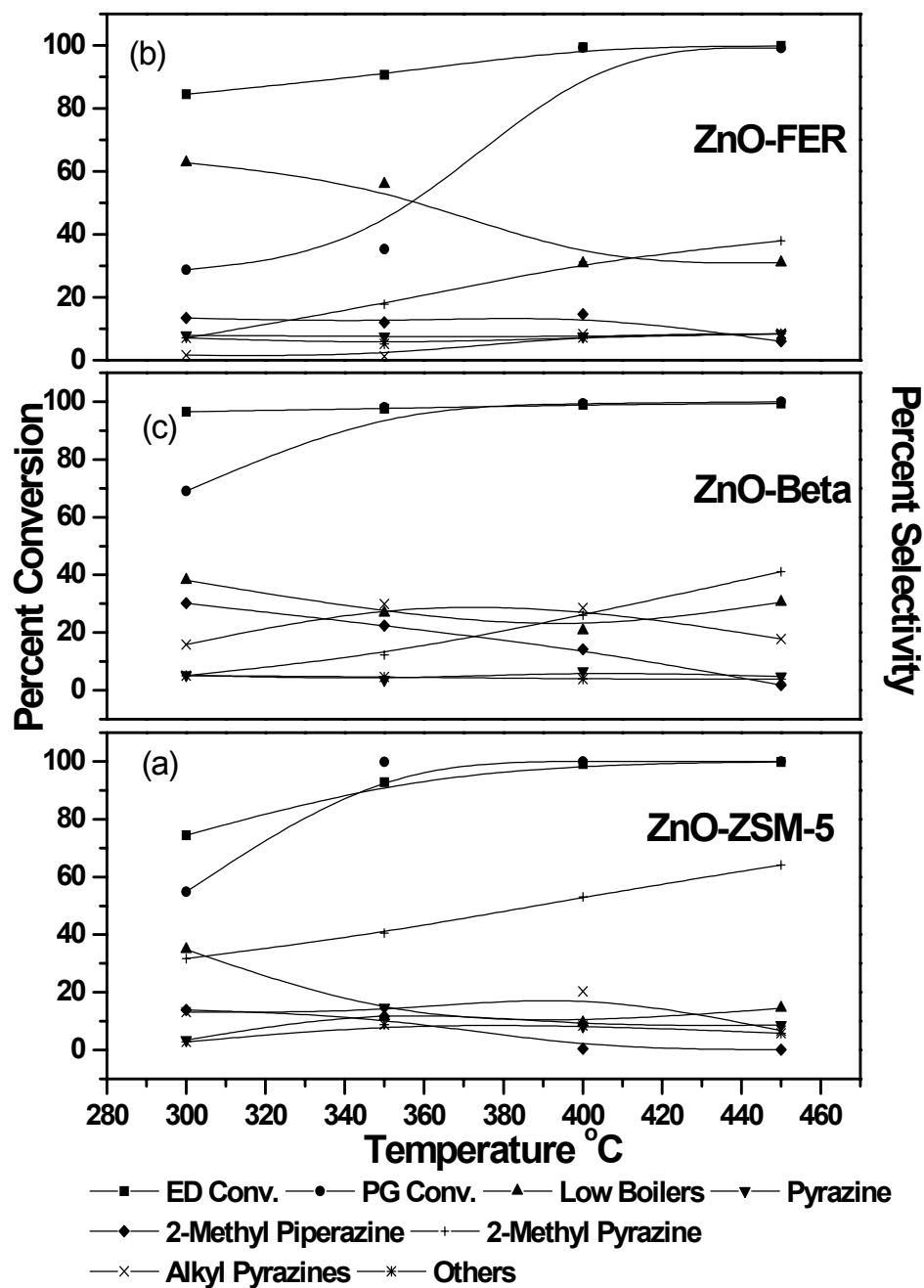
Figure 3.3.2: Effect of temperature on synthesis of 2-MP over ZnO modified zeolites.

Reaction conditions: Pressure atm., WHSV 1h^{-1}, Time 2h, ED: PG: water (1:1:5) mole ratio.

3.3.3.2. Effect of Time on stream

An investigation of the conversion and the product selectivity as a function of time over ZnO-ZSM-5 zeolite is revealed in figure 3.3.3(a). The conversion of ethylene diamine decreases from 99% to 97% after 8h of reaction. However, the methyl pyrazine concentration gradually decreased from 53 to 37% with slight increase in the selectivity for lower boilers. The major observation is that in the initial stages of the reaction the conversion of low boiling compounds and methyl piperazine to the desired products is high and at the end of the study (8h) the formation of the desired compounds is 67% of the initial indicating the deactivation of the catalyst. This phenomenon is observed for all the zeolites studied. These results indicated that this catalyst displays stable activity in the conversion of ethylene diamine and propylene glycol but not to the desired products by cyclization and successive reactions. The deactivation is comparably faster in the case of ZnO-FER (figure 3.3.3(b)); the conversion of ethylene diamine dropped from 99% sharply to 90% after 3h and maintained the constant conversion till the end (8h). The selectivity of the methyl pyrazine decreased and that of 2-methylpiperazine increased with time on stream. In case of ZnO-Beta (figure 3.3.3(c)), which is not selective for methyl pyrazine as compared to ZnO-ZSM-5, afforded a lot of dimethyl pyrazines, ethyl pyrazines, ethylmethyl pyrazines and propyl pyrazines with concomitant increase in the formation of pyrazine, which may be due to the structural differences between beta and the other zeolites apart from the acidity of these zeolites (as discussed in chapter 2).
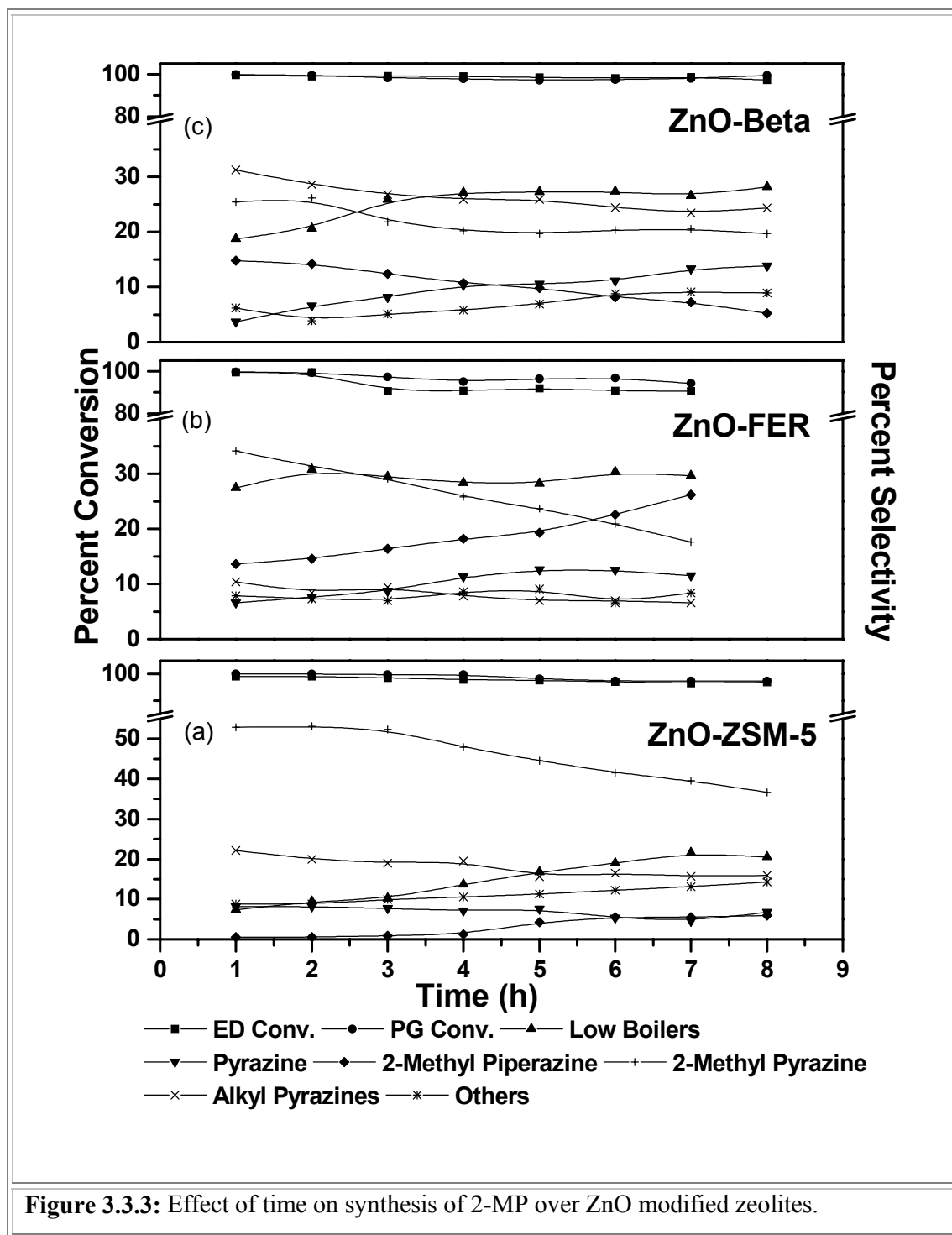
Figure 3.3.3: Effect of time on synthesis of 2-MP over ZnO modified zeolites.

Reaction conditions: Pressure atm., Temperature 400°C, WHSV 1h^{-1}, ED: PG: water (1:1:5) mole ratio

3.3.3.3. Effect of WHSV (weight hourly space velocity)

With increase in WHSV, in general, conversion as well as selectivity towards 2-MP decreases, however, that for 2-methylpiperazine, the primary product, increases indicating that dehydrogenation has not taken place when the contact time is less. At low WHSV, the formation of 2-methylpyrazine and the other alkyl pyrazines like dimethyl pyrazine, ethyl pyrazine, ethylmethyl pyrazine and propyl pyrazine were more. The effect of WHSV on conversion and product selectivity over ZnO-ZSM-5 zeolite catalyst was investigated and the results are presented in figure 3.3.4(a). As the WHSV was increased from 0.66 to $2h^{-1}$, it can be seen from the figure that there is a small decrease in conversion of ethylene diamine and propylene glycol. However, the selectivity of methyl pyrazine decreases from 57% to 26% at WHSV = $2h^{-1}$. At higher WHSV formation of methyl piperazine, assumed to be the primary product is observed where as at low WHSV pyrazines are formed due to successive reactions. It is also worth noting the formation of large amount of lower boilers, unidentifiable higher boilers and some tiny peaks at higher WHSVs. In case of ZnO-FER figure 3.3.4(b), increase in WHSV led to an increase in the selectivity of 2-methyl piperazine (8.5 to 44%) and decrease in that of methyl pyrazine (42.8 to 10.8%). As pyrazine and alkyl pyrazines are secondary products obtained from the successive reaction of piperazine and its methyl derivative either by dehydrogenation or alkylation with the low boiling compounds, the concentration of these is less at high WHSV (low contact time). Same behavior is also observed in case of ZnO-Beta figure 3.3.4(c). So it can be concluded that the dehydrogenation activity of ZnO modified FER and Beta is less than that of ZSM-5.

Figure 3.3.4: Effect of WHSV on synthesis of 2-MP over ZnO modified zeolites.
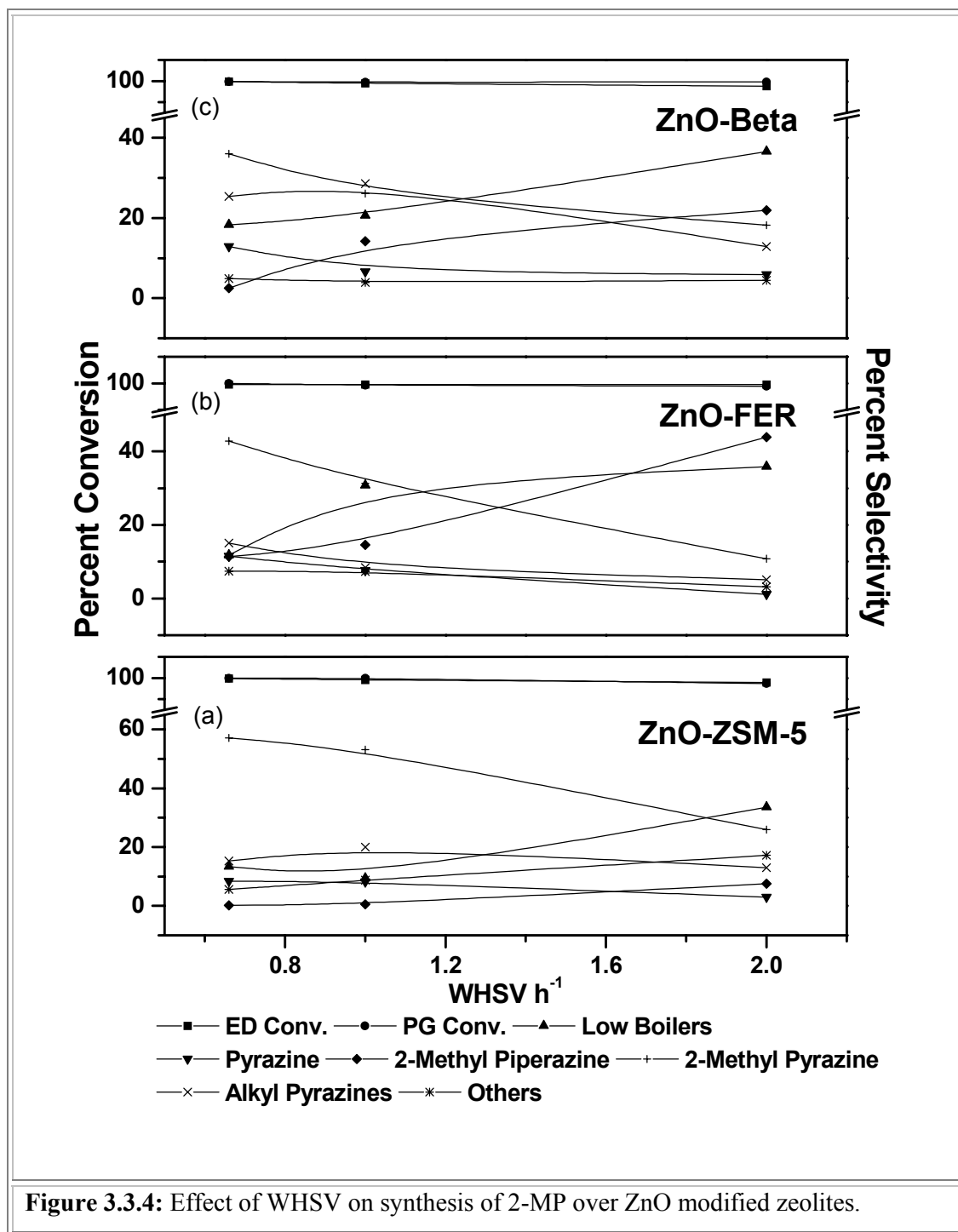
Reaction conditions: Pressure atm., Temperature 400°C, Time 2h, ED: PG: water (1:1:5) mole ratio

3.3.3.4. Effect of molar ratio of reactants

In order to find out the optimum feed ratio, a series of experiments were performed at 400°C with different mole ratios of over ZnO-ZSM5 and the results are tabulated in table 3.3.1. Molar ratio was found have a profound effect over the reaction. As seen from the table 3.3.1, the conversion of propylene glycol (PG) increases when the molar ratio of PG decreased.

Table 3.3.1: Effect of molar ratio of ethylene diamine and propylene glycol on synthesis of 2-methyl pyrazine over ZnO-ZSM-5

Molar ratio (ED:PG)	ED Conv.	PG Conv.	LB	PY	MPIP	2-MP	Alk. Pyrazine	Others
1:2	99.2	95	25.4	3.9	1	45	11.6	13.1
1:1.5	99.4	99	15.4	6	0.8	48.5	19.5	9.8
1:1	99.1	100	9.4	8.2	0.5	53.1	20.3	8.5
1.5:1	97.5	97.7	9.5	9	3.2	59.5	15	3.8
2:1	96.2	98.1	10.9	11.6	3.3	63.5	7.7	3

ED = Ethylene Diamine; PG = Propylene Glycol; LB = Low Boilers; PY = Pyrazine; MPIP = Methyl pyrazine; 2-MP = 2-methyl pyrazine;

Reaction conditions: Pressure atm., Temperature = 400°C; WHSV $1h^{-1}$; Time 2h; molar ratio of water is 5.

In a similar way the conversion of ethylene diamine (ED) decreased when the molar ratio of ED increased in the feed. The concentration of methylpyrazine increases with increase in ED concentration in the feed. This is due to the self-cyclocondensation of ED leading to pyrazine and alkylpyrazine, which was noticed in the reaction of ED alone. It can also be noted that the formation of methylpiperazine, which is primary product, was found in noticeable amount when ED concentration was more in the feed.

3.3.3.5. Effect of zinc modification

The zeolite ZSM-5 was modified with zinc by both impregnation and ion exchange. For comparison purposes ZnO and a physical mixture [of ZnO(5%) and ZSM-5(95%)] were also tested for the synthesis of 2-MP. Detailed discussion about these samples is in chapter 2 (FTIR and XPS studies). The results of the catalytic activity of these samples are shown in table 3.3.2. It is observed that the conversion of both ED and PG over ZnO is less as compared with the zinc modified ZSM-5. However, ZnO produced a little higher selectivity for MP as compared to zinc modified zeolites even though a higher amount of low boiling compounds are formed. Unmodified H-ZSM-5 showed very low selectivity to MP and produced a higher amount of other unwanted products (alkylpyrazines and higher boilers). A physical mixture of zinc oxide and H-ZSM-5 also produced similar result. For Zinc modified ZSM-5 (by ion-exchange, Zn-ZSM-5) a comparable selectivity with respect to the impregnated sample (ZnO-ZSM-5) is observed for MP, however modification by impregnation showed an increase in yield of MP and is the best catalyst studied for this reaction.

Table 3.3.2: Effect of various catalysts on synthesis of 2-methyl pyrazine

Catalyst	ED Conv.	PG Conv.	LB	PY	MPIP	2-MP	Alk. Pyrazine	Others
ZnO-ZSM-5	99.1	100	9.4	8.2	0.5	53.1	20.3	8.5
Zn-ZSM-5	96.2	99.9	12.1	11.4	7.9	44.5	15.2	8.9
ZnO+ZSM-5	97.8	96.5	16.6	14.7	9.3	27.1	21.6	10.7
H-ZSM-5	98.8	95.2	17.9	16.6	7	23.3	24.7	10.5
ZnO	77.4	85.7	22.7	4.6	2.4	59.2	3.5	7.6

ED = Ethylene Diamine; PG = Propylene Glycol; LB = Low Boilers; PY = Pyrazine; MPIP = Methyl pyrazine; 2-MP = 2-methyl pyrazine;

Reaction conditions: Pressure atm., Temperature = 400°C; WHSV 1h^{-1}; Time 2h; ED: PG: water (1:1:5) mole ratio

As seen from the XPS data (table 2.9, chapter 2) the surface Zn/Si ratio is high for zinc impregnated ZSM-5 compared to ion exchanged ZSM-5 and it suggests that zinc is not well dispersed as in the case of ion-exchanged sample. From both XPS and FTIR studies it is seen that impregnation leads to formation of extracrystalline ZnO apart from exchanged centers. A comparison between the better catalytic activity observed with impregnated catalyst may be due to its similarity with ZnO (extracrystalline ZnO) than Zn^{2+} cations and also possessing intermediate acidity of both Brönsted and Lewis as compared to unmodified and zinc ion exchanged ZSM-5 which are responsible for cyclization.

3.3.4. CONCLUSIONS

Reaction of ethylene diamine and propylene glycol over ZnO modified zeolites, in general, resulted in the formation of methyl pyrazine. ZnO-ZSM-5 displayed high selectivity towards 2-methylpyrazine compared to other zinc modified zeolites under study. Deactivation of the catalyst (ZnO-ZSM-5) during the period of study i.e. 8h is observed. ZnO-Beta and ZnO-FER are less active; ZnO-Beta is not selective. The catalyst can be easily be regenerated in situ by burning off the carbonaceous deposits with air at 500°C for 5h. A little higher concentration of ethylene diamine in the feed improves the selectivity of 2-methylpyrazine. The stability of these catalysts in terms of conversion of ethylene diamine with time on stream followed the order ZnO-ZSM-5 > ZnO-Beta > ZnO-FER.

3.4. SYNTHESIS OF ALKYLPYRAZINES FROM MONOETHANOLAMINE OVER ZINC OXIDE MODIFIED ZEOLITES

3.4.1. INTRODUCTION

Transformation of alkanolamines to piperazine and pyrazine derivatives, alkylenimines, aziridine compounds, triethylenediamines, ethylenediamine and various other important industrial products has been reported over different metal oxides, alkaline and alkaline earth phosphates and zeolite catalysts [78-98]. Piperazine was produced from monoethanolamine at low pressure by gas-solid continuous catalytic reaction using γ-aluminum oxide-support containing NiO 65~78%, CuO 15~25%, Cr_2O_3 2~10% and small quantity of Co and W [79]. A process was developed for preparation of a mixture of piperazine and $H_2NCH_2CH_2NH_2$ by reacting $HOCH_2CH_2NH_2$ with NH_3 in presence of hydrogen and a Ni-Cu-Cr catalyst [80]. The reaction of ethanolamine with diethanolamine over Ni-Cu-Cr catalyst at hydrogen pressure yielded another important chemical N-(2-hydroxyethyl)piperazine [81]. Also piperazine and triethylenediamine were prepared from reaction of an ethanolamine, ethyleneamine (e.g., diethylenetriamine), piperazine, or morpholine over a pentasil-type zeolite at elevated temperature over modified ZSM-5 [82]. In a patented literature, transformation of ethanolamine to triethylenediamine was reported over a pentasil zeolite [83]. The synthesis of ethylenediamine from ethanolamine with ammonia over acidic types of zeolite catalyst is also investigated [88-90] and dealuminated mordenite catalyst was found to be active and selective for synthesis of ethylenediamine.

Recently transformation of ethanolamine to industrially important diazabicyclo[2.2.2]octane (DABCO) over pentasil zeolites was reported [75,89]. They also observed the formation of piperazine, alkylpiperazine, pyrazine and alkylpyrazine along with DABCO. The pyrazine derivatives are formed by the dehydrogenation of the corresponding piperazine derivatives, which are in turn formed by the intermolecular

cylcocondensation reaction of monoethanolamine. We are interested to study the preparation of pyrazine derivatives by cyclocondensation of monoethanolamine over ZnO modified zeolites. The dehydrogenation activity of ZnO-containing catalysts are well known and hence it is expected that impregnation with ZnO can lead to an improvement in pyrazine selectivity [71,98]. The zeolites selected for this investigation are H-ZSM-5, H-FER and H-MOR.

3.4.2. VAPOR PHASE CONDENSATION OF MONOETHANOLAMINE (MEA)

The catalytic tests were made in a fixed-bed down flow silica reactor (figure 2.23(a)) at atmospheric pressure in the temperature range 280-400°C with a catalyst charge of about 4g loaded in the middle of the reactor in the form of pellets (10-20 mesh). The catalyst was activated at 500°C for 5h in a flow of dry air, prior to the start of each run. The dry catalyst was then cooled to the reaction temperature in a flow of dry nitrogen. Monoethanolamine (MEA) in water (solvent) was introduced from the top of the reactor at the required flow rate using a syringe feed pump (SAGE instruments, model 352,USA).

The liquid products were analyzed on a Shimadzu gas chromatograph (GC-15A with FID detector) equipped with an OV-101 column. The identification of the products was carried out on GCMS (Shimadzu GCMS-QP 2000A, SE-52 column, non-polar silicon fluid) and GC-FTIR (Perkin Elmer, FTIR spectrometer spectrum 2000).

3.4.3. RESULTS AND DISCUSSION

The vapor phase reaction of MEA over ZnO modified zeolites resulted in the formation of pyrazine, methylpyrazine, ethylpyrazine, 2,3-dimethypyrazine, piperazine, aziridine, DABCO and polyamines, along with lower boilers like ethyleneoxide, ethyleneimine, ethylenediamine and aziridine. These lower boilers are formed by the intermolecular dehydration or deamination of MEA. A general reaction scheme for the transformation of MEA is shown (figure 3.4.1). Intermolecular condensation of two

molecules of MEA resulted in the formation of piperazine, which in turn was dehydrogenated to give pyrazine. The reaction of pyrazine with the dissociation products of MEA produced alkyl pyrazines.

MEA- monoethanolamine, AZ – azridine, EO- ethyleneoxide, EDA -ethylenediamine,

EI- ethyleneimine, PIP- piperazine, PZ- pyrazine, DABCO- diazabicyclo[2.2.2]octane

EP- ethylpyrazine, MP- methylpyrazine, DMP- 2,3-dimethylpyrazine
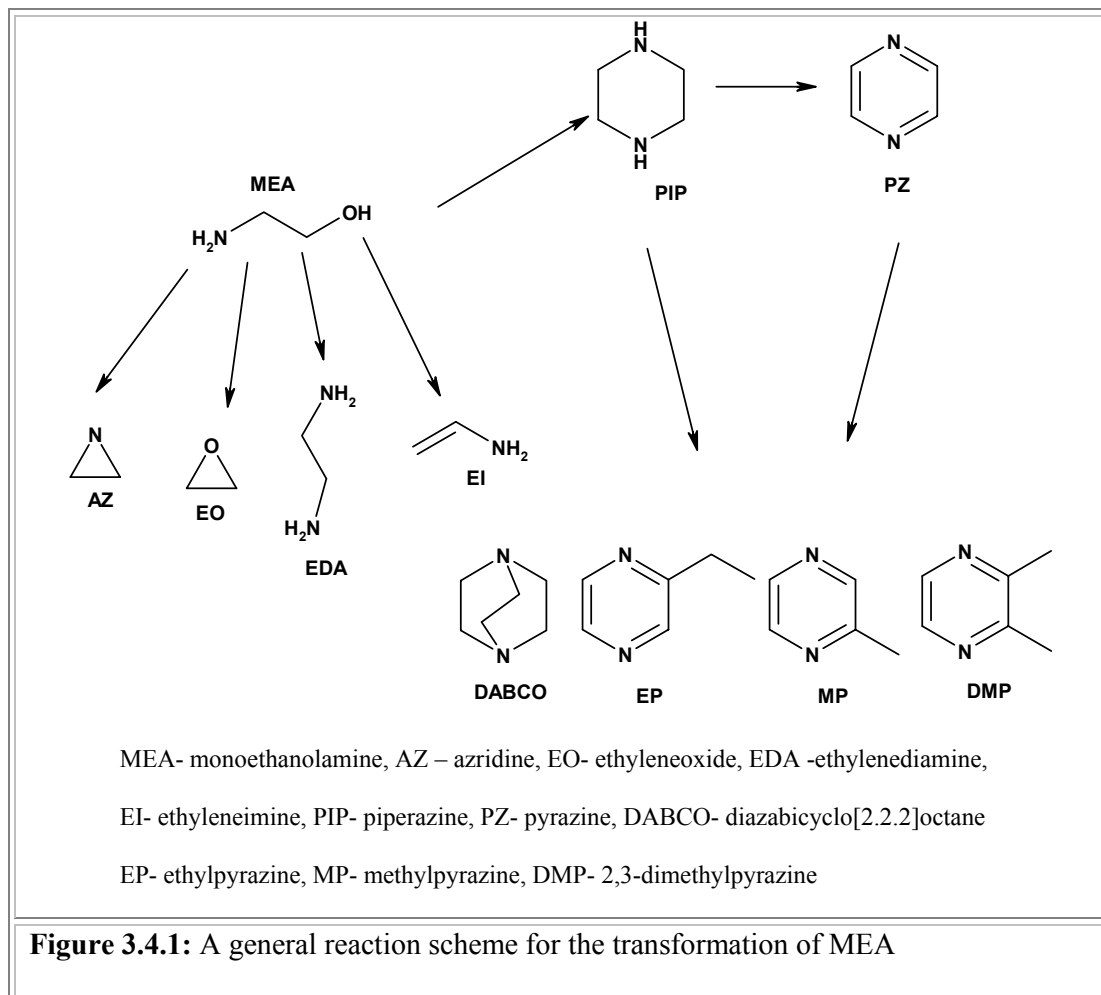
Figure 3.4.1: A general reaction scheme for the transformation of MEA

3.4.3.1. Effect of temperature

The reaction of MEA was carried out separately over three different catalysts at different temperatures. The effect of temperature on the conversion and product selectivity in the case of ZnO-ZSM-5 is depicted in table 3.4.1. The MEA conversion increased from 80 % at 280°C to 97 % at 400°C. Only small amounts of lower boilers including ethyleneimine, ethylenediamine, aziridine, ethyleneoxide etc. were detected. It is interesting to note that piperazine was not obtained as one of the products in the entire

temperature range investigated. Hence, we concluded that piperazine or its alkyl derivatives were dehydrogenated easily to corresponding pyrazine derivative over ZnO modified catalyst. Ethylpyrazine was the main product amongst the alkylpyrazines produced. A maximum ethylpyrazine selectivity of about 62% was achieved at 350°C. At higher temperature (400°C), ethylpyrazine selectivity decreased to 34%. At higher temperatures, there were a few additional tiny peaks on the chromatogram, which could not be identified even by mass spectrometry, so they were neglected and are grouped along with others in the tables. The low selectivity of pyrazine with respect to alkylpyrazines indicated that the decomposition of MEA is an important side reaction, resulting in the formation of alkyl carbocations (carbenium ions) necessary for alkylation. Bhat et al. [84] reported the selective transformation of MEA to DABCO over ZSM-5 zeolite in the temperature range 325°C to 400°C. However, the product pattern is totally different in the case of ZnO modified zeolite, which indicates small amounts of DABCO. The bicyclic compound must be formed by the reaction of a molecule of MEA and piperazine. Due to the dehydrogenation activity of the present catalyst system, piperazine is easily converted into pyrazine, and hence the reaction between piperazine and MEA to form DABCO becomes less probable.

The effect of temperature on the conversion and product selectivity in the case of ZnO-FER zeolite is given in table 3.4.2. The product pattern is similar to that obtained for ZnO modified ZSM-5 zeolite. But the conversion of MEA was low at 280°C and increased sharply to 92% at 350°C. Over this catalyst also, the formation of an appreciable amount of lower boilers was noticed at lower temperatures. An appreciable amount of piperazine was also noticed, unlike in the case of ZnO-ZSM-5. At higher temperatures (350-400°C), the selectivity towards ethylpyrazine was almost the same as that of ZnO-ZSM-5 catalyst,

whereas at lower temperature the formation of pyrazine was maximum (38%), which is due

to the low conversion of MEA.

Table 3.4.1: Influence of temperature on the transformation of MEA over ZnO-ZSM-5

T °C	MEA Conv. (Wt%)	Product Selectivities (wt%)						
		L	Py	MP	EP	2,3-DMP	DABCO	O
400	97.1	10.7	8.9	12.7	34.5	12.2	2.5	18.6
375	95.1	10.1	7.4	10.2	36.2	23.3	2.6	9.2
350	92	4.7	9.9	10.9	62.2	5.9	1.1	5.2
280	80.4	3.8	11.7	16.4	54.1	6.7	2.1	4.7

Table 3.4.2: Influence of temperature on the transformation of MEA over ZnO-FER

T °C	MEA Conv. (Wt%)	Product Selectivities (wt%)							
		L	Py	MP	EP	2,3-DMP	PIP	DABCO	O
400	94.1	7.9	6.1	16.6	36.6	12.7	4.3	3.1	12.6
375	93.7	5.1	10.9	11.8	45.9	5.05	12.3	2.4	6.3
350	92.0	5.5	16.7	11.8	40.1	12.1	3.1	1.2	8.9
280	46.1	21.9	37.7	11.7	7.6	5.6	2.5	2.5	10

Table 3.4.3: Influence of temperature on the transformation of MEA over ZnO-MOR

T °C	MEA Conv. (Wt%)	Product Selectivities (wt%)							
		L	Py	MP	EP	2,3-DMP	PIP	DABCO	O
400	97.1	26.1	15.1	12.1	11.3	13.1	1.4	12.6	7.9
375	96.9	34.7	17.8	7.1	13	6.9	4	10.5	5.9
350	85.5	11.3	46.2	13.3	2.6	8.9	4.6	7.9	4.9
280	23.3	28.6	57.1	0	0	0	2.3	11	1

Reaction conditions: TOS = 3h , Pressure atm, MEA : water = 1:1 wt% and WHSV = 0.75 h^{-1}

L = lower boilers like ethyleneimine, ethylenediamine, aziridine, ethyleneoxide, methylamine

Py = pyrazine, MP = methylpyrazine, EP = ethylpyrazine, 2,3-DMP = 2,3-dimethylpyrazine, PIP = piperazine, DABCO = diazabicyclo[2.2.2]octane, O = polyamines and other higher boilers

Table 3.4.3 presents the results of reaction temperature variation on the catalytic activity and product selectivity over ZnO-MOR catalyst. The activity of the catalyst was low at 280°C; however, at 350°C about 85 % of MEA was converted. In comparison to the other two catalysts, ZnO-modified MOR afforded a large amount of lower boilers including methyamine, aziridine, ethylamine, ethylenediamine with a relative selectivity in the order; methyamine > aziridine > ethylamine > ethylenediamine. At lower conversion levels, pyrazine was observed as the major product, with increase in temperature it gets converted to alkylpyrazines.

Unlike the case of ZnO-modified ZSM-5 and FER catalysts, different alkylpyrazines were formed in almost equal amounts. It is also worth noting that an appreciable amount of DABCO was formed as one of the side products. Segawa et al. [90] have reported that H-Mordenite catalyzes the reaction of ethanolamine and NH_3 to ethylenediamine selectively, along with small amounts of ethyleneimine and piperazine derivatives as side products. They proposed that the formation of ethylenediamine takes place over strong acid sites inside the narrow pore channels of H-MOR zeolite. Hence it is believed that the formation of larger molecules like piperazine and pyrazine takes place over weaker acid sites located on the external surface of mordenite crystals.

3.4.3.2. Effect of time on stream

An investigation of the conversion and the product selectivity as a function of time over ZnO-ZSM-5 zeolite revealed a slow catalyst deactivation. A drop in MEA conversion from 96% to 84% was noticed after 8h of reaction. Moreover, the product selectivity remained the same and did not vary much even after 8 hours. These results indicated that this catalyst displays stable activity in the reaction at least over a period of 8 hours. The results are summarized in figure 3.4.2(a).

Figure 3.4.2 (a): Influence of Time on Stream on the transformation of MEA over ZnO-ZSM-5
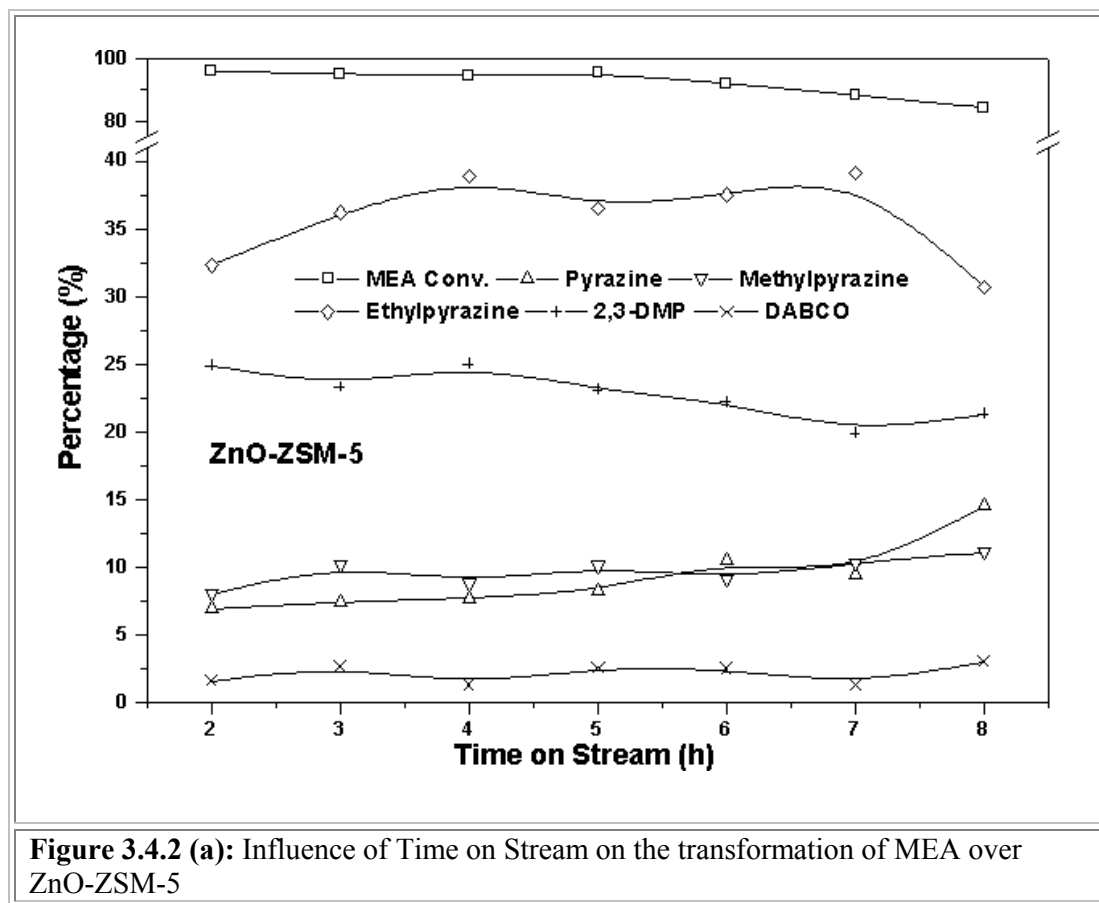
Reaction conditions: Temperature 375°C, Pressure atm, MEA : water = 1:1 wt% and WHSV = 0.75 h^{-1}

In the case of ZnO-MOR, a steady and gradual decrease in the conversion of MEA was observed from 93% to 47% in 8h. The selectivity of pyrazine derivatives dropped down appreciably with lapse of time with a concomitant increase in the selectivity of lower boilers. Results are summarized in figure 3.4.2(b). In the case of mordenite zeolite, for the diffusion of smaller molecules, one may consider that it has a two-dimensional channel system; for larger molecules, the channel system is one-dimensional and may be subjected to diffusion blocks produced by crystal stacking faults in the c-direction or by the presence of amorphous material or cations in the channels. These may be contributing factors in the catalyst deactivation.

Figure 3.4.2(b): Influence of Time on Stream on the transformation of MEA over ZnO-MOR
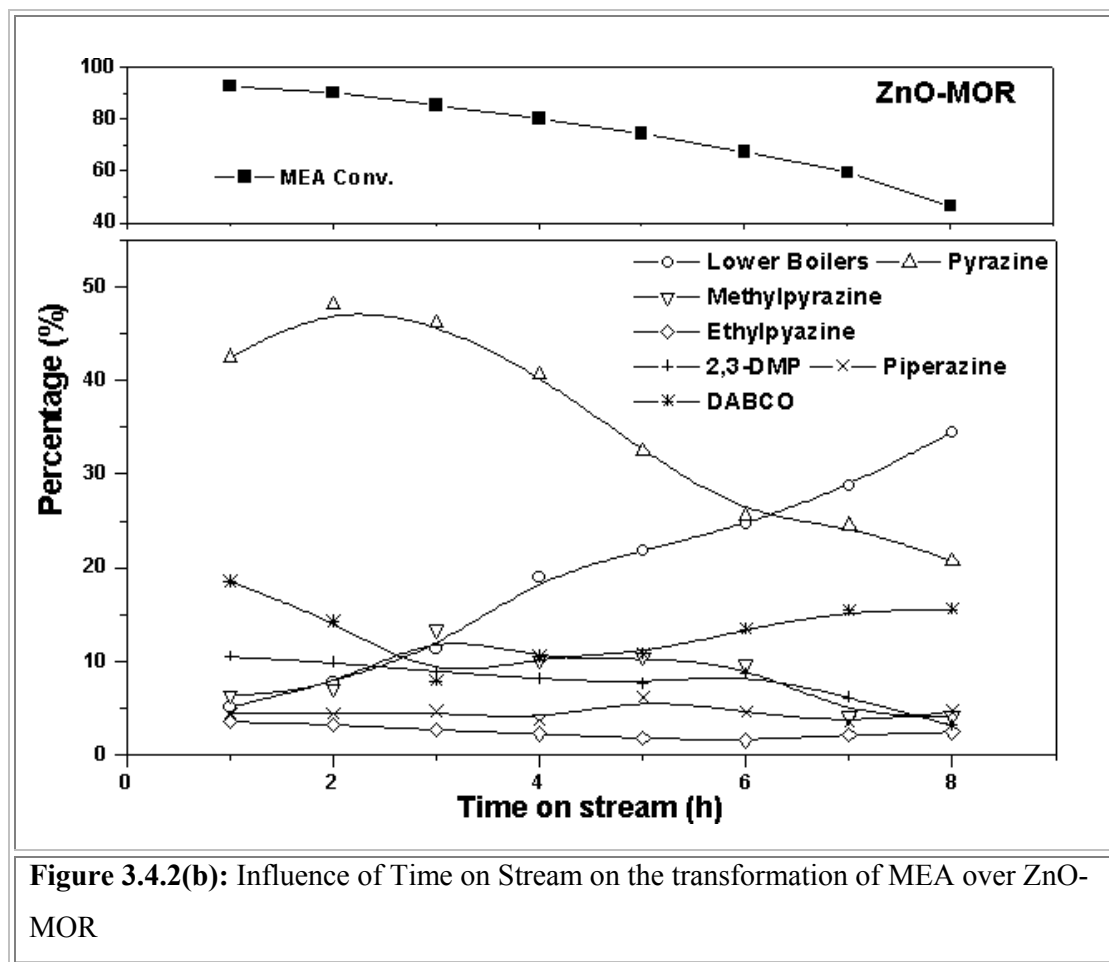
Reaction conditions: Temperature 350°C, Pressure atm, MEA : water = 1:1 wt% and WHSV = 0.75 h^{-1}

The deactivation is faster in the case of ZnO-FER; the conversion dropped from 97% to merely 6% in 8h, showing the instability of the catalyst towards the reaction. The selectivity of the ethylpyrazine decreased and that of lower boilers increased with time on stream (figure 3.4.2(c)).

Figure 3.4.2(c): Influence of Time on Stream on the transformation of MEA over ZnO-FER
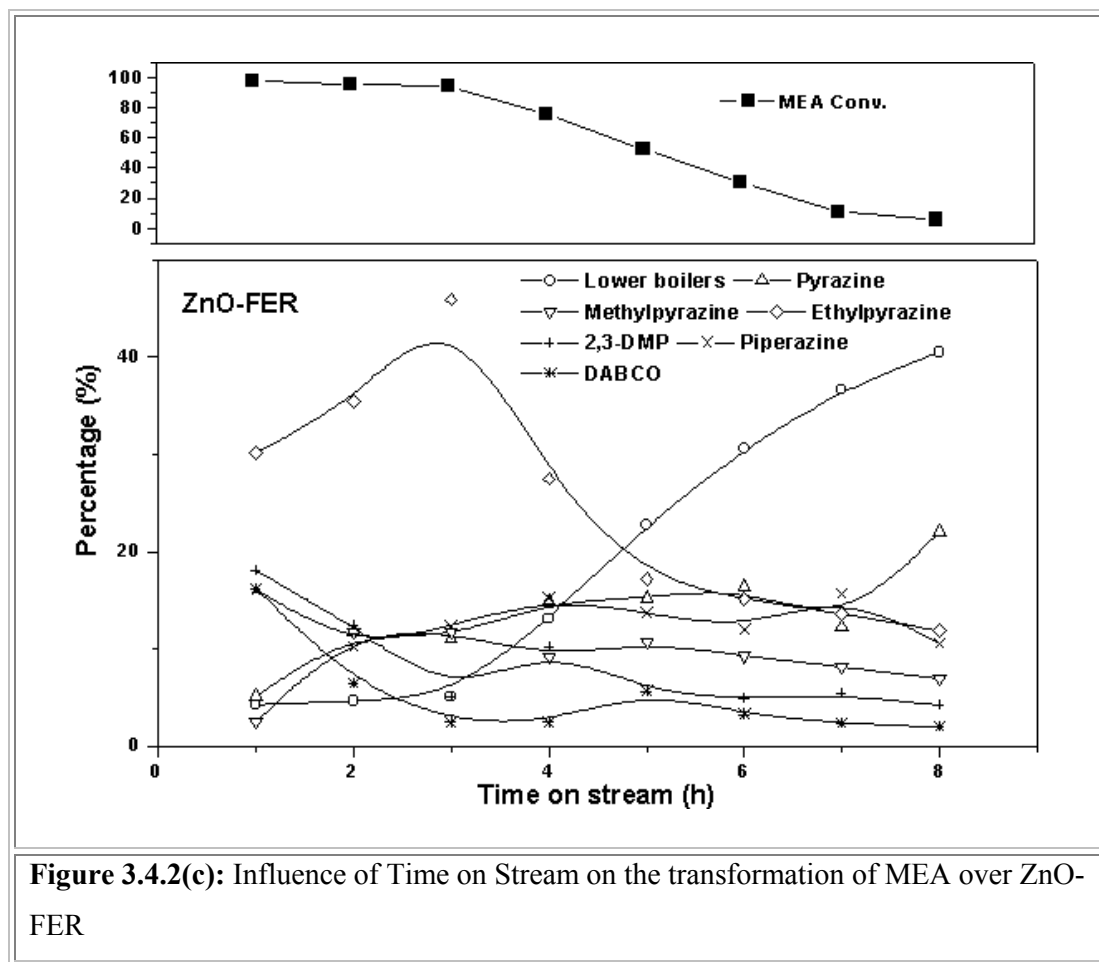
Reaction conditions: Temperature 375°C, Pressure atm, MEA : water = 1:1 wt% and WHSV = 0.75h[-1]

3.4.3.3. Effect of WHSV

The effect of WHSV (weight hourly space velocity) on MEA conversion and product selectivity over ZnO-ZSM-5 zeolite catalyst was investigated; the results are presented in figure 3.4.3(a). As expected, increasing the WHSV led to reduce in MEA conversion. As the WHSV was increased from 0.75 to 3.75h[-1], it can be seen from the figure 3.4.3(a), that the selectivity of alkylpyrazines decreased with a concomitant increase in the selectivity of piperazine. This is expected, since pyrazine derivatives were formed by the dehydrogenation of piperazine.
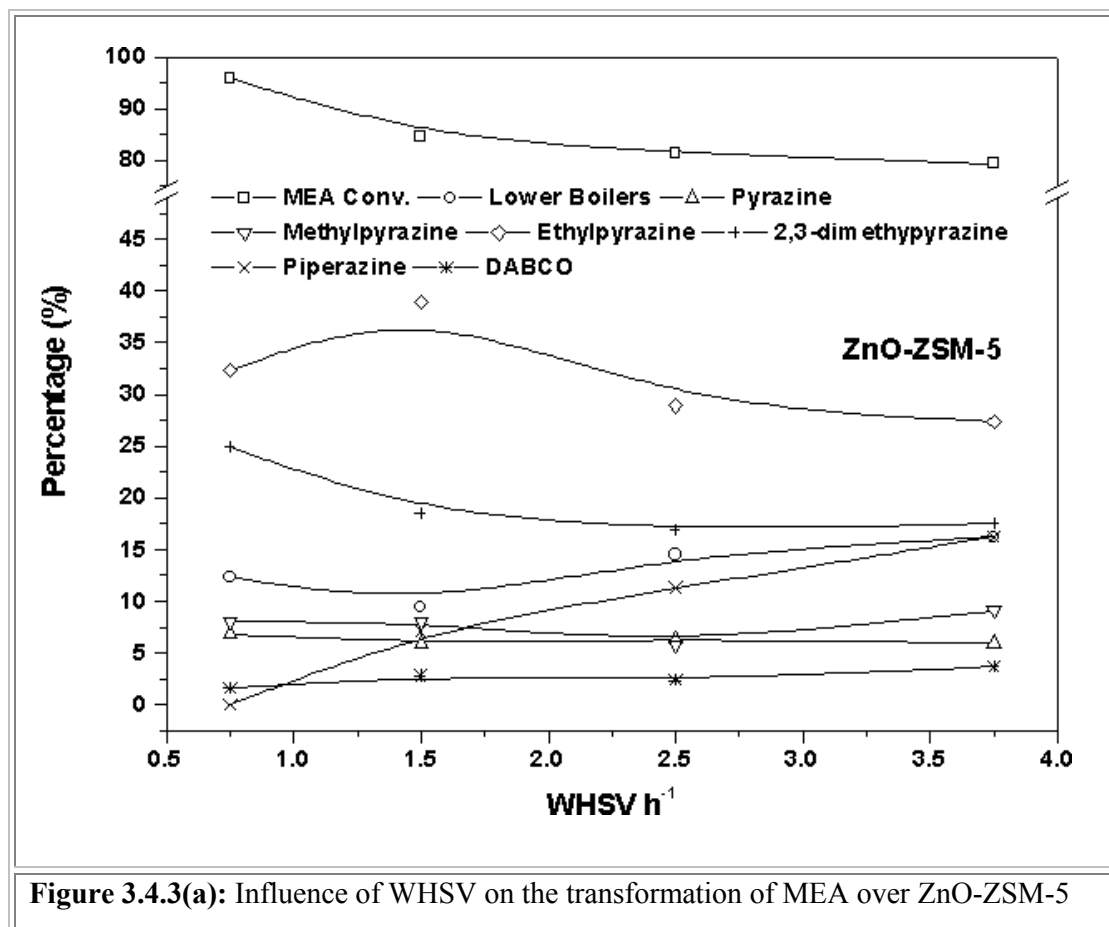
Figure 3.4.3(a): Influence of WHSV on the transformation of MEA over ZnO-ZSM-5

Reaction conditions: Temperature 375°C, Pressure atm, MEA : water = 1:1 wt% and TOS = 3h

In case of ZnO-FER catalyst (figure 3.4.3(b)), the pyrazine selectivity decreases with decrease in contact time at the expense of the selectivity of alkylpyrazines. At higher contact time (WHSV= 0.75h^{-1}) alkylpyrazines were formed as a major product, which implies that decomposition of MEA resulted in the formation of various alkyl carbenium ions. As the contact time decreases, conversion also decreases appreciably and the other secondary reactions like the formation of aziridines and amines become increasingly dominant. Hence, the reaction of the cracked products of MEA with formed pyrazine is less probable. The high selectivity of pyrazine even at low contact time (WHSV= 3.75h^{-1}) indicates the high dehydrogenation activity of the present catalyst system.

Figure 3.4.3(b): Influence of WHSV on the transformation of MEA over ZnO-FER

Reaction conditions: Temperature 375°C, Pressure atm, MEA : water = 1:1 wt% and TOS = 3h
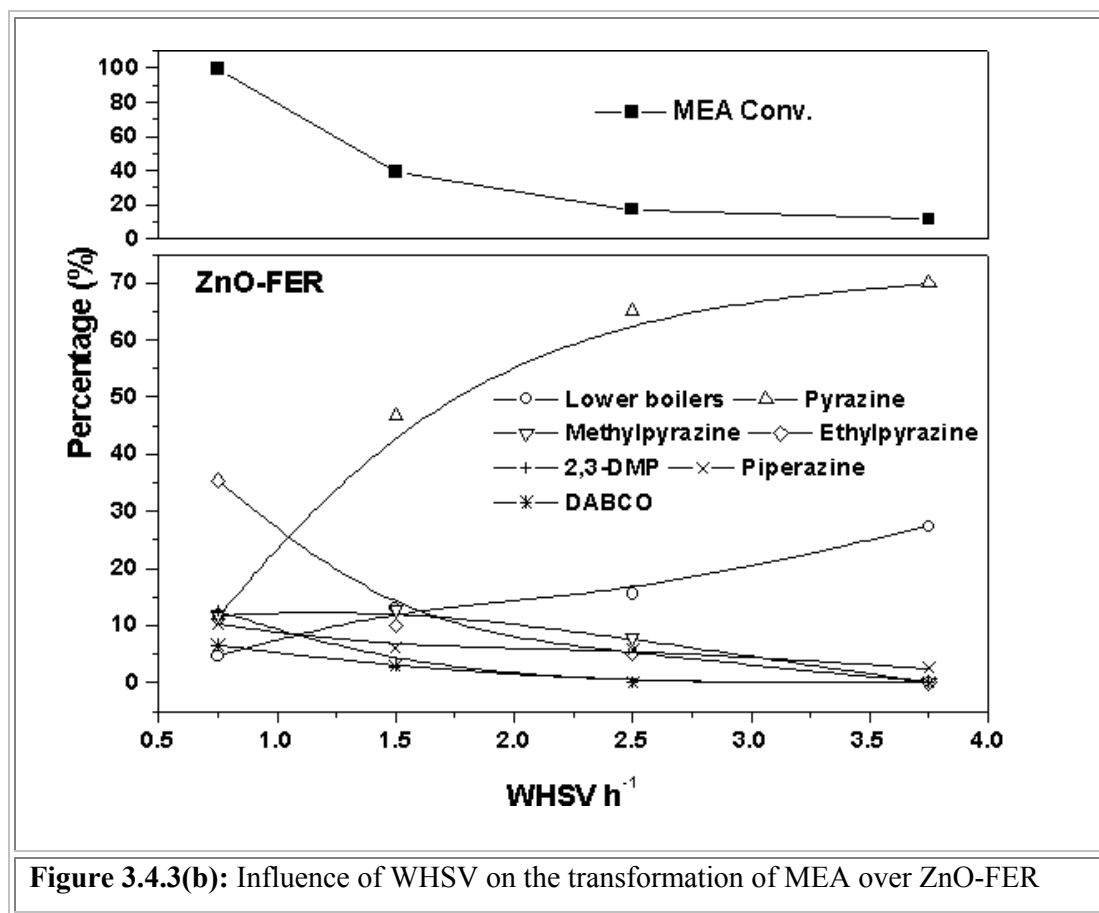
The effect of contact time on the product selectivity over ZnO-MOR catalyst is shown in figure 3.4.3(c). Increase in WHSV led to an increase in the selectivity of lower boilers. An appreciable amount of DABCO was formed irrespective of the value of contact time. So the reaction between piperazine and MEA to DABCO is an important side reaction over ZnO-MOR. As expected, the pyrazine and alkylpyrazine selectivity decreased with decrease in contact time and a steady increase in the selectivity of piperazine was observed. So it can be concluded that the dehydrogenation activity of ZnO-modified MOR is less than that of FER and ZSM-5.

Figure 3.4.3(c): Influence of WHSV on the transformation of MEA over ZnO-MOR
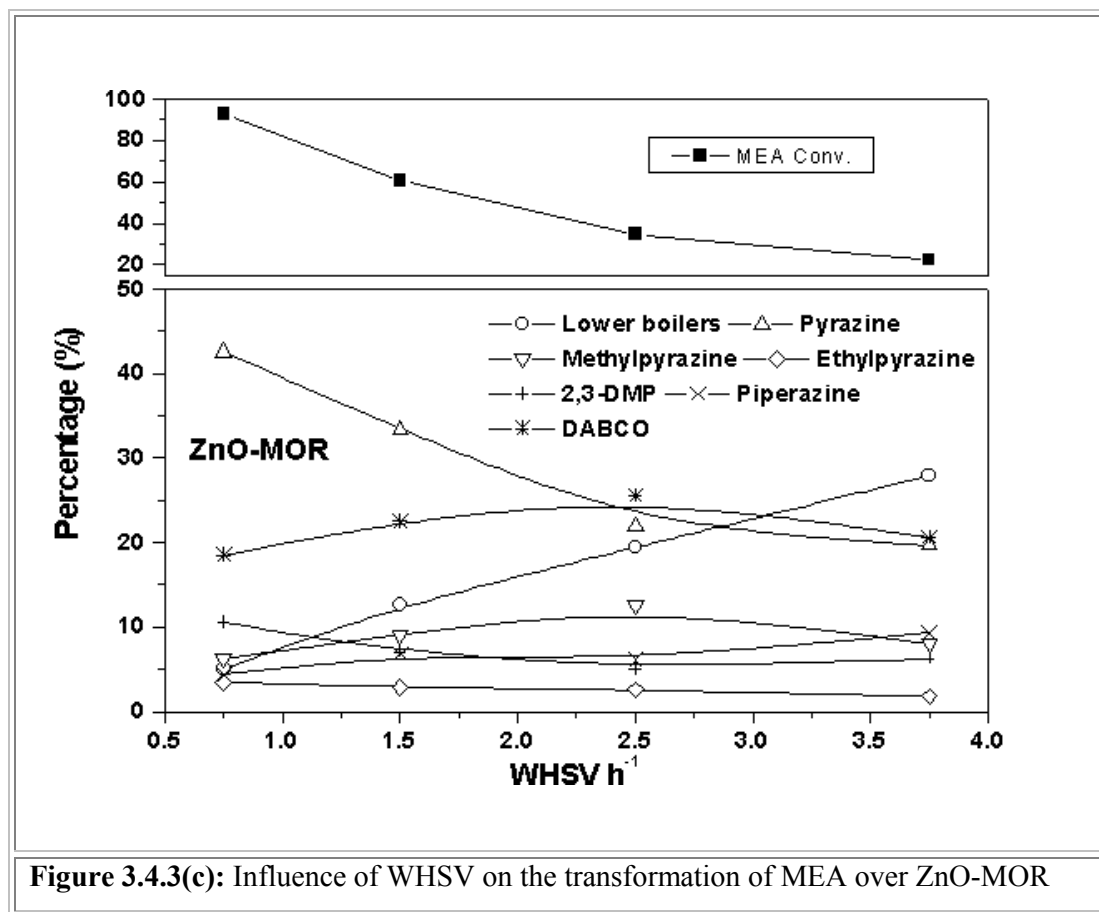
Reaction conditions: Temperature 350°C, Pressure atm, MEA : water = 1:1 wt% and TOS = 3h

3.4.4. CONCLUSIONS

Reaction of MEA over ZnO-modified zeolites in general resulted in the formation of pyrazine and alkylpyrazines. Out of different alkylpyrazines formed, ethylpyrazine was the major product in the case of ZnO-ZSM-5 and ZnO-FER catalysts. However in the case of ZnO-MOR, different alkylpyrazines were formed without showing any appreciable selectivity towards a particular compound. It was found that piperazine or its alkylderivaties were easily dehydrogenated to corresponding pyrazine derivatives over these catalysts. The formation of DABCO was appreciable over ZnO-MOR; however, it became less probable over ZnO-FER and ZnO-ZSM-5 catalyst, due to their higher dehydrogenation activity. The narrow pore inside ZnO-MOR zeolite allowed the formation of different lower boilers like methylamine, ethylamine, aziridine and ethylenediamine.

127

The stability of these catalysts in terms of conversion of MEA with time on stream followed the order: ZnO-ZSM-5 > ZnO-MOR > ZnO-FER.

3.5. REFERENCES

1. S. N. Ege, *Organic Chemistry,* 2nd ed.; D.C. Heath and Company: Lexington, MA, (1989) 915.

2. Kirk-Othmer. *Encyclopedia of Chemical Technology,* 4th ed.; John Wiley and Sons Inc.; New York, Vol. **4**, (1995) 827.

3. D. C. England, U.S. Patent 2,634,269, (1953).

4. I. S. Fisher, U.K. Patent 881,276, (1961).

5. A. Costa, P. M. Deya, J. V. Sinisterra, J. M. Marinas, *Can. J. Chem.,* **58** (1980) 1266.

6. P. Vitarelli, S. Cavallaro, R. Maggiore, G. Cimino, C. Caristi, S. Galvagno, *Gazz. Chim. Ital.,* **112** (1982) 493.

7. T. Curtin, J. B. McMonagle, B. K. Hodnett*, Appl. Catal. A,* **93** (1992) 91.

8. T. Curtin, J. B. McMonagle, B. K. Hodnett, *Appl. Catal. A,* **93** (1992) 75.

9. T. Curtin, J. B. McMonagle, M. Ruwet, B. K. Hodnett, *J. Catal.,* **142** (1993) 172.

10. S. Sato, K. Hirose, M. Kitamura, H. Tojima, N. Ishii, EP 236 092 (1987).

11. S. Sato, H. Sakurai, K. Urabe, Y. Izumi, *Chem. Lett.,* (**3**), (1985) 277.

12. T. Ushikubo, K. Wada, *J. Catal.,* **148** (1994) 138.

13. N. Katada, T. Tsubouchi, M. Niwa, Y. Murakam, *Appl. Catal. A,* **124** (1995) 1.

14. P.S. Landis, P.B. Venuto, *J. Catal.,* **6** (1966) 245.

15. A. Aucejo, M.C. Burguet, A. Corma, V. Fornes, *Appl. Catal.,* **22** (1986) 187.

16 H. Sato, K. Hirose, M. Kitamura, Y. Nakamura, *Stud. Surf. Sci. Catal.,* **49** (1989) 1213.

17. J. Sauer, A. Bleiber, *Catal. Today,* **3** (1988) 485.

18. L.-X. Dai, R. Hayasaka, Y. Iwaki, K.A. Koyano, T. Tatsumi, *Chem. Commun. (Cambridge),* (**9**), (1996) 1071.

19. H. Sato, K. Hirose, N. Ishii, Y. Umada, Eur. Patent 234088 (1986).

20. H. Sato, N. Ishii, K. Hirose, S. Nakamura, *Stud. Surf. Sci. Catal.,* **28** (1986) 775.

21. H. Sato, *Catal. Rev. -Sci. Eng.,* **39** (1997) 395.

22. P. Albers, K. Seibold, T. Haas, G. Prescher, W.F. Hoelderich, *J. Catal.,* **176** (1998) 561.

23. G.P. Heitmann, G. Dahlhoff, W.F. Hoelderich, *J. Catal.,* **186** (1999) 12.

24. J. Roseler, G. Heitmann, W.F. Hoelderich, *Appl. Catal. A,* **144** (1996) 319.

25. W.F. Hoelderich, J. Roseler, G. Heitmann, T. Liebens, *Catal. Today,* **37** (1997) 353.

26. T. Yashima, K. Miura, T. Komatsu, *Stud. Surf. Sci. Catal.,* **84** (1994) 1897.

27. A. Thangaraj, S. Sivasanker, P. Ratnaswamy, *J. Catal.,* **137** (1992) 252.

28. A. Corma, H. Garcia, J. Primo, *Zeolites,* **11**(6), (1991) 593.

29. P.S. Singh, R. Bandyopadhyay, S.G. Hegde, B.S. Rao, *Appl. Catal. A,* **136** (1996) 249.

30. J.S. Reddy, R. Ravishankar, S. Sivasankar, P. Ratnasamy *Catal. Lett.,* **17** (1993) 139.

31. T. Komatsu, T. Maeda, T. Yashima, *Microporous Mesoporous Mater,* **35-36** (2000) 173.

32. P.B. Venuto *Microporous Materials,* **2** (1994) p. 311.

33. Van Nostrand's Sci. Encyl., 6th edn. 1984, p. 2356.

34. Kirk-Othmer *Encyclopedia of Chemical Technology,* 3rd edn. Vol. 19, 1983, p.454.

35. A. Nenz, M. Pieroni, *Hydrocarbon process*, (a) **47** (11) (1968) 139 (b) **47** (12) (1968) 103.

36. D.J. Berry, *Spec. Chem.,* **3** (1983) 13.

37. Ullman's *Encyclopedia of Industrial Chemistry,* Vol. A22, VCH, Weinheim, 5th edn., 1993 pp 399-430.

38. Lummus Co. Ltd., G.B. Pat. 1182705 (1970).

39. Celanese Corp., U.S; Pat. 3970655 (1976).

40. B.P. Chemicals (U.K.) Ltd., G.B. Pat. 1235390 (1971).

41. Rfitgerswerke A.G. (a) Ger. Offen. 2203384 (1973); (b) G.B. Pat. 1302470 (1973)

42. Koei Chemical Co., G.B. Pat. 1346630 (1974).

43. Eastman Kodak Co., U.S. Pat. 3829428 (1974).

44. Asahi Kasei Kogyo Kabushiki Kaisha, G.B. Pat. 1579473 (1980).

45. Shell Oil Co., U.S. Pat. 3412096 (1968).

46. Koei Chemical Co., (a) G.B. Pat. 1216866 (1972); (b) U.S. Pat. 3932421 (1976).

47. Mobil Oil Corp., U.S. Pat. 4220783 (1980).

48. V.V. Antonova, T.I. Ovchinnikova, B.F. Ustavshchikov, V.K. Promonenkov, *Zh. Org. Khim.,* **16** (1980) 547.

49. F.J. van der Gaag, F. Louter, J.C. Oudejans, H. van Bekkum, *Appl. Catal.,* **26** (1986) 191.

50. G.W. Wheland, *Resonance in Organic Chemistry*, John Wiley & Sons, New York, NY, 1955, p. 99.

51. F.J. van der Gaag, R.J.O. Adriaansens, H. van Bekkum, P.C. van Geem, *Stud. Surf. Sci. Catal.,* **52** (1989) 283.

52. F.J. van der Gaag, F. Louter, H. van Bekkum, *Stud. Surf. Sci. Catal.,* **28** (1986) 763.

53. P.B. Venuto, P.S. Landis, *Advances in Catalysis*, Vol. 18, Academic, New York, NY, 1968, p. 344.

54. C.D. Chang, W.H. Lang, US. Pat. 4220783 (1980).

55. W.F. Hoelderich, M. Hesse, F. Naumann, *Angew. Chem. Int. Ed. Engl.,* **27** (1988) 239.

56. W.F. Hoelderich, *Stud. Surf. Sci. Catal.,* **46** (1989) 193.

57 W.F. Hoelderich, N. Goetz, G. Fouquet, Eur. Pat., 263 464 (1988).

58. F.P. Gortsema, B. Beshty, J.J. Friedman, D. Matsumoto, J.J. Sharkey, G. Wildman, T.J. B1ack1ock, S.H. Pan, paper presented at the *14th Conference on Catalysis of Organic Reactions,* Albuquerque, NM*,* April 27-29*,* 1992.

59. W.F. Hoelderich, N. Goetz, Eur. Pat., 289 924 (1988).

60. D.G. Jones, P.S. Landis, U.S. Pat., 3264 307 (1966).

61. Y. Ben Taarit, Y. Diab, B. Elleuch, M. Kerkani, M. Chihaoui, *J. Chem. Soc., Chem. Commun.,* **5** (1986) 402.

62. J. Okada, Japan 49,25,947 (1974).

63. Koei Chemical Co., Japan 53,43512 (1978).

64. Korea Research Institute of Chemical Technology, Japan 05,52829 (1993).

65. Tokai Electro-Chemical Co., Japan 55,50024 (1980).

66. Koei Chemical Co., Japan 09,48763 (1997).

67. L. Forni, P. Pollesel, *J Catal.,* **130**(2), (1991) 403.

68. L. Forni, S. Nestori, *Stud. Surf. Sci. Catal.,* **41**(1988) 291.

69. G.T. Fedolyak, L.A. Krichevskii, A.D. Kagarlitskii*, Izv. Akad. Nauk Kaz. SSR, Ser. Khim.,* **5** (1989)50.

70. T. Shoji, T. Nakaishi, M. Mikata, Ger. Offen. DE 19629258 A1 6 Feb 1997, 9 pp

71. G. T.Fedolyak, A.D. Kagarlitskii, L.A. Krichevskii, A.V. Morozov*, Izv. Akad. Nauk Resp. Kaz., Ser. Khim.*, **6** (1992) 31.

72. S.J. Kulkarni, M. Subrahmanyam, A.V. Rama Rao, *Indian. J Chem., Sect. A* **32A**(1) (1993) 28.

73. A.W. Chester, Y.F. Chu. US Pat. 4350835 (1982).

74.   Y. Ono, *Catal. Rev. –Sci. Eng.* **34** (3) (1992) 179.

75.   F. Roessner, A. Hagen, U. Mroczek, H.G. Karge, K. –H. Steinberg, *Stud. Surf. Sci. Catal.,* **75** (1993) 1707.

76.   M.S. Scurrell, *Appl. Catal.,* **32** (1987) 1.

77.   L. Froni, G. Stern, M. Gatti *Appl. Catal.,* **29** (1987) 161.

78.   S. Shimizu, T. Niwa, T. Shoji, JP 63162678 (1988).

79.   Sun, Yumeng, *Gaoxiao Huaxue Gongcheng Xuebao,* **13**(2), (1999) 178.

80.   T.T. McConnell, T.H. Cour, US 4234730 (1980).

81.   M.E. Brennan, G.P. Speranza, US 4338443 (1982).

82.   H. Li, J.G. Santiesteban, L.A. Emig, J.N. Armor, EP 952152 (1999).

83.   H. Li, J.G. Santiesteban, L.A. Emig, J.N. Armor, US 5731449 (1998).

84.   Y.S. Bhat, J. Das, S. Ali, B.D. Bhatt, A.B. Halgeri, *Appl. Catal.,A.* **148** (1996) L1 .

85.   G. H. Grosch, E. Gehrer, U. Steuerle, C. Koenig, M. Eder, EP 782985 (1997).

86.   U. Steuerle, W. Reuther, G. Schuh, DE 19548337 (1997).

87.   U. Dingerdissen, G. Lauth, P. Truebenbach, U. Steuerle DE 19533662 (1997).

88.   K. Segawa, S. Mizuno, M. Sugiura, S. Nakata, *Stud. Surf. Sci. Catal.* **101** (1996) 267.

89.   K. Segawa, S. Mizuno, Y. Maruyama, S. Nakata, *Stud. Surf. Sci. Catal.,* **84** (1994) 1943.

90.   K. Segawa, S. Mizuno, Y. Fujimoto, H. Yamamoto, *Stud. Surf. Sci. Catal.,* **83** (1994) 273.

91.   M. Huang, S. Kaliaguine, *React. Kinet. Catal. Lett.,* **56** (1995) 21.

92.   M. Ueshima, Y. Shimasaki, K. Ariyoshi, H. Yano, H. Tsuneki, *Stud. Surf. Sci. Catal.,* **75** (1993) 2447.

93.   N. Nagasaki, T. Hironaka, Y. Hara, JP 05017414 (1993).

94.   N. V. Testova, E. Paukstis, K.G. Ione, *React. Kinet. Catal. Lett.,* **44** (1991) 243.

95.   M. Ueshima, Y. Shimasaki, Y. Hino, H. Tsuneki, in *Acid-Base Catal., Proc. Int. Symp.,* Edited by: K. Tanabe. Kodansha: Tokyo, Japan. (1989).

96.   M. Ueshima, Y. Shimasaki, *Kagaku to Kogyo,* **43** (1990) 349.

97.   T. Kiyoura, Y. Kogure, JP 52005780 (1977).

98   J.Kijenski, *Bull. Acad. Pol. Sci. Ser. Sci. Chim.,* **29**, (1981) 225.

Chapter –4

Acid Catalyzed reactions of Amines

Catalysis over Medium and Large pore zeolites

4.1. SYNTHESIS OF DABCO

4.1.1. INTRODUCTION

Nitrogen-containing compounds are used as structural components of pharmaceuticals and agrochemicals due to their high biological activities. There are many nitrogen-containing chemicals, from simple structured compounds as pyridine bases to more complicated structures as pharmaceutical ingredients and their number is growing rapidly every year. Amines are an important class of compounds which find uses as intermediates in a variety of applications including pharmaceuticals, agricultural chemicals, rubber chemicals, water treatment chemicals, and solvents. Methods for commercial manufacture of amines vary depend on the specific amine to be produced and on the raw materials employed [1].

1,4-Diazabicyclo[2.2.2]octane or DABCO (also known as triethylenediamine or TEDA) is one of the principal catalysts used for production of polyurethanes [2] from polyisocyanates and polyols. It also acts as anti-fade reagent that scavenges free radicals produced by excitation of fluorochromes. It is also added to the mounting medium in fluorescence microscopy to retard photobleaching of fluorescein and other fluorescent dyes. Recently, it is reported as template (structure directing agent) in zeolite synthesis [3]. DABCO is manufactured by acid-catalyzed condensation of polyethyleneamine-based feedstocks. Early routes to DABCO involved cyclization of substituted piperazines, such as aminoethylpiperazine, *N*-(2-hydroxyethyl)piperazine, or *N,N'*-di(2-hydroxyethyl)piperazine, in the vapor phase over alumina [4,5] or in the liquid phase in the presence of an aromatic carboxylic acid catalyst [6]. Yields of DABCO were reported to be in the 50–70% range. In the mid-1980s, a strontium hydrogen phosphate catalyst was developed which produced DABCO from *N*-(2-hydroxyethyl)piperazine in 93% yield [7].

Even though zeolites have been used successfully in several commercial processes like fluid catalytic cracking, xylenes isomerization, alkylation reaction etc., they have not been fully explored so far for transformation of basic amino compounds to value added amines. Zeolite catalysts, particularly those having the pentasil structure, have also been shown to be active for these cyclization reactions, although DABCO selectivities equivalent to that obtained from the β-SrHPO$_4$ catalyst have not been achieved [8-10].

Recent efforts to identify process improvements have focused on the reaction of other polyethyleneamine feedstocks, such as monoethanolamine, ethylenediamine, and diethylenetriamine, over modified ZSM-5 zeolites [11-16]. In a broad spectrum, the amines used for DABCO synthesis are ethyleneamines (ethylenediamine, diethylenetriamine and triethylenetetramine); ethanolamines (monoethanolamine, diethanolamine and triethanolamine) isoproponalamines; piperazine and its derivates, N-hydroxyethylpiperazine, bis(hydroxyethyl)piperazine and N-aminoethylpiperazine or the mixture of the foregoing.

Few reports by Karpeiskaya et al. [17] and Scriabine [18] for the cyclization of ethanolamine showed the use of cobalt and alumina as suitable catalysts, respectively. Although conventional catalysts [17,18] gave higher yields, the selectivity was low and the product separation was difficult. Budnik and Sandner reported the synthesis of DABCO from N-aminoethyl piperazine over zeolites [19] and claimed that a zeolite based catalyst gives higher selectivities than existing industrial catalysts. The possibility of using monoethanolamine (MEA) as the starting material for the synthesis of DABCO is discussed in the open literature [20,21].

In our studies on conversion of MEA over zinc modified ZSM-5, dehydrogenation of piperazine, the intermediate product was observed with a subsequent formation of alkylpyrazines. However, the piperazine was formed over other two zinc-modified zeolites

studied (FER and MOR). Hence, we intend to study the synthesis of DABCO from piperazine over various acidic zeolite catalysts and zinc modified ZSM-5. The details of the product pattern with reaction parameters like temperature, contact time, stability of the catalyst etc. were discussed.

4.1.2.EXPERIMENTAL

4.1.2.1. Materials and Catalysts

The catalyst employed in this reaction is medium pore zeolites H-ZSM-5 and H-FER and large pore zeolites H-MOR and H-BETA (synthesis and characterization discussed in chapter 2). All the samples were exchanged with 1M aqueous NH_4NO_3 solution. The solid was filtered, washed with deionized water and dried at 110°C to yield NH_4-form of the zeolite, which was subsequently converted to the corresponding H-forms by calcination at 500°C. Piperazine (PIP) (>99% s.d. fine chemicals, India) was used as such with out further purification.

4.1.2.2. Synthesis of DABCO from PIP

The reactions were carried out in a down-flow, fixed-bed silica reactor (figure 2.23(a) in chapter 2) at atmospheric pressure and 375°C. An aqueous piperazine solution (20wt% PIP in H_2O) was fed to the reactor with an ISCO pump (Model 500D, USA) with a flow rate of $1h^{-1}$. Nitrogen gas was co-fed to the reactor at a rate of 20ml/min. Prior to each run the reactor, containing a catalyst charge of 3g (10-20 mesh size), was calcined for 4h in a flow of dry air and then cooled to the reaction temperature in a flow of N_2. The temperature was measured by a thermocouple located in the catalyst bed. The product was cooled using ice-cooled water and collected in the receiver. The products were analyzed on Shimadzu 15A gas chromatograph fitted with OV-101 column using FID detector. The products were identified by GC-MS (Shimadzu QP 5000) and GC-FTIR (Perkin Elmer Spectrum 2000).

4.1.3. RESULTS AND DISCUSSIONS

The reaction of piperazine (PIP) was carried out at 350°C reaction temperature and $1h^{-1}$ WHSV (weight hourly space velocity). Nitrogen is used as carrier gas and was fed at a rate of 20 ml/min. The major product of the reaction was the formation of DABCO over medium pore zeolites (ZSM-5 and FER) whereas the selectivity towards DABCO was decreased considerably over large pore zeolites (MOR and Beta). Apart from the formation of DABCO, other products identified include, pyrazine and methylpyrazine. The higher alkylpyrazines such as ethylpyrazine, dimethylpyrazine, and propylpyrazine were grouped under alkylpyrazines in the tables and figures. Among the various zeolites, H-ZSM-5 shows highest selectivity for DABCO (~85%) at conversions above ~ 77%.

4.1.3.1. Activity of catalysts and temperature

The catalytic activities for the PIP conversion and product selectivities over various zeolites such as H-ZSM-5, H-FER, H-Beta and H-MOR are exhibited in table 4.1.1. All catalyst showed high conversions of PIP (above 75%) at temperatures 350°C. However, the product distribution differs with the catalyst type and acidity. The medium pore zeolites (ZSM-5 and FER) produced DABCO as the major product, where as large pore zeolites (Beta and MOR) produced considerable amount of alkylpyrazines, particularly methylpyrazine.

In the case of H-ZSM-5, the conversion of PIP increases from 50.6% at 300°C to 96.5% at 450°C with an increase in temperature, correspondingly the selectivity of DABCO decreases from 87.3% at 300°C to 27.6% with concomitant increase in the side products like pyrazine and alkylpyrazines. These are formed by the decomposition and transformation of DABCO. The low boiling compounds include, methylamine, ethylenediamine, ethyleneimine, ammonia, and ethylene as identified by GC-MS. These compounds are formed by the decomposition of PIP or DABCO over the acid sites of the

zeolites. The dehydrogenation of PIP gives pyrazine; and the alkylpyrazines were formed by the reactions of the decomposed product with the pyrazine. The optimum temperature was 350°C for a high yield (66.3%) of DABCO. However, a maximum yield of 69.3% for DABCO was observed over H-ZSM-5 at a temperature of 400°C, the selectivity being 75.6%. It was reported that when the DABCO synthesis was carried out with MEA over ZSM-5 and modified ZSM-5, lower temperatures (<400 °C) do not favor the formation of pyrazine and its derivatives hence the selectivity of piperazine and DABCO increases and at higher temperature pyrazine derivatives increase [20,21]. Similar trend is also observed when piperazine is the feed over H-ZSM-5 as evident from table 4.1.1. At 350°C the yield of DABCO is 66.3% and at 400°C it is 69.3% where as at 450°C, it dropped down to a mere 22.8%. Ferrierite (FER) which is having one 10-membered and one channel system with 8-membered pore opening also shown good yield of DABCO (~54.2%) at 450°C. The product pattern in case of FER is similar to that of ZSM-5. Also, the DABCO being a bulkier molecule may not form in the channels of FER, but on the surface of the zeolite and hence showed lesser conversion than H-ZSM-5. In the case of MOR, the yield of DABCO remains the same with increase in temperature, however, the selectivity to higher alkylpyrazines decrease and that of methylpyrazine increases with temperature. The trend with the Beta zeolite is different from other zeolites under study, which showed poor yield towards DABCO. Due to the high acidic nature of Beta and MOR zeolites, cracking of PIP and subsequent alkylation reactions of the cracked product with PIP yielding alkylpyrazines. Hence H-Beta and H-MOR are not selective catalyst in the synthesis of DABCO. Also, with these large pore zeolites the formation of coke is high and the mass balance was less than 80% at high temperatures. The regeneration of these catalysts requires much longer time as compared to ZSM-5 and FER.

Table 4.1.1: Effect of reaction temperature on PIP conversion and product selectivities over various zeolites.

Catalyst	T °C	Conv. PIP	Selectivity (%)						Yield DABCO
			LB	Pz	MP	Alk.Pz	DABCO	Others	
H-ZSM-5	300	50.6	1	8.9	1.6	1.2	87.3	0	44.2
	350	77.7	1.7	6.7	1.5	4.7	85.3	0.1	66.3
	400	91.7	3.9	6.9	3.5	7.4	75.6	2.7	69.3
	450	96.5	10.6	14.9	19.8	26.1	23.6	5	22.8
H-FER	300	27.7	10.7	2.3	0	0	87	0	24.1
	350	40.1	8.3	2.6	0.6	1.2	87.3	0	35
	400	62.9	7.5	4.5	1.2	3.5	83.3	0	52.4
	450	71.7	8.9	13.1	2.5	6.5	67.6	1.4	48.4
H-MOR	300	56.3	13.4	0	0	31.6	47.2	7.8	26.6
	350	75.3	7.3	13.6	14.1	20.6	33.4	11	25.2
	400	88.2	6.5	18.1	21.7	13.9	28.2	11.6	24.9
	450	84.4	3.9	21.6	26.3	6.6	27.4	14.2	23.1
H-Beta	300	73	11.6	14.6	13.1	14.4	36.8	9.5	26.9
	350	78.3	9.5	15.7	40.3	10.2	11	13.3	8.6
	400	89.5	5.7	26.9	35.4	8.2	7.4	16.4	6.6
	450	86.1	6.4	30.7	28	6.1	6.3	22.5	5.4

LB = Lower Boilers; Pz = Pyrazine; MP = Methylpyrazine; Alk.Pz = Alkylpyrazines; Others = unidentifiers/ high boiling compounds

Reaction Conditions: Feed 20% PIP in water; WHSV = 1h^{-1}; TOS = 3h.

To account for the formation of alkylpyrazines, a reaction of ethylenediamine over H-ZSM-5 was studied. The major products are pyrazine and piperazine. Considerable amounts of methyl pyrazine, ethyl pyrazine and dimethyl pyrazine were also formed. PIP over acidic zeolites reacts to give ethylenediamine and ethylene (both are identified as

products by GC-MS), which on subsequent reaction with one more molecule of PIP to yield DABCO and N-aminoethylpiperazine. The latter compound can readily be converted to DABCO (figure 4.1.1).

Figure 4.1.1: Reaction scheme for conversion of PIP over acidic zeolites
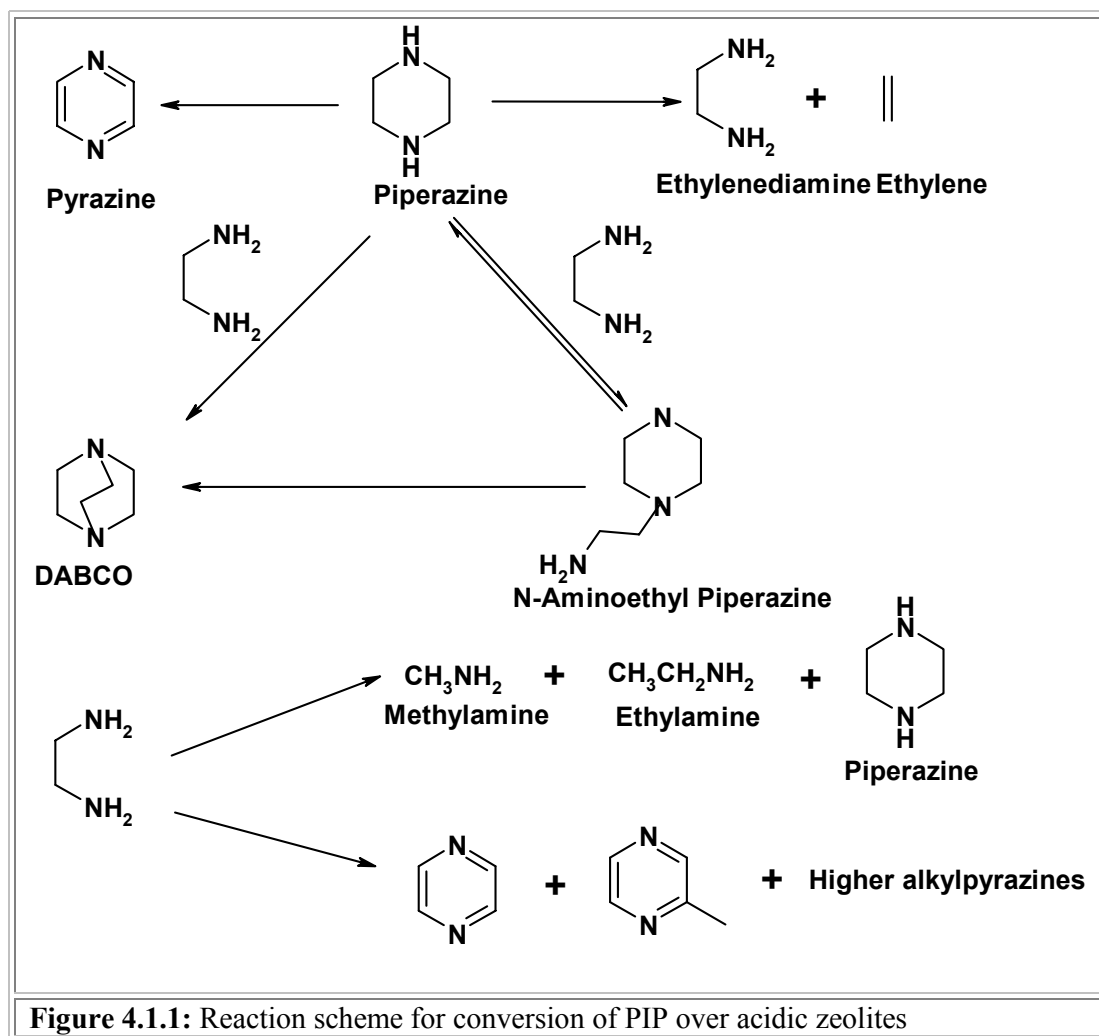
4.1.3.2. Influence of WHSV

The changes in PIP conversion and product selectivities on the reaction of PIP over H-ZSM-5 at WHSV (h^{-1}) ranging from 4 to 0.5 were shown in figure 4.1.2. There are no external mass transfer limitations as evident by the linear increase in PIP conversion with contact time. However, the selectivity to DABCO increases with decrease in contact time,

reaching 98.4% at a conversion of 44% for WHSV = 4h^{-1}. Thus keeping in view of DABCO selectivity and yield, it can be concluded that optimum WHSV was found to be 1h^{-1}.

Figure 4.1.2: Influence of space velocity on PIP conversion and product selectivities over H-ZSM-5.

Reaction Conditions: Feed 20% PIP in water; Temperature = 350°C; TOS = 3h.
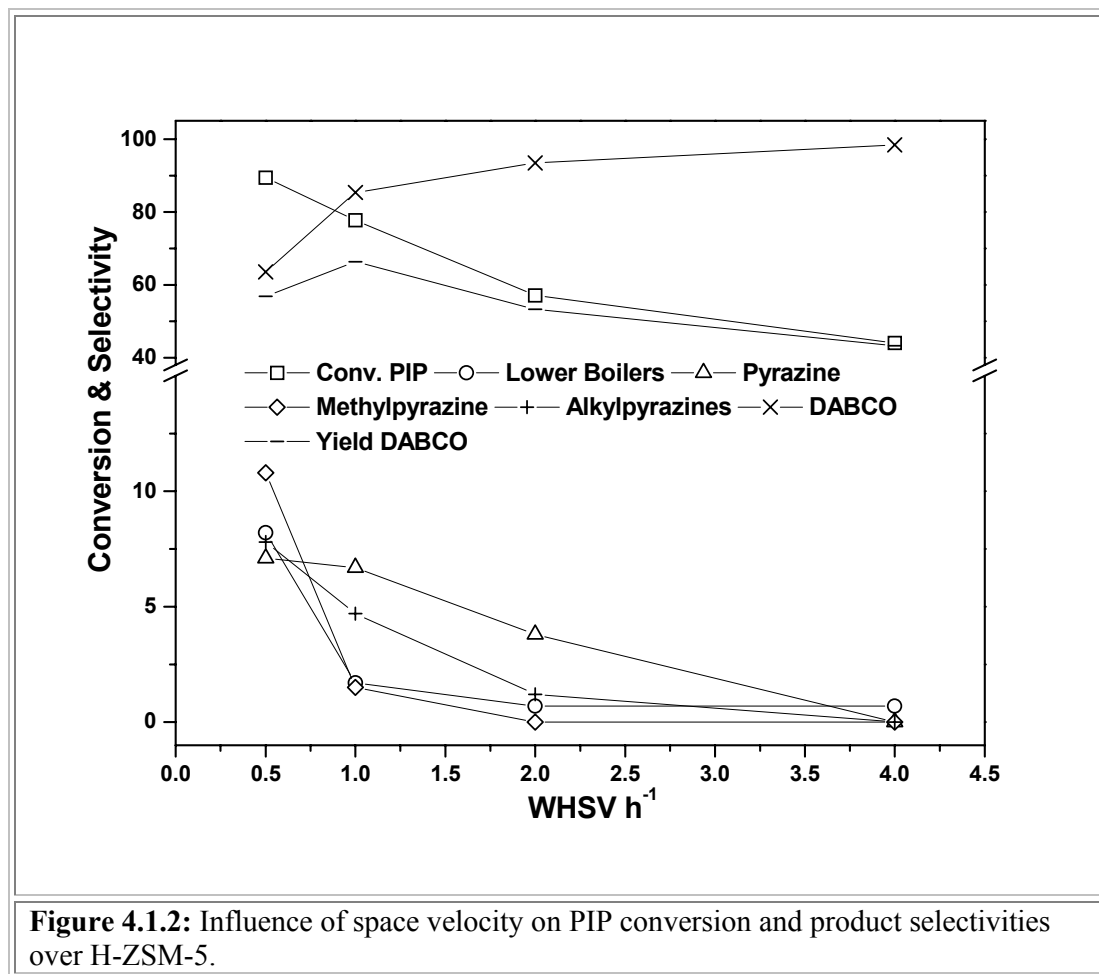
4.1.3.3. Influence of time on stream

The influence of reaction time on PIP conversion and product distribution over H-ZSM-5 at 350°C is depicted in figure 4.1.3. The conversion of PIP was high initially (91%) and decreased to 77.7% in 3h. This is due to surface coking of the zeolite, after which it showed a steady state conversion up to 12h.

Figure 4.1.3: Influence of time on stream on catalytic performance of H-ZSM-5 on PIP conversion and product selectivities.

Reaction Conditions: Feed 20% PIP in water; Temperature = 350°C; WHSV = 1h^{-1}
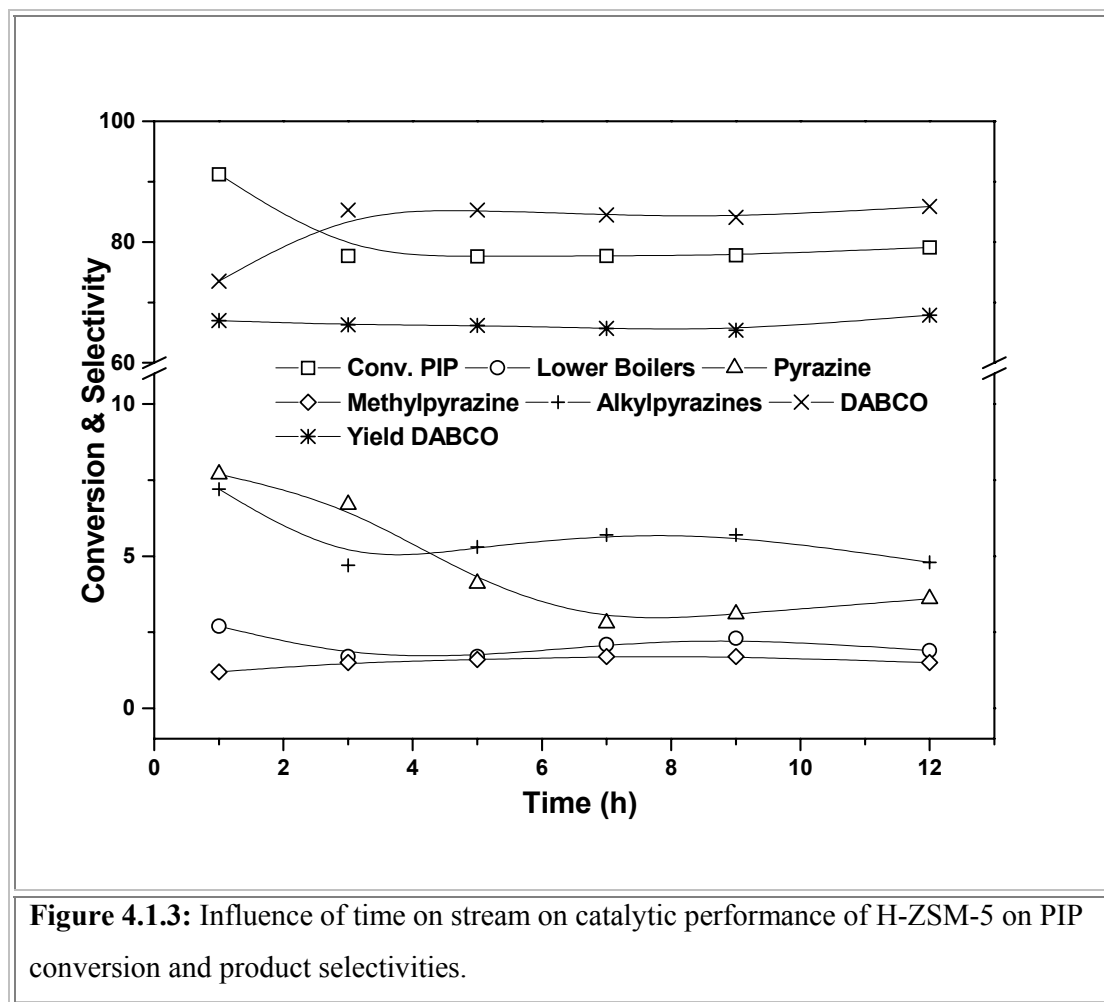
4.1.3.4. Influence of concentration of PIP

The influence of concentration of PIP in the feed was investigated over H-ZSM-5 at 350°C. As shown in table 4.1.2, a decrease in concentration of PIP (10%) in the aqueous solution of the feed improves the selectivity and yield of DABCO. At a high concentration of PIP (25%), the conversion as well as the yield of DABCO was poor and the formation of by-products was high.

4.1.3.5. Influence of silica to alumina ratio

It is well known that the increment of aluminum content determines the increase in the acid site density [22]. As shown in table 4.1.3, with increasing Si/Al ratio, the

conversion of PIP decreases from 85.5 to 38.4% and the selectivity of DABCO increase from 68.6 to 90.8%. The alkylated products or dehydrogenated products were formed more when the Si/Al ratio is low. It is reported that the coke formed on zeolite with low Si/Al ratio is olefinic and active in dehydrogenation reactions [23] and the acidity of the zeolite yields the alkylated products. Thus ZSM-5 with Si/Al ratio of 100 is optimum for the production of DABCO.

Table 4.1.2: Influence of PIP concentration on PIP conversion and DABCO selectivity using H-ZSM-5 as a catalyst.

Conc. PIP (wt%)	Conv. PIP	Selectivity (%)						Yield DABCO
		LB	Pz	MP	Alk.Pz	DABCO	Others	
10	84.9	1.1	5.5	1.2	0.9	91.3	0	77.5
20	77.7	1.7	6.7	1.5	4.7	85.3	0.1	66.3
25	58.4	9.4	10.7	4.8	7.8	60.2	7.1	35.2

LB = Lower Boilers; Pz = Pyrazine; MP = Methylpyrazine; Alk.Pz = Alkylpyrazines; Others = unidentifiers/ high boiling compounds

Reaction Conditions: Temperature = 350°C; WHSV = 1h^{-1}; TOS = 3h.

Table 4.1.3: Influence of Si/Al ratio PIP conversion and DABCO selectivity using H-ZSM-5 as a catalyst.

Si/Al ratio	Conv. PIP	Selectivity (%)						Yield DABCO
		LB	Pz	MP	Alk.Pz	DABCO	Others	
40	85.5	5.1	9.5	5.5	8.2	68.6	3.1	58.7
100	77.7	1.7	6.7	1.5	4.7	85.3	0.1	66.3
250	38.4	0.9	3.4	1.8	3	90.8	0.1	34.9

LB = Lower Boilers; Pz = Pyrazine; MP = Methylpyrazine; Alk.Pz = Alkylpyrazines; Others = unidentifiers/ high boiling compounds

Reaction Conditions: Feed 20% PIP in water; Temperature = 350°C; WHSV = 1h^{-1}; TOS = 3h.

4.1.3.6. Influence of zinc loading

In the previous chapter, we have discussed the conversion of MEA over zinc-modified zeolites. Two molecules of MEA undergo dehyrocyclization to yield piperazine, which was dehydrogenated to yield pyrazine and the reaction of cracked products of MEA with pyrazine yielded alkylpyrazines. In order to find out the role of zinc in the zinc impregnated and ion exchanged zeolite for this piperazine conversion, we have carried out this reaction over ZSM-5 zeolite with different ZnO loadings and the results are tabulated in table 4.1.4. It can be observed from the table 4.1.4 that unmodified H-ZSM-5 showed good conversion and yield to DABCO suggesting that the zeolite is good for both cracking of the piperazine and subsequent cyclization reaction to yield bicyclic compound DABCO.

Table 4.1.4: Conversion of PIP over modified ZSM-5

Catalyst	Conv. PIP	Selectivity (%)						Yield DABCO
		LB	Pz	MP	Alk.Pz	DABCO	Others	
H-ZSM-5	77.7	1.7	6.7	1.5	4.7	85.3	0.1	66.3
Zn-ZSM-5	61.2	1.9	28.5	2.5	5.1	61.3	0.7	37.5
ZnO-ZSM-5 (5)	56.8	5	16.7	4.2	10.6	61.5	2	34.9
ZnO-ZSM-5 (10)	54.1	5.1	21.3	12.2	8.9	48	4.5	25.9
ZnO-ZSM-5 (15)	47.7	6.4	25.4	12.5	8.2	42.5	5	20.3
ZnO-ZSM-5 (15)	8.5	1.5	50.7	6.8	1.1	39.9	0	4.3

LB = Lower Boilers; Pz = Pyrazine; MP = Methylpyrazine; Alk.Pz = Alkylpyrazines; Others = unidentifiers/ high boiling compounds

Reaction Conditions: Feed 20% PIP in water; Temperature = 350°C; WHSV = 1h^{-1}; TOS = 3h.

This catalyst upon modification with ZnO by impregnation (to various degree e.g. 5%, 10% etc.,) with zinc acetate followed by calcination at 550°C showed considerable decrease in conversion as well as selectivity to DABCO with concomitant increase in the formation of pyrazine suggesting that dehydrogenation activity of ZnO is more than the cyclization

activity of H-ZSM-5. This is also due to non-availability of Brönsted acid sites that are blocked by ZnO coverage. Similar effect is also observed with ion-exchanged Zn-ZSM-5 zeolite, however, showing better conversion compared to zinc impregnated ZSM-5. When the reaction is carried out over ZnO (prepared by firing zinc acetate at 550°C), the conversion of PIP is very poor (>9%) yielding pyrazine as the major product.

4.1.4. CONCLUSIONS

Piperazine can be converted to useful products like DABCO, methylpyrazine and higher alkylpyrazines over acidic zeolite catalysts. The medium pore zeolites (particularly, H-ZSM-5) are selective for the formation of DABCO where as the large pore zeolites are useful for alkylpyrazines. Catalyst with medium pore and less acidity leads to formation of DABCO; where as the one with strong and weak acidity leads to formation of dehydrogenated and alkylated products. Modification of H-ZSM-5 with ZnO by impregnation leads to diminish in conversion of PIP and selectivity to DABCO with increase in pyrazine selectivity showing the dehydrogenation activity of zinc.

4.2. ISOMERIZATION OF *ortho*-TOLUIDINE

4.2.1. INTRODUCTION

Isomerization and alkylation are acid catalyzed reactions. Friedel-Crafts catalysts (AlCl$_3$, FeCl$_3$, etc) traditionally used for acid catalyzed reactions, many a times produce undesirable products and pose difficulties such as catalyst separation as well as enhanced pollution and corrosion. Recently, K. Tanabe and W.F. Hölderich [24] published a statistical survey of industrial processes using solid acid–base catalysts. They identified and analyzed 127 different processes such as for alkylation, isomerization, amination, cracking, etherification, esterification, condensation reactions, etc. For these processes around 180 different catalyst types such as zeolites, oxides, complex oxides, phosphates, and ion-

exchange resins are employed. Among them zeolite catalysts represent, with 74 (about 45%), the largest group.

It is widely accepted that zeolites exhibit remarkable catalytic and adsorptive properties due to their well-defined pore structure with confined active sites. The size and shape of the zeolites are responsible for shape selectivity in different reactions [25]. Zeolites also find application in the synthesis of intermediates and fine chemicals [26,27].

In the past, shape selective conversions of mononuclear aromatics in zeolite catalysts have been studied extensively [25,28-32]. Industrial applications include the manufacture of ethylbenzene from benzene and ethylene [33,34] and the production of *para*-xylene by isomerization of its *ortho* and *meta* isomers [35,36]. So far, practically all commercial applications of shape selective conversion of aromatics rely on a single zeolite, viz. ZSM-5.

Toluidines are important intermediates for the manufacture of dyestuffs and agrochemicals and are generally synthesized by electrophilic nitration of toluene followed by reduction of the intermediate nitrotoluenes [37]. A mixture consisting mainly of *ortho*- and *para*- toluidines is formed in this process. *meta*- toluidine, another important chemical is produced in limited quantity in this process. The process practiced for the large volume production of this *meta*-isomer in the commercial scale is by the amination of *meta*-cresol, a relatively costly chemical [38]. A new process, the vapour phase catalytic isomerization of *ortho*- and *para*- toluidines is receiving increasing attention for producing this important chemical [39]. This isomerization chemistry provides a more commercially viable route for producing this *meta*-isomer from the readily available and cheaper *ortho*- and *para*-toluidine [40].

Many zeolite catalysts have shown outstanding ability to isomerize the di-substituted aromatics to the more value added isomer. H-ZSM-5 is a popular catalyst for

the intramolecular isomerization of substituted toluenes such as xylenes [41], cresols [42] toluonitriles [43], chlorotoluenes [44], toluidines [40,45-47], and ethylanilines [48] all equilibrate with this catalyst by 1,2-methyl migrations. The activity of H-ZSM-5 for isomerization and disproportionation reactions depends on its acid strength distribution. However, there are no reports on the comparison of zeolites with different structural properties and pore dimensions. It was therefore intended to study the isomerization of o-toluidine over zeolites such as H-ZSM-5, H-FER, H-Beta and HY having various channel tortuousity and pore dimensions. The isomerization reaction was studied in the temperature range of 300-450°C.

4.2.2.EXPERIMENTAL

4.2.2.1. Materials and Catalysts Studied

ortho-Toluidine (purity >99% Aldrich) was used as such with out any further purification. The catalysts used for this study are well-characterized (chapter 2) medium pore zeolites H-ZSM-5 and H-FER and large pore zeolites HY and H-Beta.

4.2.2.1.Isomerization of o-toluidine

The catalytic tests were carried out in a fixed bed down flow silica reactor (figure 2.23(a), Chapter 2) at atmospheric pressure in the temperature range 320-450°C with a catalyst charge of 3g loaded in the middle of the reactor in the form of pellets (10-20 mesh). The catalyst was activated at 500°C for 5h in a flow of dry air prior to the start of each run. The dry catalyst was then cooled to the reaction temperature in a flow of dry nitrogen. *ortho*-toluidine was injected at the top of the reactor at the required flow rate using a feed pump (ISCO 500D, USA).

The liquid products were analyzed on GC (Shimadzu 15A fitted with 20% KOH treated Carbowax 20M column) with a FID detector. The product identification was carried out on both GCMS (Shimadzu QP 5000) and GC-FTIR (Perkin Elmer Spectrum 2000).

The conversion, selectivity and yield are defined as follows:

$$\% \text{ o-toluidine conversion} = \frac{(\text{moles of o-toluidine in feed}) - (\text{moles of o-toluidine in product})}{\text{moles of o-toluidine in feed}} \times 100$$

$$\% \text{ selectivity to product (i)} = \frac{\text{moles of product (i)}}{\text{o-toluidine conversion}} \times 100$$

Yield = conversion X selectivity

4.2.3. RESULTS AND DISCUSSIONS

4.2.3.1. Effect of Catalyst type with temperature

Table 4.2.1(a,b) shows the results of o-toluidine isomerization on medium pore zeolites (H-ZSM-5 and H-FER) and large pore zeolites (H-Beta and HY) with increasing temperature from 325-450°C. It can be noticed that isomerization is the major reaction over medium pore zeolites whereas disproportionation is the major reaction over large pore zeolites. It is also noteworthy that total conversion was nearly equal to isomerization in the case of medium pore zeolites. The conversion of o-toluidine over H-FER is very less compared to H-ZSM-5 even though total acidity of former is higher than the latter (as seen from TPD studies, Chapter 2). This behaviour may be directly related to the structural features of ferrierite, which has 10 and 8 MR pores, and the diffusion of reagents is restricted to 10 MR pores. Further the 10 MR pores are less in number and also smaller in size due to their elliptical nature as compared to those in ZSM-5 hence the overall conversion is low.

In the case of large pore zeolites disproportionation of o-toluidine is high and HY zeolite exhibits higher conversion than H-Beta zeolite. It was believed that transalkylation requires high acid site density and the low disproportionation observed in case of medium

pore zeolites may be due to wide spacing of the acid sites [31]. Later, it was concluded that the controlling factor was restricted transition state selectivity in case of isomerization of substituted toluenes, which involves the formation of bulky diphenylmethane intermediates, medium pore zeolites like ZSM-5 and FER don't favour the bulky molecules. Also high acidity observed with wide pore zeolites favour dealkylation and disproportionation.

Table 4.2.1(a): Influence of temperature on isomerization of o-toluidine over large pore (HY and HBeta) zeolites

Catalyst	HY				H-Beta			
Temperature °C	325	350	400	450	325	350	400	450
o-toluidine Conv.	5.1	21.1	42.7	43.9	3.7	15.6	23.7	28.2
Aniline	29.8	37	31.2	32.8	22.1	26.4	26.6	30.8
p-toluidine	9.9	4.7	8.4	8.9	8.7	4.5	4.2	6.4
m-toluidine	29.3	5.5	11.9	15.9	38.3	27.5	29.6	24.8
Dimethyl anilines	28.5	45.2	30.7	25.7	29	35.9	30.2	24.6
Others	2.5	7.6	17.8	16.7	1.9	5.7	9.4	13.4
Isomerization	39.2	10.2	20.3	24.8	47.0	32.0	33.8	31.2
Disproportionation	58.3	82.2	61.9	58.5	51.1	62.3	56.8	55.4
Iso/Disp	0.7	0.1	0.3	0.4	0.9	0.5	0.6	0.6
m/p isomer ratio	3.0	1.2	1.4	1.8	4.4	6.1	7.0	3.9
Yield m-toluidine	1.5	1.2	5.1	7.0	1.4	4.3	7.0	7.0

Reaction Conditions: Feed = o-toluidine; WHSV = 0.66h^{-1}; TOS = 3h; Pressure = atm.

HZSM-5 is shape-selective because diphenylmethane type intermediates are too big to form inside its pore structure [49,50]. These intermediates can form inside larger zeolites such as HY or on the surface of amorphous solid-acids such as silica-alumina [51]. Analogous diaminodiphenylmethanes are by-products in the formation of

methylenedianiline from aniline and formaldehyde. It can be anticipated that for disproportionation of o-toluidine, the space available in the cages, lobes and intersections of the zeolite channels will be more important than the dimensions of the pore openings. As evident from the table 4.2.1(a,b) that the conversion of o-toluidine increases with temperature over all the zeolites under study. It was also observed that above 400°C, the product pattern was in the thermodynamic equilibrium. (Thermodynamic equilibrium composition of toluidine isomers [47] at 400°C: 16.1 *para*, + 33.7 *ortho*, + 50.2 *meta*).

Table 4.2.1(b): Influence of temperature on isomerization of o-toluidine over medium pore (H-ZSM-5 and H-FER) zeolites

Catalyst	H-ZSM-5				H-FER			
Temperature °C	325	350	400	450	325	350	400	450
o-toluidine Conv.	9.8	27.6	40.1	57.5	2.9	8.7	14.4	19.3
Aniline	2.9	4.3	5.7	9.4	1	0.9	1.4	2
p-toluidine	9.3	12.6	17.9	19.5	6.8	11	16.2	19.3
m-toluidine	83.6	78.4	70.5	62.5	89.4	85.8	78	71.7
Dimethyl anilines	3	4.5	5.2	6	0.1	0.5	0.7	0.9
Others	1.2	0.2	0.7	2.6	2.7	1.8	3.7	6.1
Isomerization	92.9	91.0	88.4	82.0	96.2	96.8	94.2	91.0
Disproportionation	5.9	8.8	10.9	15.4	1.1	1.4	2.1	2.9
Iso/Disp	15.7	10.3	8.1	5.3	87.5	69.1	44.9	31.4
m/p isomer ratio	9.0	6.2	3.9	3.2	13.1	7.8	4.8	3.7
Yield m-toluidine	8.2	21.6	28.3	35.9	2.6	7.5	11.2	13.8

Reaction Conditions: Feed = o-toluidine; WHSV = 0.66h^{-1}; TOS = 3h; Pressure = atm.

The m/p isomer ratio is found to be higher at lower temperature and it progressively decreases with increase in temperature due to the secondary isomerization reactions. Furthermore, it is observed that even at higher temperature disproportionation is low over

H-FER as compared with H-ZSM-5. Over Beta and HY zeolites the disproportionation passes through a maximum at 350°C and thereafter decreases due to increased dealkylation, subsequent realkylation and other hydrocarbon formations at higher temperatures.

4.2.3.2. Mechanism

The isomerization of o-toluidine is unimolecular reaction, however, formation of DMAs (Dimethyl anilines) is a bimolecular reaction and proceeds via diaryl intermediate. Thus, in the case of medium pore zeolites, monomolecular mechanism involving successive 1,2- methyl shifts around the ring and protonated benzenium ion can be visualized. At high temperatures the protonated benzenium ion (σ complex) is formed followed by a single or successive 1,2-methyl shifts resulting n the formation of *meta* and *para* isomers of toluidine as follows
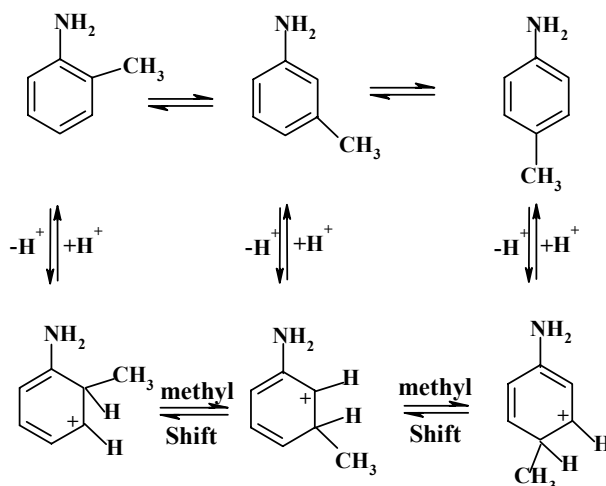
4.2.3.3. Effect of WHSV

Table 4.2.2 summarizes the effect of WHSV on the o-toluidine isomerization over H-ZSM-5 and HY zeolites. In both the cases the conversion decreases with the increase in WHSV. However, there is no change in the m/p isomer ratio over both the zeolites. It is

149

also observed that a huge amount of unidentified compounds (high boiling compounds) and hydrocarbons are formed at lower WHSV. Secondary reactions are favored at high contact time. Even at higher WHSV, we observed that disproportionation is the main reaction over HY zeolite. It is also reported that the initial reaction was disproportionation of the o-toluidine to aniline and 2,4- and 2,6-DMA over HY zeolite and DMAs then exchange methyls to produce DMA isomers with *meta*- methyls [52]

Table 4.2.2: Influence of space velocity on isomerization of o-toluidine over HY and H-ZSM-5 zeolites

Catalyst	HY					H-ZSM-5				
WHSV h^{-1}	0.33	0.66	1	2	4	0.33	0.66	1	2	4
o-toluidine Conv.	62	42.7	37.4	34.3	18.9	49.8	40.1	37.9	25.6	18.1
Aniline	26.8	31.2	30.8	32.3	35.5	8.5	5.7	4.7	3.5	1.1
p-toluidine	8.7	8.4	8.8	7	5.3	18.3	17.9	19	18.9	18.5
m-toluidine	5.2	11.9	13.1	10.5	9	65.8	70.5	72.5	75.3	79.7
Dimethyl anilines	24.5	30.7	30.9	37.4	41.7	5.6	5.2	3.3	1.9	0.7
Others	34.8	17.8	16.4	12.8	8.5	1.8	0.7	0.5	0.4	0
Isomerization	13.9	20.3	21.9	17.5	14.3	84.1	88.4	91.5	94.2	98.2
Disproportionation	51.3	61.9	61.7	69.7	77.2	14.1	10.9	8.0	5.4	1.8
Iso/Disp	0.3	0.3	0.4	0.3	0.2	6.0	8.1	11.4	17.4	54.6
m/p isomer ratio	0.6	1.4	1.5	1.5	1.7	3.6	3.9	3.8	4.0	4.3
Yield m-toluidine	3.2	5.1	4.9	3.6	1.7	32.8	28.3	27.5	19.3	14.4

Reaction Conditions: Feed = o-toluidine; Temperature = 400°C; TOS = 3h; Pressure = atm.

4.2.3.4. Effect of time on stream

The effect of time on stream on the o-toluidine conversion at atmospheric pressure for HY and H-ZSM-5 are compared in both figure 4.2.1 and table 4.2.3(a,b).

Table 4.2.3(a): Influence of time on isomerization of o-toluidine over HY zeolite

Catalyst	HY						
Time (h)	2	3	4	6	8	10	12
o-toluidine Conv.	43.3	42.7	26.5	15.2	10.6	6.9	5.2
Aniline	30.5	31.2	33.6	34.2	37.1	36.2	37.3
p-toluidine	7.6	8.4	6.8	7.2	2.4	2.9	2
m-toluidine	10.9	11.9	12.5	16.5	19.1	20.3	21.6
Dimethyl anilines	29.8	30.7	36.6	37.5	35.3	34.8	33.3
Others	21.3	17.8	10.6	4.6	6.1	5.8	5.9
Isomerization	18.5	20.3	19.3	23.7	21.5	23.2	23.6
Disproportionation	60.3	61.9	70.2	71.7	72.4	71.0	70.6
Iso/Disp	0.3	0.3	0.3	0.3	0.3	0.3	0.3
m/p isomer ratio	1.4	1.4	1.8	2.3	8.0	7.0	10.8
Yield m-toluidine	4.7	5.1	3.3	2.5	2.0	1.4	1.1

Reaction Conditions: Feed = o-toluidine; Temperature = 400°C; WHSV = 0.66h^{-1}; Pressure = atm.

Table 4.2.3(b): Influence of time on isomerization of o-toluidine over H-ZSM-5 zeolite

Catalyst	H-ZSM-5						
Time (h)	2	3	4	6	8	10	12
o-toluidine Conv.	42.6	40.1	39.4	37.3	33.8	32.6	30.9
Aniline	5.6	5.7	4.3	2.4	2.4	2.5	2.9
p-toluidine	18.7	17.9	20.3	20.9	20.4	22	19.8
m-toluidine	71	70.5	72.1	74	74.8	72.4	74.3
Dimethyl anilines	4.3	5.2	2.8	1.7	1.8	1.9	2
Others	0.4	0.7	0.5	1	0.6	1.2	1
Isomerization	89.7	88.4	92.4	94.9	95.2	94.4	94.1
Disproportionation	9.9	10.9	7.1	4.1	4.2	4.4	4.9
Iso/Disp	9.1	8.1	13.0	23.1	22.7	21.5	19.2
m/p isomer ratio	3.8	3.9	3.6	3.5	3.7	3.3	3.8
Yield m-toluidine	28.5	**28.3**	28.4	27.6	25.3	23.6	23.0

Reaction Conditions: Feed = o-toluidine; Temperature = 400°C; WHSV = 0.66h^{-1}; Pressure = atm.

Figure 4.2.1. Variation conversion of o-toluidine on time on stream over HY and H-ZSM-5 zeolites
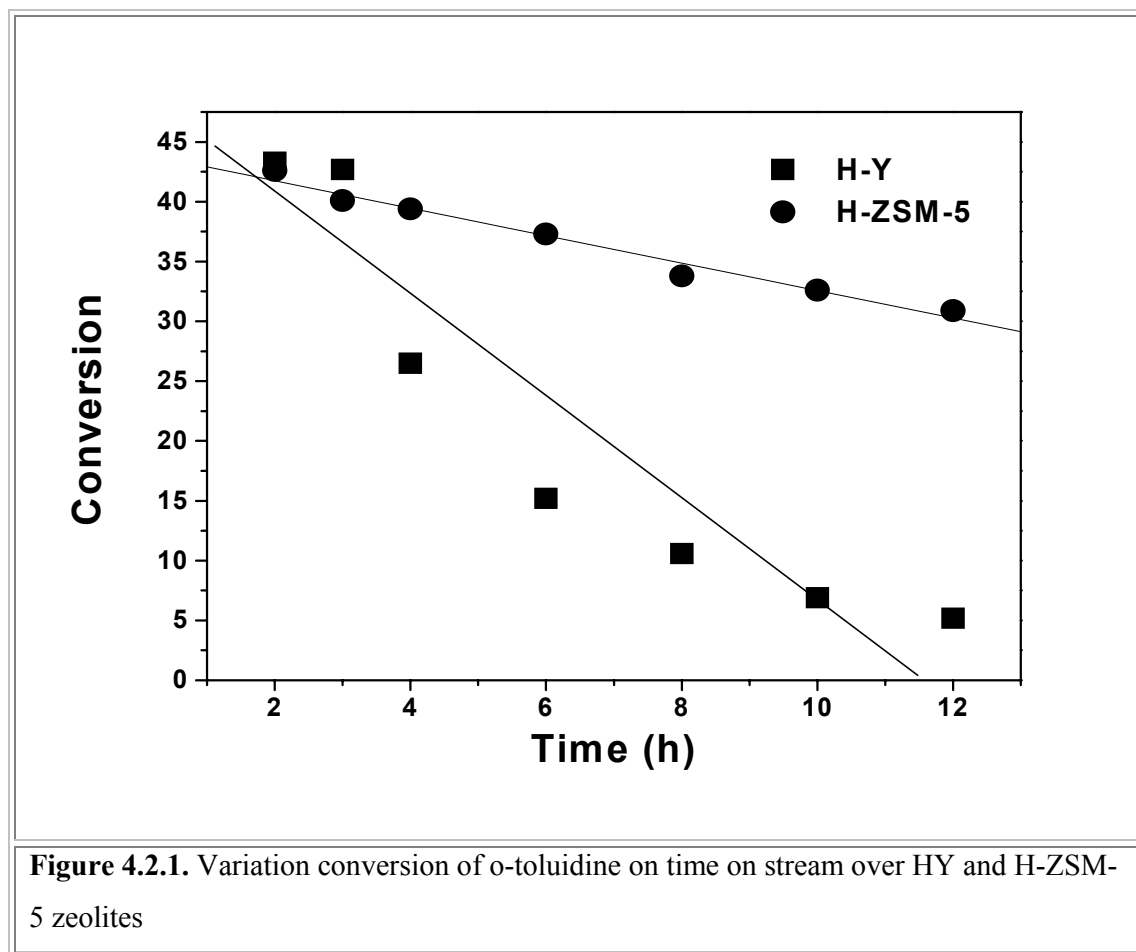
The activity over HY zeolite dropped rapidly from 43.3 to 5.2% over a period of 12h showing a rapid deactivation. However, over H-ZSM-5 the activity is marginally decreased from 42.6 to 30.9% for the same duration of time suggesting the better stability of the catalyst compared to HY zeolite. It is also worth noting that the ratio of isomerization to disproportionation remains almost same during the period of study over HY zeolite whereas it increases with time over H-ZSM-5 zeolite. Also m/p isomer ratio increases with time over HY, however it remains almost same over H-ZSM-5.

4.2.4. CONCLUSIONS

The channel dimensionality and pore openings of different zeolites studied, reveals that the H-ZSM-5 (medium pore) zeolite favours isomerization contrary to wide pore zeolites favoring disproportionation. The m/p isomer ratio is found to be higher at lower temperature and it progressively decreases with increase in temperature however, with contact time, there is not much change in the m/p isomer ratio over both the zeolites. The deactivation is found to be more for wide pore zeolite than the medium pore H-ZSM-5.

4.3. METHYLATION OF *ortho*-TOLUIDINE

4.3.1. INTRODUCTION

The alkylation of aniline with methanol is industrially important reaction as it gives toluidine, N-methylaniline (NMA) and N,N-dimethylaniline (NNDMA) as major compounds which are important intermediates in the manufacture of dyes, plastics and explosives. The vapour-phase process was initially studied by Hill et al.[53], using Al_2O_3 as catalyst and obtained a high aniline conversion [54]. In recent years, this process has been investigated over various zeolites [55-58]. A review on the aniline alkylation over solid acid catalysts also appeared recently [59]. The results suggest that the major factors influencing the activity and selectivity of the gas phase alkylation of aniline are the acid-base properties and shape selectivity of the solid catalyst.

It was shown that on faujasite catalysts, dimethyl carbonate (methylating agent) is very selective for the alkylation of aniline to N-methylaniline. Thus, zeolites K-EMT and K-Y are selective catalysts (99.6% conversion with 93.5% N-methylaniline selectivity even at 408 or 453 K) [60,61]. Alkaline X zeolites are the best catalysts for the production of N,N-dimethylaniline (a 75% selectivity at 97% aniline conversion) [61]. Barthomeuf et al. [57,58] studied this reaction over different zeolites. They concluded that it involves acid

(cations) and basic (oxygen) sites. The more basic zeolites (X and Y exchanged with K, Rb or Cs) favour production of N-alkylates. The zeolites with the more acidic cations, amongst alkali metals, Li and Na, lead to C-alkylation. In addition to acid and basic sites, the reaction involves variables that are specific to each structure. Woo et al. [62,63] investigated the selective alkylation of aniline with methanol over several metallosilicates. They suggested that strong acid sites, medium acid sites, and weak acid sites, are all active sites that yield C-alkylate and coke, NNDMA and N-methyltoluidine (NMT), and NMA, respectively.

Despite many studies on the aniline methylation, there are not many reports in the literature describing alkylation of o-toluidine. Choi et al. [64] has studied N-alkylation of o-toluidine with ether on HX zeolite catalysts modified with K, Cs, K-Mg and MgO and reported that HX zeolite gives maximum conversion at 300°, while the catalysts, modified catalysts with less acidity exhibit maximum conversions at higher temperatures. Synthesis of 2,6-dimethylaniline (2,6-DMA) is also an important industrial process and a potential route to 2,6-DMA might involve the direct *ortho*-methylation of aniline similar to the commercially used process to make 2,6-dimethylphenol [65] and the selective catalysts for this reaction have been reported [66]. Catalytic *ortho*-ethylation of aniline is a well-established process [67]. Zhang et al. [68] has studied synthesis of 2,6-DMA from *ortho* -toluidine and methanol by vapor phase alkylation over solid V_2O_5 catalyst. They reported that the optimum cocatalyst is Cr_2O_3 and the optimum ratio is $V_2O_5/ Cr_2O_3 =$ 10/1(mol/mol), o-toluidine/MeOH molar ratio 1/3, and liq. velocity $0.5h^{-1}$ for the synthesis of 2,6-DMA and its selectivity can be improved by addition of water in the feed. Chen et al. [69-71] studied the alkylation of o-toluidine with methanol over V_2O_5- Cr_2O_3-Al_2O_3 mixture and γ-Al_2O_3- V_2O_5 mixture separately. However, there are no reports on the methylation of o-toluidine with methanol or dimethylcarbonate as alkylating agent over

zeolite catalysts. It was therefore intended to study the methylation of o-toluidine with methanol over both medium and large pore zeolites and the distribution of product selectivities was discussed with structural differences of the zeolites and their acidity.

4.3.2. EXPERIMENTAL

4.3.2.1. Materials and Catalysts

Methanol (E-Merck) and o-toluidine (Aldrich) were used as such without further purification. Catalysts screened for this reaction are H-FER, H-ZSM-5, H-Beta, H-MOR and HY. Synthesis and detailed characterizations of these zeolites are discussed in chapter 2. The catalyst studied and their acidity values are given in table 4.3.1

Table 4.3.1: Characteristics of zeolites studied for *ortho*-toluidine methylation.

Zeolite	SiO$_2$/Al$_2$O$_3$	TPD acidity mmol/g		FTIR Pyridine adsorption (B/L Ratio)	
		LT	HT	200	300
H-ZSM-5	200	0.12	0.16	10.7	-
H-FER	34	0.53	0.39	6.66	6
HY	4.76	1.34	3.2	1.56	1.85
H-Beta	30	0.69	1.14	1	2.7
H-MOR	25	0.8	0.96	18.7	22

4.3.2.2. Reaction procedure

The catalytic alkylation of o-toluidine with methanol at temperatures 250-450°C was carried out at atmospheric pressure using a fixed-bed down flow reactor (figure 2.23, chapter 2) containing 3g of previously calcined zeolite catalyst and activated under a stream of nitrogen for 30min prior to the experiment. A mixture of o-toluidine and methanol with the required molar ratio was introduced into the reactor by means of a syringe pump (ISCO, 500D, USA). The liquid products were collected every hour, and quantified by gas chromatograph (GC) using a flame ionization detector and HP-1 capillary

column. Reaction products were identified by GC-MS (Shimadzu QP 5000) and GC-FTIR (Perkin Elmer Spectrum 2000).

4.3.3. RESULTS AND DISCUSSION

The major products of the reaction of OTD (*o*-toluidine) methylation were NM-OTD (N-methyl-*o*-toluidine), NNDM-OTD (N,N-dimethyl-*o*-toluidine,), 2,4-DMA (2,4-dimethyl aniline), NM-Xy (N-methyl Xylidines) and 2,4,6-TMA (2,4,6- trimethylaniline), and minor amounts of 2,6-DMA (2,6-dimethylaniline), NNDM-Xy (N,N-dimethyl Xylidines) and other unidentified compounds on all the zeolites under study.

4.3.3.1. Effect of Catalyst type and temperature

Table 4.3.2(a,b) shows the activity and selectivity of various catalysts for the methylation of o-toluidine at different reaction temperatures (250-450°C) for a time on stream of 2h. The main products of the reaction are both NMOTD and 2,4-DMA. The medium pore zeolites H-ZSM-5 and H-FER showed very less conversion (>30%, even at 400°C) and are selective to N-mono-methylation of o-toluidine. However, the large pore zeolite, H-Beta showed more selectivity towards C-alkylated product, 2,4-DMA. Due to pore restrictions in H-MOR, both NMOTD and 2,4-DMA are formed in equal amounts at higher temperatures. HY showed very low activity than other two large pore zeolites H-Beta and H-MOR. Even at higher temperature, 400°C, the selectivity of NM-OTD is higher than 2,4-DMA. Similar effect is also observed for aniline methylation and is reported that for a given structure the N-alkylation is favored on basic zeolites ZSM-5 or faujasite [57, 72] while protonic ZSM-5 gives C-alkylation [56].

The activity of the catalyst follows the order (at 350°C)

H-Beta > H-MOR > HY > H-ZSM-5 > H-FER (based on OTD conversion)

H-Beta > H-ZSM-5 > H-MOR > HY > H-FER (based on NM-OTD yield)

H-Beta > H-MOR > HY > H-ZSM-5 > H-FER (based on 2,4-DMA yield)

It can be generalized that in the reaction of o-toluidine with methanol, the medium pore zeolite favors the formation of N-alkylates and large pore zeolites has a bias towards C-alkylation based on acidity and the structural features

With the increase of temperature (table 4.3.2a,b), in general, the conversion of o-toluidine increases over all the catalysts. At low temperature formation of N-mono methylation is favoured over all the zeolites. At high temperature, formation of 2,4-DMA is favoured over large pore zeolites. The selectivity of NMOTD decreases with temperature with concomitant increase in that of 2,4-DMA.

Table 4.3.2(a): Catalytic properties of Medium pore zeolites studied in o-toluidine methylation

Catalyst	ZSM-5					HFER			
T °C	250	300	350	400	450	300	350	400	450
Conv. OTD	5.5	26.8	34.9	42.5	55.7	10.8	17.1	24.3	33.4
Product Selectivity (%)									
Lower Boilers	0	0	0.3	0.4	0.4	0	0.7	0.8	0.5
NNDM-OTD	8.7	6.5	3.9	1.4	1.3	9.5	6.6	4.8	2.5
NNDM-Xy	0	0	0	0	0	0	0	0	0
NM-OTD	80.7	72.6	65.4	56.5	47.1	83.1	78.5	73.7	62.8
2,6-DMA	0.3	0.7	0.7	1.5	2.1	0.2	0.5	0.5	1.2
2,4-DMA	10.3	19.1	25.6	34.4	40	6.9	11.6	16.6	27.1
NM-Xy	0	0	1.1	1.7	2	0	0	0.5	0.9
2,4,6-TMA	0	1	2.7	3.7	6.6	0.2	1.7	2.6	4.5
Others	0	0.1	0.3	0.4	0.5	0.1	0.4	0.5	0.5

Reaction conditions: Methanol : o-Toluidine = 2:1 (mol), WHSV = 1h^{-1}, TOS = 2h

The higher conversion obtained on large pore zeolites than on medium pore zeolites can be attributed to the number and nature of acid sites. Nitrogenous bases are known to poison the acid sites on zeolites by strong adsorption and hence the available Brönsted

acid sites on medium pore zeolites are quickly poisoned where as the number of Brönsted acid sites available in large pore zeolites are higher and are not poisoned to the same degree.

Table 4.3.2(b): Catalytic properties of Large pore zeolites studied in o-toluidine methylation

Catalyst	HB				MOR					HY				
T °C	300	350	400	450	250	300	350	400	450	250	300	350	400	450
Conv. OTD	24.5	61.1	77.1	83.5	22.2	37.3	41	51	65.2	19	28.8	36.7	45.7	56.2
Product Sel. (%)														
Lower Boilers	0.4	0.3	0.6	3.1	0.9	0.5	0.8	1.5	1.7	0	3	1	1.6	0.6
NNDM-OTD	9.1	3.1	1	0.4	3.9	4.2	4.1	3.8	3.6	4.7	4.4	2.6	1.4	0.7
NNDM-Xy	0	0.2	0.4	0.2	0	0	0	0.2	0.2	0	0.1	0.2	0.4	0.4
NM-OTD	69.7	43.7	3.8	1.1	81.8	68	44.8	35.9	23.5	79.4	60.6	48.7	41.4	23.6
2,6-DMA	1.2	1.8	2.4	1.9	0.2	1.5	2.9	3.1	3.5	0.5	0.9	1.4	1.5	1
2,4-DMA	14.3	32	69.1	57.8	8.9	17.9	35.8	37.8	43.3	13.7	21.1	30.2	31	44.8
NM-Xy	2.7	7.8	8.3	6.8	0	2.4	2.3	2.1	2	1.2	2.7	2.7	3.5	2.9
2,4,6-TMA	2.4	10.9	12.9	26.4	3.6	5.1	8.7	14.5	20.5	0.5	4.2	6.5	8.5	16.6
Others	0.2	0.2	1.5	2.3	0.7	0.4	0.6	1.1	1.7	0	3	6.7	10.7	9.4

Reaction conditions: Methanol : o-Toluidine = 2:1 (mol), WHSV = 1h^{-1}, TOS = 2h

It is also seen from table 4.3.2b that the zeolite H-Beta catalyzes the reaction efficiently towards C-alkylation more than the other zeolites under study. The selectivity to 2,4-DMA and 2,4,6-TMA increased while that of NNDM-OTD and NM-OTD decreased at higher reaction temperatures. The selectivity towards NMOTD decreased steadily with reaction temperature from 79.8% to a mere 1.1% at 250 and 450°C respectively. At lower temperature (250°C), there is no formation of NM-Xy and NNDM-Xy, however, with increase of temperature, these products also are formed which are due to the methylation of DMA and NM-Xy respectively. Strong acid sites are required to produce C-methylation

and coke. Weak acid sites are active for NMOTD, whereas medium acid sites are active for formation of NNDM-OTD and NM-Xy. A moderate reaction temperature (400°C) was helpful to enhance the product selectivity to 2,4-DMA. Considering the o-toluidine conversion and product distribution, the optimum reaction temperature is 400°C. At this reaction temperature, the selectivity to 2,4-DMA is the highest (69.1% and yield 53.3%) at high o-toluidine conversions (77.1%).

4.3.3.2. Influence of acidity

 . In the alkylation of aromatic amines, the studies show that the reaction is acid catalyzed and the product distribution primarily depends up on the nature and strength of acid sites. The preponderance of the interaction of zeolite with the lone pair of electrons on "N" in amine group or with the π electrons of aromatic ring dictates the product distribution in favour of side chain alkylation or ring alkylation respectively. Hence, the product distribution seems to depend on the relative amount of Brönsted and Lewis acid sites on the zeolite surface. Table 4.3.2a,b shows that the product distribution not only depends on the pore structure of the catalysts but also on acid site distribution. It is known that Lewis acid sites form N-methylated products in the methylation reaction of alkylaromatic amines. Comparing the Lewis acid site distribution over the temperature range of our study (discussed in chapter 2, given in table 4.3.1) and product distribution in table 4.3.2(a,b), similar trends can be noted. C-alkylation is found to follow the concentration of Brönsted acid sites except H-β zeolite, which showed more Lewis acid sites at lower temperatures and Brönsted acid sites at higher temperature above 300°C and this may be responsible for marked increase in the conversion of o-toluidine as compared with the other zeolite systems under study. Also a sudden drop in N-alkylation and an increase in C-alkylation from 350 to 400°C is observed which can be attributed to the increase in Brönsted acidity of Beta zeolite. Even though HY possess higher number of

acid sites, the conversion is less than H-Beta and H-MOR. Also the C-alkylation is less compared to H-Beta. This can be due to the fact that HY possessed almost same B/L ratio above 200°C and hence it produced both N- and C-alkylated products.

At higher temperatures (≥ 400) over H-Beta, the selectivity to NMOTD decreased to less than 4% and a marked increase in selectivities of 2,4-DMA. This may be due to isomerization of NMOTD to 2,4-DMA at higher temperatures by Brönsted acid sites. Pyridine cannot access the internal acid sites of 8-membered ring of H-FER and hence some of the product (dialkylated product) may be produced on the surface of the zeolite. The lower conversion than H-ZSM-5, even though the Si/Al ratio is lesser than that of H-ZSM5, can be correlated to this.

4.3.3.3. Influence of molar ratio

The effect of varying molar ratio of methanol/o-toluidine on the activity and selectivity of zeolite H-Beta at 400°C and a space velocity (WHSV (h^{-1})) of 1 is depicted in table 4.3.3. The results show that the conversion of o-toluidine and selectivity to 2,4,6-TMA increased with increasing molar ratios. The conversion of o-toluidine is almost complete at methanol / o-toluidine molar ratio of 7. Also it is interesting to note the formation of NNDM-2,4,6-TMA at molar ratios ≥ 5. The product selectivity to 2,4-DMA reached 69.1% at 77.1% o-toluidine conversion at a molar ratio of 2:1 with very less side products. The formation of side products (N-, N,N-, C-, C,N- alkylated products) was observed at higher concentration of methanol. It is noteworthy that at lower molar ratio (0.5), apart from the decrease in conversion, formation of aniline in considerable amount shows that the disproportionation of o-toluidine has taken place.

4.3.3.4. Influence of WHSV

The influence of space velocity on the activity and selectivity of zeolite H-Beta catalyst was studied at 400°C for a methanol/o-toluidine (molar ratio) of 2:1. Figure 4.3.1

shows o-toluidine conversion and product distribution of the reaction at WHSV (h^{-1}) ranging from 5 to 0.5. It is clear from fig. 4.3.1 that o-toluidine conversion decreases from 84.9% to 56.9% with increase in WHSV from 0.5 to $5h^{-1}$ respectively and product selectivity to 2,4-DMA remains almost unchanged. The linear increase in OTD conversion up to 84.9% with contact time indicates that there are no external mass transfer limitations. At longer contact times, the selectivity to 2,4,6-TMA increased approximately to 14%. The selectivity towards NM-OTD decreased with increase in contact time, due to further methylation of NMOTD to NNDM-OTD and NM-Xy. However, the increase in concentration of NM-Xy was up to 8.9% at WHSV ($2h^{-1}$), a further increase in contact time resulted in a decrease in its selectivity with concomitant increase in the formation of NNDM-Xy. Also the selectivity towards NNDM-OTD was nearly same, suggesting that NNDM-Xy is produced by methylation of NM-Xy and not by NNDM-OTD.

Table 4.3.3: Influence of reactant molar ratio (methanol: *o*-toluidine) on *o*-toluidine methylation over Hβ

MeOH/o-toluidine molar ratio	7	5	2	1	0.5
Conv. o-Toluidine	100	92.9	77.1	51.7	29.3
Product Selectivity (%)					
Lower Boilers	0.9	0.6	0.6	0.5	0.5
Aniline	0	0	0	2.9	6.9
NNDM-OTD	7.2	3.9	1	1.2	0.5
NNDM-Xy	18.2	10.6	0.4	0	0
NM-OTD	15.3	9.5	3.8	3.4	2
2,6-DMA	4.3	3.6	2.4	3.1	0.5
2,4-DMA	20.4	45	69.1	78.3	83.1
NNDM-2,4,6-TMA	3.9	2.1	0	0	0
NM-Xy	10.1	9.4	8.3	2.1	1
2,4,6-TMA	19.3	14.8	12.9	7.2	4.5
Others	0.4	0.5	1.5	1.3	1

* N,N-dimethyl-2,4,6-trimethylaniline **Reaction Conditions:** Temperature: 400°C; TOS = 2h. WHSV = 1 h^{-1}

4.3.3.5. Influence of time on stream

The activity and product selectivity of zeolite H-Beta catalyst as a function of time for the reaction of o-toluidine alkylation with methanol at 400°C, WHSV of 1 h^{-1} and molar ratio of methanol to o-toluidine of 2:1 was depicted in figure 4.3.2 for a period of 12h. The OTD conversion decreases slightly during initial 2h on stream and thereafter remains stable up to 12h. The catalytic activity and product selectivity remained almost same during the period of study.

Figure 4.3.1: Influence of WHSV on o-toluidine methylation and product selectivities over Hβ	**Figure 4.3.2:** Influence of Time on stream on o-toluidine methylation and product selectivities over Hβ
Reaction Conditions: Temperature = 400°C; catalyst: H-Beta; Methanol: o-Toluidine = 2:1 (mol), TOS = 2h	**Reaction Conditions:** Temperature = 400°C; Methanol: o-Toluidine = 2:1 (mol), TOS = 2h.

.
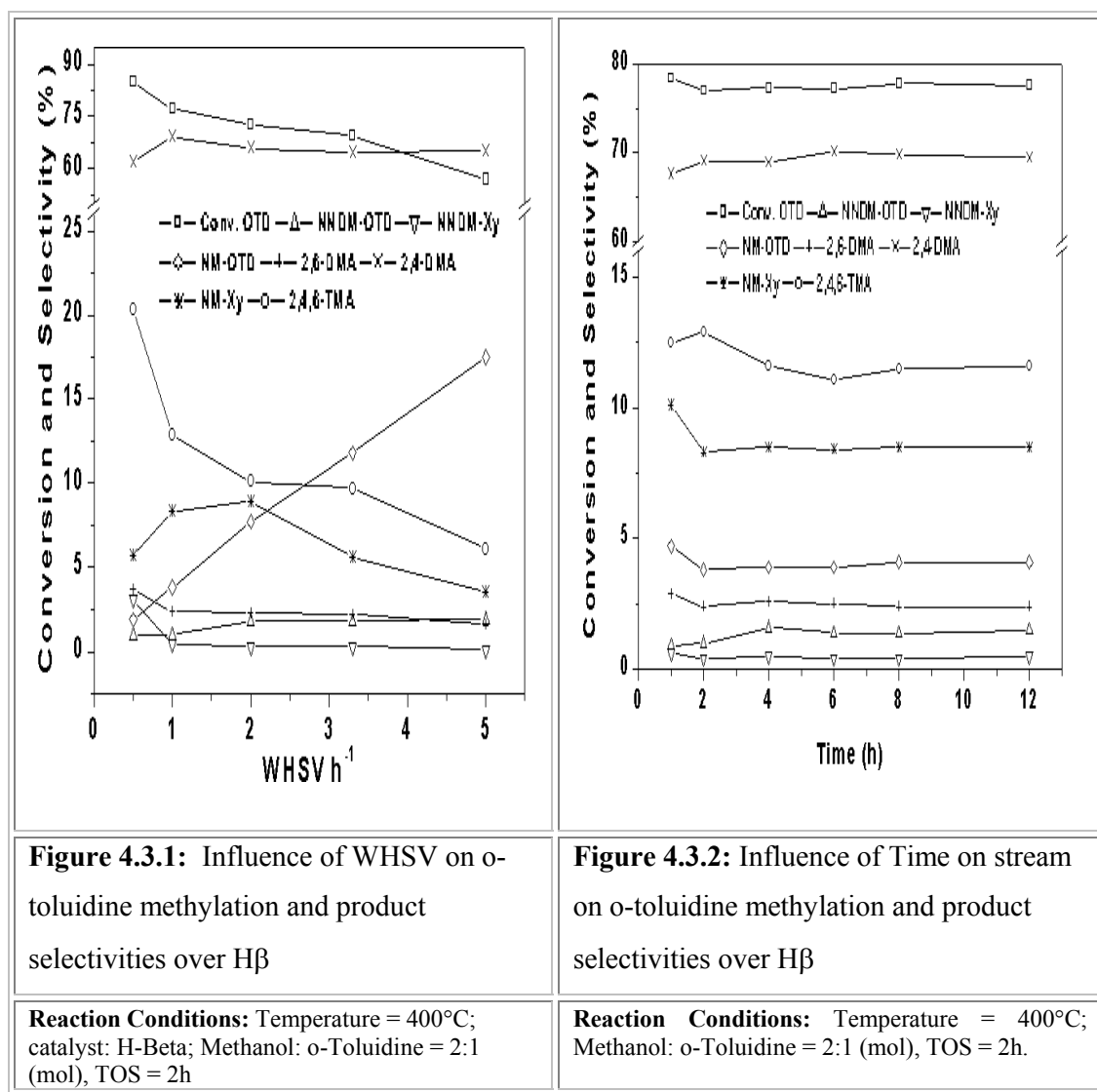
In broad outline, the scheme of methylation of o-toluidine (figure 4.3.3) may be presented as follows:
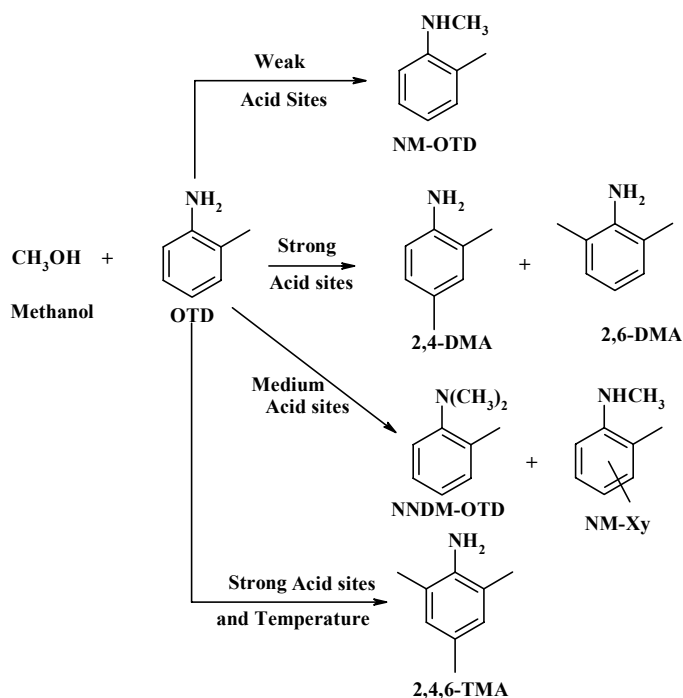
Figure 4.3.3: Scheme of methylation of o-toluidine over acidic zeolites.

4.3.4. CONCLUSIONS

The main products of the reaction of OTD (*o*-toluidine) methylation are both NMOTD and 2,4-DMA. All the zeolites are selective for N-mono-methylation of o-toluidine at lower temperatures. C-alkylation is favoured over large pore zeolites at higher temperatures. Weak acid sites are active for NMOTD, whereas medium acid sites are active for formation of NNDM-OTD and NM-Xy and strong acid sites are responsible for 2,4-DMA, 2,6-DMA and 2,4,6-TMA. Lower molar ratios are beneficial to xylidines and higher ones are helpful to produce poly-methylated products. The catalytic activity and product selectivity remained almost same during the period of study of 12h over Hβ zeolite.

4.4. REFERENCES

1.   K.S. Hayes *Appl. Catal. A,* **221** (2001) 187.

2.   Ullmann's *Encyclopedia of Industrial Chemistry*, vol. A2, VCH, 1998, p. 16.

3.   A. Belhekar, T.K. Das, K. Chaudhari, S.G. Hegde, A.J. Chandwadkar, *Stud. Surf. Sci. Catal.,* **113** (1998) 195.

4.   H.G. Bosche, K. Baer, K. Schneider, DE Patent 2,442,929 (1976).

5.   I. Hudea, M. Biemel Werner, R. Czifra, RO Patent 85,563 (1984).

6.   G. Engemann, G. Spielberger, US Patent 3,080,371 (1963).

7.   J.E. Wells, US Patent 4,514,567 (1985).

8.   T. Ogawa, N. Mizui, S. Tate, S. Kumoi, Japan Patent 5,017,460 (1993).

9.   T. Ogawa, N. Mizui, S. Tate, S. Kumoi, Japan Patent 5,017,461 (1993).

10.   T. Ogawa, N. Mizui, S. Tate, S. Kumoi, Japan Patent 5,017,462 (1993).

11.   H.J. Buysch, A. Botta, L. Puppe, DE Patent 3,934,459 (1991).

12.   W.T. Reichle, *J. Catal.,* **144** (1993) 556.

13.   H.-X. Li, J.G. Santiesteban, J.N. Armor, US Patent 5,731,449 (1998).

14.   J.G. Santiesteban, H.-X. Li, J.N. Armor, US Patent 5,741,906 (1998).

15.   J.N. Armor, J.G. Santiesteban, H.-X. Li, US Patent 5,756,741 (1998).

16.   H.-X. Li, J.G. Santiesteban, L.A. Emig, J.N. Armor, European Patent 952,152 (1999).

17.   E.I. Karpeiskaya, L.S. Gorshakowa, *Bull. Acad. Sci. USSR,* **19** (1970) 255.

18.   I. Scriabine, *Bull. Soc. Chim. Fr.,* **5** (1947) 454.

19.   R.A. Budnik, M.R. Sander, Eur. Pat. 158 (1985)139.

20.   N. Srinivas, D. Venu Gopal, B. Srinivas, S.J. Kulkarni, M. Subrahmanyam *Microporous Mesoporous Mater,* **51** (2002) 43.

21.   Y. Bhat, J. Das, S. Ali, B.D. Bhatt, A.B. Halgeri, *Appl. Catal. A*, 148(1), (1996) L1.

22.   S.G. Hedge, R. Kumar, R.N. Bhat, P. Ratnasamy, *Zeolites,* **9** (1989) 231.

23.   S. J. Kulkarni, H. Hattori, I. Toyoshima, *Zeolites*, 7(3), (1987) 178.

24.   K. Tanabe, W.F. Hölderich, *Appl. Catal. A,* **181** (1999) 399.

25.   P.B. Weisz, *Pure Appl. Chem.,* **52** (1980) 2091.

26.   W. F. Hoelderich, *Appl. Catal. A,* **194-195**, (2000) 487.

27.   W. F. Hoelderich, *Catal. Today,* **62**(1), (2000) 115.

28.   S.M. Csicsery, *Pure Appl. Chem.*, **58** (1986) 841.

29.   J. Weitkamp, S. Ernst, H. Dauns, E. Gallei, *Chem.-Ing.-Tech.,* **58** (1986) 623.

30.   S.M. Csicsery, *J. Catal.,* **23** (1971) 124.

31.   D.H. Olson, W.O. Haag, in T.E. Whyte, Jr., R.A. Dalla Betta, E.G. Derouane and R.T.K. Baker (Editors), *Catalytic Materials: Relationship Between Structure and Reactivity*, ACS Symposium Series, Vol. 248, American Chemical Society, Washington, D.C., 1984, pp. 275-307.

32.   W.O. Haag, D.H. Olson, P.B. Weisz, in H. Grtinewald (Editor), *Chemistry for the Future, Proc. 29th IUPAC Congress,* Pergamon Press, Oxford, New York, Toronto, Sydney, Paris, Frankfurt, 1984, pp. 327-336.

33.   F.G. Dwyer, in W.R. Moser (Editor), *Catalysis of Organic Reactions*, Marcel Dekker, Inc., New York, Basel, 1981, pp. 39-50.

34.   J. Weitkamp, *Proc. Intern. Symposium on Zeolite Catalysis*, Sibfok, Hungary, May 13 - 16, 1985, pp. 271-290.

35.   H. Heinemann, in J.R. Anderson and M. Boudart (Editors), *Catalysis Science and Technology*, Vol. 1, Springer-Verlag, Berlin, Heidelberg, New York, 1981, pp. 1-41.

36.   W. Hoelderich, E. Gallei, *Chem.-Ing.-Tech*., **56** (1984) 908-915.

37.   Industrial Organic Chemistry (1997), VCH, New York, p. 376.

38.   K. Weisermal, H. J. Aree in: *Industrial Organic Chemistry*, Verlag Chemie, (1978) p. 329.

39.   W. F. Hoelderich. in: *Introduction to zeolite science and practice*, (Eds. H. Van Bekkum, E.M. flanigen, J. C. Jansen), Elsevier, (1991) p. 661.

40.   F. J. Weigert, *J. Org. Chem.,* **52** (1987) 3296.

41.   D.J. Collins, R.J. Medina, B.H. Davis, *Can. J. Chem. Eng.,* **61** (1983) 29.

42.   US Patent No. 4 283 571.

43.   F.J. Weigert, *J. Org. Chem.,* **51** (1986) 2653.

44.   K. Eichler, H.J. Arpe, H. Baltes, E.I. Leupold, Ger. Offen. DE 3420707 (1985).

45.   F.J. Weigert, US Pat. 4,593,124 (1986).

46.   H.J. Arpe, H. Litterer, Eur. Pat. 92 103 (1982).

47.   R.H. Hardy, B.H. Davis, *J. Catal.,* **111** (1988) 146.

48.   Ger. Offen. DE 3,420,706 (1985).

49.   P.B. Weisz, V.J. Frilette, *J. Phys. Chem.,* **64** (1960) 382.

50.   S.M., Csicsery, *Zeolite Chemistry and Catalysis,* ACS Monogr., 171 (1976) 680.

51.   A. Corma, E. Sastre, *J. Chem. Soc., Chem. Commun.,* (1991) 594.

52.   F.J. Weigert, R.S. Mitchell *J. Mol. Catal.,* **89** (1994) 191.

53.   A.G. Hill, J.H. Shipp, A.J. Hill, *Ind. Eng. Chem.,* **43** (1951) 1579.

54.   L.K. Doraiswamy, G.R.W. Krishnan, S.P. Mukherjee, *Chem.Eng.,* **88**(14), (1981) 78.

55.   P.Y. Chen, S.J. Chu, N.S. Chang, T.K. Chuang, *Stud. Surf. Sci. Catal.,* **49**B (1989) 1105.

56.   K.G. Ione, O.V. Kikhtyanin, *Stud. Surf. Sci. Catal.,* **49**B (1989) 1073.

57.   B.L. Su, D. Barthomeuf, *Appl. Catal. A,* **124** (1995) 73.

58.   B.L. Su, D. Barthomeuf, *Appl. Catal. A,* **124** (1995) 81.

59.   S. Narayanan, K. Deshpande, *Appl. Catal. A,* **199** (2000) 1.

60.   Z. Fu, Y. Ono, *Catal. Lett.,* **22** (1993) 277.

61.   P.R.H.P. Rao, P. Massiani, D. Barthomeuf, *Catal. Lett.,* **31** (1995) 115..

62.   S.I. Woo, J.K. Lee, S.B. Hong, Y.K. Park, Y.S. Uh, *Stud. Surf. Sci. Catal.,* **49** (1989) 1905.

63.   Y.K. Park, K.Y. Park, S.I. Woo, *Catal. Lett.,* **26** (1994) 169.

64.   B. –Y. Choi, W. –C. Chang, K. –S. Kim, T. –J. Lee, *Hwahak Konghak,* 38(2), (2000) 123.

65.   H. Le Blanc, K. Wedemeyer, Eur. Pat. Appl. EP 68283 (1983).

66.   K. Takahata, T. Murashige, S. Hirokane, Jpn. Kokai Tokkyo Koho, JP 86/238766 (1986); Jpn Kokai Tokkyo Koho JP 86/238767 (1986); W. Zielinski, *Chem. Stosow.,* 34 (1990) 311.

67.   G.S.J. Lee, D.V. Rao, K.D. Anderson, L.N. Moreno, N.N.Shah, Eur.Pat.Appl, EP422590 (1991).

68.   X.–C. Zhang, L.-Y. Chen, W. Dong, *Shiyou Huagong,* **29**(2), (2000) 93.

69.   L.-Y. Chen X.-C. Zhang, W. Dong, H.-K. Chen, *Jingxi Huagong,* **17**(1), (2000) 19.

70.   L.-Y. Chen X.-C. Zhang, L. Yu, *Ranliao Gongye,* **36**(1), (1999) 35-37,40.

71.   L.-Y. Chen X.-C. Zhang, W. Dong, *Huaxue Fanying Gongcheng Yu Gongyi,* **16**(2), (2000) 193.

72.   P.Y. Chen, M.C. Chen, H.Y. Chu, N.S. Chang,T.K. Chang, *Stud. Surf. Sci. Catal.,* **28** (1986) 739.

Chapter –5

Summary & Conclusions

The thesis is a study of synthesis of nitrogen containing heterocyclic compounds and acid catalyzed reactions of aromatic amines. The catalysts investigated are both medium (H-FER and H-ZSM-5) and large pore (HY, H-BETA and H-MOR) zeolites and their modifications with zinc. The reactions investigated are vapor phase Beckmann rearrangement (over various FER zeolites), condensation of acetone, acetaldehyde and ammonia to yield pyridine bases (over H-FER zeolite), intermolecular cyclization of ethylene diamine and propylene glycol to yield methylpyrazine (over ZnO modified zeolites), intramolecular cyclization of MEA to yield alkylpyrazines (over ZnO modified zeolites). The acidic form of medium and large pore zeolites (H-zeolites) are utilized to investigate the synthesis of a bicyclic amine DABCO, isomerization of o-toluidine and methylation of o-toluidine.

The various zeolites have been prepared by hydrothermal methods, calcined and ion-exchanged with ammonium nitrate to yield H-zeolites. These zeolites are modified with zinc by wet impregnation method. Zeolite H-ZSM-5 is modified with zinc by ion-exchange also. FER zeolite is steam treated to yield highly stable steamed ferrierite (St-H-FER). All these samples were characterized by XRD for structural purity and surface area. All the zeolite showed excellent crystallinity, and there is no change in the peak intensities of the zeolite samples modified with zinc by impregnation. At higher loadings, however, a decrease in intensity is noted. Also the surface area of zinc-modified samples is less than that of the parent sample.

The acid sites of these zeolites were characterized by temperature programmed desorption of ammonia and FTIR spectra of adsorbed pyridine. In the case of TPD, the spectra were resolved and the HT B peak was analyzed. According to the total acidity, the following order can be observed for H-zeolites: H-Y > H-BETA > H-MOR > H-ZSM-5 > H-FER, and zinc modified ZSM-5 samples: ZnO-ZSM-5 > Zn-ZSM-5 > H-ZSM-5, and

FER zeolites can be arranged in the following order: Na-FER > H-FER (20) > H-FER (34) > H-FER (50) > St-H-FER (37) > Si-FER (the values in the parentheses represents SiO_2/Al_2O_3 ratio), and for zinc modified zeolites: ZnO-BETA > ZnO-MOR > ZnO-ZSM-5 > ZnO-FER.

The FTIR study of adsorbed pyridine gives a clear distinction between Bronsted and Lewis acidic sites at around 1540 and 1450cm^{-1} respectively and these peak areas are utilized to estimate the relative acidity of various zeolites. From the structural hydroxyl region and pyridine adsorption region, for zinc modified ZSM-5, a remarkable difference in the relative concentration of different kind of –OH groups is observed. A decrease in concentration of bridging hydroxyl groups due to Zn^{2+} exchange of a H^+ cation is considerably less than in zinc-impregnated sample. The concentration of the internal silanol groups at 3740cm^{-1} in impregnated sample has decreased more than that in ion-exchanged sample indicating in addition to exchangeable positions, zinc may be present as bulk ZnO on the surface of the sample in not much dispersed state.

XPS studies of the above said zinc modified samples revealed that there are two different zinc species at different BE. Intermediate value of Zn/Si ratio suggests that the distribution of Zn species is more uniform and well separated in case of ion exchanged sample than the impregnated or physical mixture of ZnO and ZSM-5.

From the studies of vapor phase Beckmann rearrangement of cyclohexanone oxime, it can be concluded that using appropriate Si/Al ratio or highly dealuminated H-ferrierite and an appropriate diluent can increase catalytic performance of H-ferrierite zeolite catalysts. H-FER and St-H-FER catalysts show good activity at 350°C. Solvent polarity also strongly affects the conversion of cyclohexanone oxime and selectivity of ε-caprolactam. Acetonitrile has been found to be the best solvent for cyclohexanone oxime to improve the selectivity for ε-caprolactam formation. Also ferrierite zeolite was shown to be

active in the synthesis of pyridine bases in the liquid phase and under autogeneous pressure.

Reaction of ethylene diamine and propylene glycol over ZnO modified zeolites, in general, resulted in the formation of methyl pyrazine. ZnO-ZSM-5 displayed high selectivity towards 2-methylpyrazine compared to other zinc modified zeolites under study. Deactivation of the catalyst (ZnO-ZSM-5) during the period of study i.e. 8h is observed. ZnO-Beta and ZnO-FER are less active; ZnO-Beta is not selective. A little higher concentration of ethylene diamine in the feed improves the selectivity of 2-methylpyrazine. A comparison between the better catalytic activity observed with impregnated catalyst may be due to its similarity with ZnO (extracrystalline ZnO) than Zn^{2+} cations (from XPS study) and also possessing intermediate acidity of both Brönsted and Lewis (from FTIR study) as compared to unmodified and zinc ion exchanged ZSM-5 which are responsible for cyclization.

Reaction of MEA over ZnO-modified zeolites resulted in the formation of pyrazine and alkylpyrazines. Ethylpyrazine was the major product in the case of ZnO-ZSM-5 and ZnO-FER catalysts. Selectivity towards a particular compound was not observed over ZnO-MOR. It was found that piperazine or its alkylderivaties were easily dehydrogenated to corresponding pyrazine derivatives over these catalysts. The formation of DABCO was appreciable over ZnO-MOR; however, it became less probable over ZnO-FER and ZnO-ZSM-5 catalyst, due to their higher dehydrogenation activity. The narrow pore inside ZnO-MOR zeolite allowed the formation of different lower boilers like methylamine, ethylamine, aziridine and ethylenediamine. The stability of these catalysts in terms of conversion of MEA with time on stream followed the order ZnO-ZSM-5 > ZnO-MOR > ZnO-FER.

Piperazine can be converted to useful products like DABCO, methylpyrazine and higher alkylpyrazines over acidic zeolite catalysts. The medium pore zeolites (particularly, H-ZSM-5) are selective for the formation of DABCO where as the large pore zeolites are useful for alkylpyrazines. Catalyst with medium pore and less acidity leads to formation of DABCO; where as the one with strong and weak acidity leads to formation of dehydrogenated and alkylated products. Modification of H-ZSM-5 with ZnO by impregnation leads to diminish in conversion of PIP and selectivity to DABCO with increase in pyrazine selectivity showing the dehydrogenation activity of zinc.

The channel dimensionality and pore openings of different zeolites studied for o-toluidine isomerization, reveals that the H-ZSM-5 (medium pore) zeolite favours isomerization contrary to wide pore zeolites favoring disproportionation. The m/p isomer ratio is found to be higher at lower temperature and it progressively decreases with increase in temperature however, with contact time, there is not much change in the m/p isomer ratio over both the zeolites. The deactivation is found to be more for wide pore zeolite (HY) than the medium pore H-ZSM-5.

The main products of the reaction of OTD (o-toluidine) methylation are both NMOTD and 2,4-DMA. All the zeolites are selective for N-mono-methylation of o-toluidine at lower temperatures. C-alkylation is favoured over large pore zeolites at higher temperatures. Weak acid sites are active for NMOTD, whereas medium acid sites are active for formation of NNDM-OTD and NM-Xy and strong acid sites are responsible for 2,4-DMA, 2,6-DMA and 2,4,6-TMA. Lower molar ratios are beneficial to xylidines and higher ones are helpful to produce poly-methylated products. The catalytic activity and product selectivity remained almost same during the period of study of 12h over Hβ zeolite.

The above studies reveal that FER are active in vapor phase Beckmann rearrangement of cyclohexanone oxime and pyridine bases synthesis by batch process in liquid phase autogeneous pressure conditions. Zinc modified zeolites are excellent in dehydrocyclization reactions especially for the conversion of simpler molecules like MEA to alkylpyrazines. Also incorporation of zinc leads to generation of new Lewis acidic sites, which are active for these reactions apart from the dehydrogenating activity of ZnO. The zeolites with various channel dimensions and their acidity are proven to be crucial in acid catalyzed reactions of aromatic amines and in synthesis of DABCO.

List of Publications

1. Epoxidation of styrene with TBHP/O2 over Ferrierite (FER) type molecular sieves
   R.Anand, Siddhesh Shevade, R.K.Ahedi and B.S.Rao
   Catalysis Letters 62 (1999) 209-13

2. A comparative study on the catalytic activity of ZnO modified zeolites in the synthesis of alkylpyrazines
   R.Anand, T.M. Jyothi and B.S.Rao
   Applied Catalysis A: General 208 (2001) 203–211

3. Catalytic acetylation of alcohols, phenols, thiols and amines with zeolite H-FER under solventless conditions
   Subhash. P. Chavan, **R. Anand**, K. Pasupathy and B. S. Rao
   Green Chemistry, 3 (2001) 320–322

4. Synthesis of 2-methyl pyrazine over zinc-modified ferrierite (FER) catalysts
   R. Anand and B.S. Rao
   Catalysis Communications 3 (2002) 29–35

5. Vapor phase Beckmann rearrangement of cyclohexanone oxime over different ferrierite Zeolite catalysts
   R. Anand, R. B. Khomane, B. S. Rao and B. D. Kulkarni
   Catalysis Letters 78 (2002) 189-194

6. Alkylation of phenol with cyclohexanol and cyclohexene using HY and modified HY zeolites
   R. Anand, K.U. Gore and B.S. Rao
   Catalysis Letters in press

7. Selective alkylation of Phenol with cyclohexanol over large pore zeolites
   R.Anand, Thomas Daniel, R.J. Lahoti, K.V. Srinivasan and B.S.Rao
   Catalysis Letters in press

8. FTIR and *o*-toluidine methylation studies over USY zeolites
   K.U. Gore, **R. Anand**, B.B. Tope, S.G. Hegde and B.S. Rao
   Communicated to *Appl. Catal. A*

9. Tertiary butylation of phenol over HY and dealuminated HY zeolites
   R. Anand, V. R. Chumbhale, K. U. Gore, B. B. Tope and S. G. Hegde
   Communicated to *J. Mol. Catal. A*

10**.** Selective alkylation of catechol with t-butylalcohol over HY and modified HY Zeolites
   R. Anand, K. U. Gore and V. R. Chumbhale
   Communicated to *Catalysis Communication*

List of Papers presented at Symposia

1. Synthesis of ε-Caprolactam over Ferrierite (FER) type zeolite
   R.Anand, S.S.Shevade , R.K.Ahedi and B.S.Rao
   Presented at NCL Golden Jubilee Symposium on Catalysis, 1999.

2. Synthesis of 2-Methyl Pyrazine over Modified Zeolites
   R.Anand, P.S. Mukund, R.K. Ahedi and B.S. Rao
   Presented at International Symposium On Zeolites And Microporous Crystals, ZMPC 2000, Sendai, Japan

Manuscripts under Preparation

1. Synthesis of DABCO over acidic zeolites
   R. Anand and B.S. Rao

2. Synthesis of 2-methyl pyrazine over zinc modified zeolites
   R. Anand, C.S.Gopinath, S.G. Hegde and B.S. Rao

3. Methylation of *ortho*-toluidine over acidic zeolites
   R. Anand, K.U. Gore, B.B. Tope, S.G. Hegde and B.S. Rao